

SYNTHESIS AND AROMATIZATION OF BIOBASED CYCLOHEXENES

By

Yukari Nishizawa-Brennen

A DISSERTATION

Submitted to  
Michigan State University  
in partial fulfillment of the requirements  
for the degree of

Chemistry–Doctor of Philosophy

2017

# ABSTRACT

## SYNTHESIS AND AROMATIZATION OF BIOBASED CYCLOHEXENES

By

Yukari Nishizawa-Brennen

In recent years, the cost of petrochemicals has declined by increasing production of unconventional gases such as shale gas, tight gas and coalbed methane. The main component of the unconventional gases is methane. Aromatic compounds are ubiquitous in commodity, specialty and pharmaceutical chemicals. Many aromatic chemicals are derived from benzene, toluene and xylenes (BTX), which could be derived from methane. Biobased aromatic chemicals production may appear unnecessary since we can produce BTX from methane. However, other factors need to be considered such as climate change, avoidance of toxic starting materials and/or byproducts, and significant consumer preference for biobased products.

Because aromatics are generally toxic to microbes, biobased aromatic compounds are often synthesized from nontoxic biobased intermediates. An ideal strategy is a synthesis of biobased hydroaromatics that can be either dehydrated or dehydrogenated to aromatics in a single step. We can perform elimination reactions on biobased cyclohexenes possessing appropriately placed leaving groups. In the absence of leaving groups, dehydrogenation reactions need to be employed. This thesis focuses on biobased cyclohexenes that are aromatized either by dehydration reactions or by dehydrogenation reactions.

Copyright by  
YUKARI NISHIZAWA-BRENNEN  
2017

This dissertation is dedicated to Mike and Ike  
Thank you for coming to Michigan with me.

## ACKNOWLEDGMENTS

First, I would like to thank my research adviser, Professor John W. Frost, for his patience and guidance. Even though, I was clueless in chemistry laboratory, he never gave up on me. I would like to thank the members of my guidance committee, Professor Babak Borhan, Professor Xuefei Huang and Professor Gary J. Blanchard for their intellectual input throughout the graduate school.

I am grateful for Dr. Karen Draths for detail guidance in experimental techniques and intelligent input. I extremely appreciate all of former group members for their research and strain collections. Lastly, I am deeply indebted to my lab mate, Kelly K. Miller, for help during the writing of this thesis.

## TABLE OF CONTENTS

LIST OF TABLES .....	xi
LIST OF FIGURES .....	xiii
LIST OF SCHEMES .....	xiv
KEY TO ABBREVIATIONS.....	xvii
CHAPTER ONE .....	1
1. Introduction.....	1
REFERENCES .....	14
CHAPTER TWO .....	20
Synthesis of Biobased <i>p</i> -Hydroxybenzoic Acid .....	20
1. Introduction.....	20
2. <i>p</i> -Hydroxybenzoic Acid Production .....	21
3. Toxicity of Benzene and Phenol.....	24
4. Biocatalytic Routes to <i>p</i> -Hydroxybenzoic Acid .....	26
5. Results.....	33
5.1. Conversion of Shikimic Acid to <i>p</i> -Hydroxybenzoic Acid in Ionic Liquid Bromides .....	33
5.2. Dehydration of Shikimic Acid in non-Bromide Ionic Liquids .....	38
5.3. A Possible Mechanism for Bromide-Catalyzed Dehydration of Shikimic Acid .....	39
5.4. Lewis Acid Catalyzed Conversion of Shikimic Acid to <i>p</i> -Hydroxybenzoic Acid in 1- Butyl-3-methylimidazolium Salts .....	41
5.5. Conversion of (3 <i>R</i> ,4 <i>S</i> ,5 <i>R</i> )-Triacetoxy-1-cyclohexene-1-carboxylic Acid to <i>m</i> -Hydroxybenzoic Acid in 1-Butyl-3-methylimidazolium Salts.....	44
6. Discussion .....	47
7. Experimental .....	49
7.1. General.....	49
7.2. Product Analysis .....	50
7.3. Screening of Ionic Liquid for Dehydration of Shikimic Acid .....	50
7.4. Comparison of Shikimic Acid Concentration in Dehydration of Shikimic Acid .....	50
7.5. Synthesis of 1-Butyl-3-methylimidazolium Bromide.....	51
7.6. Recycling 1-Butyl-3-methylimidazolium Bromide .....	51
7.7. Lewis Acid Catalysts Screening for Dehydration of Shikimic Acid .....	53
7.8. Synthesis of Tetra-( <i>n</i> )-butylphosphonium Iodide .....	54
7.9. (3 <i>R</i> ,4 <i>S</i> ,5 <i>R</i> )-Triacetoxy-1-cyclohexenecarboxylic Acid .....	55
7.10. Screening of Ionic Liquid for <i>m</i> -Hydroxybenzoic Acid Synthesis from (3 <i>R</i> ,4 <i>S</i> ,5 <i>R</i> )- Triacetoxy-1-cyclohexenecarboxylic Acid .....	55
7.11. 1-Butyl-3-methylimidazolium Chloride .....	56
7.12. <i>m</i> -Hydroxybenzoic Acid Synthesis from (3 <i>R</i> ,4 <i>S</i> ,5 <i>R</i> )-Triacetoxy-1-cyclohexenecarboxylic Acid .....	56

REFERENCES .....	58
CHAPTER THREE .....	66
Scale-Up of the Synthesis of Biobased <i>p</i> -Hydroxybenzoic Acid .....	66
1. Introduction.....	66
2. <i>E. coli</i> SP1.1/pKD15.071B .....	67
3. Countercurrent Flow Extraction .....	69
4. Tangential (Cross) Flow Filtration.....	73
5. Results.....	75
5.1. Shikimic Acid Titers and Yield .....	75
5.2. Shikimic Acid Extraction Solvent Screening .....	75
5.3. Countercurrent Extraction of Shikimic Acid .....	76
5.4. Comparison of Shikimic Acid Crystallization Solvents .....	79
5.5. Purification of Shikimic Acid .....	80
5.6. Scale Up Synthesis of <i>p</i> -Hydroxybenzoic Acid.....	81
6. Discussion .....	82
7. Experimental .....	84
7.1. General.....	84
7.2. Product Analysis .....	84
7.3. Culture Medium .....	85
7.4. Bacterial Strain and Plasmid.....	86
7.5. Fed-Batch Fermentation (General) .....	86
7.6. Fed-Batch Fermentation of Shikimic Acid .....	87
7.7. Cell Removal .....	89
7.8. Protein Removal.....	90
7.9. Shikimic Acid Extraction Solvent Screening in Vials .....	90
7.10. KARR® Column General .....	90
7.11. Comparison of Shikimic Acid Extraction Solvents in KARR® Column .....	91
7.12. Comparison of Shikimic Acid Crystallization Solvents .....	91
7.13. Decolorizing Isopropanol/Water (9:1 v/v) Extract and Evaporative Crystallization from <i>n</i> -Butanol of Shikimic Acid .....	92
7.14. Scale-up Dehydration of Shikimic Acid in 1-Butyl-3-methylimidazolium Bromide.....	93
REFERENCES .....	95
CHAPTER FOUR.....	99
Synthesis of Biobased Terephthalic Acid .....	99
1. Introduction.....	99
2. Terephthalic Acid and Isophthalic Acid Production.....	100
3. Biobased Terephthalic Acid.....	102
4. Results .....	107
4.1. Cycloaddition of Acrylic Acid and Isoprene .....	107
4.2. Aromatization of 4-Methyl-3-cyclohexenecarboxylic Acid and 3-Methyl-3-cyclohexenecarboxylic Acid.....	110
4.2.1. H <sub>2</sub> SO <sub>4</sub> Oxidation .....	110
4.2.2. Dehydrogenation Catalyzed by Pd/C in Solvents .....	112
4.2.3. Catalytic Oxidative Dehydrogenation.....	113

4.2.4. Aerobic Dehydrogenation .....	114
4.2.5. Aerobic Oxidative Dehydrogenation .....	114
4.2.6. Vapor Phase Dehydrogenation .....	116
5. Discussion .....	119
6. Experimental .....	120
6.1. General .....	120
6.2. Cycloaddition Products 39 and 40 Analysis .....	120
6.3. Analysis of Aromatization Products: <i>p</i> -Toluic Acid 41 and 4-Methyl-3-cyclohexenecarboxylic Acid 44 .....	121
6.4. Analysis of Aromatization Products: <i>p</i> -Toluic Acid 41, <i>m</i> -Toluic Acid 42, 4-Methylcyclohexanecarboxylic Acid 44, 3-Methylcyclohexanecarboxylic Acid 47, Unreacted 4-Methyl-3-cyclohexenecarboxylic Acid 39, and Unreacted 3-Methyl-3-Cyclohexenecarboxylic Acid 40 .....	122
6.5. Uncatalyzed Cycloaddition of Acrylic Acid 38 and Isoprene 37 at rt .....	123
6.6. Uncatalyzed Cycloaddition of Acrylic Acid and Isoprene in a High Pressure Reactor ....	124
6.7. Silica Gel Catalyzed Cycloaddition of Acrylic Acid 38 and Isoprene 37 at 25 °C .....	124
6.8. Silica Gel Catalyzed Cycloaddition of Acrylic Acid 38 and Isoprene 37 at 50 °C .....	125
6.9. Silica Gel Catalyzed Cycloaddition of Acrylic Acid 38 and Isoprene 37 at 95 °C .....	125
6.10. Zeolite $\beta$ Catalyzed Cycloaddition of Acrylic Acid 38 and Isoprene 37 (Table 4.1, entry 6).....	126
6.11. Zeolite $\beta$ Catalyzed Cycloaddition of Acrylic Acid 38 and Isoprene 37 (Table 4.1, entry 7).....	126
6.12. Zeolite $\beta$ Catalyzed Cycloaddition of Acrylic Acid 38 and Isoprene 37 (Table 4.1, entry 8).....	127
6.13. Zeolite $\beta$ Catalyzed Cycloaddition of Acrylic Acid 38 and Isoprene 37 (Table 4.1, entry 9).....	127
6.14. H <sub>2</sub> SO <sub>4</sub> Oxidation of 4-Methyl-3-cyclohexenecarboxylic Acid 39 to <i>p</i> -Toluic Acid 41 ..	128
6.15. H <sub>2</sub> SO <sub>4</sub> Oxidation of a Mixture of 4-Methyl-3-cyclohexenecarboxylic Acid 39 and 3- Methyl-3-cyclohexenecarboxylic Acid 40 to <i>p</i> -Toluic Acid 41 and <i>m</i> -Toluic Acid 42..	128
6.16. Dehydrogenation of 4-Methyl-3-cyclohexenecarboxylic Acid 39 in Water .....	129
6.17. Dehydrogenation of 4-Methyl-3-cyclohexenecarboxylic Acid 39 in Acetic Acid .....	130
6.18. Dehydrogenation of 4-Methyl-3-cyclohexenecarboxylic Acid 39 in <i>p</i> -Xylene .....	130
6.19. Dehydrogenation of 4-Methyl-3-cyclohexenecarboxylic Acid 39 in Mesitylene .....	131
6.20. Dehydrogenation of 4-Methyl-3-cyclohexenecarboxylic Acid 39 in <i>n</i> -Decane .....	131
6.21. Dehydrogenation of 4-Methyl-3-cyclohexenecarboxylic Acid 39 and 3-Methyl-3- Cyclohexenecarboxylic Acid 40 with Pd/C and Nitrobenzene in Mesitylene.....	132
6.22. PdCl <sub>2</sub> -AMS Catalyzed Dehydrogenation of 4-Methyl-3-cyclohexenecarboxylic Acid 39 .....	132
6.23. Pd/C-AMS Catalyzed Dehydrogenation of 4-Methyl-3-cyclohexenecarboxylic Acid 39	132
6.24. Aerobic Dehydrogenation of 4-Methyl-3-cyclohexenecarboxylic Acid 39 .....	133
6.25. Aerobic Dehydrogenation of 4-Methyl-3-cyclohexenecarboxylic Acid 39 and 3-Methyl-3-cyclohexenecarboxylic Acid 40 .....	133
6.26. Aerobic Oxidative Dehydrogenation of 4-Methyl-3-cyclohexenecarboxylic Acid 39....	134
6.27. Vapor Phase Dehydrogenation of 4-Methyl-3-cyclohexenecarboxylic Acid 39 .....	134
6.28. Vapor Phase Dehydrogenation of a Mixture of 4-Methyl-3-cyclohexenecarboxylic Acid 39 and 3-Methyl-3-cyclohexenecarboxylic Acid 40 .....	135

REFERENCES .....	137
CHAPTER FIVE .....	143
Synthesis of Biobased Trimethyl Trimellitate .....	143
1. Introduction.....	143
2. Trimellitic Acid Production .....	144
3. Biobased Trimellitic Acid / Trimethyl Trimellitate.....	146
4. New Synthesis Route of Biobased Trimellitic Acid.....	147
5. Protocatechuate 3,4-Dioxygenase.....	149
6. 1,2,4-Butanetricarboxylic Acid.....	152
6.1. Introduction.....	152
6.2. Synthesis of Biobased 1,2,4-Butanetricarboxylic Acid .....	152
7. Results.....	154
7.1. Microbial Synthesis of 2 <i>E</i> ,4 <i>Z</i> -3-Carboxylic Acid .....	154
7.1.1. <i>E. coli</i> WN1/pYNB6.009A.....	154
7.1.1.1. Cloning Overview.....	154
7.1.1.2. Construction of pKD16.179A and pYNB6.009A.....	155
7.1.1.3. Host Strain <i>E. coli</i> WN1 Phenotype Confirmation.....	158
7.1.2. Protocatechuate 3,4-Dioxygenase Activity.....	159
7.1.3. Fed-Batch Fermentor Synthesis of 2 <i>E</i> ,4 <i>Z</i> -3-Carboxymuconic Acid.....	159
7.1.3.1. Glucose-rich Condition Fermentation.....	159
7.1.3.2. Glucose-limited Condition Fermentation .....	161
7.2. Isolation of 2 <i>E</i> ,4 <i>E</i> -3-Carboxymuconic Acid from Fermentation Broth .....	163
7.3. Synthesis of Biobased Trimethyl Trimellitate .....	164
7.3.1. Isomerization of 2 <i>E</i> ,4 <i>E</i> -3-Carboxymuconic Acid 54 to 2 <i>Z</i> ,4 <i>E</i> -3-Carboxymuconic Acid 13.....	164
7.3.2. Cycloaddition of 2 <i>E</i> ,4 <i>E</i> -3-Carboxymuconic Acid 54 and Ethylene.....	165
7.3.3. Esterification of 2 <i>E</i> ,4 <i>E</i> -3-Carboxymuconic Acid 54.....	165
7.3.4. Cycloaddition of Trimethyl 3-Carboxymuconate 56 and Ethylene .....	166
7.3.5. Aromatization of Cycloadduct 57 .....	167
7.3.5.1. Dehydrogenation Catalyzed by Pd/C in Solvents.....	167
7.3.5.2. Aerobic Oxidative Dehydrogenation of Cycloadduct 57.....	168
7.3.5.3. Vapor Phase Dehydrogenation of Cycloadduct 57 Catalyzed by Pd/SiO <sub>2</sub> .....	169
7.4. Synthesis of Biobased 1,2,4-Butanetricarboxylic Acid .....	170
8. Discussion .....	171
9. Experimental .....	172
9.1 Spectroscopic Measurements.....	172
9.2. Gas Chromatography .....	172
9.3. Bacterial Strains and Plasmids.....	172
9.4. Storage of Bacterial Strains and Plasmids .....	173
9.5. Culture Medium .....	173
9.6. Preparation and Transformation of Electrocompetent Cell .....	174
9.7. Small Scale Purification of Plasmid DNA.....	175
9.8. Large Scale Purification of Plasmid DNA.....	176
9.9. Isolation of <i>Klebsiella pneumoniae</i> subsp. <i>pneumoniae</i> (ATCC25597) Genomic DNA ..	176
9.10. Plasmid pKD16.179A.....	177

9.11. Plasmid pYNB6.009B .....	178
9.12. Plasmid pYNB6.009A .....	180
9.13. <i>E. coli</i> WN1 .....	180
9.14. Protocatechuate 3,4-Dioxygenase Activity.....	181
9.15. Fed-Batch Fermentation General .....	182
9.16. Glucose-rich Condition Fermentation.....	184
9.17. Glucose-limited Condition Fermentation .....	185
9.18. Removal of Cells and Protein .....	187
9.19. Isolation of 2 <i>E</i> ,4 <i>E</i> -3-Carboxymuconic Acid 54 .....	187
9.20. 2 <i>E</i> ,4 <i>E</i> -3-Carboxymuconic Acid 54 isolation Process Investigation.....	188
9.21. Isomerization of 2 <i>E</i> ,4 <i>E</i> -3-Carboxymuconic Acid 54 to 2 <i>Z</i> ,4 <i>E</i> -3-Carboxymuconic Acid 13 .....	188
9.22. Cycloaddition of 2 <i>E</i> ,4 <i>E</i> -3-Carboxymuconic Acid 54 and Ethylene.....	189
9.22.1. Reaction in 1,4-Dioxane at 164 °C .....	189
9.22.2. Reaction in <i>m</i> -Xylene at 150 °C .....	189
9.22.3. Reaction in 1,4-Dioxane at 100 °C .....	190
9.22.4. Reaction in <i>m</i> -Xylene at 100 °C .....	190
9.23. Esterification of 2 <i>E</i> ,4 <i>E</i> -3-Carboxymuconic Acid 54.....	190
9.24. Cycloaddition of Trimethyl 3-Carboxymuconate 56 and Ethylene .....	191
9.25. Dehydrogenation of Cycloadduct 57 Catalyzed by Pd/C in Decane .....	192
9.26. Dehydrogenation of Cycloadduct 57 Catalyzed by Pd/C in Dichlorobenzene.....	193
9.27. Aerobic Oxidative Dehydrogenation of Cycloadduct 57.....	193
9.28. Vapor Phase Dehydrogenation of Cycloadduct 57 .....	193
9.29. Synthesis of Biobased 1,2,4-Butanetricarboxylic Acid 37 .....	194
REFERENCES .....	196

## LIST OF TABLES

Table 2.1. Dehydration of Shikimic Acid in Various 1-Butyl-3-methylimidazolium Salts <b>40a-40e</b> .....	34
Table 2.2. Impact of Shikimic Acid Concentration in 1-Butyl-3-methylimidazolium Bromide <b>40b</b> on Dehydration Yield and Accountability of Shikimic Acid Consumption .....	34
Table 2.3. 1-Butyl-3-methylimidazolium Bromide <b>40b</b> Recycle .....	36
Table 2.4. Dehydration of Shikimic Acid in Various Ionic Liquids <b>41-45</b> .....	37
Table 2.5. Lewis Acid 20 mol% Catalyzed Dehydration of Shikimic Acid in 1-Butyl-3-methylimidazolium Bromide <b>40b</b> .....	42
Table 2.6. Lewis Acid 20 mol% Catalyzed Dehydration of Shikimic Acid in 1-Butyl-3-methylimidazolium Chloride <b>40a</b> .....	42
Table 2.7. Lewis Acid 20 mol% Catalyzed Dehydration of Shikimic Acid in 1-Butyl-3-methylimidazolium Iodide <b>40c</b> .....	43
Table 2.8. Lewis Acid 2 mol% Catalyzed Dehydration of Shikimic Acid in 1-Butyl-3-methylimidazolium Bromide <b>40b</b> .....	43
Table 2.9. <i>m</i> -Hydroxybenzoic Acid Synthesis from Acetylated Shikimic Acid in Various 1-Butyl-3-methylimidazolium Salts <b>40a-40e</b> .....	45
Table 3.1. Shikimic Acid Partition Coefficient in Various Solvents .....	76
Table 3.2. Problems Seen During KARR® Column Optimization .....	77
Table 3.3. Countercurrent Extraction of Microbe-Synthesized Shikimic Acid .....	79
Table 3.4. % Purity and % recovery of Crystallized Shikimic Acid .....	80
Table 3.5. Instrument Setting of First Phase .....	88
Table 3.6. Instrument Setting of Second Phase .....	89
Table 3.7. Auto-antifoam Setting .....	89
Table 4.1. Cycloaddition of Acrylic Acid and Isoprene .....	108
Table 4.2. Dehydrogenation of 4-Methyl-3-cyclohexenecarboxylic Acid in Various Solvents ..	112

Table 5.1. Cycloaddition of 2 <i>E</i> ,4 <i>E</i> -3-Carboxymuconic Acid <b>54</b> and Ethylene.....	165
Table 5.2. Dehydrogenation of Cycloadduct <b>57</b> Catalyzed by Pd/C in Solvents .....	168
Table 5.3. PCR Cycle for <i>pcaHG</i> .....	177
Table 5.4. PCR Cycle for <i>serA</i> – <i>aroF</i> <sup>FBR</sup> – <i>P</i> <sub><i>aroF</i></sub> Cassette .....	179
Table 5.5. First Phase of Glucose-rich Fermentation .....	184
Table 5.6. Second Phase of Glucose-rich Fermentation .....	185
Table 5.7. First Phase of Glucose-limited Fermentation .....	186
Table 7.8. Second Phase of Glucose-limited Fermentation .....	186

## LIST OF FIGURES

Figure 2.1. <i>ortho</i> - and <i>para</i> -intermediate .....	22
Figure 3.1. A: Centrifugal Extractor, B: Rotor of Centrifugal Extractor.....	70
Figure 3.2. A: Packed Column, B: Sieve Tray Column, C: RDC Extractor, D: SCHEIBEL® Column .....	70
Figure 3.3. KARR® Column .....	70
Figure 3.4. KARR® Column Configuration.....	73
Figure 3.5. A: Tangential (Cross) Flow Filtration, B: Dead-End Filtration .....	74
Figure 3.6. Hollow Fibers .....	74
Figure 3.7. Continuous Liquid-Liquid Extractor .....	82
Figure 4.1. Vapor Phase Plug Reactor .....	117
Figure 5.1. Preparation of Plasmid pKD16.179A.....	156
Figure 5.2. Preparation of Plasmid pYNB6.009B .....	157
Figure 5.3. Preparation of Plasmid pYNB6.009A .....	158
Figure 5.4. Glucose-rich/IPTG(+) Fermentation .....	161
Figure 5.5. Glucose-limited/IPTG(+) Fermentation .....	162

## LIST OF SCHEMES

Scheme 1.1 Methane is an Ozone Precursor.....	4
Scheme 1.2. Formation of Cyclohexane during Aromatization of Cyclohexene .....	6
Scheme 1.3. Palladium Catalyst Cycle with Anthraquinone-2-sulfonate Sodium Salt .....	8
Scheme 1.4. Proposed Mechanism for Regeneration of Pd(TFA) <sub>2</sub> with Oxygen.....	9
Scheme 1.5. Proposed Mechanism for Pd <sup>II</sup> Catalyzed Aerobic Dehydrogenation .....	9
Scheme 1.6. Aromatization of 3,4-Dimethylcyclohex-3-enecarboxylic Acid.....	10
Scheme 1.7. Aerobic Oxidative Dehydrogenation of Cyclohexenes to Arene Derivatives .....	11
Scheme 1.8. Dehydration of Microbially Synthesized Shikimic Acid .....	12
Scheme 1.9. Synthesis of Biobased <i>p</i> -Toluic Acid <i>m</i> -Toluic Acid .....	13
Scheme 1.10. Synthesis of Biobased Trimethyl Trimellitate .....	13
Scheme 2.1. <i>p</i> -Hydroxybenzoic Acid Production from Benzene .....	23
Scheme 2.2. Benzene Metabolism .....	25
Scheme 2.3. Biocatalytic Routes to <i>p</i> -Hydroxybenzoic Acid.....	27
Scheme 2.4. Biocatalytic Routes to <i>p</i> -Hydroxybenzoic Acid.....	29
Scheme 2.5. Shikimic Acid Dehydration in Ionic Liquid.....	33
Scheme 2.6. Ionic Liquids Used in Shikimic Acid Dehydration .....	33
Scheme 2.7. Possible Mechanism of Shikimic Acid Dehydration .....	40
Scheme 2.8. Aromatization of Acetylated Shikimic Acid .....	44
Scheme 2.9. Possible Mechanism of Acetylated Shikimic Acid Aromatization .....	46
Scheme 3.1. The Common Pathway of Aromatic Amino Acid Biosynthesis .....	67
Scheme 3.2. Biosynthesis of Erythrose-4-phosphate.....	68

Scheme 3.3. Increasing Phosphoenolpyruvic Acid Availability .....	68
Scheme 3.4. Dehydration of Shikimic Acid .....	81
Scheme 4.1. Aerobic Catalytic Oxidation of <i>p</i> -Xylene to Terephthalic Acid .....	101
Scheme 4.2. Catalytic Pathway for Amoco Mid-Century Oxidation of <i>p</i> -Toluic Acid .....	101
Scheme 4.3. Biobased <i>p</i> -Xylene .....	103
Scheme 4.4. Xylene-Free Synthesis of Biobased Terephthalic Acid .....	104
Scheme 4.5. Alder's Reaction Sequence .....	105
Scheme 4.6. Cycloaddition of Acrylic Acid and Isoprene.....	107
Scheme 4.7. Aromatization of 4-Methyl-3-cyclohexenecarboxylic acid <b>39</b> and 3-methyl-3-cyclohexenecarboxylic acid <b>40</b> .....	110
Scheme 4.8. H <sub>2</sub> SO <sub>4</sub> Oxidation.....	111
Scheme 4.9. Proposed Reaction Mechanism of H <sub>2</sub> SO <sub>4</sub> Oxidation .....	111
Scheme 4.10. Dehydrogenation of 4-Methyl-3-cyclohexenecarboxylic Acid on Pd/AMS.....	113
Scheme 4.11. Stahl's Reported Reaction .....	114
Scheme 4.12. Aerobic Dehydrogenation of 4-Methyl-3-cyclohexenecarboxylic Acid and 3-Methyl-3-cyclohexenecarboxylic Acid.....	114
Scheme 4.13. Aerobic Oxidative Dehydrogenation of Cyclohexenes to Arene Derivatives .....	115
Scheme 4.14. Aerobic Oxidative Dehydrogenation of 4-Methyl-3-cyclohexenecarboxylic Acid.....	115
Scheme 4.15. Vapor Phase Aromatization of 4-Methyl-3-cyclohexenecarboxylic Acid and 3-Methyl-3-cyclohexenecarboxylic Acid .....	118
Scheme 5.1. Plasticizers.....	143
Scheme 5.2. Oxidation of Pseudocumene.....	145
Scheme 5.3. Biobased Trimellitate .....	147
Scheme 5.4. New Synthesis Route of Biobased Trimellitic Acid .....	148

Scheme 5.5. Biosynthesis Pathway of <i>2E,4Z</i> -3-Carboxymuconic Acid.....	149
Scheme 5.6. $\beta$ -Ketoadipate Pathway .....	151
Scheme 5.7. First Phase of Aromatic Compound Degradation .....	151
Scheme 5.8. Synthesis of 1,2,4-Butanetricarboxylic Acid from <i>2E,4Z</i> -3-Carboxymuconic Acid.....	152
Scheme 5.9. Biobased 1,2,4-Butanetricarboxylic Acid Synthesis Route .....	153
Scheme 5.10. Lysine Biosynthesis Pathway.....	154
Scheme 5.11. Protocatechuate 3,4-Dioxygenase .....	159
Scheme 5.12 Fermentation Products.....	160
Scheme 5.13. Isomerization of <i>2E,4E</i> -3-Carboxylic Acid <b>54</b> .....	164
Scheme 5.14. Nuclear Overhauser Effect .....	164
Scheme 5.15. Cycloaddition of <i>2E,4E</i> -3-Carboxymuconic Acid <b>54</b> and Ethylene .....	165
Scheme 5.16. Esterification of <i>2E,4E</i> -3-Carboxymuconic Acid <b>54</b> .....	166
Scheme 5.17. Nuclear Overhauser Effect .....	166
Scheme 5.18. Cycloaddition of Trimethyl 3-Carboxymuconate <b>56a,b</b> and Ethylene .....	167
Scheme 5.19. Dehydrogenation of Cycloadduct <b>57</b> Catalyzed by Pd/C in Solvent .....	167
Scheme 5.20. Aerobic Oxidative Dehydrogenation of Cycloadduct <b>57</b> .....	168
Scheme 5.21. Vapor Phase Dehydrogenation of Cycloadduct <b>57</b> Catalyzed by Pd/SiO <sub>2</sub> .....	169
Scheme 5.22. Synthesis of 1,2,4-Butanetricarboxylic Acid <b>37</b> .....	170

## KEY TO ABBREVIATIONS

Ac	acetyl
AcOH	acetic acid
AMS	anthraquinone-2-sulfonate sodium salt
Ap	ampicillin
Ap <sup>R</sup>	ampicillin resistance
ASA	acetylated shikimic acid
ADP	adenosine monophosphate
ATP	adenosine triphosphate
BMI <sub>m</sub>	1-butyl-3-methylimidazolium
Bp	base pair
BSTFA	<i>N,O</i> -bis(trimethylsilyl)trifluoroacetamide
BTEX	benzene, toluene, ethylbenzene and xylenes
BTX	benzene, toluene and xylenes
BuOH	butanol
CIAP	calf intestinal alkaline phosphatase
CoA	coenzyme A
DAHP	3-deoxy-D- <i>arabino</i> -heptulosonate 7-phosphate
DHQ	3-dehydroquinic acid
DHS	3-dehydroshikimic acid
DIPEA	<i>N,N</i> -diisopropylethylamine
DMF	dimethylformamide

DNA	deoxyribonucleic acid
dNTP	Deoxynucleotide solution mix
DO	dissolved oxygen
E4P	D-erythrose 4-phosphate
E.C.	enzyme commission number
<i>E. coli</i>	<i>Escherichia coli</i>
EPA	United Sates Environmental Protection Agency
EtOAc	ethyl acetate
EtOH	ethanol
FBR	feed back resistant
GC	gas chromatography
h	hour
HPLC	high-performance liquid chromatography
IPTG	isopropyl $\beta$ -D-1-thiogalactopyranoside
<i>K. pneumoniae</i>	<i>Klebsiella pneumoniae</i>
LCP	liquid crystalline polymer
MCL	maximum contaminant limit
MeOH	methanol
MHBA	<i>m</i> -hydroxybenzoic acid
Min	minute
MS	mass spectrometer
NAD	nicotinamide adenine dinucleotide
NMP	<i>N</i> -methyl-2-pyrrolidone

NOE	nuclear Overhauser effect spectroscopy
mp	melting point
NMR	nuclear magnetic resonance spectroscopy
OD	optical density
OTf	trifluoromethanesulfonate
OSHA	Occupational Safety and Health Administration
PCA	protocatechuic acid
PCR	polymerase chain reaction
PEP	phosphoenolpyruvate
PET	polyethylene terephthalate
PHBA	<i>p</i> -hydroxybenzoic acid
Ppm	parts per million
PTS	PEP:carbohydrate phosphotransferase
PVC	polyvinylchloride
RDC	rotating disc contactor
ROS	reactive oxygen species
rt	room temperature
SA	shikimic acid
sec	second
<i>sp.</i>	species
subsp.	subspecies
TCA	tricarboxylic acid cycle
Temp	temperature

TFA	trifluoroacetate
THF	tetrahydrofuran
TLC	thin-layer chromatography
TsOH	<i>p</i> -toluenesulfonic acid
TSP	sodium salt of 3-(trimethylsilyl) propionic-2,2,3,3-d <sub>4</sub> acid

## CHAPTER ONE

### 1. Introduction

As part of the generation that was born and raised during the 1970's oil crisis, the fear of decreasing petrochemical availability was omnipresent. This fear has declined today due to exponentially increasing production of unconventional gases such as shale gas, tight gas and coalbed methane. Unconventional gas is the gas that can be produced by using hydraulic fracturing, horizontal drilling or other techniques to expose additional reservoirs of hydrocarbons.<sup>1</sup> Use of hydraulic fracturing to extract oil and gas from shale/rock/coalbed formations, has advanced rapidly over the last two decades.<sup>2</sup> Extraction of shale gas in the United States has increased more than ten times in the last decade alone.<sup>3</sup> The United States has become self-sufficient in gas production despite recently being one of the largest importers of natural gas in the world.<sup>2</sup> According to the U.S. Department of Energy, the United States had  $3.5 \times 10^{11} \text{ m}^3$  of proven coalbed methane reserves and  $5.0 \times 10^{12} \text{ m}^3$  of proven reserves of shale gas methane.<sup>4a</sup> They also estimated the United States had  $3000 \times 10^{12} \text{ m}^3$  of methane as methane hydrate.<sup>4b</sup> Even though there is no commercial production of methane from methane hydrate, Japan recently reported the world's first offshore methane hydrate production field test.<sup>4c</sup>

Many aromatic chemicals are derived from benzene, toluene and xylenes (BTX) but the challenge of deriving BTX from methane remains. The conversion of methane to BTX via methanol has been suggested to be the most promising route for conversion of methane to BTX.<sup>5</sup> Methane is converted to methanol via steam reforming. The catalysts for steam reforming are quartz (silica) or metal exchanged zeolite.<sup>6,7</sup> Selective conversion of methanol to aromatics is catalyzed by metal exchanged ZSM-5.<sup>8</sup> The highest distribution of products among BTX from this process is xylenes, while the lowest is benzene.<sup>8</sup> The selective disproportionation of toluene

over zeolite can yield *p*-xylene and benzene.<sup>9</sup>

Biobased aromatic chemicals production may appear unnecessary since we can produce BTX from methane. However, other factors need to be considered such as climate change, avoidance of toxic starting materials and/or byproducts, and significant consumer preference for biobased products. The United Nations encourages implementation of carbon pricing systems for greenhouse gas emissions such as carbon taxation and cap-and-trade policies.<sup>10</sup> A carbon pricing system has already been implemented or is scheduled for implementation in small number of countries, states and provinces. A cap-and-trade program has been in place in California since 2012.<sup>11</sup> Washington and Oregon have been deliberating the implementation of a carbon tax since 2015.<sup>10,12</sup> Although the first carbon tax proposal in Washington was rejected by voters in November 2016, the proposed legislation is currently being revised.<sup>13</sup>

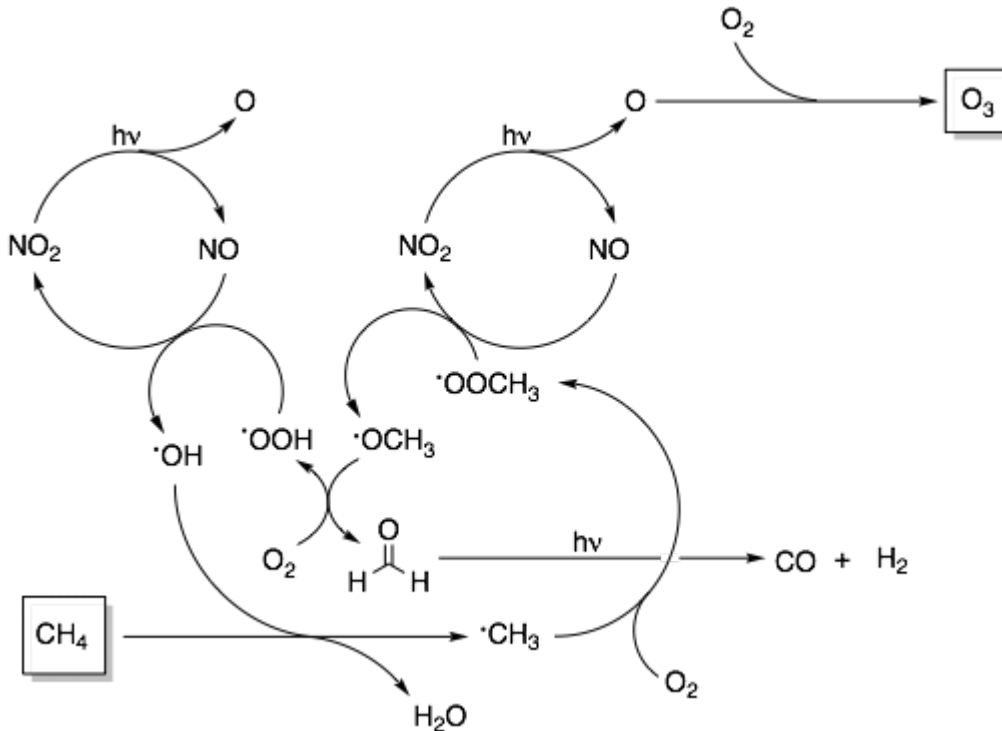
In petrochemical production, significant amounts of carbon are wasted as CO<sub>2</sub>. As an example, 30-40% of carbon is wasted as CO<sub>2</sub> and CO during the production of maleic anhydride from *n*-butane.<sup>14</sup> Synthesis of biobased maleic anhydride from furfural, which is obtained from hydrolysis of biomass, also loses 40% of carbon during oxidation,<sup>15,16</sup> although this lost carbon originated from atmospheric CO<sub>2</sub> fixed by plants. The U.S. Department of Agriculture (USDA) encourages production and use of biobased products as part of the BioPreferred® program. The USDA reported that the total contribution of the biobased product industry to the U.S. economy in 2013 was \$369 billion and employed four million workers.<sup>17</sup> One example of a commercial biobased product is the 30% (by weight) biobased polyethylene terephthalate water bottle produced for and marketed by The Coca-Cola Company.<sup>18</sup>

The radiation from sunlight bounces off the Earth surface and emits longwave radiation. Absorbance of longwave radiation and emission of the energy by CO<sub>2</sub> is the basis of its

greenhouse effect.<sup>19a</sup> There is also a report that elevated CO<sub>2</sub> concentrations in the atmosphere affects plant physiology, which increases greenhouse effect.<sup>19b</sup> The elevated CO<sub>2</sub> concentrations in the atmosphere reduces the evapotranspiration of plants, which is reducing the concentration of water vapor in the atmosphere.<sup>19b</sup> Even though water has a greenhouse gas effect,<sup>19a</sup> clouds near the land keeps temperature low by increasing the planetary albedo and causing less solar radiation to reach the surface. The decreasing the greenhouse gas effect of water cannot compensate the increased solar radiation to reach the surface.<sup>19b</sup> Methane has more of a greenhouse gas effect than CO<sub>2</sub> because methane absorbs shorter wavelength (8 μm) radiation than CO<sub>2</sub> (10 μm and 14 μm).<sup>19a</sup> Degradation of methane produces ozone, which is also a greenhouse gas.<sup>20</sup> The ozone layer in the stratosphere protects us by absorbing UV radiation. Ozone in the troposphere leads to a greenhouse effect by absorbing longwave (9 μm) radiation.<sup>19a,20a</sup>

High concentrations of methane along with nitrogen oxides (NO<sub>x</sub>) increases the concentration of ozone in the troposphere (Scheme 1).<sup>20</sup> Hydroxyl radical abstracts a hydrogen from methane, forming •CH<sub>3</sub>. The •CH<sub>3</sub> reacts with molecular oxygen to form •OOCH<sub>3</sub>. An oxygen atom is abstracted from •OOCH<sub>3</sub> by NO, yielding •OCH<sub>3</sub>. Formaldehyde is produced when •OCH<sub>3</sub> reacts with molecular oxygen. Formaldehyde is photolyzed to CO and H<sub>2</sub> by sunlight.<sup>20e</sup> An oxygen atom is released from NO<sub>2</sub> upon photolysis by sunlight, and the oxygen atom reacts with molecular oxygen, forming ozone (Scheme 1.1).<sup>20</sup>

Scheme 1.1. Methane is an Ozone Precursor



Methane gas leakage at shale gas drilling and production sites is a problem. It is estimated that  $2.2 \times 10^9$  kg/yr of methane is emitted annually in the United States.<sup>21</sup> Another problem at shale gas drilling site is a groundwater contamination from the shale gas/oil, chemicals used during hydraulic fracturing and disturbance of surface soil.<sup>22</sup> Dichloromethane was detected from private, residential water wells (within one mile) the Barnett shale region in Texas.<sup>22a</sup> The average dichloromethane concentration was 0.08 mg/L while the maximum contaminant limit (MCL) of dichloromethane suggested by the U.S. Environmental Protection Agency is 0.005 mg/L.<sup>22a</sup> The source of dichloromethane is thought to be from disturbance of surface soil, which was already contaminated with dichloromethane. Methane contaminates underground water at active shale gas extraction sites. The highest methane level in the underground water from Wyoming, north-east Pennsylvania and New York was 70 mg/L.<sup>22b</sup> All the samples with high methane concentration was obtained within 1 km from the active shale gas

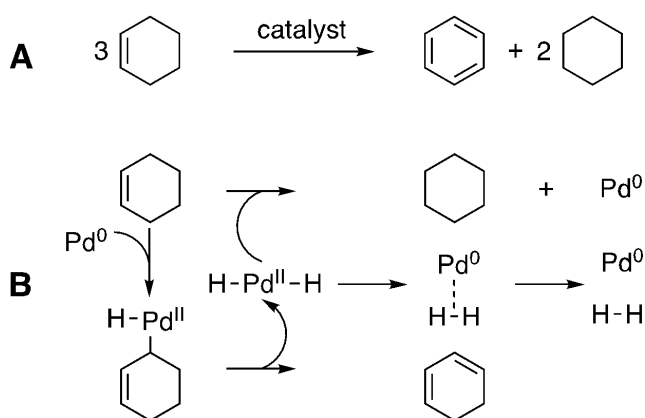
extraction sites.<sup>22b</sup> Hydraulic fracturing utilizes organic solvents containing benzene, toluene, ethylbenzene and xylenes (BTEX).<sup>22c</sup> The contaminated water and soil produced from drilling and hydraulic fracturing are injected into a ground. The shallow groundwater near the disposal ground contained 390 µg/L of benzene and 150 µg/L of *m/p*-xylenes while EPA's maximum concentration level for benzene was 5 µg/L.<sup>22c</sup> There was an incident caused by Marcellus shale gas wells in Pennsylvania. Natural gas flooded into initially drinkable groundwater used by several households.<sup>22d</sup> The groundwater was located to 1-3 km from hydraulic fracturing areas. In addition to methane (47 mg/L), the water was observed to foam.<sup>22d</sup> Later, the cause of foaming was linked to 2-*n*-butoxyethanol, which was one component of the fracturing fluid.<sup>22d</sup>

In addition to greenhouse gas emissions and groundwater contamination, earthquakes related to shale gas production is a concern. The magnitude and the area impacted by reported earthquakes related to hydraulic fracturing are relatively small (magnitude 2-3) relative to tectonic earthquake activity.<sup>23ab</sup> However, there were some significant earthquakes in Oklahoma caused by injection of wastewater produced from hydraulic fracturing. On September 3rd 2016, there was the earthquake with magnitude 5.8, which occurred approximately 15 km to the northwest of the town Pawnee.<sup>23c</sup> It damaged several buildings in the town. The earthquake was felt across multiple states up to distance over 1500 km.<sup>23c</sup>

Aromatic compounds are ubiquitous in commodity, specialty and pharmaceutical chemicals. Because aromatics are generally toxic to microbes,<sup>24</sup> biobased aromatic compounds are often synthesized from nontoxic biobased intermediates. An ideal strategy is a synthesis of biobased hydroaromatics that can be either dehydrated or dehydrogenated to aromatics in a single step. We can perform elimination reactions on biobased cyclohexenes possessing appropriately placed leaving groups. In the absence of leaving groups, dehydrogenation

reactions need to be employed. This thesis focuses on biobased cyclohexenes that are aromatized either by dehydration reactions or by dehydrogenation reactions. On its face, selective aromatization of cyclohexenes seems easy, but it has troubled chemists for more than 50 years. The difficulty of this transformation is a formation of cyclohexanes. One theory is that cyclohexenes can disproportionate into one equivalent of benzene and two equivalents of cyclohexane (Scheme 1.2A).<sup>25</sup> The other theory could be the reduction timing of H-Pd<sup>II</sup>-H to Pd<sup>0</sup>-H<sub>2</sub> complex (Scheme 1.2B). The H-Pd<sup>II</sup>-H needs to be reduced to Pd<sup>0</sup>-H<sub>2</sub> complex before it hydrogenates other alkene (Scheme 1.2B).

Scheme 1.2. Formation of Cyclohexane during Aromatization of Cyclohexene



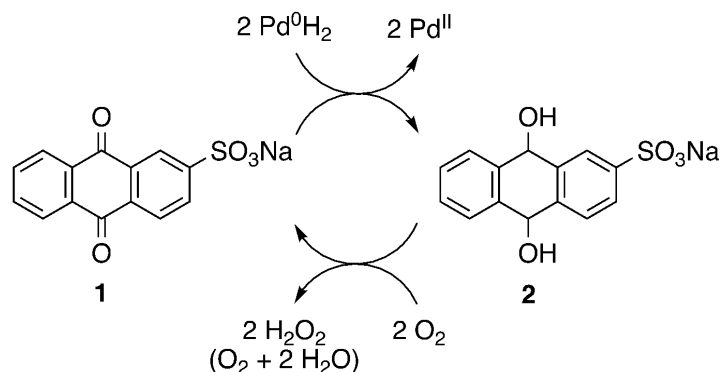
Early research examined the aromatization of cyclohexane and cyclohexene to benzene using a Ni catalyst.<sup>28ab</sup> In the 1970's, Pd and Pt became popular catalysts for investigation of the reaction conditions required for cyclohexene aromatization. A catalyst that works well for dehydrogenation of cyclohexene tends to work better for hydrogenation of cyclohexene.<sup>27a</sup> In order to lead the reaction toward dehydrogenation instead of hydrogenation, high temperatures are required for the reactions.<sup>27a</sup> For example, the suggested reaction temperature by Johnson Matthey is 5-100 °C for hydrogenation reaction in solvent while 180-250 °C is suggested for dehydrogenation reaction in solvents.<sup>27c</sup> C-C bond cleavage with attendant formation of coke

becomes a problem at high temperatures.<sup>27a</sup> Hydrogenolysis of ethane to methane with metal catalysts under hydrogen gas at 205°C was used to compare the ease of C-C bond cleavage.<sup>27b</sup> When the relative reaction rates per unit surface area of metal were compared as C-C bond cleavage relative activity, Ni had 10<sup>5</sup> higher relative specific activity when compared with Pd and Pt.<sup>27b</sup> This trend suggested Ni would have more of a coke formation problem than Pd or Pt during dehydrogenation reaction.<sup>27ab</sup>

Trost and Metzner used palladium(II) trifluoroacetate (TFA) and a hydrogen acceptor to prevent the disproportionation of cyclohexene to benzene and cyclohexane in 1980.<sup>28</sup> They examined multiple molecules as hydrogen acceptors although most inhibited the reaction. The selectivity towards benzene was slightly improved using three equivalents of maleic acid as the hydrogen acceptor.<sup>28</sup> Later, chemists started focusing on a catalytic cycle between Pd<sup>II</sup> and Pd<sup>0</sup> such as that seen in the Wacker process. For example, the oxidation of ethylene to acetaldehyde utilizes PdCl<sub>2</sub> and CuCl<sub>2</sub> as cocatalysts. Pd<sup>II</sup> oxidizes ethylene to acetaldehyde as it is reduced to Pd<sup>0</sup>. Cu<sup>II</sup> oxidizes Pd<sup>0</sup> back to Pd<sup>II</sup> while being reduced to Cu<sup>I</sup>. Oxygen oxidizes Cu<sup>I</sup> back to Cu<sup>II</sup>.<sup>29</sup>

One issue of the Wacker process is the production of a chlorinated side product.<sup>30</sup> In order to avoid the chlorinated side product, an alternative electron-transfer system for the reoxidation of Pd<sup>0</sup> was desired. Sheldon and Sobczak proposed anthraquinone-2-sulfonate sodium salt (AMS) as a cocatalyst with either PdCl<sub>2</sub> or Pd/C for aromatization of cyclohexene to benzene in 1991. They chose AMS for their catalyst system because it was found to be reoxidized easily by molecular oxygen (Scheme 1.3). They reported quantitative yields of benzene on a Pd/AMS catalytic system with molecular oxygen.<sup>31</sup> They did not demonstrate the utility of their system to substituted cyclohexenes.

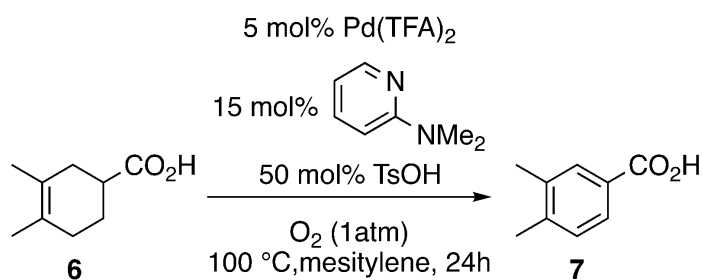
Scheme 1.3. Palladium Catalyst Cycle with Anthraquinone-2-sulfonate Sodium Salt



There was no progress in aromatization of cyclohexenes during the 1990's and 2000's. However, there was significant progress in elaborating catalytic cycles between Pd<sup>II</sup> and Pd<sup>0</sup> suitable for aerobic Pd-catalyzed oxidation of alcohols/alkenes to a ketones/aldehydes,<sup>32-34</sup> aminations<sup>34</sup> and annulations.<sup>33-35</sup> Nitrogen-donor ligands were commonly used in those transformations in order to initiate and/or accelerate the reactions.<sup>32-34</sup> Later Stahl explained the role of nitrogen-donor ligands were to form soluble Pd nanoparticles.<sup>36</sup> Labinger reported 100% selectivity for aromatization of cyclohexene to benzene using a Pd(TFA)<sub>2</sub>/O<sub>2</sub> system.<sup>25</sup> They suggested that insertion of O<sub>2</sub> into a Pd-H bond **3** produces a peroxy intermediate **4**, which reacts with trifluoroacetic acid to regenerate the catalyst **5** (Scheme 1.4). The shortcoming of their approach was a low conversion.<sup>25</sup>

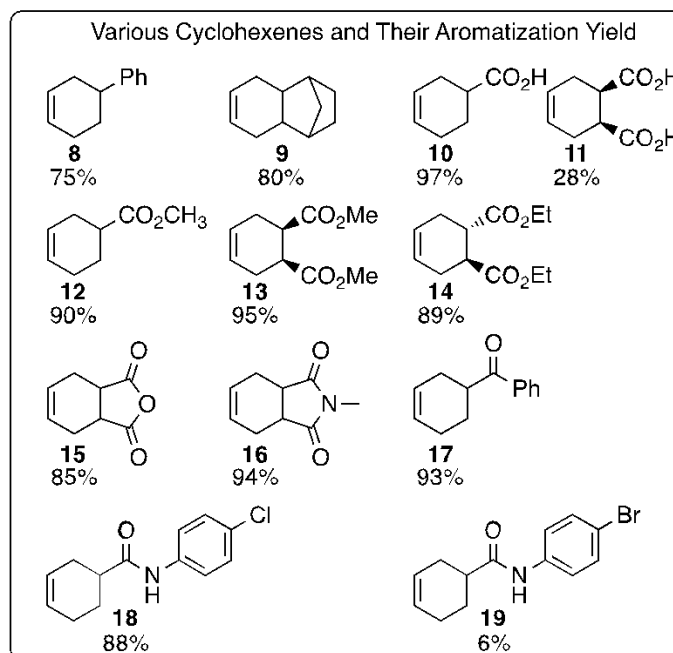
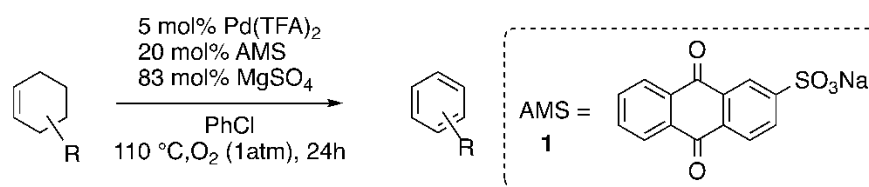


Scheme 1.6. Aromatization of 3,4-Dimethylcyclohex-3-enecarboxylic Acid<sup>37</sup>



A few years later, Stahl published a tandem oxidative coupling/dehydrogenation reaction. The catalyst system was modified to employ a different nitrogen-donor ligand and a different additive. The most significant change was the additive. TsOH interfered with oxidative coupling reactions but quinones, particularly AMS, were beneficial.<sup>39</sup> Stahl's research in oxidative dehydrogenation continued to focus on the aromatization of cyclohexanone to phenol.<sup>39</sup> The aromatization of cyclohexene came back under the spotlight in 2015.<sup>40</sup> Stahl reported a catalyst system consisted of Pd(TFA)<sub>2</sub>, AMS and MgSO<sub>4</sub> as a drying agent which could aromatize cyclohexenes.<sup>40</sup> The quantitative or near quantitative yields were reported with various substituted cyclohexenes including: aromatic, alkyl, ester, cyclic anhydride, ketone, imide and carboxylic acid groups (Scheme 1.7).<sup>40</sup>

Scheme 1.7. Aerobic Oxidative Dehydrogenation of Cyclohexenes to Arene Derivatives<sup>40</sup>

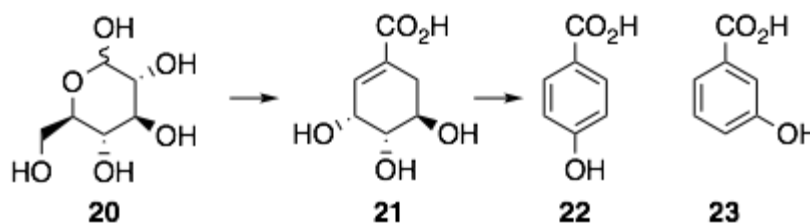


However, this reaction is very sensitive to minor changes in the substituents. The reaction yield was nearly quantitative when the substituent was an *N*-aryl amide bearing chloride **18**. The reaction yield was very poor when the substituent was an *N*-aryl amide bearing bromide **19** (Scheme 1.7).<sup>40</sup> One carboxylic acid as a substituent **10** produced a quantitative yield of benzoic acid; two carboxylic acids substituents **11** produce a poor yield of phthalic acid with a significant quantity of benzoic acid from decarboxylation (Scheme 1.7).<sup>40</sup> Stahl's research is a significant development in aromatization of cyclohexenes, but all of his reported successes were limited to substituents in the 4- and/or 5-position of the cyclohexenes without any substituent at other positions.<sup>40</sup>

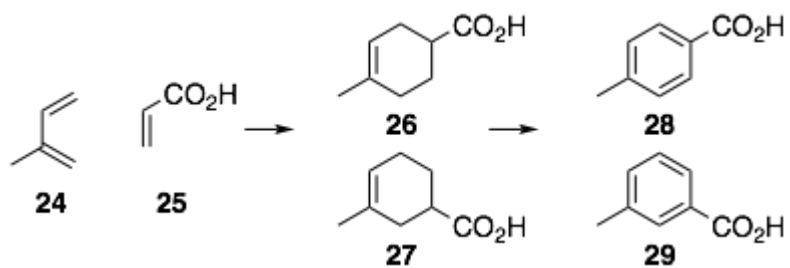
This thesis focuses on synthesis and aromatization of biobased cyclohexenes. An

elimination reaction was performed on biobased cyclohexene **21** possessing appropriately placed leaving groups. In the absence of leaving groups, dehydrogenation reactions were employed. In Chapter 2, microbially synthesized shikimic acid **21** is aromatized to *p*-hydroxybenzoic acid **22** and *m*-hydroxybenzoic acid **23** by a dehydration reactions (Scheme 1.8). 4-Methylcyclohex-3-enecarboxylic acid **26** and 3-methylcyclohex-3-enecarboxylic acid **27**, which are formed by cycloaddition of acrylic acid **25** with isoprene **24**, are aromatized to *p*-toluic acid **28** and *m*-toluic acid **29** by dehydrogenation in Chapter 4 (Scheme 1.9). In Chapter 5, (*2E,4Z*)-hexa-2,4-diene-1,3,6-tricarboxylic acid ((*2E,4Z*)-3-carboxymuconic acid) **30** is synthesized by a recombinant *E. coli* strain. The biobased cyclohexene **32** is synthesized by cycloaddition of the trimethyl 3-carboxymuconate **31** and ethylene and then aromatized by dehydrogenation (Scheme 1.10). A vapor phase plug reactor was developed for the dehydrogenation reaction to aromatize biobased cyclohexenes **26**, **27**, **32**. Stahl's oxidative aerobic dehydrogenation reaction was also tested to aromatize the biobased cyclohexenes **26** and **32**. No aromatization of cyclohexenes **26** or **32** was observed.

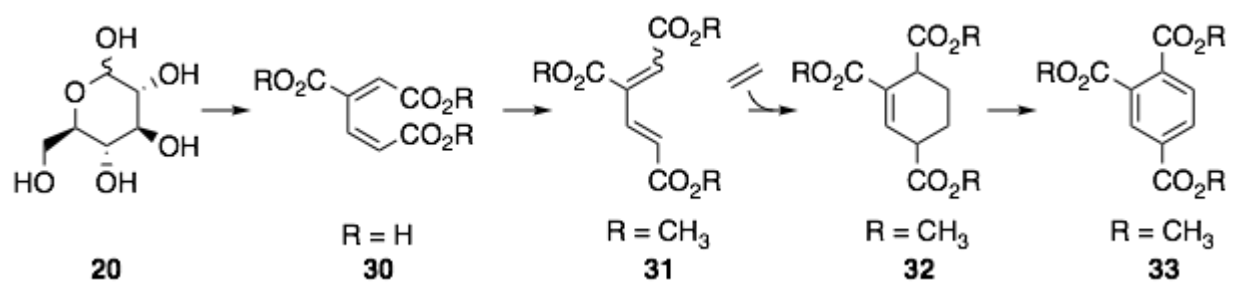
Scheme 1.8. Dehydration of Microbially Synthesized Shikimic Acid



Scheme 1.9. Synthesis of Biobased *p*-Toluic Acid *m*-Toluic Acid



Scheme 1.10. Synthesis of Biobased Trimethyl Trimellitate



## REFERENCES

## REFERENCES

1. Alberta Energy Regulator. What is Unconventional Oil and Gas? <https://www.aer.ca/about-aer/spotlight-on/unconventional-regulatory-framework/what-is-unconventional-oil-and-gas> (accessed Mar 30, 2017).
2. Stephenson, M. H. Shale gas in North America and Europe. *Energy Sci. Eng.* **2016**, *4*, 4-13. DOI: 10.1002/ese3.96.
3. U.S. Energy Information Administration. U.S. Shale Production. [https://www.eia.gov/dnav/ng/hist/res\\_epg0\\_r5302\\_nus\\_bcfa.htm](https://www.eia.gov/dnav/ng/hist/res_epg0_r5302_nus_bcfa.htm) (accessed Dec. 19, 2016).
4. (a) U.S. Department of Energy, U.S. Crude Oil and Natural Gas Proved Reserves, Year-end 2015. <https://www.eia.gov/naturalgas/crudeoilreserves/pdf/usreserves.pdf> (accessed Mar 13, 2017). (b) United States Department of Energy. Fiscal Year 2013 Methane Hydrate Program, Report to Congress October 2014. Washington, DC. (c) Konno, Y.; Fujii, T.; Sato, A.; Akamine, K.; Naiki, M.; Masuda, Y.; Yamamoto, K.; Nagao, J. Key finding of the world's first offshore methane hydrate production test off the Coast of Japan: toward future commercial production. *Energy Fuels* **2017**, *31*, 2607-2616. DOI: 10.1021/acs.energyfuels.6b03143.
5. Niziolek, A. M.; Onel, O. Production of benzene, toluene, and xylene from natural gas via methanol: process synthesis and global optimization. *AIChE J.* **2016**, *62*, 1531-1556 DOI: 10.1002/aic.15144.
6. (a) De Winne, H.; Jacobs, P.; Sels, B.; Vermeiren, W. Process for the selective oxidation of methane. US 2010280289, November 04, 2010. (b) Zhang, Q.; He, D.; Li, J.; Xu, B.; Liang, Y.; Zhu, Q. Comparatively high yield methanol production from gas phase partial oxidation of methane. *Applied Catalysis A: General* **2002**, *224*, 201-207.
7. Ranocchiari, M.; Tomkins, P.; Van Bokhoven, J. A process for methane to methanol conversion at low temperature. EP 3090997, September 11, 2016.
8. (a) Ono, Y.; Adachi, H.; Senoda, Y. J. Selective conversion of methanol into aromatic hydrocarbons over zinc-exchanged ZSM-5 zeolites. *Chem. Soc., Faraday Trans. 1* **1988**, *84*, 1091-1099. (b) Inoue, Y.; Nakashiro, K.; Ono, Y. Selective conversion of methanol into aromatic hydrocarbons over silver-exchanged ZSM-5 zeolites. *Microporous Materials* **1995**, *4*, 379-383. (c) Lopez-Sanchez, J. A.; Conte, M.; Landon, P.; Zhou, W.; Bartley, J. K.; Taylor, S. H.; Carley, A. F.; Kiely, C. J.; Khalid, K.; Hutchings, G. J. Reactivity of Ga<sub>2</sub>O<sub>3</sub> clusters on zeolites ZSM-5 for the conversion of methanol to aromatics. *Catal. Lett.* **2012**, *142*, 1049-1056 DOI: 10.1007/s10562-012-0869-2. (d) Conte, M.; Lopez-Sanchez, J. A.; He, Q.; Morgan, D. J.; Ryabenkova, Y.; Bartley, J. K.; Carley, A. F.; Taylor, S. H.; Keily, C. J.; Khalid, K.; Hutchings, G. J. Modified zeolite ZSM-5 for the methanol to aromatics reaction. *Catal. Sci. Technol.* **2012**, *2*, 105-112 DOI: 10.1039/c1cy00299f.

9. (a) Koster, S. C.; Holmgren, J. S. Selective disproportionation catalysis and process. US 6872865, March 29, 2005. (b) Beck, J. S.; Cheng, J. C.; McCullen, S. B.; Olson, D. H.; Stern, D. L. Binderless ex situ selectivated zeolite catalyst. US 6576582, June 10, 2003.
10. Cuevas, S.; Haines, A. Health benefits of a carbon tax. *The Lancet* **2016**, 387, 7-9. DOI: 10.1016/S0140-6736(15)00994-0.
11. Center for Climate and Energy Solutions. California Cap-andTrade Program Summary. <https://www.c2es.org/us-states-regions/key-legislation/california-cap-trade> (accessed Mar 30, 2017).
12. World Bank Group Climate Change. State and Trends of Carbon Pricing. 99533 <http://documents.worldbank.org/curated/en/636161467995665933/State-and-trends-of-carbon-pricing-2015> (downloaded Mar 30, 2017).
13. (a) IP, G. A growth-friendly climate change proposal. *The Wall Street Journal* **2016**, Sept. 28. <http://www.wsj.com/articles/a-growth-friendly-climate-change-proposal-1475079939>. (b) Lavelle, M. Washington state voters reject nation's first carbon tax. Inside Climate News **2016**, <https://insideclimatenews.org/news/09112016/washington-state-carbon-tax-i-732-ballot-measure> (accessed Dec 12, 2017).
14. (a) Mestl, G.; Lesser, D.; Turek, T. Optimum performance of vanadyl pyrophosphate catalysts. *Top Catal.* **2016**, 59, 1533-1544. DOI: 10.1007/s11244-016-0673-0 (b) Dente, M.; Pierucci, S.; Tronconi, E.; Cecchini, M.; Ghelfi, F. Selective oxidation of *n*-butane to maleic anhydride in fluid bed reactors: detailed kinetic investigation and reactor modelling. *Chem. Eng. Sci.* **2003**, 58, 643-648.
15. Tachibana, Y.; Kimura, S.; Kasuya, K. Synthesis and verification of biobased terephthalic acid from furfural. *Sci. Rep.* **2015**, 5, 8249.
16. Chheda, J. N.; Weider, P. R.; Blackburn, R. L.; Lange, J. P. A. M. J. G. Process for preparing furfural from biomass. WO 2016025673, February 18, 2016.
17. Golden, J. S.; Handfield R.; Daystar, J.; McConnell, E. *An Economic Impact Analysis of the U.S. Biobased Products Industry: A Report to the Congress of the United States of America* U.S. Department of Agriculture's Biopreferred® program **2015**.
18. U.S. Department of Agriculture (USDA). Biopreferred Product: Product Packaging. <https://www.biopreferred.gov/BioPreferred/faces/catalog/Catalog.xhtml#> (accessed Mar 16, 2017).
19. (a) Harries, J. E.; Brindley, H. E.; Sagoo, P. J.; Bantges, R. J. Increases in greenhouse forcing inferred from the outgoing longwave radiation spectra of the Earth in 1970 and 1997. *Nature* **2001**, 410, 355-357. (b) Gao, L.; Bala, G.; Caldeira, K.; Nemani, R.; Ban-Weiss, G. Importance of carbon dioxide physiological forcing to future climate change. *Proc. Natl. Acad. Sci. U.S.A.* **2010**, 107, 9513-9518. DOI:10.1073/pnas.0913000107.

20. (a) Dzierzynska, A. “Good” and “bad” ozone-evaluation on the basis of plant reaction to ozone. *Chem. Diact. Ecol. Metrol.* **2012**, *17*, 97-112. DOI: 10.2478/cdem-2013-0009. (b) Department of Earth and Planetary Sciences, Harvard University. EPS 281 Great Papers in Earth Sciences. Part1: Oxidation and OH radicals. <https://courses.seas.harvard.edu/climate/eli/Courses/EPS281r/Sources/OH-reactivity/www.atmosphere.mpg.de-oxidation-and-OH-radicals.pdf> (accessed Mar 15, 2017). (c) Avino, P.; Manigrasso, M. Ozone formation in relation with combustion process in highly populated urban areas. *Environm. Sci.* **2015**, *2*, 764-781. (d) National Aeronautics and Space Administration (NASA). Chemistry in the Sunlight. [https://earthobservatory.nasa.gov/Features/ChemistrySunlight/chemistry\\_sunlight3.php](https://earthobservatory.nasa.gov/Features/ChemistrySunlight/chemistry_sunlight3.php) (accessed Mar 15, 2017) (e) Nilsson, E. J. K.; Andersen, V. F.; Skov, H.; Johnson, M. S. Pressure dependence of the deuterium isotope effect in the photolysis of formaldehyde by ultraviolet light. *Atoms. Chem. Phys.* **2010**, *10*, 3455-3463.
21. Allen, D. T.; Sullivan, D. W.; Zavala-Araiza, D.; Pacsi, A. P.; Harrison, M.; Keen, K.; Fraser, M. P.; Hill, D.; Lamb, B. K.; Sawyer, R. F. Methane emission from process equipment at natural gas production sites in the United States: liquid unloadings. *Environ. Sci. Technol.* **2015**, *49*, 641-648. DOI: 10.1021/es504016r.
22. (a) Hildenbrand, Z. L.; Carlton, D. D. Jr.; Fontenot, B. E.; Meik, J. M.; Walton, J. L.; Taylor, J. T.; Thacker, J. B.; Korlie, S.; Shelor, C. P.; Henderson, D.; Kadjo, A. F.; Roelke, C. E.; Hudak, P. F.; Burton, T.; Rifai, H. S.; Schug, K. A. A comprehensive analysis of ground water quality in the Barnett shale region. *Environ. Sci. Technol.* **2015**, *49*, 8254-8262. DOI: 10.1021/acs.est.5b01526. (b) Al-Bajalan, A. R. To what extent could shale gas “fracking” contaminate ground water. *J. Pet. Environ. Biotechnol.* **2015**, *6*, 236. DOI: 10.4172/2157-7643.1000236. (c) DiGiulio, D. C.; Wilkin, R. T.; Miller, C.; Oberley, G.; Investigation of Ground Water Contamination near Pavilion, Wyoming (draft Report); U.S. Environmental protection Agency, 2011. (d) Llewellyn, G. T.; Dorman, F.; Westland, J. L.; Yoxtheimer, D.; Grieve, P.; Sowers, T.; Humston-Fulmer, E. Evaluating a groundwater supply contamination incident attributed to Marcellus shale gas development. *Proc. Natl. Acad. Sci. USA* **2015**, *112*, 6325-6330. DOI: 10.1073/pnas.1420279112.
23. (a) Frohlich, C. Two-year survey comparing earthquake activity and injection-well locations in the Barnett shale, Texas. *P. Natl. Acad. Sci. U.S.A.* **2012**, *109*, 13934-13938. DOI: 10.1073/pnas.1207728109. (b) BC Oil & Gas Commission. Investigation of Observed Seismicity in the Horn River Basin. <https://www.bcogc.ca/node/8046/download> (downloaded Mar 30, 2017). (c) Yeck, W. L.; Hayes, G. P.; McNamara, D. E.; Rubinstein, J. L.; Barnhart, W. D.; Earle, P. S.; Benz, H. M. Oklahoma experiences largest earthquake during ongoing regional wastewater injection hazard mitigation efforts. *Geophys. Res. Lett.* **2017**, *44*, 711-717. DOI: 10.1002/2016GL071685.
24. Heipieper, H. J.; Martinez, P. M. Toxicity of Hydrocarbon to Microorganisms. Cellular Ecophysiology: Problem of Solventogenicity, Solvent Tolerance. In *Handbook of Hydrocarbon and Lipid Microbiology*, Timmis, K. N.; McGenity, T. J.; van der Meer, J. R.; de Lorenzo, V. Ed.; Springer-Verlag: Berlin Heidelberg, 2010; p1563-1573

25. Bercaw, J. E.; Hazari, N.; Labinger, J. A. Oxidative aromatization of olefins with dioxygen catalyzed by palladium trifluoroacetate. *J. Org. Chem.* **2008**, *73*, 8654-8657
26. (a) Ross, R. A.; Valentine, J. H. The dehydrogenation of cyclohexane vapor on silica-supported nickel catalysts. *J. Catal.* **1963**, *2*, 39-44. (b) Tetenyi, P.; Schachter, K. On the kinetics of the catalytic dehydrogenation of hydroaromatic compounds, VIII: The catalytic activity of metals in the dehydrogenation of cyclic hydrocarbon. *Acta Chim. Hung.* 1966, *50*, 129-144.
27. (a) Holderich, W. F.; Roberge, D. M. Dehydrogenation. In *Fine Chemicals Through Heterogeneous Catalysis*; Sheldon, R.A.; van Bekkum, H. Ed.; Wiley-VCH; Weinheim, 2001; pp427-437. (b) Sinfelt, J. H. Catalysis by metals: the P. H. Emmett award address. *Cataly. Rev.* **1974**, *9*, 147-168. (c) Johnson Matthey Catalysts. The Catalyst Technical Handbook. 2008.
28. Trost, B. M.; Metzner, P. J. Reaction of olefins with palladium trifluoroacetate. *J. Am. Chem. Soc.* **1980**, *102*, 3572-3577.
29. Smidt, J.; Hafner, W.; Jira, R.; Sieber, R.; Sedlmeier, J.; Sabel, A. The oxidation of olefins with palladium chloride catalysts. *Angew. Chem. Int. Edit.* **1962**, *1*, 80-88.
30. Iriuchijima, M. Study for manufacturing methyl ethyl ketone from *n*-butene by Wacker process (Part 2): Reaction of 1-butene with palladium chloride-cupric chloride aqueous solution at elevated temperature and Pressure *Sekiyu Gakkaishi* **1983**, *26*, 8-14
31. Sheldon, R. A.; Sobczak, J. M. Catalytic oxidative dehydrogenation of cyclohexene. *J. Mol. Catal.* **1991**, *68*, 1-6
32. Nishimura, T.; Uemura, S. Novel palladium catalytic systems for organic transformations. *Synlett* **2004**, 201-216.
33. Stoltz, B. M. Palladium catalyzed aerobic dehydrogenation: from alcohols to indoles and asymmetric catalysis. *Chem. Lett.* **2004**, *33*, 362-367.
34. Sigman, M. S.; Schultz, M. J. The renaissance of palladium(II)-catalyzed oxidation chemistry. *Org. Biomol. Chem.* **2004**, *2*, 2551-2554.
35. Toyota, M.; Ihara, M. Development of palladium-catalyzed cycloalkenylation and its application to natural product synthesis. *Synlett* **2002**, 1211-1222.
36. Pun, D.; Diao, T.; Stahl, S. S. Aerobic dehydrogenation of cyclohexanone to phenol catalyzed by Pd(TFA)<sub>2</sub> / 2-dimethylaminopyridine: evidence for the role of Pd nanoparticles. *J. Am. Chem. Soc.* **2013**, *135*, 8213-8221. DOI: 10.1021/ja403165u.
37. Izawa, Y.; Pun, D.; Stahl, S. S. Palladium-catalyzed aerobic dehydrogenation of substituted cyclohexanones to phenols. *Science* **2011**, *333*, 209-213. DOI: 10.1126/science.1204183.

38. Diao, T.; Stahl, S. S. Synthesis of cyclic enones via direct palladium-catalyzed aerobic dehydrogenation of ketones. *J. Am. Chem. Soc.* **2011**, *133*, 14566-14569. DOI: 10.1021/ja206575j.
39. Izawa, Y.; Zheng, C.; Stahl, S. S. Aerobic oxidative Heck / dehydrogenation reaction of cyclohexanones: efficient access to *meta*-substituted phenols. *Angew. Chem. Int. Ed.* **2013**, *52*, 3672-3675. DOI: 10.1002/anie.201209457.
40. Iosub, A. V.; Stahl, S. S. Palladium-catalyzed aerobic oxidative dehydrogenation of cyclohexenes to substituted arene derivatives. *J. Am. Chem. Soc.* **2015**, *137*, 3454-3457. DOI: 10.1021/ja512770u.

## CHAPTER TWO

### Synthesis of Biobased *p*-Hydroxybenzoic Acid

#### 1. Introduction

*p*-Hydroxybenzoic acid is used in the manufacture of liquid crystalline polymers (LCPs). The first LCP developed and commercialized in 1955 was poly(*p*-hydroxybenzoic acid).<sup>1</sup> This polymer was insoluble in standard organic solvents and possessed a high melting temperature (350 °C). These properties allow *p*-hydroxybenzoic acid to be used for many useful applications but also cause difficulty in processing.<sup>1</sup> In order to alleviate processing challenges, various comonomers are employed, such as *m*-hydroxybenzoic acid, 6-hydroxynaphthoic acid, isophthalic acid, terephthalic acid, hydroquinone, bisphenol, 1,4-naphthalene dicarboxylic acid, 1,5-naphthalene dicarboxylic acid and 2,6-naphthalene dicarboxylic acid.<sup>2</sup> Though the presence of comonomers in the crystal lattice lowers the melting temperature of LCPs, the polymer as a whole is nonetheless heat resistant. A physical term, coefficient of thermal expansion, describes how much a material expands when it is heated. The expansion coefficient of some LCPs are comparable to the expansion coefficient of glass, steel, ceramic and glass fiber/epoxy materials. LCPs, which are used in the construction of circuit boards,<sup>3</sup> have a low expansion coefficient. This is very desirable for electronic device casings, connectors and other parts. LCP use also addresses the demand to reduce chip size and weight. The physical strength and thermostability of LCPs require less thickness to hold components of the circuit board than glass fiber/epoxy resin.<sup>4b</sup> Therefore, the use of LCPs has increased quickly over time in electronic devices such as circuit boards, semiconductors and liquid crystal displays.<sup>4</sup> Applications extend beyond electronic devices. LCPs' high melting temperature allows them to form nonstick bakewares.<sup>5</sup> LCPs are also quite strong and are being used to create cut-resistant yarns, which can be

manufactured into a material for lightweight garments that protect against sharps object and knives.<sup>6</sup>

Esterified *p*-hydroxybenzoic acids (parabens) are widely used as preservatives in cosmetics, creams, and oral aqueous medicines such as cough syrup and some intravenous medicines. The most widely marketed parabens are: methylparaben, ethylparaben, propylparaben and butylparaben. Different esters of parabens lead to different solubilities and different antimicrobial activities.<sup>7</sup> Parabens have also been shown to bind to human estrogen receptors.<sup>7b</sup> However, the affinities of parabens to the estrogen receptors are  $10^4$  to  $10^6$  times less than estradiol.<sup>7c</sup> Methyl and ethylparaben have lower in vitro and in vivo estrogenic activity than butyl or propylparaben.<sup>7b</sup> Even though there are concerns about the possible role of parabens in decreased sperm viability and incidence of breast cancer, current data does not support these concerns.<sup>7c</sup>

*p*-Hydroxybenzoic acid (\$5.40/kg) is more expensive than other monomers such as terephthalic acid (\$0.73/kg).<sup>8</sup> Global LCP production was estimated at  $58.7 \times 10^6$  kg/yr with a market size of \$950 million in 2016. The market size of LCPs has been increasing every year based on data between 2012 and 2015.<sup>9</sup> Grand View Research reported the revenue from parabens in the global cosmetic preservative market was valued at only \$33 million in 2015.<sup>10</sup>

## **2. *p*-Hydroxybenzoic Acid Production**

In 1860, Kolbe discovered that the reaction of sodium phenoxide with carbon dioxide could produce salicylic acid (*o*-hydroxybenzoic acid).<sup>11</sup> He later filed a patent in which the selectivity of the reaction could be altered to *p*-hydroxybenzoic acid by using potassium hydroxide instead of sodium hydroxide.<sup>12</sup> The selectivity of *p*-hydroxybenzoic acid increases

with an increasing ionic radius of the alkali metal (Figure 2.1).<sup>13</sup> The carboxylation of metal phenoxide salts was improved by Kolbe himself in 1875 then by Schmitt in 1885.<sup>14</sup> This Kolbe-Schmitt reaction is still the basis for manufacture of hydroxybenzoic acids.

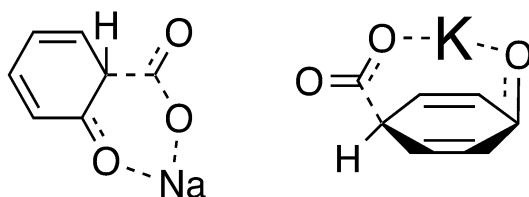
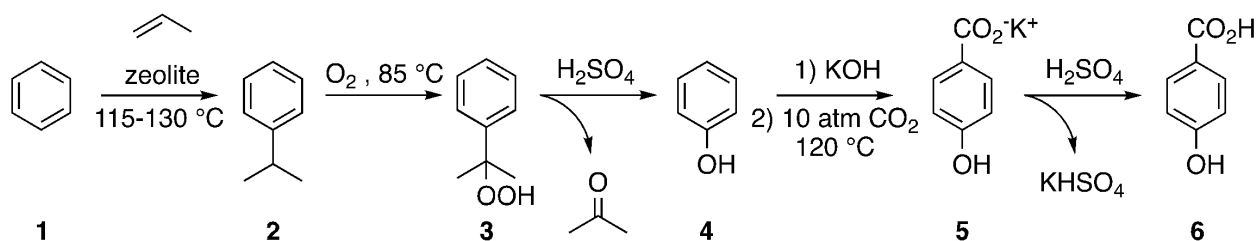


Figure 2.1. *ortho*- and *para*-intermediate

*p*-Hydroxybenzoic acid **6** is currently manufactured from benzene **1** (Scheme 1). Benzene **1** is transformed to cumene **2** by the acid-catalyzed reaction of benzene **1** and propylene. Currently, zeolites are employed as the acid catalysts.<sup>15</sup> In 1944, Hock reported the synthesis of phenol **4** and acetone from cumene **2**. Cumene **2** is first oxidized by molecular oxygen to cumene hydroperoxide **3**, which is then cleaved to phenol **4** and acetone by a Brønsted acid.<sup>16</sup> After World War II, the Hock process became the standard commercial method to manufacture phenol **4** and acetone.<sup>17</sup> In the Kolbe-Schmitt reaction, potassium phenolate, which results from deprotonation of phenol **4** using KOH, is reacted at 120 °C with carbon dioxide at 10 atm pressure. The potassium *p*-hydroxybenzoate **5** is neutralized with H<sub>2</sub>SO<sub>4</sub> which produces a stoichiometric amount of potassium salt byproduct, KHSO<sub>4</sub>.<sup>13</sup>

Scheme 2.1. *p*-Hydroxybenzoic Acid Production from Benzene



It is not difficult to obtain the starting materials required for the manufacture of *p*-hydroxybenzoic acid thanks to many years of process development. Benzene and propylene are produced from petroleum and natural gas/shale gas (Chapter 1). Potassium hydroxide is manufactured by potassium chloride electrolysis. In the United States, potassium chloride is obtained from the Great Salt Lake Desert in Utah and subterranean brines of Searles Lake in California.<sup>18</sup> Carbon dioxide is recovered as a byproduct of ammonia and hydrogen production.<sup>19</sup> Sulfuric acid is manufactured from either pyrites (FeS<sub>2</sub>) or elemental sulfur. Combustion of elemental sulfur or heating pyrites produces sulfur dioxide gas which is oxidized to sulfur trioxide gas by a vanadium oxide catalyst (V<sub>2</sub>O<sub>5</sub>).<sup>20a,b</sup> Reaction of sulfur trioxide with water leads to sulfuric acid. In the United States, 80% of sulfuric acid is produced from elemental sulfur combustion which produces electrical power in addition to sulfuric acid.<sup>20c</sup> Most mining of elemental sulfur in North America is localized near the Gulf of Mexico and spans a region extending through parts of Mexico, Texas and Louisiana.<sup>20d,e</sup> Therefore, raw materials for *p*-hydroxybenzoic acid production are readily available. There are some significant concerns with current manufacture of *p*-hydroxybenzoic acid, which include occupational hazards from exposure to carcinogenic benzene and toxic phenol.

### 3. Toxicity of Benzene and Phenol

Benzene causes acute myeloid leukemia,<sup>21a-g</sup> hematotoxicity (decrease in blood cells counts)<sup>21d,e,g</sup> and is suspected of causing non-Hodgkin lymphoma.<sup>21b,j,k</sup> The permissible occupational exposure limit to benzene in the U.S. is 1 part per million (8h time-weighted average) and actual occupational exposure levels are typically below the limit.<sup>21a,e</sup> However, benzene still causes hematotoxicity in workers exposed to below 1 part per million.<sup>21a,e</sup> Some individuals are more susceptible to benzene toxicity than the other.<sup>21e</sup> Single-nucleotide polymorphisms in the genes encoding cytochrome-P450, myeloperoxidase and quinone oxidoreductase were observed in those more susceptible to benzene toxicity than the other.<sup>21e</sup> The various metabolites of benzene are thought to be critical factors in benzene toxicity (Scheme 2.2).<sup>21a-d,f</sup> Benzene **1** is metabolized in the liver and lungs.<sup>21a</sup> Some of those metabolites are excreted<sup>21i</sup> while others are metabolized further in the bone marrow.<sup>21a</sup> Benzene is oxidized to benzene oxide **7** by cytochrome-P450 that exists in equilibrium with its tautomer, oxepin **9**.<sup>21a</sup> The majority of benzene oxide **7** rearranges to phenol **4** spontaneously.<sup>21a</sup> The remainder is converted to catechol, *trans,trans*-muconaldehyde **10** or *S*-phenylmercapturic acid **8**.<sup>21a</sup> Phenol **4** is either excreted<sup>21i</sup> or metabolized to 1,4-hydroquinone **12**.<sup>21a</sup> 1,4-Hydroquinone **12** is converted to either the reactive metabolite 1,2,4-benzenetriol **18** in the liver / lungs or to another reactive metabolite 1,4-benzoquinone **14**.<sup>21a</sup> Metabolism of oxepin **9** produces the reactive *trans,trans*-muconaldehyde **10**.<sup>21a,b,d,f</sup> Because benzene oxide **7**, 1,4-benzoquinone **14** and *trans,trans*-muconaldehyde **10** are electrophiles, they can react with peptides and proteins easily and interfere with cellular function.<sup>21a,b,d,f,h</sup> The reactive oxygen species (ROS) **19** produced from the metabolites by peroxidases in the bone marrow can bind to cellular macromolecules and also generate oxygen radicals.<sup>21a,f</sup> The formation of 1,4-benzoquinone **14** in the bone marrow by



The Occupational Safety and Health Administration (OSHA) set the occupational exposure limit to phenol at 5 parts per million (8h time-weighted average).<sup>22</sup> Most of the severe health problems from phenol exposure occur due to skin contact with phenol. Phenol is absorbed through the skin rapidly and taken into blood stream. Though most of absorbed phenol will be excreted in the urine, skin contact with large quantity of phenol can be lethal. A case wherein 25% of an individual's skin was exposed to liquid phenol resulted in a rapid death within 10 minutes.<sup>22</sup> This was one of several rapid death cases caused by dermal exposure to phenol. The causes of death were respiratory depression, cardiac arrest and renal failure.<sup>22</sup> Chronic dermal exposure to small quantities of phenol also causes health problems, such as cardiac arrhythmias, muscle pain, enlarged and tender liver, kidney damage, emaciation, skin inflammation and necrosis.<sup>22</sup> The mechanisms of toxicity of phenol are unknown, although phenol is metabolized via the same pathway responsible for benzene metabolism. Phenol has not been found to cause hematotoxicity or leukemia.<sup>22</sup>

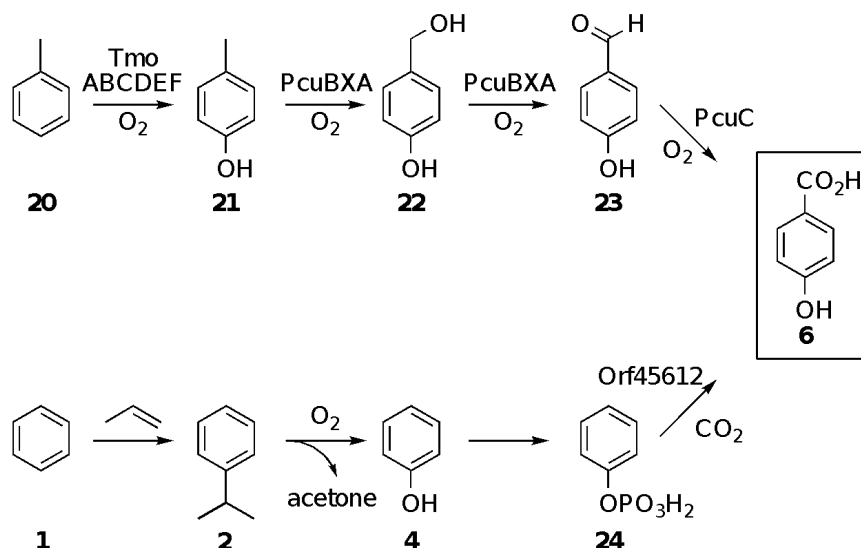
#### 4. Biocatalytic Routes to *p*-Hydroxybenzoic Acid

Biocatalytic synthesis of *p*-hydroxybenzoic acid has been attempted as an alternative to the Kolbe-Schmitt synthesis. One approach used the microbial oxidation of toluene **20** to *p*-hydroxybenzoic acid **6** (Scheme 2.3). Various *Pseudomonas putida* hosts have been engineered to heterologously express *tmoABCDEF*-encoded toluene monooxygenase from *Pseudomonas mendocina* KR1.<sup>23</sup> The toluene 4-monooxygenase catalyzes the conversion of toluene **20** into *p*-cresol **21**, which is converted in three steps by *pcu* genes to *p*-hydroxybenzoic acid **6** (Scheme 2.3).<sup>23</sup> An advantage to this approach is that substrate, toluene **20** is not toxic. However, the rates to convert toluene **20** to *p*-hydroxybenzoic acid **6** are slow and the titer of *p*-

hydroxybenzoic acid in the culture medium is low (2 g/L).<sup>23</sup> Also the low solubility of toluene in water would become a problem in large scale fermentation.

Phenylphosphate carboxylase from the strict anaerobe *Thauera aromatica* has been used to convert phenylphosphate **24** into *p*-hydroxybenzoic acid **6** (Scheme 2.3).<sup>24a-d</sup> A partially purified oxygen sensitive enzyme, phenylphosphate carboxylase has been used for this conversion.<sup>24a-d</sup> This route cannot avoid use of benzene **1** and phenol **4**. It also requires phenol **4** to be phosphorylated to phenylphosphate **24** prior to carboxylation. There was one report of in vitro phenol phosphorylation with enzymes isolated from *Shigella flexneri*.<sup>24e</sup> Genetic engineering of *Thauera aromatica* has not progressed to the point where conversion of phenol **4** to *p*-hydroxybenzoic acid **6** has been achieved.

Scheme 2.3. Biocatalytic Routes to *p*-Hydroxybenzoic Acid



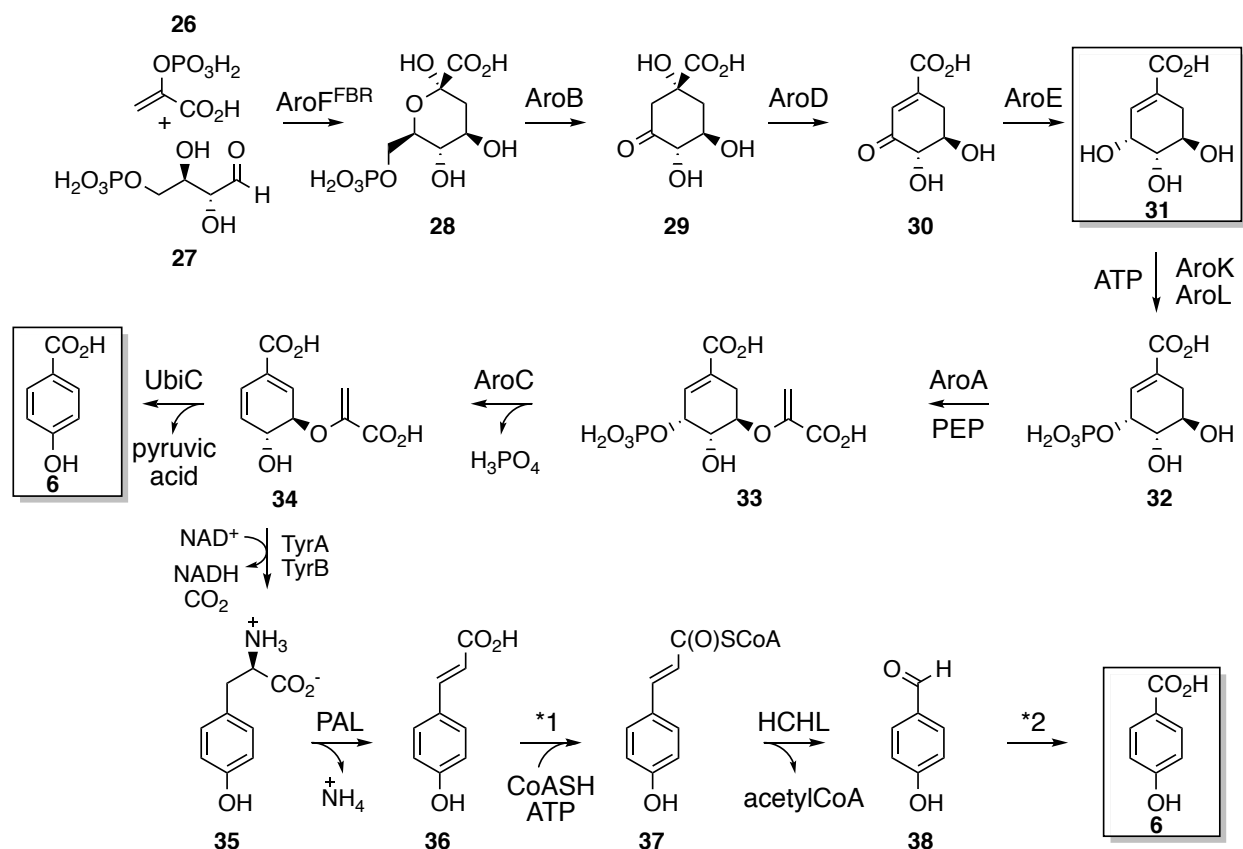
TmoABCDEF: toluene 4-monooxygenase; PcuBXA: *p*-cresol utilization gene; PcuC: *p*-hydroxybenzaldehyde dehydrogenase

Microbe-catalyzed conversion of glucose into *p*-hydroxybenzoic acid (Scheme 2.4) has the advantage of using nontoxic, renewable glucose as a starting material.<sup>25</sup> Carbon flow is

directed into and through the common pathway of aromatic amino acid biosynthesis to chorismic acid (Scheme 4, **26/27** to **34**).<sup>25</sup> Chorismate lyase encoded by *ubiC* in *E. coli* then catalyzes the conversion of chorismic acid **34** into *p*-hydroxybenzoic acid **6** with pyruvic acid formed as the byproduct (Scheme 2.4).<sup>25</sup> Numerous strategies have been developed for directing carbon flow into chorismic acid **34**. However, *ubiC*-encoded chorismate lyase is a problematic enzyme having a very low turnover of about 1 sec<sup>-1</sup> and inhibited by the *p*-hydroxybenzoic acid **6** produced with an inhibition constant ( $K_i$ ) of 2.1  $\mu\text{M}$ .<sup>25c</sup> For comparison, the chorismate lyase  $K_m$  for substrate chorismic acid **34** is 29  $\mu\text{M}$ .<sup>25c</sup>

The toxicity of *p*-hydroxybenzoic acid synthesized from glucose towards microbes has been reduced with resin-based extraction.<sup>26</sup> During microbial synthesis of *p*-hydroxybenzoic acid under fermentor-controlled conditions, culture broth is continuously passed through an anion exchange resin,<sup>26</sup> which is a polystyrene support functionalized with quaternary amine groups.<sup>27</sup> Phenolics such as *p*-hydroxybenzoic acid bind to the resin and are removed from the fermentation broth. Resin-based extraction increases the titers of microbially synthesized, resin-bound *p*-hydroxybenzoic acid by a factor of about fourfold over the concentration of *p*-hydroxybenzoic acid synthesized in lieu of resin based extraction.<sup>26</sup> The total *p*-hydroxybenzoic acid afforded was equivalent to a titer of 23 g/L.<sup>26</sup>

Scheme 2.4. Biocatalytic Routes to *p*-Hydroxybenzoic Acid



PEP: phosphoenolpyruvate; E4P: D-erythrose 4-phosphate; DAHP: 3-deoxy-D-*arabino*-heptulosonate 7-phosphate; DHQ: 3-dehydroquinic acid; DHS: 3-dehydroshikimic acid; AroF<sup>FBR</sup>: DAHP synthase; AroB: DHQ synthase; AroD: DHQ dehydratase; AroE: shikimate dehydrogenase; AroK: shikimate kinase I; AroL: shikimate kinase II; AroA: 5-enolpyruvylshikimate 3-phosphate synthase; AroC: chorismate synthase; UbiC: chorismate lyase; TyrA: chorismate mutase-prephenate dehydrogenase; TyrB: tyrosine aminotransferase; PAL: phenylalanine ammonia lyase; \*1: *p*-coumaroyl-CoA synthetase; HCHL: 4-hydroxycinnamoyl-CoA hydratase/lyase; \*2: *p*-hydroxybenzaldehyde dehydrogenase

An alternative microbial synthesis of *p*-hydroxybenzoic acid **5** has been created in *Pseudomonas putida* S12 where either glucose or glycerol was converted into tyrosine **35**<sup>28</sup> followed by phenylalanine ammonia lyase-catalyzed conversion of tyrosine into *p*-coumaric acid **36** (Scheme 2.4).<sup>29</sup> A series of enzymes native to *Pseudomonas putida* S12 including *p*-coumaroyl-CoA synthetase, 4-hydroxycinnamoyl-CoA hydratase/lyase and *p*-hydroxybenzaldehyde dehydrogenase catalyzed the conversion of *p*-coumaric acid **36** into *p*-hydroxybenzoic acid **6** (Scheme 2.4). Native *p*-hydroxybenzoate hydroxylase was inactivated to

prevent catabolism of product *p*-hydroxybenzoic acid **6** in *Pseudomonas putida* S12.<sup>29</sup> This combination of anabolism and catabolism avoids the challenges inherent in employing chorismate lyase in microbial synthesis of *p*-hydroxybenzoic acid **6** from glucose (Scheme 2.4). The yields of *p*-hydroxybenzoic acid obtained were competitive with the yields of *p*-hydroxybenzoic acid microbially synthesized from glucose via chorismate lyase in lieu of resin-based extraction. However, the yield is too low (16 %) to be suitable for commercial production.<sup>29b</sup>

Synthesis of *p*-hydroxybenzoic acid in transgenic plants has also been accomplished. Expression of either *E. coli* *ubiC*-encoded chorismate lyase (Scheme 2.4) and *Pseudomonas fluorescens hchl*-encoded 4-hydroxycinnamoyl-CoA hydratase/lyase (Scheme 2.4) in tobacco (*Nicotiana tabacum*)<sup>30-32</sup> and sugar cane (*Saccharum* hybrids)<sup>33</sup> has led to formation of glucosylated *p*-hydroxybenzoic acid. The majority of the glucosylated *p*-hydroxybenzoic acid is conjugated as an ether through the C-4 phenolic oxygen while the remainder is conjugated as an ester at the C-1 carboxylate.<sup>30-32</sup> This glucosylation with subsequent accumulation of the conjugated *p*-hydroxybenzoic acid in vacuoles is essential to the successful management of *p*-hydroxybenzoic acid's toxicity in plants. An additional critical role of glucosylation is the elimination of *p*-hydroxybenzoic acid's severe feedback inhibition of *ubiC*-encoded chorismate lyase activity.

Nuclear transformation with chloroplast-targeted *ubiC* and *hchl* has dominated approaches to achieving synthesis of glucosylated *p*-hydroxybenzoic acid in plants.<sup>30,31,33</sup> However, the highest levels of glucosylated *p*-hydroxybenzoic acid in plant leaves has been achieved with integration of *ubiC* into the chloroplast genome.<sup>32</sup> Nuclear transformation of *ubiC* led to phenotypically healthy tobacco plants, which accumulated glucosylated *p*-hydroxybenzoic

acid to 0.52 dry wt% in leaves.<sup>30</sup> This corresponds to 0.24 dry wt% of *p*-hydroxybenzoic acid after correcting for the mass of the glucose conjugate. Nuclear transformation of tobacco with *hchl* gave phenotypically unhealthy tobacco plants accumulating 1.3 dry wt% glucosylated *p*-hydroxybenzoic acid in leaves corresponding to approximately 0.61% dry wt% of *p*-hydroxybenzoic acid.<sup>31</sup> In sugar cane, nuclear transformation with *ubiC* yielded plants that accumulate a mean value of 0.41 dry wt% glucosylated *p*-hydroxybenzoic acid (0.19 dry wt% equivalent of *p*-hydroxybenzoic acid).<sup>33</sup> Nuclear transformation of sugarcane with *hchl* led to plants that accumulate a mean value of 0.7 dry wt% glucosylated *p*-hydroxybenzoic acid (0.32 dry wt% equivalent of *p*-hydroxybenzoic acid).<sup>33</sup> Integration of *ubiC* into the tobacco chloroplast genome afforded phenotypically healthy plants accumulating a mean value of 14 dry wt% glucosylated *p*-hydroxybenzoic acid (6.6 dry wt% equivalent of *p*-hydroxybenzoic acid).<sup>32</sup>

In 1892, Eykman reported dehydration of shikimic acid **31** to form *p*-hydroxybenzoic acid **5**.<sup>34</sup> This reaction has been revisited recently with a report of the formation of *p*-hydroxybenzoic acid and *m*-hydroxybenzoic acid in 40% and 13% yields, respectively by refluxing in 12 M HCl for 14 h.<sup>35</sup> Heating shikimic acid at 120 °C with 1 M H<sub>2</sub>SO<sub>4</sub> in acetic acid solution for 16 h led to a 57% yield of *p*-hydroxybenzoic acid and a 9% yield of *m*-hydroxybenzoic acid.<sup>35</sup> Although all of the shikimic acid was consumed in these reactions, mass accountability was poor.<sup>35</sup> Significant quantities of an uncharacterized black precipitate were formed in addition to the *p*-hydroxybenzoic acid and *m*-hydroxybenzoic acid.<sup>35</sup>

An appealing advantage of synthesizing *p*-hydroxybenzoic acid from shikimic acid follows from commercial sourcing of shikimic acid from select plants or microbial synthesis of shikimic acid from glucose. These sources of shikimic acid were identified during commercialization of the anti-influenza drug Tamiflu<sup>®</sup>,<sup>36</sup> which is synthesized from shikimic

acid. Commercially, shikimic acid is obtained from the star fruit and leaves of *Illicium verum*<sup>36</sup> in China and Vietnam,<sup>37</sup> and microbial synthesis from glucose under fermentor-controlled conditions.<sup>38</sup> A number of plants other than *Illicium verum* have been reported to produce significant concentrations of shikimic acid.<sup>39</sup> The shikimic acid is found in unconjugated, free-acid form in plant tissue.<sup>39b</sup>

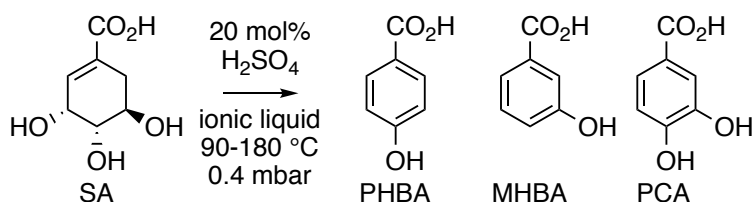
In this chapter, various ionic liquids are explored as solvent and co-catalyst for the synthesis of *p*-hydroxybenzoic acid by acid-catalyzed dehydration of shikimic acid. Chemical dehydration of nontoxic shikimic acid for synthesis of *p*-hydroxybenzoic acid allows us to avoid use of toxic phenol derived from carcinogenic benzene and the large salt wastes streams from Kolbe-Schmitt synthesis.

## 5. Results

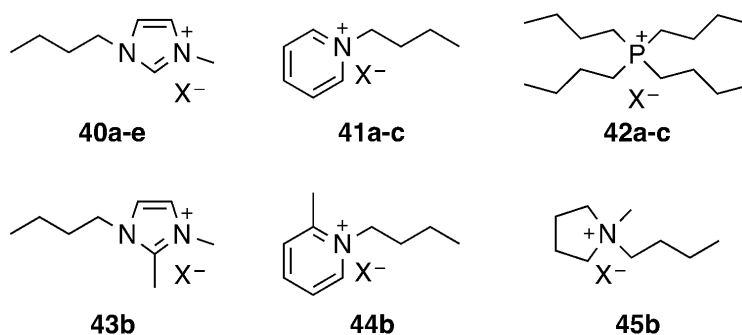
### 5.1. Conversion of Shikimic Acid to *p*-Hydroxybenzoic Acid in Ionic Liquid Bromides

Unlike earlier reported dehydrations of shikimic acid,<sup>34,35</sup> acid-catalyzed dehydration of shikimic acid using a number of different ionic liquid bromides has been discovered to undergo essentially quantitative conversion to a mixture of *p*-hydroxybenzoic acid and *m*-hydroxybenzoic acid. The earlier reported acid-catalyzed dehydrations of shikimic acid in acetic acid yielded 57% of *p*-hydroxybenzoic acid and 9% of *m*-hydroxybenzoic acid.<sup>35</sup> Typical reaction conditions involved heating a 20 weight percent (wt%) solution of shikimic acid in ionic liquid bromide at its melting point under reduced pressure (0.4 mbar) with 20 mol % H<sub>2</sub>SO<sub>4</sub> (Scheme 2.5). The vacuum was employed to remove water byproduct.

Scheme 2.5. Shikimic Acid Dehydration in Ionic Liquid



Scheme 2.6. Ionic Liquids Used in Shikimic Acid Dehydrations



The ionic liquid bromides that were examined included: 1-butyl-3-methylimidazolium bromide **40b** (Table 2.1, entry 2), 1-butylpyridinium bromide **41b** (Table 2.4, entry 2), tetrabutylphosphonium bromide **42b** (Table 2.4, entry 5), 1-butyl-2,3-dimethylimidazolium

bromide **43b** (Table 2.4, entry 7), 1-butyl-2-methylpyridinium bromide **44b** (Table 2.4, entry 8), and 1-butyl-1-methylpyrrolidinium bromide **45b** (Table 2.4, entry 9).

Table 2.1. Dehydration of Shikimic Acid in Various 1-Butyl-3-methylimidazolium Salts **40a-40e**

Entry	Ionic Liquid	Temp	Time	% Yield			% SA <sup>4</sup>
				PHBA <sup>1</sup>	MHBA <sup>2</sup>	PCA <sup>3</sup>	
1	<b>40a</b> X=Cl	90 °C	13 h	1	0	0	78
2	<b>40b</b> X=Br	90 °C	13 h	76	19	0	1
3	<b>40c</b> X=I	90 °C	13 h	1	0	1	79
4	<b>40d</b> X=HSO <sub>4</sub>	90 °C	13 h	3	0	0	2
5	<b>40e</b> X=BF <sub>4</sub>	90 °C	13 h	9	0	0	38

<sup>1</sup> PHBA=*p*-hydroxybenzoic acid; <sup>2</sup> MHBA=*m*-hydroxybenzoic acid; <sup>3</sup> PCA=protocatechuic acid  
<sup>4</sup>% SA=percent remaining shikimic acid.

Table 2.2. Impact of Shikimic Acid Concentration in 1-Butyl-3-methylimidazolium bromide **40b** on Dehydration Yield and Accountability of Shikimic Acid Consumption

Entry	IL <sup>1</sup>	[SA] <sup>2</sup>	Temp	Time	% Yield		% SA <sup>5</sup>
					PHBA <sup>3</sup>	MHBA <sup>4</sup>	
1	<b>40b</b>	20 wt %	90 °C	13 h	76	19	1
2	<b>40b</b>	40 wt %	90 °C	13 h	73	17	0
3	<b>40b</b>	50 wt %	90 °C	13 h	70	16	0
4	<b>40b</b>	60 wt %	90 °C	13 h	62	13	6

<sup>1</sup> IL=ionic liquid; <sup>2</sup> [SA]=shikimic acid concentration in IL; <sup>3</sup> PHBA=*p*-hydroxybenzoic acid;  
<sup>4</sup> MHBA=*m*-hydroxybenzoic acid; <sup>5</sup> % SA=percent remaining shikimic acid

Acid-catalyzed dehydrations in various ionic liquid bromides afforded differing yields of *p*-hydroxybenzoic acid and ratios of *p*-hydroxybenzoic acid to *m*-hydroxybenzoic acid formed with a range of 2:1 to 4:1. Furthermore, the mass balance and reaction selectivity favoring *p*-hydroxybenzoic acid and *m*-hydroxybenzoic acid varied as a function of the ionic liquid employed. 1-Butyl-3-methylimidazolium bromide **40b** (Table 2.1, entry 2) gave the highest yields for acid-catalyzed formation of *p*-hydroxybenzoic acid.

The highest weight percent of shikimic acid that could be dehydrated without a reduction in percent yield of *p*-hydroxybenzoic acid was also a consideration given the expense of ionic liquids relative to more traditional organic solvents. With 1-butyl-3-methylimidazolium bromide **40b** as solvent, the wt% of shikimic acid could be increased from 20 wt% to 40 wt% without

significant diminution in the yield of *p*-hydroxybenzoic acid, the ratio of *p*-hydroxybenzoic acid to *m*-hydroxybenzoic acid formed or the nearly quantitative conversion of shikimic acid to these two dehydration products (Table 2.2, entry 2 vs. entry 1). Increasing the concentration of shikimic acid to 50 wt% relative to 1-butyl-3-methylimidazolium bromide **40b** resulted in a 10% reduction in the combined formation of *p*-hydroxybenzoic acid and *m*-hydroxybenzoic acid (Table 2.2, entry 1 vs. 3). Increasing the concentration of shikimic acid to 60 wt% relative to 1-butyl-3-methylimidazolium bromide **40b** resulted in significant reductions in the yield of *p*-hydroxybenzoic acid and the mass balance (Table 2.2, entry 1 vs. entry 4). The wt% of shikimic acid was kept at 20 wt% during evaluation of all other ionic liquids as solvents for acid-catalyzed dehydration of shikimic acid.

Recycling the ionic liquid helps to avoid costly waste of these relatively expensive solvents. Fresh 1-butyl-3-methylimidazolium bromide **40b** was synthesized *in situ* from 1-methylimidazole and 1-bromobutane. Shikimic acid 40 wt% (12 g) in 1-butyl-3-methylimidazolium bromide **40b** (30 g) was heated at 90 °C under reduced pressure (0.4 mbar) with 20 mol % H<sub>2</sub>SO<sub>4</sub> for 24 h. After addition of water to the reaction crude, *p*-hydroxybenzoic acid and *m*-hydroxybenzoic acid were extracted into EtOAc. This initial run gave an 80% yield of *p*-hydroxybenzoic acid and an 18% yield of *m*-hydroxybenzoic acid (Table 2.3, entry 1). The aqueous layer was concentrated and dried under reduced pressure and then used as the 1-butyl-3-methylimidazolium bromide **40b** for a second dehydration of shikimic acid using the same ionic liquid used for the first dehydration. This second dehydration using recycled 1-butyl-3-methylimidazolium bromide **40b** afforded a 77% yield of *p*-hydroxybenzoic acid and a 16% yield of *m*-hydroxybenzoic acid with 2% of unreacted shikimic acid (Table 2.3, entry 2). The viscosity of this reaction solution was significantly higher than first reaction, and the magnetic

stir bar was barely stirring the solution. After addition of water to the reaction crude, *p*-hydroxybenzoic acid and *m*-hydroxybenzoic acid were extracted into EtOAc. The aqueous layer was treated with activated carbon, and then concentrated and dried under reduced pressure. This activated carbon-treated 1-butyl-3-methylimidazolium bromide **40b** was used for a third dehydration of shikimic acid. This third dehydration afforded a 72% yield of *p*-hydroxybenzoic acid and a 11% yield of *m*-hydroxybenzoic acid (Table 2.3, entry 3). In the second reaction, the ionic liquid performed nearly as well as the first reaction. In the third reaction, the ionic liquid showed a significant reduction in the yield of *p*-hydroxybenzoic acid and *m*-hydroxybenzoic acid with poor mass balance. Bromide is known to be oxidized by H<sub>2</sub>SO<sub>4</sub> forming Br<sub>2</sub> and SO<sub>2</sub> when H<sub>2</sub>SO<sub>4</sub> is used as the solvent.<sup>40</sup> For the second and third dehydration reactions, 20 mol% H<sub>2</sub>SO<sub>4</sub> was added each time. This suggests a possible redox between bromide and H<sub>2</sub>SO<sub>4</sub> in the ionic liquid. The reduction of the recycled ionic liquid performance could be due to a loss of bromide.

Table 2.3. 1-Butyl-3-methylimidazolium Bromide **40b** Recycle

Entry	IL <sup>1</sup>		% Yield		% SA <sup>5</sup>
			PHBA <sup>3</sup>	MHBA <sup>4</sup>	
1	<b>40b</b>	First Dehydration	80	18	0
2	<b>40b</b>	Second Dehydration	77	16	2
3	<b>40b</b>	Third Dehydration	72	11	0

<sup>1</sup> IL=ionic liquid; <sup>2</sup> [SA]=shikimic acid concentration in IL; <sup>3</sup> PHBA=*p*-hydroxybenzoic acid;

<sup>4</sup> MHBA=*m*-hydroxybenzoic acid; <sup>5</sup> % SA=percent remaining shikimic acid

Dehydration of shikimic acid in 1-butylpyridinium bromide **41b** gave a 62% yield of *p*-hydroxybenzoic acid. Of the shikimic acid consumed 77% could be accounted for in the formation of *p*-hydroxybenzoic acid and *m*-hydroxybenzoic acid (Table 2.4, entry 2). As with the 1-butyl-3-methylimidazolium halides **40a-c**, dehydration of shikimic acid in 1-butylpyridinium bromide **41b** gave a much larger yield of *p*-hydroxybenzoic acid relative the corresponding dehydration yields in 1-butylpyridinium chloride **41a** and 1-butylpyridinium iodide **41c** (Table 2.4, entry 1 and

3). 1-Butylpyridinium salts **41** reactions were run at 140 °C, which was the melting temperature of 1-Butylpyridinium chloride **41a**.

Table 2.4. Dehydration of Shikimic Acid in Various Ionic Liquids **41-45**.

Entry	Ionic Liquid	Temp	Time	% Yield			% SA <sup>4</sup>	
				PHBA <sup>1</sup>	MHBA <sup>2</sup>	PCA <sup>3</sup>		
1	<b>41a</b>	X=Cl	140 °C <sup>5</sup>	13 h	8	7	0	58
2	<b>41b</b>	X=Br	140 °C <sup>5</sup>	13 h	62	15	0	0
3	<b>41c</b>	X=I	140 °C <sup>5</sup>	13 h	15	3	0	29
4	<b>42a</b>	X=Cl	110 °C <sup>6</sup>	13 h	0	0	0	80
5	<b>42b</b>	X=Br	110 °C <sup>6</sup>	13 h	44	23	0	0
6	<b>42c</b>	X=I	110 °C <sup>6</sup>	13 h	0	0	8	82
7	<b>43b</b>	X=Br	110 °C <sup>7</sup>	13 h	66	19	0	0
8	<b>44b</b>	X=Br	160 °C <sup>8</sup>	13 h	54	16	0	0
9	<b>45b</b>	X=Br	180 °C <sup>9</sup>	13 h	35	10	0	0

<sup>1</sup> PHBA=*p*-hydroxybenzoic acid; <sup>2</sup> MHBA=*m*-hydroxybenzoic acid; <sup>3</sup> PCA=protocatechuic acid; <sup>4</sup> % SA=percent remaining shikimic acid, <sup>5</sup>140 °C was the melting temperature of **41a**, <sup>6</sup>110 °C was the melting temperature of **42c**, <sup>7</sup>110 °C was the melting temperature of **43b**, <sup>8</sup>160 °C was the melting temperature of **44b**, <sup>9</sup>180 °C was the melting temperature of **45b**.

Tetrabutylphosphonium salts **42** reactions were run at 110 °C, which was the melting temperature of tetrabutylphosphonium iodide **42c**. Tetrabutylphosphonium bromide **42b** (Table 2.4, entry 5) afforded a unique result leading to the highest ratio of *m*-hydroxybenzoic acid to *p*-hydroxybenzoic acid of any ionic liquid bromide examined. 1-Butyl-2,3-dimethylimidazolium bromide **43b** (Table 2.4, entry 7), 1-butyl-2-methylpyridinium bromide **44b** (Table 2.4, entry 8), and 1-butyl-1-methylpyrrolidinium bromide **45b** (Table 2.4, entry 9) were also examined as ionic liquid solvents with the reaction temperatures at their melting temperature. Among all of ionic liquid bromides, 1-butyl-1-methylpyrrolidinium bromide **45b** (Table 2.4, entry 9) gave the lowest yield of *p*-hydroxybenzoic acid with the lowest mass balance.

## 5.2. Dehydrations of Shikimic Acid in non-Bromide Ionic Liquids

While ionic liquid bromides were the best solvents for acid-catalyzed dehydration of shikimic acid, the corresponding ionic liquid chlorides showed low reactivity when employed as solvents. Only a 1% yield of *p*-hydroxybenzoic acid was obtained when acid-catalyzed dehydration of shikimic acid was run in 1-butyl-3-methylimidazolium chloride **40a** (Table 2.1, entry 1). Use of 1-butylpyridinium chloride **41a** as the solvent for acid-catalyzed dehydration of shikimic acid led to only an 8% yield of *p*-hydroxybenzoic acid (Table 2.4, entry 1). No *p*-hydroxybenzoic acid was detected when dehydration of shikimic acid was run in tetrabutylphosphonium chloride **42a** (Table 2.4, entry 4).

Poor results were also encountered when hydrogen sulfate and tetrafluoroborate were used as counteranions (Table 2.1, entry 4-5). A 3 % yield of *p*-hydroxybenzoic acid was obtained when 1-butyl-3-methylimidazolium hydrogen sulfate **40d** was used (Table 2.1, entry 4) as the solvent for acid-catalyzed dehydration of shikimic acid. Of the shikimic acid consumed only this 3% could be accounted for in the formation of *p*-hydroxybenzoic acid. Use of 1-butyl-3-methylimidazolium tetrafluoroborate **40e** as solvent for shikimic acid dehydration also led to a low yield of *p*-hydroxybenzoic acid with a modest mass balance (Table 2.1, entry 5).

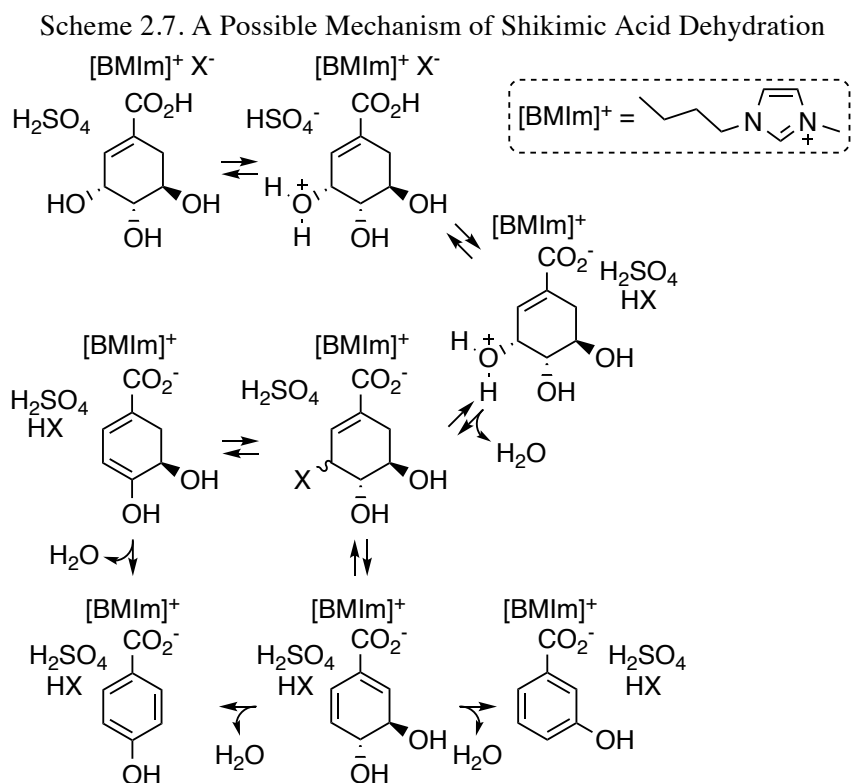
Use of ionic liquid iodides as the solvent for acid-catalyzed dehydration of shikimic acid gave yields of *p*-hydroxybenzoic acid that were uniformly lower relative to the corresponding ionic liquid bromides. An interesting feature of ionic liquid iodides was the formation of protocatechuic acid (3,4-dihydroxybenzoic acid) as a product. Protocatechuic acid formation requires oxidation of the C-3 alcohol of shikimic acid. The resulting dehydroshikimic acid will dehydrate to the observed protocatechuic acid.<sup>41</sup> 1-Butyl-3-methylimidazolium iodide **40c** afforded a 1% yield of *p*-hydroxybenzoic acid, 1% yield of protocatechuic acid, and no detectable formation of *m*-

hydroxybenzoic acid (Table 2.1, entry 3). Dehydration of shikimic acid in 1-butylpyridinium iodide **41c** led to a 15% yield of *p*-hydroxybenzoic acid and a 3 % yield of *m*-hydroxybenzoic acid (Table 2.4, entry 3). An 8% yield of protocatechuic acid with no *p*-hydroxybenzoic acid or *m*-hydroxybenzoic acid was detected when dehydration of shikimic acid was run in tetrabutylphosphonium iodide **42c** (Table 2.4, entry 6).

### 5.3. A Possible Mechanism for Bromide-Catalyzed Dehydration of Shikimic Acid

The much higher yields of hydroxybenzoic acids when shikimic acid is dehydrated in ionic liquid bromides relative to ionic liquid chlorides, ionic liquid iodides, or ionic liquids with other counteranions is particularly striking. This suggests that the ionic liquid bromides are playing an essential catalytic role in addition to serving as the solvents for the dehydrations. Protonation by H<sub>2</sub>SO<sub>4</sub> of the C-3 hydroxyl group of shikimic acid (Scheme 2.7) may precede deprotonation of the shikimate carboxylic acid and may result in an exchange of the resulting shikimate carboxylate with the bromide counteranion (Scheme 2.7). Nucleophilic attack by bromide at C-3 would displace water and generate a bromoshikimate intermediate (Scheme 2.7). This bromoshikimate could then partition between elimination reactions that ultimately lead to either *p*-hydroxybenzoic acid or *m*-hydroxybenzoic acid (Scheme 2.7). Bromide is a good nucleophile<sup>42</sup> and a good leaving group.<sup>43</sup> By contrast, chloride is not as good a nucleophile<sup>42</sup> or as good of a leaving group<sup>43</sup> as bromide. Chloride may consequently be diminished relative to bromide in its ability to nucleophilically displace water from the protonated shikimate intermediate (Scheme 2.7). Subsequently, a chloroshikimate intermediate may undergo elimination to the diolefin intermediates (Scheme 2.7) less readily than a bromoshikimate intermediate. This could explain the poor yields of hydroxybenzoic acid products when shikimic acid dehydration is run in ionic liquid chlorides. The low yields or absence of *p*-hydroxybenzoic acid formation with ionic liquids

with counteranions such as hydrogen sulfate (Table 2.1, entry 4) and tetrafluoroborate (Table 2.1, entry 5) may be explained by the non-nucleophilic nature of these anions.



In contrast to chloride, iodide is a better nucleophile<sup>42</sup> and a better leaving group<sup>43</sup> relative to bromide. This might lead to the expectation of ionic liquid iodides performing at least as well as ionic liquid bromides in the dehydration of shikimic acid. However, ion exchange considerations may be important with exchange of the carboxylate of shikimic acid with the counteranion of the ionic liquid being an essential step in the overall dehydration. With formation of an intimate ion pair between the shikimate carboxylate and the ionic liquid ammonium cation, the counteranion is released to play its essential role in the subsequent nucleophilic covalent catalysis. Using data from ion exchange resins, the binding affinity of anions with organic ammonium cations is ranked in the order: iodide  $\gg$  bromide  $>$  chloride  $\gg$  acetate.<sup>44</sup> As a consequence, exchange of shikimate with the iodide of ionic liquid iodides may be a slow step.

This slower formation of an intimate ion pair between shikimate and the organic ammonium cation component of ionic liquid iodides may explain the lower rates and lower yields for shikimic acid dehydration in ionic liquid iodides.

#### **5.4. Lewis Acid Catalyzed Conversion of Shikimic Acid to *p*-Hydroxybenzoic Acid in 1-Butyl-3-methylimidazolium Salts**

Lewis acid-catalyzed reactions of shikimic acid dissolved in 1-butyl-3-methylimidazolium salts **40** in the absence of sulfuric acid were also explored. The reaction conditions entailed heating a 20 weight percent (wt%) solution of shikimic acid in 1-butyl-3-methylimidazolium salts **40** with 20 mol % Lewis acids at 120 °C under reduced pressure (0.4 mbar) except when lower boiling Lewis acids were used. In these cases, the reaction was conducted under N<sub>2</sub>. Boron tribromide, zirconium(IV) bromide, scandium(III) bromide, hafnium(IV) bromide, germanium(IV) bromide and aluminium bromide were observed to catalyze essentially quantitative dehydration of shikimic acid to a mixture of *p*-hydroxybenzoic acid and *m*-hydroxybenzoic acids in 1-butyl-3-methylimidazolium bromide **40b** (Table 2.5, entry 1-6). Interestingly CuBr<sub>2</sub>, FeBr<sub>3</sub> and AuBr<sub>3</sub> formed almost as much protocatechuic acid as *m*-hydroxybenzoic acid (Table 2.5, entry 8-10). The oxidation state of the metals affected significantly to the reaction. There was no reaction with CuBr or FeBr<sub>2</sub> (Table 2.5, entry 18 and 19).

The importance of bromide as the counteranion of the ionic liquid was very similar to H<sub>2</sub>SO<sub>4</sub>-catalyzed reactions. Boron trichloride, zirconium(IV) chloride, hafnium(IV) chloride, and aluminium chloride catalyzed reactions of shikimic acid dissolved in 1-butyl-3-methylimidazolium chloride **40a** afforded little to no hydroxybenzoic acid (Table 2.6, entry 1-4).

Table 2.5. Lewis Acid 20 mol% Catalyzed Dehydration of Shikimic Acid in 1-Butyl-3-methylimidazolium Bromide **40b**

Entry	catalyst	% Yield			
		PHBA <sup>1</sup>	MHBA <sup>2</sup>	PCA <sup>3</sup>	% SA <sup>4</sup>
1	*BBr <sub>3</sub>	76%	21%	0%	0%
2	ZrBr <sub>4</sub>	74%	21%	0%	0%
3	ScBr <sub>3</sub>	73%	20%	0%	0%
4	HfBr <sub>4</sub>	73%	21%	0%	3%
5	*GeBr <sub>4</sub>	72%	21%	0%	0%
6	AlBr <sub>3</sub>	71%	19%	0%	7%
7	YBr <sub>3</sub>	66%	19%	0%	8%
8	CuBr <sub>2</sub>	64%	16%	15%	0%
9	FeBr <sub>3</sub>	63%	18%	13%	0%
10	AuBr <sub>3</sub>	61%	16%	22%	0%
11	VBr <sub>3</sub>	61%	16%	1%	0%
12	TiBr <sub>4</sub>	58%	18%	0%	1%
13	CrBr <sub>3</sub>	57%	16%	0%	0%
14	SnBr <sub>4</sub>	22%	6%	0%	57%
15	LaBr <sub>3</sub>	21%	6%	0%	69%
16	PdBr <sub>2</sub>	4%	1%	0%	91%
17	InBr <sub>3</sub>	3%	1%	0%	96%
18	CuBr	0%	0%	0%	99%
19	FeBr <sub>2</sub>	0%	0%	0%	99%

\*rxn = under N<sub>2</sub>(g); <sup>1</sup> PHBA=*p*-hydroxybenzoic acid; <sup>2</sup> MHBA=*m*-hydroxybenzoic acid; <sup>3</sup>PCA=protocatechuic acid; <sup>4</sup> % SA=percent remaining shikimic acid

Table 2.6. Lewis Acid 20 mol% Catalyzed Dehydration of Shikimic Acid in 1-Butyl-3-methylimidazolium Chloride **40a**

Entry	catalyst	% Yield			
		PHBA <sup>1</sup>	MHBA <sup>2</sup>	PCA <sup>3</sup>	% SA <sup>4</sup>
1	*BCl <sub>3</sub>	26%	10%	0%	54%
2	ZrCl <sub>4</sub>	0%	0%	0%	93%
3	HfCl <sub>4</sub>	0%	0%	0%	92%
4	AlCl <sub>3</sub>	0%	0%	0%	94%
5	*TiCl <sub>4</sub>	12%	6%	3%	46%

\*rxn = under N<sub>2</sub>(g); <sup>1</sup> PHBA=*p*-hydroxybenzoic acid; <sup>2</sup> MHBA=*m*-hydroxybenzoic acid; <sup>3</sup>PCA=protocatechuic acid; <sup>4</sup> % SA=percent remaining shikimic acid

Boron triiodide, zirconium(IV) iodide, hafnium(IV) iodide, and aluminium iodide catalyzed reactions of shikimic acid dissolved in 1-butyl-3-methylimidazolium iodide **40c** afforded moderate yields of *p*-hydroxybenzoic acid and *m*-hydroxybenzoic acid in addition to formation of protocatechuic acid (Table 2.7, entry 1-4). However, the percentage of shikimic acid

consumed that could be accounted for in formation of *p*-hydroxybenzoic acid, *m*-hydroxybenzoic acid and protocatechuic acid was low.

Table 2.7. Lewis Acid 20 mol% Catalyzed Dehydration of Shikimic Acid in 1-Butyl-3-methylimidazolium Iodide **40c**

Entry	catalyst	% Yield			
		PHBA <sup>1</sup>	MHBA <sup>2</sup>	PCA <sup>3</sup>	% SA <sup>4</sup>
1	BI <sub>3</sub>	32%	5%	14%	23%
2	ZrI <sub>4</sub>	26%	5%	10%	2%
3	HfI <sub>4</sub>	33%	6%	13%	1%
4	AlI <sub>3</sub>	32%	6%	12%	2%

<sup>1</sup> PHBA=*p*-hydroxybenzoic acid; <sup>2</sup> MHBA=*m*-hydroxybenzoic acid; <sup>3</sup> PCA=protocatechuic acid; <sup>4</sup> % SA=percent remaining shikimic acid

The catalyst loading of boron tribromide, zirconium(IV) bromide, scandium(III) bromide, hafnium(IV) bromide, germanium(IV) bromide and aluminium bromide in the catalyzed dehydration of shikimic acid in 1-butyl-3-methylimidazolium bromide **40b** could be lowered to 2 mol % without significant reduction of yield and mass accountability (Table 2.5, entry 1-6 vs. Table 8 entry 1-6). When 2 mol% of H<sub>2</sub>SO<sub>4</sub> was used as the catalyst, the conversion of shikimic acid became noticeably reduced (Table 2.8, Entry 7). This might be due to the redox reaction between H<sub>2</sub>SO<sub>4</sub> and bromide.

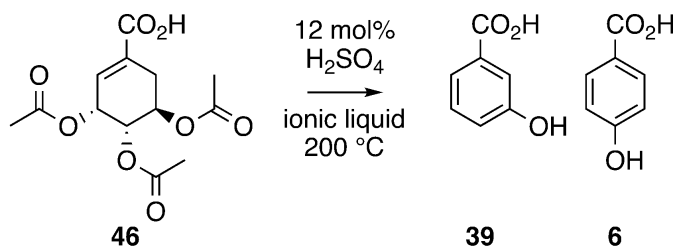
Table 2.8. Lewis Acid 2 mol% Catalyzed Dehydration of Shikimic Acid in 1-Butyl-3-methylimidazolium Bromide **40b**

Entry	catalyst	% Yield		
		PHBA <sup>1</sup>	MHBA <sup>2</sup>	% SA <sup>3</sup>
1	*BBr <sub>3</sub>	74%	21%	0%
2	ZrBr <sub>4</sub>	70%	20%	0%
3	ScBr <sub>3</sub>	71%	20%	1%
4	HfBr <sub>4</sub>	71%	20%	1%
5	*GeBr <sub>4</sub>	75%	21%	0%
6	AlBr <sub>3</sub>	72%	20%	1%
7	H <sub>2</sub> SO <sub>4</sub>	67%	18%	7%

\*rxn = under N<sub>2</sub>(g); <sup>1</sup> PHBA=*p*-hydroxybenzoic acid; <sup>2</sup> MHBA=*m*-hydroxybenzoic acid; <sup>3</sup> % SA=percent remaining shikimic acid

## 5.5. Conversion of (3*R*,4*S*,5*R*)-Triacetoxy-1-cyclohexenecarboxylic Acid to *m*-Hydroxybenzoic Acid in 1-Butyl-3-methylimidazolium Salts

Scheme 2.8. Aromatization of Acetylated Shikimic Acid



The elimination reaction of acetoxy groups from (3*R*,4*S*,5*R*)-triacetoxy-1-cyclohexenecarboxylic acid (acetylated shikimic acid) **46** in various 1-butyl-3-methylimidazolium salts **40** were explored. This reaction was very slow and it required higher temperatures and longer reaction times to achieve complete conversion than the dehydration of non-acetylated shikimic acid. *m*-Acetoxybenzoic acid, *p*-acetoxybenzoic acid, *m*-hydroxybenzoic acid and *p*-hydroxybenzoic acid were observed by <sup>1</sup>H NMR in the reaction solution during the course of the reaction. In small scale reactions, acetoxybenzoic acids were hydrolyzed by the time acetylated shikimic acid had been completely consumed. Despite the 1-butyl-3-methylimidazolium salts were dried before reaction, there must have been enough water to hydrolyze the product because of the hygroscopicity of ionic liquids. The reaction conditions entailed heating a 10 weight percent (wt%) solution of acetylated shikimic acid **46** in 1-butyl-3-methylimidazolium salts **40** at 200 °C under active flow of nitrogen (bubbler) with 12 mol % H<sub>2</sub>SO<sub>4</sub> (Scheme 2.8).

While the selectivity of shikimic acid dehydration reaction in 1-butyl-3-methylimidazolium salts **40** favors *p*-hydroxybenzoic acid, the elimination reaction of acetoxy groups from acetylated shikimic acid favors the formation of *m*-hydroxybenzoic acid (Table 2.9, entry 1-4). Selectivity favoring *m*-hydroxybenzoic acid was highest in 1-butyl-3-

methylimidazolium chloride **40a** to produce a 73% yield of *m*-hydroxybenzoic acid (Table 2.9, entry 1).

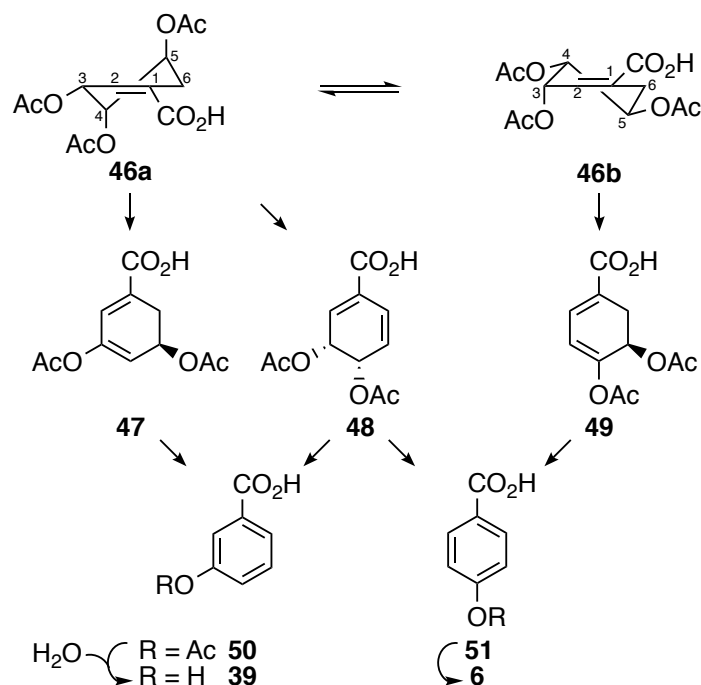
Table 2.9. *m*-Hydroxybenzoic Acid Synthesis from Acetylated Shikimic Acid in Various 1-Butyl-3-methylimidazolium Salts **40a-40e**

Entry	Ionic Liquid	Temp	Time	% Yield		% ASA <sup>3</sup>
				PHBA <sup>1</sup>	MHBA <sup>2</sup>	
1	<b>40a</b> X=Cl	200 °C	1 d	0	73	0
2	<b>40b</b> X=Br	200 °C	1 d	14	48	0
3	<b>40c</b> X=I	200 °C	1 d	0	40	0
4	<b>40d</b> X=HSO <sub>4</sub>	200 °C	1 d	0	6	0
5	<b>40e</b> X=BF <sub>4</sub>	200 °C	1 d	21	15	0

<sup>1</sup> PHBA=*p*-hydroxybenzoic acid; <sup>2</sup> MHBA=*m*-hydroxybenzoic acid;  
<sup>3</sup> % ASA=percent remaining acetylated shikimic acid

Acetoxy group elimination of acetylated shikimic acid **46** showed a different trend in product selectivity relative to shikimic acid dehydration, which suggests a different mechanism is at play. A stronger base shows more selectivity to the *meta* product when chloride, bromide and iodide are compared (Table 2.9, entry 1-3). If this is an E2 reaction, the first step is a protonation of pseudo axial acetoxy groups (Scheme 2.9).

Scheme 2.9. Possible Mechanism of Acetylated Shikimic Acid Aromatization



There are two pseudo axial acetoxy groups in the conformation **46a** at C-4 and C-5. Elimination of C-4 acetoxy group would lead to *meta* product only (Scheme 2.9). Elimination of the C-5 acetoxy yields the intermediate **48**, which can lead to either *para* or *meta* products. The C-3 proton of the intermediate **48** is more acidic than the C-4 proton and therefore would lead to *meta* product. There is only one pseudo axial acetoxy group in conformer **46b**, and the elimination of this acetoxy group leads to a *para* product (Scheme 2.9). The conformer **46a** possesses two pseudo axial acetoxy groups while the conformer **46b** possesses only one pseudo axial acetoxy group. The pseudo axial interaction in cyclohexene is less sterically strained than the diaxial interaction in cyclohexanes.<sup>45</sup> There are three possible acetoxy groups for a trans diaxial elimination at the first step (scheme 2.9). Two of them would lead to *meta* product. Of the two trans diaxial elimination, one is exclusively leads to *meta* product. The other can lead to either *meta* or *para* product. Since the C-3 proton is most acidic, the C-3 proton and the C-4 acetoxy group would more likely eliminated leading *meta* product. This might be the reason that

*meta* product is predominant in the reaction of chloride, bromide and iodide (Table 2.9, entry 1-3).

## 6. Discussion

Microbial synthesis of shikimic acid from glucose<sup>38</sup> has the advantage of utilizing a starting material that is nontoxic and renewable. This differs from the use of toxic toluene<sup>46</sup> and toxic phenol<sup>22</sup>, which are derived from carcinogenic benzene,<sup>21a-g</sup> as the starting materials in the microbial oxidation of toluene<sup>23</sup> to *p*-hydroxybenzoic acid and the enzymatic conversion of phenyl phosphate<sup>24a-d</sup> to *p*-hydroxybenzoic acid (Scheme 2.3).

Microbial synthesis of shikimic acid from glucose followed by chemical dehydration of shikimic acid to *p*-hydroxybenzoic acid lacks the conciseness of the direct microbial syntheses of *p*-hydroxybenzoic acid from glucose. One of the direct microbial syntheses of *p*-hydroxybenzoic acid from glucose involving chorismate lyase has titer of 23 g/L (Scheme 2.4).<sup>26</sup> This was achieved by employment of ion exchange resins during fermentation in order to prevent enzyme feedback inhibition.<sup>26</sup> Ion exchange resins are relatively expensive and introduce an external loop to the fermentation involving passage of culture broth through a resin bed which increases the risk of contamination. The other direct microbial syntheses of *p*-hydroxybenzoic acid from glucose involves tyrosine as one of the intermediates. It does not require employment of ion exchange resins during the fermentation, however the yield of *p*-hydroxybenzoic acid is low (16%).<sup>29b</sup>

Plant-synthesized versus microbe-synthesized shikimic acid is another comparison to consider. Shikimic acid can be synthesized from glucose in 34% yield affording shikimic acid concentrations of 72 g/L (Chapter 3). Plants that synthesize shikimic acid require a growing season before plant tissue containing shikimic acid can be harvested. By contrast, microbial synthesis of

shikimic acid only requires 61 h for microbial growth/microbial production with an additional 24 h for fermentor setup, harvesting, and fermentor cleanout.

Transgenic plants produce *p*-hydroxybenzoic acid directly. However, *p*-hydroxybenzoic acid is conjugated as either a phenolic or carboxylate glucoside.<sup>30,31,33</sup> The highest producing transgenic plant produces (after correcting for the mass of the conjugated glucose) the equivalent of 6.6 dry wt% of *p*-hydroxybenzoic acid.<sup>32</sup> There is no report in the literature that describes how *p*-hydroxybenzoic acid glucosides are extracted from transgenic plants. Also, the process to extract *p*-hydroxybenzoic acid from the transgenic plant generates a stoichiometric amount of glucose as byproduct, which will need to be captured and utilized. Utilization of fields only for one molecule is not economically efficient. Another advantage of a synthesis with plants is the low turnover. It is not flexible to the market change.

The chemical dehydration of shikimic acid in 1-butyl-3-methylimidazolium bromide using H<sub>2</sub>SO<sub>4</sub> can yield 80% of *p*-hydroxybenzoic acid and 18% *m*-hydroxybenzoic acid (Table 2.3, entry 1). The concentration of shikimic acid in the reaction solution can be up to 40 wt% of 1-butyl-3-methylimidazolium bromide. Employment of recycled 1-butyl-3-methylimidazolium bromide provides comparable yields of *p*-hydroxybenzoic acid and *m*-hydroxybenzoic acid to using fresh ionic liquid (Table 2.3). The *m*-hydroxybenzoic acid can be separated from *p*-hydroxybenzoic acid by crystallization. *m*-Hydroxybenzoic acid is also used as one of the copolymers in LCPs.<sup>2</sup> Therefore, the mixture of *p*-hydroxybenzoic acid and *m*-hydroxybenzoic acid in the mother liquor is a valuable product.

## 7. Experimental

### 7.1. General

$^1\text{H}$  NMR spectra were recorded on a 500 MHz spectrometer. Chemical shifts for  $^1\text{H}$  NMR spectra are reported (in parts per million) relative to residual non-deuterated solvent in  $\text{CDCl}_3$  ( $\delta = 7.26$  ppm) and  $\text{CD}_3\text{OD}$  ( $\delta = 3.34$  ppm). Chemical shifts for  $^1\text{H}$  NMR spectra in  $\text{D}_2\text{O}$  is reported (in parts per million) relative to residual non-deuterated sodium salt of 3-(trimethylsilyl) propionic-2,2,3,3- $\text{d}_4$  acid, TSP ( $\delta = 0.00$  ppm).  $^{13}\text{C}$  NMR spectra were recorded at 125 MHz and chemical shifts for these spectra were reported (in parts per million) relative to  $\text{CDCl}_3$  ( $\delta = 77.4$  ppm) and  $\text{CD}_3\text{OD}$  ( $\delta = 49.9$  ppm).

1-Butyl-3-methylimidazolium iodide, 1-butyl-3-methylimidazolium hydrogen sulfate, 1-butyl-3-methylimidazolium tetrafluoroborate, 1-butylpyridinium bromide, 1-butyl-1-methylpyrrolidinium bromide, 1-iodobutane, tributylphosphine, 1-methylimidazole, 1-chlorobutane, 1-bromobutane, acetic anhydride, pyridine and 3-(trimethylsilyl) propionic-2,2,3,3- $\text{d}_4$  acid were purchased from Sigma-Aldrich. 1-Butyl-2,3-dimethylimidazolium bromide, 1-butylpyridinium chloride, 1-butylpyridinium iodide, 1-butyl-2-methylpyridinium bromide and tetrabutylphosphonium chloride were purchased from Ionic Liquid Technologies. Tetrabutylphosphonium bromide was purchased from CYTEC. 1-Iodobutane and tributylphosphine were distilled prior to use. Acetic anhydride was dried with  $\text{P}_2\text{O}_5$ , and then distilled. Pyridine was dried over MS 4 Å. Other chemicals were used without further purification.

## 7.2. Product Analysis

HPLC analysis was performed on an Agilent 1100. Shikimic acid was quantified by HPLC using a Grace Alltima™ amino column (4.6 × 250 mm, 5 μm particle size) and isocratic elution with 60/40, (v/v); CH<sub>3</sub>CN/H<sub>2</sub>O (140 mM NH<sub>4</sub><sup>+</sup>HCO<sub>2</sub><sup>-</sup>, pH 4.0). The amino column was stored in a solution of 5/95, (v/v); methanol/hexane when it was received from the manufacture. In order to convert the column to weak base ion-exchange mode, the column was washed with 1 L of reagent grade isopropanol (0.2 mL/min) followed by 1 L of HPLC grade acetonitrile (0.2 mL/min) prior to the first use. Shikimic acid molecular standard was obtained from Roche. *p*-Hydroxybenzoic acid and *m*-hydroxybenzoic acid were separated from one another with baseline resolution and quantified by HPLC using an Agilent ZORBAX SB-C18 (4.6 x 150 mm, 5 μm particle size) column and isocratic elution with 15/85, (v/v); CH<sub>3</sub>CN/H<sub>2</sub>O (100 mM NH<sub>4</sub><sup>+</sup>HCO<sub>2</sub><sup>-</sup>, pH 2.5). The ZORBAX was stored in a solution of 85/15, (v/v); methanol/H<sub>2</sub>O when it was received from the manufacture. The column was washed with 1 L of HPLC grade acetonitrile prior to the first use. *p*-Hydroxybenzoic acid molecular standard was obtained from Spectrum while the *m*-hydroxybenzoic acid molecular standard was obtained from Sigma-Aldrich. The deionized, distilled water used to make the required buffer solutions was filtered with a DURAPORE® 0.45 μm HV filter (MILLIPORE). The acetonitrile was HPLC grade. Syringe filtration (0.45 μm Whatman filter) was followed by HPLC analysis for all the sample.

## 7.3. Screening of Ionic Liquid for Dehydration of Shikimic Acid

Screening of ionic liquid for dehydration of shikimic acid employed a 25 mL stripping flask fitted with a magnetic stir bar and a gas adaptor. Approximately 5 g of ionic liquid was dried in the flask overnight under reduced pressure at 50 °C. The oil bath temperature was raised

to a temperature high enough to melt the ionic liquid under the reduced pressure: 1-butyl-3-methylimidazolium salts at 90 °C, 1-butylpyridinium salts at 140 °C, tetrabutylphosphonium salts at 110 °C, 1-butyl-2,3-dimethylimidazolium bromide at 110 °C, 1-butyl-2-methylpyridinium bromide at 160 °C, 1-butyl-1-methylpyrrolidinium bromide at 180 °C. The flask containing dry ionic liquid was opened under N<sub>2</sub> and weighed. Shikimic acid 20 wt% relative to the ionic liquids' weight was added. Shikimic acid was dissolved at the melting temperature of the ionic liquid under N<sub>2</sub>, and then maintained at that temperature for 30 min under vacuum (0.4 mbar). The flask was opened under N<sub>2</sub> and H<sub>2</sub>SO<sub>4</sub> (0.2 eq) was added. The reaction solution was heated for 13 h under vacuum (0.4 mbar) and the resulting crude solution was analyzed by HPLC.

#### **7.4. Comparison of Shikimic Acid Concentration in Dehydration of Shikimic Acid**

Determining the maximum concentration limit of shikimic acid in 1-butyl-3-methylimidazolium bromide ([BMIm]Br) for the dehydration of shikimic acid employed a 25 mL stripping flask fitted with a magnetic stir bar and a gas adaptor. Approximately 5 g of [BMIm]Br was dried in the flask overnight under reduced pressure at 50 °C. The flask containing dry [BMIm]Br was weighed and opened under N<sub>2</sub>. Shikimic acid 20 wt% relative to the [BMIm]Br weight was added. Shikimic acid was dissolved at 90 °C under N<sub>2</sub> and heat was maintained for 30 min under vacuum (0.4 mbar). The flask was opened under N<sub>2</sub> and H<sub>2</sub>SO<sub>4</sub> (0.2eq) was added. The reaction solution was heated at 90 °C for 13 h under vacuum (0.3 mmHg) and the resulting crude solution was analyzed by HPLC.

## 7.5. Synthesis of 1-Butyl-3-methylimidazolium Bromide<sup>47a</sup>

1-Bromobutane (101 mL, 0.936 mol) was added to 49.5 mL (0.621 mol) of 1-methylimidazole in a 500 mL round bottom flask heated in a 70 °C oil bath fitted with a reflux condenser open to the atmosphere. A vigorous exothermic reaction was observed after heating at 70 °C for approximately 15 min. The flask was removed from the oil bath until the vigorous exothermic reaction ceased and then placed back in the 70 °C oil bath for 13 h. 1-Bromobutane (30.0 mL, 0.279 mol) was added to the flask, and continued heating at 70 °C oil for an additional 6 h. Unreacted 1-bromobutane was removed under reduced pressure at 55 °C. This afforded 1-butyl-3-methylimidazolium bromide (135 g, 99%) as a yellow solid. <sup>1</sup>H NMR (CDCl<sub>3</sub>) δ = 10.6 (s, 1H), 7.32 (dd, *J* = 3.5, 2 Hz, 1H), 7.25 (dd, *J* = 3.5, 2 Hz, 1H), 4.31 (dd, *J*<sub>1</sub> = *J*<sub>2</sub> = 7.5 Hz, 2H), 4.11 (s, 3H), 1.86-1.92 (m, 2H), 1.37 (m, 2H), 0.950 (dd, *J* = 7.5, 7.0 Hz, 3H). <sup>13</sup>C NMR (CDCl<sub>3</sub>) δ = 138.2, 123.6, 122.0, 50.3, 37.1, 32.5, 19.8, 13.8. mp: 72.0-76.0 °C (lit.<sup>47b</sup> 69-70 °C).

## 7.6. Recycling 1-Butyl-3-methylimidazolium Bromide

*In situ* synthesized 1-Butyl-3-methylimidazolium bromide (29.9 g, 136 mmol) ([BMIm]Br) was dried in a 200 mL stripping flask overnight at 90 °C under vacuum. The flask containing dry [BMIm]Br was opened under N<sub>2</sub> and shikimic acid (11.9 g, 68.5 mmol) was added. After dissolving shikimic acid at 90 °C under N<sub>2</sub>, the temperature was maintained for 30 min under vacuum (0.4 mbar). The flask was opened under N<sub>2</sub> and H<sub>2</sub>SO<sub>4</sub> (0.730 mL, 13.7 mmol) was added. The acidified reaction solution was then heated at 90 °C for 24 h under vacuum (0.4 mbar). After cooling the reaction solution to rt, it was diluted with H<sub>2</sub>O (30 mL) and extracted with EtOAc (300 mL) for 6 h in a liquid-liquid continuous extractor. Concentrating the organic layer gave a beige-colored solid consisting of 7.52 g of *p*-

hydroxybenzoic acid (80%), and 1.69 g of *m*-hydroxybenzoic acid (18%) based on HPLC analysis.

Water was removed from the aqueous layer on a rotary evaporator under high vacuum. The concentrated brown oil was dried under reduced pressure and solidified overnight giving 28.0 g (128 mmol) of [BMIm]Br as a brown solid. The flask containing this recycled [BMIm]Br was opened under N<sub>2</sub> and shikimic acid (11.2 g, 64.1 mmol) was added. After the shikimic acid dissolved by heating at 90 °C under N<sub>2</sub>, heating was continued under vacuum (0.4 mbar) for 30 min. The flask was opened under N<sub>2</sub>, and H<sub>2</sub>SO<sub>4</sub> (0.684 mL, 12.8 mmol) was added. The acidified reaction solution was then heated at 90 °C for 24 h under vacuum (0.4 mbar). The reaction solution after cooling was diluted with H<sub>2</sub>O (30 mL), and extracted with EtOAc (300 mL) for 6 h in a liquid-liquid continuous extractor. Concentrating the organic layer gave brown-colored solids consisting of 6.85 g of *p*-hydroxybenzoic acid (77%) and 1.40 g of *m*-hydroxybenzoic acid (16 %) based on HPLC analysis.

In addition to further discoloration, viscosity of the [BMIm]Br had increased during its second use. Activated carbon (DARCO®, KB-B 100 mesh) (4.00 g) was added to the aqueous layer of the extraction from the second shikimic acid dehydration using recycled [BMIm]Br, and the mixture was swirled with an orbital shaker at rt and 200 rpm. The activated carbon was removed by filtration. Concentrating and drying this filtrate gave a yellow-colored oil. Adding a small crystal of [BMIm]Br resulted in solidification of the ionic liquid (17.0 g, 77.6 mmol) as a yellow-colored solid. This twice recycled [BMIm]Br was then used for a third dehydration of shikimic acid. The [BMIm]Br was dried in a 200 mL stripping flask overnight at 90 °C under vacuum. The flask containing dry [BMIm]Br was opened under N<sub>2</sub>, and shikimic acid (7.06 g, 40.5 mmol) was added. There was shikimic acid (0.20 g, 1.2 mmol) carried over from the

second reaction. After the shikimic acid dissolved with heating at 90 °C under N<sub>2</sub>, heating at 90 °C was continued under vacuum (0.4 mbar) for 30 min. The flask was opened under N<sub>2</sub>, and H<sub>2</sub>SO<sub>4</sub> (0.432 mL, 8.11 mmol) was added. The acidified reaction solution was then heated at 90 °C for 24 h under vacuum (0.4 mbar). The reaction solution after cooling was diluted with H<sub>2</sub>O (30 mL), and extracted with EtOAc (300 mL) for 6 h in a liquid-liquid continuous extractor. Concentrating the organic layer gave a beige-colored solid consisting of 4.13 g of *p*-hydroxybenzoic acid (72%), and 0.61 g of *m*-hydroxybenzoic acid (11 %) based on HPLC analysis.

### 7.7. Lewis Acid Catalysts Screening for Dehydration of Shikimic Acid

The ionic liquid was dried in the flask overnight under reduced pressure at 50 °C. The oil bath temperature was raised to 90 °C to melt the ionic liquid under reduced pressure. The melted ionic liquid (5 g) was poured into a 25 mL stripping flask containing a magnetic stir bar. Shikimic acid (1 g, 5.74 mmol) and a Lewis acid catalyst were added. Shikimic acid was dissolved at 90 °C under N<sub>2</sub> and then vacuum (0.4 mbar) was applied. BCl<sub>3</sub>, TiCl<sub>4</sub>, BBr<sub>3</sub> and GeBr<sub>4</sub> reactions were run under active flow of N<sub>2</sub> due to their low boiling points. The oil bath temperature was raised to 120 °C and held at that temperature for 9 h. The resulting crude solution was analyzed by HPLC.

### 7.8. Synthesis of Tetra-(*n*)-butylphosphonium Iodide<sup>48</sup>

1-Iodobutane (53.6 mL, 471 mmol) was added to tri-(*n*)-butylphosphine (59 mL, 236 mmol) in a 500 mL round bottom flask fitted with a reflux condenser connected to an active Ar flow using a gas bubbler. The solution was stirred for 1 h at rt then 20 h at 100 °C under an active flow of Ar. Addition of diethyl ether (80 mL) to the reaction solution after cooling the

reaction to rt gave a white solid precipitate. Filtration and drying under reduced pressure allowed tetra-(*n*)-butylphosphonium iodide (91.0 g, 100 %) as a white solid. <sup>1</sup>H NMR ((CD<sub>3</sub>)<sub>2</sub>CO): δ = 2.47-2.53 (m, 2H), 1.66-1.73 (m, 2H), 1.52 (dddd,  $J_1 = J_2 = J_3 = J_4 = J_5 = 7.34$  Hz, 2H), 0.956 (t,  $J = 7.0$  Hz, 3H). <sup>13</sup>C NMR ((CD<sub>3</sub>)<sub>2</sub>CO) δ = 24.4, 24.2, 23.8, 23.7, 19.0, 18.7, 13.4. mp: 98-100 °C (Lit.<sup>48</sup> 95-96°C).

### 7.9. (3*R*,4*S*,5*R*)-Triacetoxyl-1-cyclohexenecarboxylic Acid

Shikimic acid (32.2 g, 185 mmol) was stirred with acetic anhydride (156 mL, 1.65 mol) and pyridine (156 mL, 1.93 mol) at rt for 24 h in a 1 L stripping flask. The reaction solution was concentrated *in vacuo*. The residue was diluted with a solution of hexanes/EtOAc (1:2) with 0.5% AcOH and washed with 200 mL of 1% (v/v) H<sub>2</sub>SO<sub>4</sub> (3x). A plug of chromatographic grade silica gel (60 Å pore size, 40-63µm mesh) was prepared with a solution of hexanes/EtOAc with AcOH (3:1, 0.5%). The crude solution was filtered through the plug of silica gel. Concentrating the filtrate *in vacuo* afforded a colorless oil (42.1 g, 76%). <sup>1</sup>H NMR (CDCl<sub>3</sub>) δ = 6.83-6.85 (m, 1H), 5.72-5.73 (m, 1H), 5.23-5.28 (m, 2H), 2.85 (ddd,  $J = 19, 4.5, 2$  Hz, 1H), 2.41 (ddd,  $J = 19, 3.5, 2$  Hz, 1H), 2.06 (s, 3H), 2.04 (s, 3H), 2.03 (s, 3H). <sup>13</sup>C NMR (CDCl<sub>3</sub>) δ = 170.8, 170.3, 170.2, 135.4, 130.9, 67.7, 67.0, 66.3, 28.3, 21.3, 21.0.

### 7.10. Screening of Ionic Liquid for *m*-Hydroxybenzoic Acid Synthesis from (3*R*,4*S*,5*R*)-Triacetoxyl-1-cyclohexenecarboxylic Acid

Screening of ionic liquid for *m*-hydroxybenzoic acid synthesis from (3*R*,4*S*,5*R*)-triacetoxyl-1-cyclohexene-1-carboxylic acid employed a 25 mL stripping flask fitted with a magnetic stir bar and a gas adaptor. Ionic liquid (5 g) was added to (3*R*,4*S*,5*R*)-triacetoxyl-1-cyclohexene-1-carboxylic acid (0.5 g). It was dried overnight under reduced pressure at 50 °C.

The flask containing dry ionic liquid and (3*R*,4*S*,5*R*)-triacetoxy-1-cyclohexene-1-carboxylic acid was weighed. The flask was opened under N<sub>2</sub>, and H<sub>2</sub>SO<sub>4</sub> (0.12eq) was added. It was heated for 24 h under an active flow of N<sub>2</sub> using a gas bubbler and the resulting crude solution was analyzed by HPLC.

### 7.11. 1-Butyl-3-methylimidazolium Chloride<sup>49a</sup>

1-Chlorobutane (230 mL, 2.20 mol) was added to 122 mL (1.53 mol) of 1-methylimidazole in a 500 mL round bottom flask heated in a 95 °C oil bath fitted with a reflux condenser connected to an active flow of N<sub>2</sub> using a gas bubbler. The solution was heated at 95 °C for 38 h. Another 40 mL of 1-chlorobutane (0.383 mol) was added, and then continued heating at 95 °C for total 3 days. Removing unreacted substrate with a rotary evaporator and drying under reduced pressure overnight allowed 1-butyl-3-methylimidazolium chloride (267 g, 100 %) as a yellow solid. <sup>1</sup>H NMR (CDCl<sub>3</sub>): δ 11.2 (s, 1H), 7.16 (dd, *J* = 3, 1.5 Hz, 1H), 7.14 (dd, *J* = 3.5, 2 Hz, 1H), 4.31 (dd, *J*<sub>1</sub> = *J*<sub>2</sub> = 7.5 Hz, 2H), 4.11 (s, 3H), 1.85-1.92 (m, 2H), 1.38 (m, 2H), 0.958 (dd, *J* = 7.5, 7.0 Hz, 3H). <sup>13</sup>C NMR (CDCl<sub>3</sub>) δ = 139.5, 123.1, 121.6, 50.3, 37.0, 32.5, 19.9, 13.8. mp: 60.0-65.0 °C (Lit.<sup>49b</sup> 65-69 °C).

### 7.12. *m*-Hydroxybenzoic Acid Synthesis from (3*R*, 4*S*, 5*R*)-Triacetoxy-1-cyclohexenecarboxylic Acid

1-Butyl-3-methylimidazolium chloride ([BMIm]Cl) was dried and melted in a round bottom flask at 90 °C under vacuum overnight. The [BMIm]Cl (211 g, 1.20 mol) was poured into a 2 L three neck round bottom flask containing (3*R*,4*S*,5*R*)-triacetoxy-1-cyclohexene-1-carboxylic acid (20.9 g, 69.5 mmol) and then H<sub>2</sub>SO<sub>4</sub> (0.445 mL, 8.34 mmol) was added. The

solution was stirred with an overhead stirrer under an active flow of N<sub>2</sub> and heated at 200 °C for 24 h. 0.7 M NaOH (240 mL) was added to the solution and heated at 100 °C for 3 h. The solution was acidified with H<sub>2</sub>SO<sub>4</sub> to pH 3.4 and then extracted with EtOAc (750 mL) for 3 days in a continuous liquid-liquid extractor. The organic extract was concentrated to afford brown oil containing 6.7 g (70%) of *m*-hydroxybenzoic acid based on HPLC analysis. This brown oil was decolorized using continuous flow conditions. A decolorizing column (D = 5.4 cm) was constructed with a piece of Kimwipe to plug the column outlet below a layer of 6.7 g Celite® 545 topped with a layer consisting of 3.6 g activated charcoal (DARCO® G-60, 100 mesh) dispersed in 15.4 g flash chromatography grade silica gel (60 Å pore size, 40-63µm mesh). After loading, the decolorizing column was washed with an EtOAc/AcOH (98.6:1.4 v/v) solution. Concentrating this solution gave a light brown oil. This light brown oil was diluted with 2 M NaOH (50 mL) and washed with CH<sub>2</sub>Cl<sub>2</sub> (50mL). The remaining aqueous solution was acidified with HCl to pH 0.0, crystallized at 4 °C, filtered, and dried to afford *m*-hydroxybenzoic acid 5.3 g (54%) as a white solid with a 97.8% purity based on HPLC analysis. <sup>1</sup>H NMR (CD<sub>3</sub>OD): δ = 7.52 (dt, *J* = 8.0, 1.3 Hz, 1H), 7.45 (dd, *J* = 2.5, 1.5 Hz, 1H), 7.30 (t, *J* = 8.0 Hz, 1H), 7.03 (ddd, *J* = 8.5, 3.0, 1.0 Hz, 1H). <sup>13</sup>C NMR (CD<sub>3</sub>OD) δ = 170.8, 159.6, 134.0, 131.3, 122.7, 121.8, 118.1. mp: 196-198 °C (Lit.<sup>50</sup> 197-200 °C).

## REFERENCES

## REFERENCES

1. Aelony, D.; Renfrew, M. M. Polyester resins. US 2728747, December 27, 1955.
2. (a) Hanabatake, M. Production method of aromatic polyesters. JP S5657821, May 20, 1981. (b) Layton, R.; Cleay, J. W. Wholly aromatic polyesters with reduced char content. EP 0347228, December 20, 1989. (c) Huspeni, P. J.; Stern, B. A.; Frayer, P. D. Blends of liquid crystalline polymers of hydroquinone poly(iso-terephthalates) p-hydroxybenzoic acid polymers and another LCP containing oxybisbenzene and naphthalene derivatives. WO 9004002, April 04, 1990. (d) Waggoner, M. Liquid crystalline polymer composition. WO 9606888, July 03, 1996. (e) Shepherd, J. P.; Linstid, C. H. III. Stretchable liquid crystal polymer composition. WO 02064661, August 22, 2002.
3. Ticona, GmbH, Vectra®: *Liquid Crystalline Polymer (LCP)*, Frankfurt, 2001. <http://www.hipolymers.com.ar/pdfs/vectra/diseno/Vectra%20brochure.pdf> (accessed Mar 31, 2017)
4. (a) Adlem, K.; Parri, O.; Wiles, D.; Saxton, P. E. Polymerisable L.C. Material and polymer film with negative optical dispersion. US 20120224245, September 06, 2012. (b) King, A. C.; Weatherspoon, M. R.; Rendek, L. J. Jr. Method for making electronic device with liquid crystal polymer and related device. US 20140217618, August 07, 2014.
5. Yung, P. C.; Juenger, O. Metal detectable liquid crystalline polymer composition. US 20150173564, June 25, 2015.
6. Blake, K. Cut resistant yarn. GB 2446866, August 27, 2008.
7. (a) Hiom, S. J. Preservation of Medicines and Cosmetics. In *Russel, Hugo & Ayliffe's: Principles and Practice of Disinfection, Preservation and Sterilization, 5<sup>th</sup> Ed.* Willey-Blackwell: West Sussex, 2012; pp388-407. (b) Cashman, A. L.; Warshaw, E. M. Parabens: A review of epidemiology, structure, allergenicity, and hormonal properties. *Dermatitis* **2005**, *16*, 57-66. (c) Kirchhof, M. G.; de Gannes, G. C. The health controversies of parabens. *Skin Therapy Letter* **2013**, *18*, 5-7.
8. (a) Molbase. 99-96-7 4-Hydroxybenzoic Acid. [http://www.molbase.com/en/search.html?search\\_type=text&search\\_keyword=99-96-7](http://www.molbase.com/en/search.html?search_type=text&search_keyword=99-96-7) (accessed Dec. 21, 2016). (b) Molbase. 100-21-0 Terephthalic Acid. [http://www.molbase.com/en/search.html?search\\_keyword=100-21-0](http://www.molbase.com/en/search.html?search_keyword=100-21-0) (accessed Dec. 21, 2016).
9. (a) Radiant Insights. Liquid Crystal Polymer (LCP) Market Size, 2020. <http://www.radiantinsights.com/research/liquid-crystal-polymer-lcp-market> (accessed Dec. 21, 2016). (b) Markets and Markets. Liquid Crystal Polymer Market Worth 1.2 Billion USD by 2020. <http://www.marketsandmarkets.com/PressReleases/liquid-crystal-polymer-resin.asp>

(accessed Dec. 21, 2016).

10. Grand View Research. Cosmetic Preservative Market Analysis By Product (Paraben Esters, Formaldehyde Donors, Phenol Derivative, Alcohol, Quaternary Compounds, Organic Acid), By Application (Skin & Sun Care, Hair Care, Toiletries, Fragrances & Perfumes, Makeup & Color) and Segment Forecasts to 2024. <http://www.grandviewresearch.com/industry-analysis/cosmetic-preservative-market> (accessed Dec. 21, 2016).
11. Kolbe, H. Ueber synthese der salicylsäure. *Just. Liebigs Ann. Chem.* **1860**, *113*, 12-127.
12. Kolbe, H. Improvement in the processes of preparing salicylic acid and other acids. US 150867, April 20, 1874.
13. Zevaco, T.; Dinjus, E. Main Group Element- and Transition Metal-Promoted Carboxylation of Organic Substrates (Alkanes, Alkenes, Alkynes, Aromatics, and Others). In *Carbon Dioxide as Chemical Feedstock*; Aresta, M., Ed.; Wiley-VCH Verlag: Weinheim, 2010; pp89-119.
14. (a) Kolbe, H. Ueber eine neue darstellungsmethode und einige bemerkenswerthe eigenschaften der salicylsäure. *J. Prakt. Chem.* **1875**, *10*, 89-112. (b) Schmitt, R. Beitrag zur kenntniss der Kolbe'schen salicylsäure synthese. *J. Prakt. Chem.* **1885**, *31*, 397-411.
15. (a) Buelna, G.; Nenoff, T.M. Catalytic reactive separation system for energy-efficient production of cumene. US 7566429, July 28, 2009 (b) Brown, S. H. Production of high purity cumene from non-extracted feed and hydrocarbon composition useful therein. US 7683228, March 23, 2010
16. Hock, H.; Lang, S. Autoxydation von Kohlenwasserstoffen, IX. Mitteil.: Über peroxide von benzol-derivaten. *Ber. Dtsch. Chem. Ges.* **1944**, *3-4*, 257-264.
17. Basil, V. A.; Reginald, H. H.; Denis, C. Q.; Heinrich, W. T. K. Manufacture of phenol. US 2628983, February 17, 1953.
18. (a) Schultz, H.; Bauer, G.; Schachl, E.; Hagedorn, F.; Schmittinger, P. Potassium Compounds. In *Ullmann's Encyclopedia of Industrial Chemistry*; Wiley-VCH: Weinheim, 2012; pp 639-704. DOI: 10.1002/14356007.a22\_039. (b) Sato, H.; Imai, S. Electrolytic method of aqueous potassium chloride solution. JP S5967379, April 17, 1984. (c) Butts, D. Chemicals from Brine. In *Kirk-Othmer Encyclopedia of Chemical Technology*; Wiley, 2003; pp784-803.
19. Topham, S.; Bazzanella, A.; Schiebahn, S.; Luhr, S.; Zhao, L.; Otto, A.; Stolen, D. Carbon Dioxide. In *Ullmann's Encyclopedia of Industrial Chemistry*; Wiley-VCH: Weinheim, 2014; pp 1-43. DOI: 10.1002/14356007.a05\_165.pud2.
20. (a) Muller, H. Sulfuric Acid and Sulfur Trioxide. In *Ullmann's Encyclopedia of Industrial Chemistry*; Wiley-VCH: Weinheim, 2012; pp 141-211. DOI: 10.1002/14356007.a25\_635

(b) Muller, H. Sulfur Dioxide. In *Ullmann's Encyclopedia of Industrial Chemistry*; Wiley-VCH: Weinheim, 2012; pp 73-118. DOI: 10.1002/14356007.a25\_569. (c) Garcia-Labiano, F.; de Diego, L. F.; Gabello, A.; Gayan, P.; Abad, A. Adanez, J.; Sprachmann, G. Sulphuric acid production via chemical looping combustion of elemental Sulphur. *Applied Energy* **2016**, *178*, 736-745. DOI: 10.1016/j.apenergy.2016.06.110. (d) Zakiewicz, B. Recent developments in Sulphur mining by underground melting. Thermofluid mining of Sulphur deposits. *Sulphur* **1986**, *184*, 26-32. (e) Nehb, W.; Vydra, K. Sulfur. In *Ullmann's Encyclopedia of Industrial Chemistry*; Wiley-VCH: Weinheim, 2012; pp 5-71. DOI: 10.1002/14356007.a25\_507.pub2.

21. (a)McHale, C. M.; Zhang, L. Smith, M. T. Current understanding of the mechanism of benzene-induced leukemia in humans: implications for risk assessment. *Carcinogenesis* **2012**, *33*, 240-252. DOI: 10.1093/carcin/bgr297. (b) Rappaport, S. M.; Kim, S.; Lan, Q.; Vermeulen, Roel, Waidyanatha, W.; Zhang, L.; Li, G.; Yin, S.; Hayes, R.B.; Rothman, N.; Smith, M. T. Evidence that humans metabolize benzene via two pathways. *Environmental Health Perspectives* **2009**, *117*, 946-952. (c) Smith, M. T.; Zhang, L.; Jeng, M.; Wang, Y.; Guo, W.; Duramad, P.; Hubbard, A. E.; Hofstadler, G.; Holland, N. T. Hydroquinone, a benzene metabolite, increases the level of aneusomy of chromosomes 7 and 8 in human CD34-positive blood progenitor cells. *Carcinogenesis* **2000**, *21*, 1485-1490. (d) Zhang, Z.; Kline, S. A.; Kirley, T. A.; Goldstein, B. D.; Witz, G. *Arch.* Pathways of trans,trans-muconaldehyde metabolism in mouse liver cytosol: reversibility of monoreductive metabolism and formation of end products. *Toxicol.* **1993**, *67*, 461-467. (e) Lan, Q.; Zhang, L. Li, G.; Vermeulen, R.; Weinberg, R. S.; Dosemeci, M.; Rappaport, S. M.; Shen, M.; Alter, B. P.; Wu, Y.; Kopp, W.; Waidyanatha, S.; Rabkin, C.; Guo, W.; Chanock, S.; Hayes, R. B.; Linet, M.; Kim, S.; Yin, S.; Rothman, N.; Smith, M. T. Hematotoxicity in workers exposed to low levels of benzene. *Science* **2004**, *306*, 1774-1776. (f) Smith, M. T. The mechanism of benzene-induced leukemia: a hypothesis and speculations on the causes of leukemia. *Environ. Health Persp.* **1996**, *104*, suppl. 6, 1219-1225. (g) Stillman, W. S.; Varella-Garcia, M.; Irons, R. D. The benzene metabolite, hydroquinone, selectivity induced 5q31 – and – 7 in human CD34<sup>+</sup> CD19<sup>-</sup> bone marrow cells. *Exp. Hematol.* **2000**, *28*, 169-176. (h) Esterbauer, H.; Schaur, R. J.; Zollner, H. Chemistry and biochemistry of 4-hydroxynonenal, malonaldehyde and related aldehydes. *Free Radical Biol. Med.* **1991**, *11*, 81-128. (i) Marrubini, G.; Calleri, E.; Coccini, T.; Castoldi, A. F.; Manzo, L. Direct analysis of phenol, catechol and hydroquinone in human urine by coupled-column HPLC with fluorimetric detection. *Chromatographia* **2005**, *62*, 25-31. DOI: 10.1365/s10337-005-0570-3. (j) Yin, S.; Hayes, R. B.; Linet, M. S.; Li, G.; Dosemeci, M.; Travis, L. B.; Li, C.; Zhang, Z.; Li, D.; Chow, W.; Wacholder, S.; Wang, Y.; Jiang, Z.; Dai, T.; Zhang, W.; Chao, X.; Ye, P.; Kou, Q.; Zhang, X.; Lin, X.; Meng, J.; Ding, C.; Zho, J. Blot, W. A cohort study of cancer among benzene-exposed workers in China: overall results. *Am. J. Ind. Med.* **1996**, *29*, 227-235. (k) Hayes, R. B.; Yin, S.; Dosemeci, M.; Li, G.; Wacholder, S.; Travis, L. B.; Li, C.; Rothman, N.; Hoover, R. N.; Linet, M. S. Benzene and the dose-related incidence of hematologic neoplasms in China. *Journal of the National Cancer Institute* **1997**, *89*, 1065-1071.
22. (a) Beckman-Sundh, U.; Binderup, M-L.; Bolognesi, C.; Brimer, L.; Castle, L.; Di Domenico, A.; Engel, K.; Franz, R.; Gontard, N.; Gurtler, R.; Husoy, T.; Jany, K.; Kolf-

- Clauw, M.; Leclercq, C.; Mennes, W.; Milana, M. R.; de Fatima Pocas, M.; Prarr, I.; Svensson, K.; Toldra, F.; Wolfle, D. Scientific opinion on the toxicological evaluation of phenol. *EFSA Journal* **2013**, *11*, 3189. DOI: 10.2903/j.efsa.2013.3189. (b) Frumkin, H.; Gerberding, J. L. *Toxicological Profile for Phenol*; U.S. Department of Health and Human Services: Washington D.C., 2008 pp 21-93.
23. (a) Miller, E. S.; Peretti, S. W. Toluene bioconversion to *p*-hydroxybenzoate by Fed-Batch cultures of recombinant *Pseudomonas putida*. *Biotechnol. Bioeng.* **2002**, *77*, 340-351. DOI: 10.1002/bit.10071. (b) Ramos-González, M.-I.; Ben-Bassat, A.; Campos, M.-J.; Ramos, J. L. Genetic engineering of a highly solvent-tolerant *Pseudomonas putida* strain for biotransformation of toluene to *p*-hydroxybenzoate. *Appl. Environ. Microb.* **2003**, *69*, 5120-5127. DOI: 10.1128/AEM.69.9.5120-5127.2003.
24. (a) Aresta, M.; Quaranta, E.; Liberio, R.; Dileo, C.; Tommasi, I. Enzymatic synthesis of 4-OH benzoic acid from phenol and CO<sub>2</sub>: the first example of a biotechnological application of a carboxylase enzyme. *Tetrahedron* **1998**, *54*, 8841-8846. (b) Aresta, M.; Dibenedetto, A. Development of environmentally friendly syntheses: use of enzymes and biomimetic systems for the direct carboxylation of organic substrates. *Rev. Mol. Biotechnol.* **2002**, *90*, 113-128. (c) Schüle, K.; Fuchs, G. Phenylphosphate carboxylase: a new C-C lyase involved in anaerobic phenol metabolism in *Thauera aromatica*. *J. Bacteriol.* **2004**, *186*, 4556-4567. DOI: 10.1128/JB.186.14.4556-4567.2004. (d) Dibenedetto, A.; Lo Noce, R.; Pastore, C.; Aresta, M.; Fragale, C. First in vitro use of the phenylphosphate carboxylase enzyme in supercritical CO<sub>2</sub> for the selective carboxylation of phenol to 4-hydroxybenzoic acid. *Environ. Chem. Lett.* **2006**, *3*, 145-148. DOI: 10.1007/s10311-005-0019-9. (e) van Herk, T.; Hartog, A. F.; van der Burg, A. M.; Wever, R. Regioselective phosphorylation of carboxylates and various alcohols by bacterial acid phosphatases; probing the substrate specificity of the enzyme from *Shigella flexneri*. *Adv. Synth. Catal.* **2005**, *347*, 1155-1162. DOI: 10.1002/adsc.200505072.
25. (a) Barker, J. L.; Frost, J. W. Microbial synthesis of *p*-hydroxybenzoic acid from glucose. *Biotechnol. Bioeng.* **2001**, *76*, 376-390. (b) Nichols, B. P.; Green, J. M. Cloning and sequencing of *Escherichia coli* *ubiC* and purification of chorismate lyase. *J. Bacteriol.* **1992**, *174*, 5309-5316. (c) Holden, M. J.; Mayhew, M. P.; Gallagher, D. T.; Vilker, V. L. Chorismate lyase: kinetics and engineering for stability. *Biochim. Biophys. Acta* **2002**, *1594*, 160-167.
26. Johnson, B. F.; Amaratunga, M.; Lobos, J. H. Method for increasing total production of 4-hydroxybenzoic acid by biofermentation. US 6114157, September 5, 2000.
27. Sigma-Aldrich. Amberlite® IRA-400 Chloride Form. <http://www.sigmaaldrich.com/catalog/product/aldrich/247669?lang=en&region=US> (accessed Dec 27, 2016).
28. Camakaris, H.; Pittard, J. Tyrosine Biosynthesis. In *Amino Acids: Biosynthesis and Genetic Regulation*. Herrmann, K. M. Ed.; Somerville, R. L., Ed.; Addison-Wesley: Massachusetts, 1983; p339-350.

29. (a) Verhoef, S.; Ruijsenaars, H. J.; de Bont, J. A. M.; Wery, J. Bioproduction of *p*-hydroxybenzoate from renewable feedstock by solvent-tolerant *Pseudomonas putida* S12. *J. Biotechnol.* **2007**, *132*, 49-56. DOI: 10.1016/j.jbiotec.2007.08.031. (b) Meijnen, J.-P.; Verhoef, S.; Briedjal, A. A.; Ruijsenaars, H. J. Improved *p*-hydroxybenzoate production by engineered *Pseudomonas putida* S12 by using a mixed-substrate feeding strategy. *Appl. Microbiol. Biotechnol.* **2011**, *90*, 885-893. DOI: 10.1007/s00253-011-3089-6.
30. Siebert, M.; Sommer, S; Li, S.-M.; Wang, Z.-X.; Severin, K.; Heide, L. Genetic engineering of plant secondary metabolism. *Plant Physiol.* **1996**, *112*, 811-819.
31. Mayer, M. J.; Narbad, A.; Parr, A. J.; Parker, M. L.; Walton, N. J.; Mellon, F. A.; Michael, A. J. Rerouting the plant phenylpropanoid pathway by expression of a novel bacterial enoyl-CoA hydratase/lyase enzyme function. *Plant Cell* **2001**, *13*, 1669-1682.
32. Viitanen, P. V.; Devine, A. L.; Khan, M. S.; Deuel, D. L.; Van Dyk, D. E.; Daniell, H. Metabolic engineering of the chloroplast genome using the *Escherichia coli* *ubiC* gene reveals that chorismate is a readily abundant plant precursor for *p*-hydroxybenzoic acid biosynthesis. *Plant Physiol.* **2004**, *136*, 4048-4060.
33. McQualter, R. B.; Chong, B. F.; Meyer, K.; Van Dyk, D. E.; O'Shea, M. G.; Walton, N. J.; Viitanen, P. V.; Brumbley, S. M. Initial evaluation of sugarcane as a production platform for *p*-hydroxybenzoic acid. *Plant Biotechnol. J.* **2005**, *3*, 29-41.
34. Eykman, J. F. Ueber die shikimisaure. *Ber. Dtsch. Chem. Ges.* **1891**, *24*, 1278-1303.
35. Gibson, J. M.; Thomas, P. S.; Thomas, J. D.; Barker, J. L.; Chandran, S. S.; Harrup, M. K.; Draths, K. M.; Frost, J. W. Benzene-free synthesis of phenol. *Angew. Chem. Int. Ed.* **2001**, *40*, 1945-1948.
36. Abrecht, S.; Harrington, P.; Idling, H.; Karpf, M.; Trussardi, R.; Wirz, B.; Zutter, U. The synthetic development of the anti-influenza neuraminidase inhibitor Oseltamivir phosphate (Tamiflu®): a challenge for synthesis & process research. *Chimia* **2004**, *58*, 621-629.
37. Rapisarda, A. Economic Importance and Market Trends of the Genera *Pimpinella*, *Illicium*, and *Foeniculum*. In *Illicium, Pimpinella and Foeniculum*. Jodral, M. M., Ed.; CRC: Boca Raton, 2004; p 191-218.
38. (a) Draths, K. M.; Knop, D. R.; Frost, J. W. Shikimic acid and quinic acid: replacing isolation from plant sources with recombinant microbial biocatalysis. *J. Am. Chem. Soc.* **1999**, *121*, 1603-1604. DOI: 10.1021/ja9830243. (b) Knop, D. R.; Draths, K. M.; Chandran, S. S.; Barker, J. L.; von Daeniken, R.; Weber, W.; Frost, J. W. Hydroaromatic equilibration during biosynthesis of shikimic acid. *J. Am. Chem. Soc.* **2001**, *123*, 10173-10182. DOI: 10.1021/ja0109444. (c) Chandran, S. S.; Yi, J.; Draths, K. M.; von Daeniken, R.; Weber, W.; Frost, J. W. Phosphoenolpyruvate availability and the biosynthesis of shikimic acid. *Biotechnol. Prog.* **2003**, *19*, 808-814. DOI: 10.1021/bp025769p.

39. (a) Avula, B.; Wang, Y.-H.; Smillie, T. J.; Khan, I. A. Determination of shikimic acid in fruits of *Illicium* species and various other plant samples by LC-UV and LC-ESI-MS. *Chromatographia* **2009**, *69*, 307-314. DOI: 10.1365/s10337-008-0884-z. (b) Bohm, B. A. Shikimic acid (3,4,5-trihydroxy-1-cyclohexene-1-carboxylic acid). *Chem. Rev.* **1965**, *65*, 435-466.
40. Hirayama, Y. ICL-IP Japan. Global Bromine Industry and Its Outlook. [http://www.bromine.chem.yamaguchi-u.ac.jp/library/L02\\_Global%20Bromine%20Industry.pdf](http://www.bromine.chem.yamaguchi-u.ac.jp/library/L02_Global%20Bromine%20Industry.pdf) (accessed 6/14/2017).
41. Li, W.; Xie, D.; Frost, J.W. Benzene-free synthesis of catechol: interfacing microbial and chemical catalysis. *J. Am. Chem. Soc.* **2005**, *127*, 2874-2882. DOI: 10.1021/ja045148n.
42. Pearson, R. G.; Songstad, J. Application of the principle of hard and soft acids and bases to organic chemistry. *J. Am. Chem. Soc.* **1967**, *89*, 1827-1836.
43. Noyce, D. S.; Virgilio, J. A. The synthesis and solvolysis of 1-phenylethyl disubstituted phosphinates. *J. Org. Chem.* **1972**, *37*, 2643-2647.
44. Alexandratos, S. D. ion-exchange resins: a retrospective from *industrial and engineering chemistry research*. *Ind. Eng. Chem. Res.* **2009**, *48*, 388-398. DOI: 10.1021/ie801242v.
45. Rickborn, B.; Lwo, S. Conformational effects in cyclic olefins. Kinetic and stereochemistry of epoxidation of some alkyl-substituted cyclohexenes. *J. Org. Chem.* **1965**, *30*, 2212-2216.
46. Flowers, L.; Boyes, W.; Foster, S.; Gehlhaus, M.; Hogan, K.; Marcus, A.; McClure, P.; Osier, M.; Ronney, A. Toxycological Review of Toluene; U.S. Environmental Protection Agency; Washington D.C., 2005.
47. (a) Gruzdev, M. S.; Ramenskaya, L. M.; Chervonova, U. V.; Kumeev, R. S. Preparation of 1-butyl-3-methylimidazolium salts and study of their phase behavior and intramolecular interactions. *Russ. J. Gen. Chem.* **2009**, *79*, 1720-1727. (b) Golovanov, D. G.; Lyssenko, K. A.; Antipin, M. Y.; Vygodskii, Y. S.; Lozinskaya, E. I.; Shaplov, A. S. Cocrystal of an ionic liquid with organic molecules as a mimic of ionic liquid solution. *Cryst. Growth Des.* **2005**, *5*, 337-340. DOI: 10.1021/cg030086i.
48. Rodriguez-Zubiri, M.; Anguille, S.; Brunet, J. Intermolecular hydriamination of non-activated alkenes catalyzed by Pt(II) or Pt(IV)-*n*-Bu<sub>4</sub>PX (X = Cl, Br, I) systems: key effect of the halide anion. *J. Mol. Catal. A-Chem.* **2007**, *271*, 145-150. DOI: 10.1016/j.molcata.2007.02.011.
49. (a) Khrizman, A.; Chen, H.; Moyna, G. Synthesis of sequentially deuterated 1-*n*-butyl-3-methylimidazolium ionic liquids. *J. Labelled Compd. Rad.* **2011**, *54*, 401-407. DOI: 10.1002/jlcr.1884. (b) Wilkes, J. S.; Levisky, J. A.; Wilson, R. A.; Hussey, C. L. Dialkylimidazolium chloroaluminate melts: a new class of room-temperature ionic liquids for

electrochemistry, spectroscopy, and synthesis. *Inorg. Chem.* **1982**, *21*, 1263-1264.

50. Elming, N. Transformation of 2-( $\beta$ ,  $\beta$ -dicarbomethoxyethyl)-furan into *m*-hydroxybenzoic acid. *Acta Chem. Scand.* **1956**, *10*, 1664-1666.

## CHAPTER THREE

### Scale-Up of the Synthesis of Biobased *p*-Hydroxybenzoic Acid

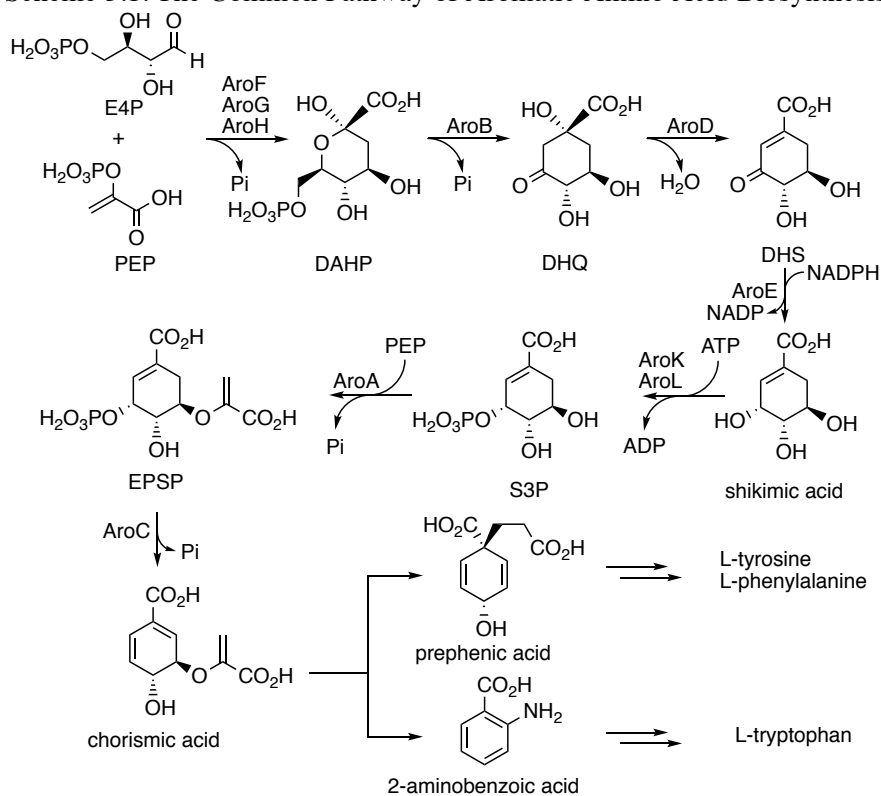
#### 1. Introduction

The reaction conditions for the synthesis of biobased *p*-hydroxybenzoic acid were described in Chapter 2. This chapter focuses on the scale-up of the synthesis of biobased *p*-hydroxybenzoic acid. Scale-up includes: (a) the microbial synthesis of shikimic acid from glucose under fermentor-controlled conditions from 1 L to 20 L; (b) elaboration and scale-up of a modified isolation and purification of shikimic acid from fermentation broth; (c) scale-up of the aromatization of shikimic to form *p*-hydroxybenzoic acid from 1 g reaction to 250 g reaction; (d) scale-up of the purification of biobased *p*-hydroxybenzoic acid. The starting material, shikimic acid, is microbially synthesized with *E. coli* SP1.1/pKD15.071B, which was previously genetically engineered in the Frost group.<sup>1</sup> Although fed-batch fermentation at 1 L scale with this strain had been performed routinely, scale-up of the microbial synthesis to 20 L scale in the Frost group has not been previously attempted. The current commercial method for isolation of shikimic acid from fermentation broth employs ion exchange columns followed by crystallization from highly flammable solvents. Use of ion exchange columns requires evaporating large quantities of water and generates large salt waste streams associated with regeneration of the ion exchange resins. The aromatization of shikimic to form *p*-hydroxybenzoic acid was scaled up from 1 g reaction to 250 g reaction. In addition to biobased *p*-hydroxybenzoic acid synthesis, microbial synthesis of shikimic acid is also scaled up from a 1 L fermentation to a 20 L fermentation in this chapter. Furthermore, downstream isolation and purification of shikimic acid is developed. Employment of hollow fiber filtration for cell removal and tangential flow filtration systems for protein removal from the 30 L fermentation

broth greatly expedited cell removal and broth clarification. Shikimic acid is highly water soluble, which makes isolation from fermentation broth challenging. A continuous countercurrent extraction of shikimic acid was developed to overcome this challenge.

## 2. *E. coli* SP1.1/pKD15.071B

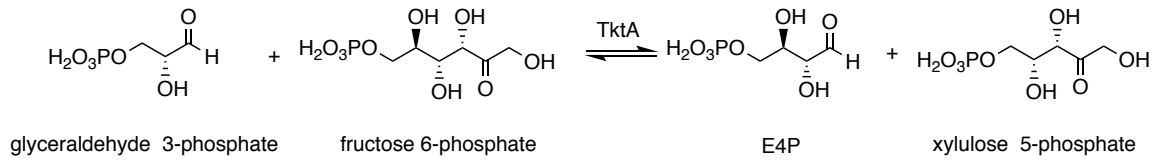
Scheme 3.1. The Common Pathway of Aromatic Amino Acid Biosynthesis



E4P: erythrose 4-phosphate; PEP: phosphoenolpyruvate;  
 DAHP: 3-deoxy-D-*arabino*-heptulosonic acid 7-phosphate; DHQ: 3-dehydroquinic acid;  
 DHS: 3-dehydroshikimic acid; S3P: shikimate 3-phosphate; EPSP: 5-enolpyruvylshikimate 3-phosphate;  
 AroF: DAHP synthase (tyrosine feedback); AroG: DAHP synthase (phenylalanine feedback);  
 AroH: DAHP synthase (tryptophan feedback); AroB: DHQ synthase; AroD: DHQ dehydratase;  
 AroE: shikimate dehydrogenase; AroK: shikimate kinase I; AroL: shikimate kinase II;  
 AroA: EPSP synthase; AroC: chorismate synthase

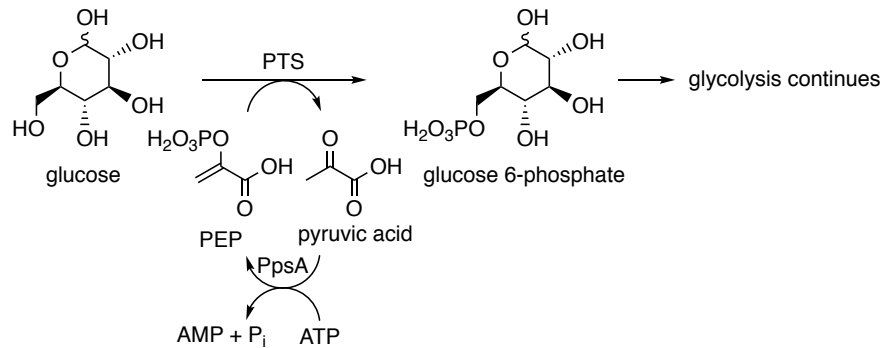
Shikimic acid is a key intermediate in the common pathway of aromatic amino acid biosynthesis. This pathway, which is found in plants, bacteria, fungi and parasites,<sup>2</sup> converts phosphoenolpyruvic acid (PEP) and erythrose 4-phosphate (E4P) into chorismic acid via seven enzyme-catalyzed reactions (Scheme 3.1).<sup>2a,3</sup>

Scheme 3.2. Biosynthesis of Erythrose 4-phosphate



TktA: transketolase; E4P: erythrose 4-phosphate

Scheme 3.3. Increasing Phosphoenolpyruvic Acid Availability



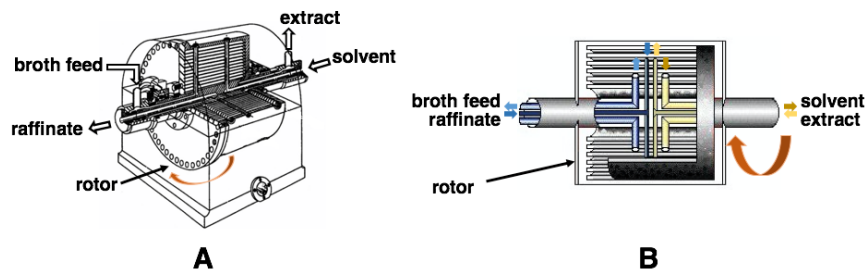
PEP: phosphoenolpyruvic acid; PpsA: PEP synthase; PTS: PEP:carbohydrate phosphotransferase

Modification of the host genome for microbial synthesis of shikimic acid included the insertion of *aroB* into the *serA* locus and disruption of *aroL* and *aroK* genes in the genome of *E. coli* SP1.1.<sup>1a,1b,4,5</sup> An extra copy of *aroB* enables overexpression of 3-dehydroquinic acid synthase, while disruption of shikimate kinase-encoding *aroL* and *aroK* prevents phosphorylation of shikimic acid. Disruption of L-serine biosynthesis due to loss of genomic *serA*-encoded phosphoglycerate dehydrogenase ensures that plasmid pKD15.071B, which encodes *serA*, *aroF<sup>FBR</sup>*, *aroE*, *tktA* and *ppsA* is retained by *E. coli* SP1.1 during cultivation in minimal salts medium in the absence of L-serine supplementation.<sup>1a-c,4ab,6,7a,8a</sup> Overexpression of *aroF<sup>FBR</sup>*, which encodes a mutant isozyme of 3-deoxy-D-arabino-heptulosonic acid 7-phosphate synthase insensitive to feedback inhibition by tyrosine, helps to increase carbon flow into the common pathway.<sup>1a,4b</sup> Shikimate dehydrogenase, encoded by *aroE*, was overexpressed to compensate for feedback inhibition of AroE by shikimic acid.<sup>1a,4a</sup> *In vitro* experiments have

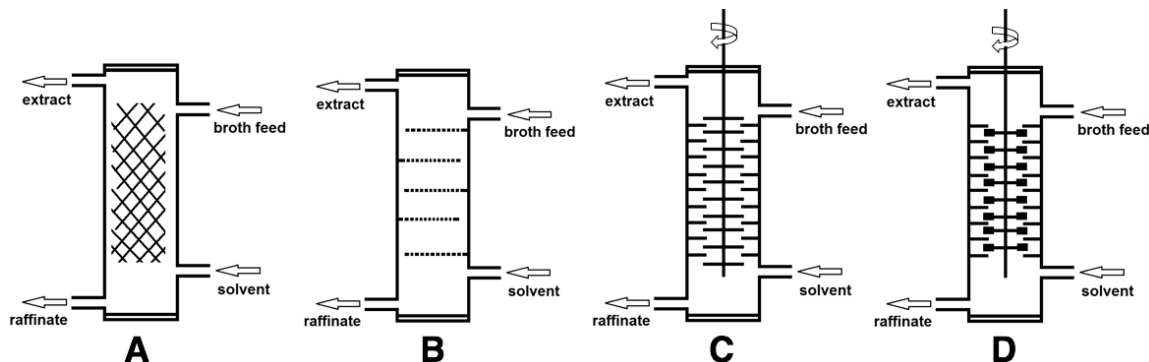
shown that E4P dimerization occurs at high concentrations of E4P in aqueous solutions.<sup>7b</sup> By balancing the rate of E4P consumption with the rate of E4P synthesis in vivo, the steady state concentration of E4P may be sufficiently low to avoid dimerization.<sup>7a</sup> The maintenance of a low steady state concentration of E4P in vivo to avoid dimerization may explain why E4P has never been detected in biological systems. In order to increase the availability of E4P to the common pathway, *tktA*-encoded transketolase was also overexpressed (Scheme 3.2).<sup>1b,9</sup> PEP drives PTS-mediated transport and phosphorylation of glucose to glucose 6-phosphate. There is a competition for PEP between PTS-mediated glucose transport and biosynthesis of DAHP (Scheme 3.3).<sup>8b</sup> In order to compensate for the competition with PTS-mediated glucose transport, PEP availability was increased by amplified expression of *ppsA*-encoded PEP synthase so that pyruvic acid is recycle back to PEP (Scheme 3.3).<sup>1c</sup>

### 3. Countercurrent Flow Extraction

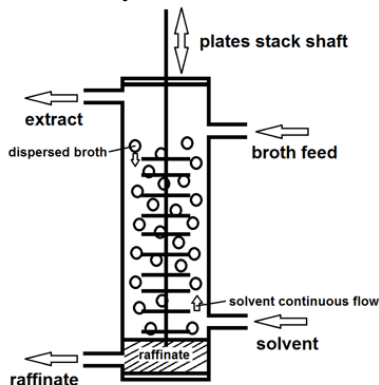
There are two general methods of liquid-liquid extraction in the chemical industry. One employs a mix/decant tank, which is similar to a huge separatory funnel. The other is countercurrent extraction. Disadvantages to a mix/decant tank include the requirement of multiple solvent additions to achieve the desired number of theoretical plates (one extraction is equivalent to one theoretical plate), recovery and recycling of the large volume of solvent required for each extraction and the requirement that the extraction be performed in batches. Countercurrent extraction, on the other hand, has several advantages over the mix/decant method of extraction. These include a higher number of theoretical extraction plates and the ability to be operated continuously. There are different types of countercurrent extraction equipment such as a centrifugal extractor, packed column, sieve tray column, rotating disc contactor (RDC) extractor, SCHEIBEL® column and KARR® reciprocating column.<sup>10a</sup>



\* Configuration example when solvent density is lower than broth  
 Figure 3.1. A: Centrifugal Extractor, B: Rotor of Centrifugal Extractor<sup>10</sup>



\* Configuration example when solvent density is lower than broth  
 Figure 3.2. A: Packed Column, B: Sieve Tray Column, C: RDC Extractor, D: SCHEIBEL® Column



\* Configuration example when solvent density is lower than broth; broth is dispersed in the solvent.  
 Figure 3.3. KARR® Column

In these countercurrent extraction systems, a high density liquid (heavy phase) and a lower density liquid (light phase) flow in opposite directions. In a centrifugal extractor, a heavy phase and a light phase are mixed in a rotor (Figure 3.1A).<sup>10</sup> The heavy phase is siphoned off from the outer area of the rotor while the light phase is collected near the center of the rotor (Figure 3.1B).<sup>10</sup> Packed columns have a mesh structure in the column which disrupts the flow of one of

the phases, breaking it up into droplets. These droplets have a high surface area which facilitates the interaction between the heavy and light phases (Figure 3.2A).<sup>10a</sup> A sieve tray column use sieves rather than a mesh column to break up one of the phases into droplets (Figure 3.2B).<sup>10a</sup> Rotating disc contactor (RDC) extractors and SCHEIBEL® columns have rotating impellers for the same reason (Figure 3.2C and 2D).<sup>10a</sup> KARR® reciprocating columns (KARR® column) have a stack of plates on a shaft, which oscillates up-and-down in order to disrupt one of the phases into droplets (Figure 3.3).<sup>10a</sup> Each instrument has different characteristics. Centrifugal extractors can handle small density differences between two phases while providing several theoretical plates. However, these extractors are susceptible to fouling and plugging.<sup>10a</sup> Packed columns and sieve tray columns can process larger volumes per unit time than the other four extraction systems, although the number of theoretical plates is lower than the other four extraction systems. Also, packed columns are not suitable for small scale extractions.<sup>10a</sup> RDC extractors are suitable for viscous material but have fewer theoretical plates than centrifugal extractors, SCHEIBEL® columns or KARR® columns.<sup>10a</sup> SCHEIBEL® columns have a high number of theoretical plates and are suitable for a wide range of sample volumes.<sup>10a</sup> KARR® columns also have a high number of theoretical plates and can be suited to a wide range of sample volumes but they have the additional advantage of having the highest process volume per unit time .<sup>10a</sup>

In this chapter, a KARR® column was employed to extract shikimic acid from fermentation broth. The fermentation broth and the extraction solvent are fed into the KARR® column, one from the top and the other from the bottom, and flow through the column in opposite directions. The fermentation broth feed and the extraction solvent are assigned for different phases. One phase, called the continuous phase, fills the column chamber and is fed at

a high flow rate. The other phase is fed more slowly and therefore disperses into small droplets. (Figure 3.3). This dispersion of one phase into a continuous phase affords a high extraction surface area. Whether the broth feed is used as the continuous or dispersed phase depends on the molecule to be extracted and the characteristics of both broth and solvent. Four configuration choices using light or heavy extraction solvents are illustrated in Figure 3.4.<sup>10</sup> A light solvent such as *n*-butanol or EtOAc will have a lower density than the fermentation broth. A heavy solvent such as dichloromethane or chloroform will have a higher density than the broth. The interface level of each configuration is adjusted so as to not disturb the addition of either feed nor solvent (Figure 3.4).<sup>10a</sup> The solvent of configuration A and B has a lower density than the broth (Figure 3.4A and B). The column is filled with broth and the solvent is dispersed in the configuration A (Figure 3.4A). In the configuration B, the column is filled with solvent and the broth is dispersed (Figure 3.3 and 4B). The solvent of configuration C and D has a higher density than broth (Figure 3.4C and D). The column is filled with broth and the solvent is dispersed in configuration C (Figure 3.4C). In configuration D, the column is filled with solvent and the broth is dispersed (Figure 3.4D). The configuration of the KARR® column, the flow rate of the solvent and feed, the stroke rate of the plates stack shaft (agitation speed) and the material that the plates stack shaft is made of are experimentally determined.

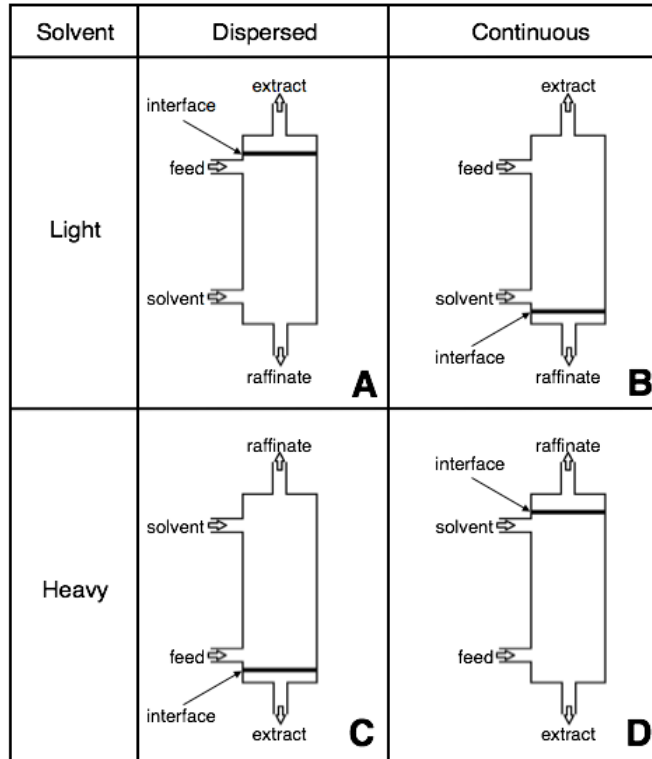


Figure 3.4. KARR® Column Configuration<sup>10</sup>

#### 4. Tangential (Cross) Flow Filtration

Employment of a tangential (cross) flow filtration shortens the time required to remove cells and proteins from fermentation broth. In a tangential flow filtration system, the feed stream flows perpendicularly to pores of the filter (Figure 3.5A).<sup>12</sup> The retentate is recirculated as a portion of the feed stream to complete filtration without clogging the filter with cells or proteins. In a dead-end filtration system, the feed stream flows parallel to the pores of the filter resulting in a buildup of cells or proteins on the filter (Figure 3.5B),<sup>12</sup> which slows and eventually halts filtration.

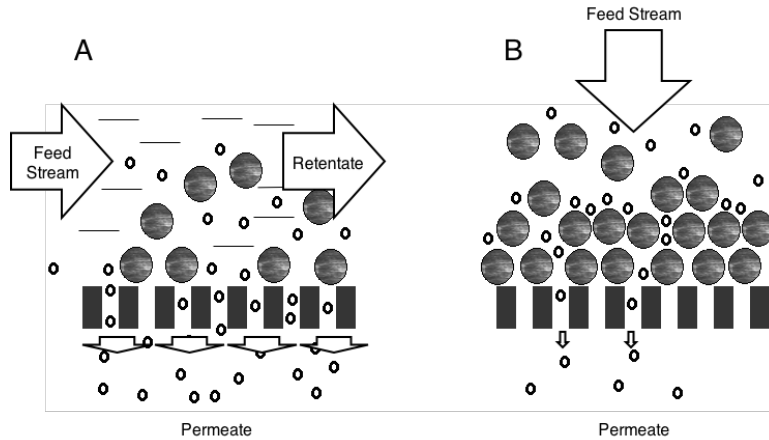


Figure 3.5. A: Tangential (Cross) flow filtration, B: Dead-End Filtration

A hollow fibers cartridge is made of multiple straw-shaped filters (Figure 3.6A). The feed stream enters the one end of straws and the retentate comes out from the other end. Each straw possesses numerous pores that can separate various particle by their sizes (Figure 3.6B).

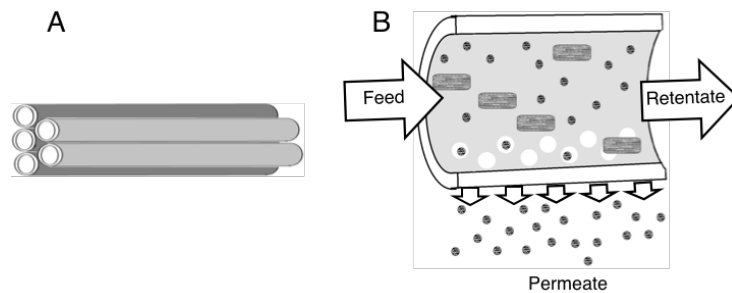


Figure 3.6. Hollow Fibers

In this chapter, microbial synthesis of shikimic acid from glucose is scaled up to 20 L scale. Downstream processing of the fermentation broth employs tangential flow filtration to remove cells and proteins followed by a countercurrent extraction of shikimic acid with a KARR® column. 1-Butyl-3-methylimidazolium bromide is employed as both solvent and catalyst in the scaled up synthesis of biobased *p*-hydroxybenzoic acid from the microbially synthesized shikimic acid.

## 5. Results

### 5.1. Shikimic Acid Titrers and Yield

The shikimic acid synthesizing strain,<sup>1</sup> *E. coli* SP1.1/pKD15.071B was cultured at 20 L scale in a 30 L working volume fermentor at pH 7.0 and 33 °C. Glucose-rich culture conditions were employed such that the concentration of glucose in the medium was maintained in the range of 19-43 g/L throughout the run. The stir and airflow rate were allowed to vary in order to maintain dissolved O<sub>2</sub> level at 10% of air saturation. The air flow was supplemented with O<sub>2</sub> when the stir and airflow rate could not maintain dissolved O<sub>2</sub> levels. This 20 L cultivation of *E. coli* SP1.1/pKD15.071B was run for 61 h and achieved a shikimic acid titer of 72 g/L synthesized in a 34% yield from glucose. The final fermentation broth volume was 30 L after addition of glucose solution, NH<sub>4</sub>OH and 2N H<sub>2</sub>SO<sub>4</sub> to control pH. Prior to isolation and purification of shikimic acid, cells were removed from crude fermentation broth by filtration through a hollow fiber membrane column (GE Healthcare). Protein was then removed using a tangential flow filtration apparatus fitted with four 10 kD ultrafiltration cassettes (Sartorius).

### 5.2. Shikimic Acid Extraction Solvent Screening

The partition coefficient of shikimic acid in several solvents was measured (Table 3.1). Cell-free, protein-free shikimic acid fermentation broth was concentrated by boiling off water to approximately 1/5 of the original broth volume and then acidified with H<sub>2</sub>SO<sub>4</sub> to pH 2.5. The final volume was adjusted with water to 1/4 of original broth volume. Each extraction was performed in a vial with 0.5 mL concentrated broth and 0.5 mL solvent. The solvent and the broth were mixed by continuously rotating vertically (7 rotations/min) for 12 h using a hybridization incubator. The shikimic acid concentration of extracts and raffinate were

determined by HPLC. The partition coefficient of shikimic acid was calculated using Formula 1.

Formula 1. Partition Coefficient

$$\text{Partition Coefficient} = \frac{[\text{SA}] \text{ in extract}}{[\text{SA}] \text{ in raffinate}}$$

The total of 14 solvents were tests including nine alcohols, three ketones and two carboxylic acids (Table 3.1). Methanol, ethanol, *n*-propanol, isopropanol, acetone, acetic acid and propionic acid are miscible with water. Surprisingly, not only could *n*-propanol, isopropanol and acetone work as extraction solvents, they were the best three solvents in the screening experiments (Table 3.1, entry 6, 7 and 10). These three solvents were miscible with a fermentation broth when it was not concentrated. However, highly concentrated fermentation broth led to a two-phase mixture upon addition of the water-miscible solvents.

Table 3.1. Shikimic Acid Partition Coefficient in Various Solvents

entry	solvent	relative polarity <sup>13a</sup>	solubility in H <sub>2</sub> O <sup>13b</sup> (g/L at pH 2)	partition coefficient
1	methanol	0.762	234	no separation
2	ethanol	0.654	183	no separation
3	<i>n</i> -butanol	0.586	48	0.192
4	2-butanol	0.506	68	0.234
5	isobutanol	0.552	68	0.161
6	<i>n</i> -propanol	0.617	100	0.466
7	isopropanol	0.546	141	0.627
8	<i>n</i> -hexanol	0.559	9	0.055
9	cyclohexanol	0.509	44	0.181
10	acetone	0.355	95	0.957
11	4-methyl-2-pentanone	0.327	12	0.113
12	2-butanone	0.269	47	0.100
13	acetic acid	0.648	197	no separation
14	propionic acid	0.611	96	no separation

### 5.3. Countercurrent Extraction of Shikimic Acid

The configuration of the KARR® column, the flow rate of the solvent and feed, the stroke rate of the plates stack shaft (agitation speed) and the impact of the materials used to

construct the plates stack shaft among other valuable were experimentally determined. There are some clues that assist in making these decisions. The guidelines to make the decisions were collected and summarized in Table 2.<sup>10,11</sup> If following suggestion of the table 2 does not solve a coalesce, a different solvent should be used (Table 3.2, entry 1). A rag layer is a layer of solids that builds up at the interface. This might be prevented by reversing phases (Table 3.2, entry 2). If the solids are impurities, the rag layer may be filtered and the filtrate is recirculated into the column. When a band of droplets builds up at the interface (emulsion band), this indicates that there is not enough time to let the dispersed phase settle. Reversing phases, slowing down the flow rates or reducing agitation rate will give the dispersed phase more time to settle at the interface (Table 3.2, entry 3). When a phase exits from the wrong exit port, it is called entrainment. Reducing flow rates and/or reducing agitation rate will prevent an entrainment. Alternatively, a mixture of two phases can be separated outside of the column (Table 3.2, entry 4). If a second interface forms in the column (flooding), the flow rate should be increased or agitation rate should be reduced (Table 3.2, entry 5).

Table 3.2. Problems Seen During KARR® Column Optimization<sup>10,11</sup>

entry	Problem	Description	Suggestion
1	Coalesce	dispersed phase is fused	Increase agitation speed Change flow rate Reverse phases Change solvent
2	Rag layer	solids built up at the interface	Reverse phases Filter the rag layer liquid and recirculate
3	Emulsion band	a band of droplets built up at interface	Reverse phases Slow down flow rate Reduce agitation speed
4	Entrainment	a phase exits from the from the wrong exit port	Reduce flow rate Reduce agitation speed Separate into two phase outside of column
5	Flooding	second interface forms in the column	Increase the flow rate Reduce agitation speed

The cell-free, protein-free shikimic acid fermentation broth was concentrated by boiling off water to approximately 20% of the original broth volume. Concentrated H<sub>2</sub>SO<sub>4</sub> was then added to adjust the concentrated fermentation broth to pH 2.5. Water was subsequently added so that the final volume of the concentrated, pH-adjusted solution was 25% of the starting fermentation broth volume. A KARR® column (Figure 3.3) was used to extract shikimic acid from the concentrated fermentation broth. Water-miscible solvents (*t*-butanol, acetone, *n*-propanol, isopropanol) and water-immiscible solvents (*n*-butanol, 2-butanol) were examined as extracting solvents. Acidified concentrated broth (100 mL) containing shikimic acid (30 g) was subjected to countercurrent extraction using *n*-butanol, 2-butanol and *t*-butanol. *t*-Butanol was melted before use. A broth feed flow rate of 5 mL/min and a solvent flow rate of 40 mL/min were used (Figure 3.3). The % recovery of shikimic acid from the fermentation broth for *n*-butanol, 2-butanol and *t*-butanol were 57%, 60% and 73% respectively (Table 3.3). The acidified concentrated broth (100 mL) containing shikimic acid (30 g) was also submitted to countercurrent extraction using *n*-propanol, acetone and isopropanol. A broth feed flow rate of 5 mL/min and a solvent flow rate of 10 mL/min were used in these instances (Figure 3.3). The % recovery of shikimic acid from the fermentation broth for *n*-propanol, acetone and isopropanol were 77%, 80% and 80% respectively (Table 3.3). These water-miscible solvents led to a thick, doughy raffinate that clogged the countercurrent extraction column resulting in termination of the extraction during scale-up. The % recovery of the isopropanol and acetone extractions were better than *n*-propanol. The clogging problem was worse in acetone extraction than isopropanol. Therefore, isopropanol was chosen as the extraction solvent. An isopropanol/water (9:1, v/v) solution was used as the extraction solvent. Addition of water to the isopropanol eliminated the problem of raffinate clogging of the countercurrent extractor. Finally, acidified concentrated

broth (1000 mL) containing shikimic acid (272 g) was submitted to countercurrent extraction using isopropanol/water, 9:1, v/v. A broth feed flow rate of 10 mL/min and a solvent flow rate of 20 mL/min were used (Figure 3.3). This extraction with isopropanol/water, 9:1, v/v solution achieved a 95% recovery (Table 3.3).

Table 3.3. Countercurrent Extraction of Microbe-Synthesized Shikimic Acid

Entry	Solvent	Shikimic Acid (g) in Broth	Shikimic Acid (g) Extracted	Shikimic Acid % Recovery
1	<i>n</i> -butanol	30	17	57
2	2-butanol	30	18	60
3	<i>t</i> -butanol	30	22	73
4	<i>n</i> -propanol	30	23	77
5	acetone	30	24	80
6	isopropanol	30	24	80
7	isopropanol/water, 9:1, v/v	272	259	95

#### 5.4. Comparison of Shikimic Acid Crystallization Solvents

*n*-Butanol, 2-butanol, *n*-propanol, isopropanol, *t*-butanol and acetone containing varying contents of shikimic acid (Table 3.3) were concentrated using a rotary evaporator until formation of the first solid was observed, and crystallization subsequently allowed to proceed at rt overnight. The amount of shikimic acid obtained, % recovery, and purity as a function of solvent is summarized in Table 2. *n*-Butanol resulted in the highest % recovery (75%) and the best purity (94.3%) among these solvents (Table 3.4). No precipitate of shikimic acid was observed after standing at rt overnight for *t*-butanol and acetone extracts.

Table 3.4. % Purity and % Recovery of Crystallized Shikimic Acid

Entry	Solvent (azeotrope °C, wt% water) <sup>14</sup>	Shikimic Acid			
		in Extract (g)	Isolated (g)	% Recovery	%Purity
1	<i>n</i> -butanol (93 °C, 43%)	17.0	13.6	75	94.3
2	2-butanol (87 °C, 27%)	17.5	9.5	51	93.1
3	<i>n</i> -propanol (88 °C, 29%)	23.3	8.8	34	89.4
4	isopropanol (80 °C, 13%)	24.4	12.2	47	94.1

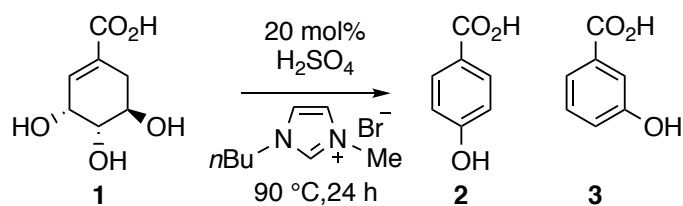
### 5.5. Purification of Shikimic Acid

The cell-free, protein-free shikimic acid fermentation broth 4 L was aliquoted from 30 L broth. A concentrated, pH-adjusted solution 1 L was prepared as aforementioned. Shikimic acid was extracted from this concentrated, pH-adjusted solution to isopropanol/water, 9:1, v/v with a KARR® column. Isopropanol/water, 9:1, v/v extract (2910 mL) containing shikimic acid (257 g) was decolorized with activated charcoal (10 wt% of shikimic acid). This solution was filtered and then concentrated. The residue was dissolved in boiling water (250 mL) prior to addition of *n*-butanol (1500 mL). Azeotropic removal of water using a rotary evaporator was conducted until crystallization was first observed and the solution immediately poured into a crystallization dish to afford the first crop of shikimic acid. During the azeotropic removal of water, a dark, brown-colored solid formed gradually at the bottom of the stripping flask. This was kept in the stripping flask when the crystallization solution was poured out. The dark, brown-colored solid remaining in the stripping flask was dissolved in boiling water (100 mL). *n*-Butanol (550 mL) was then added to the solution. The water was once again removed using a rotary evaporator until crystallization just began. The solution was poured into a crystallization dish to afford a

second crop of shikimic acid. The first and second crops of crystallized shikimic acid were collected by filtration after solutions of crystallizing shikimic acid were allowed to stand at rt overnight. For the first crop, 160 g of shikimic acid was obtained (61% recovery) with a purity of 98.4%. For the second crop, 36 g of shikimic acid was obtained (14% recovery) with a purity of 97.9%. This overall process afforded 196 g of shikimic acid (75% recovery).

## 5.6. Scale Up Synthesis of *p*-Hydroxybenzoic Acid

Scheme 3.4. Dehydration of Shikimic Acid



The dehydration reaction was scaled up to 250 g of shikimic acid **1** in 1-butyl-3-methylimidazolium bromide. 1-Butyl-3-methylimidazolium was synthesized *in situ* from 1-methylimidazole and 1-bromobutane. Shikimic acid in 1-butyl-3-methylimidazolium bromide (40 wt%) was heated at 90 °C with 20 mol % H<sub>2</sub>SO<sub>4</sub> for 24 h. The headspace of the reaction vessel was swept with a vigorous flow of N<sub>2</sub>. This reaction afforded a 74% yield of *p*-hydroxybenzoic acid **2** and a 19% yield of *m*-hydroxybenzoic acid **3**. The *p*-hydroxybenzoic acid **2** and *m*-hydroxybenzoic acid **3** were extracted into EtOAc with a continuous liquid-liquid extractor (Figure 3.7) followed by decolorization with activated charcoal. Concentration of the decolorized extract followed by crystallization in water afforded 64% *p*-hydroxybenzoic acid **2** as a white solid with a purity of 98.9%.

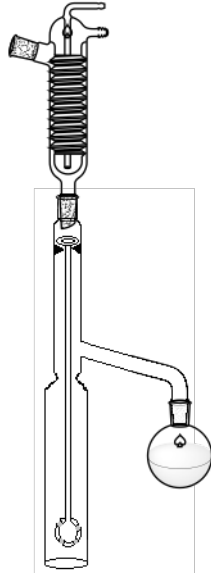


Figure 3.7. Continuous Liquid-Liquid Extractor

## 6. Discussion

The scale-up of the microbial synthesis of shikimic acid to 20 L scale employed  $O_2$ -supplemented air to afford a shikimic acid concentration in the fermentor broth of 72 g/L synthesized in 34% yield from glucose. Hollow fiber filtration of the 30 L of fermentation broth removed *E. coli* SP1.1/pKD15.071B cells followed by tangential flow filtration of the cell-free fermentation broth to remove protein resulting from cell lysis. The both filtration processes are suitable for 30 L or higher volume fermentation broth.

With respect to reported strategies for isolation of shikimic acid, Royal DSM performed countercurrent extraction of shikimic acid from concentrated fermentation broth residue using 2-butanone.<sup>15</sup> The DSM process began with the removal of water in the fermentation broth and ended with the crystallization of shikimic acid, achieving a 57% overall recovery of shikimic acid with 96% purity. During their countercurrent extraction, 1.2 L of the extraction solvent, 2-butanone, was used to extract only 10 g of shikimic acid.<sup>15</sup> This use of a large volume of solvent for isolation of a small quantity of shikimic acid is not practical. Unlike DSM's shikimic acid

extraction method, the countercurrent extraction using isopropanol/water, 9:1, v/v required only 77 mL of the solvent per 10 g of shikimic acid. Starting from concentration of fermentation broth to crystallization of shikimic acid, this novel process achieved a 71% overall recovery of shikimic acid with 98% purity.

The dehydration reaction of shikimic acid was successfully scaled up with a nearly quantitative conversion into *p*-hydroxybenzoic acid (74%) and *m*-hydroxybenzoic acid (19%). The isolated yield of *p*-hydroxybenzoic acid was 64% with a purity of 98.9%. The impurity in the isolated product was *m*-hydroxybenzoic acid (1%). The mother liquor from the crystallization contained *p*-hydroxybenzoic acid (10%) and *m*-hydroxybenzoic acid (17%). *m*-Hydroxybenzoic acid is often used as one of copolymers in LCPs.<sup>16</sup> Therefore, the mixture of *p*-hydroxybenzoic acid and *m*-hydroxybenzoic acid in the mother liquor can be used in polymerizations to afford melt-processible LCPs.

## 7. Experimental

### 7.1. General

$^1\text{H}$  NMR spectra were recorded on a 500 MHz spectrometer. Chemical shifts for  $^1\text{H}$  NMR spectra are reported (in parts per million) relative to residual non-deuterated solvent in  $\text{CDCl}_3$  ( $\delta = 7.26$  ppm) and  $\text{CD}_3\text{OD}$  ( $\delta = 3.34$  ppm). Chemical shifts for  $^1\text{H}$  NMR spectra in  $\text{D}_2\text{O}$  is reported (in parts per million) relative to residual non-deuterated sodium salt of 3-(trimethylsilyl) propionic-2,2,3,3- $\text{d}_4$  acid, TSP ( $\delta = 0.00$  ppm).  $^{13}\text{C}$  NMR spectra were recorded at 125 MHz and chemical shifts for these spectra were reported (in parts per million) relative to  $\text{CDCl}_3$  ( $\delta = 77.4$  ppm) and  $\text{CD}_3\text{OD}$  ( $\delta = 49.9$  ppm).

1-methylimidazole, 1-bromobutane and 3-(trimethylsilyl) propionic-2,2,3,3- $\text{d}_4$  acid were purchased from Sigma-Aldrich.

### 7.2. Product Analysis

HPLC analysis was performed on an Agilent 1100. Shikimic acid was quantified by HPLC using a Grace Alltima<sup>TM</sup> amino column (4.6 x 250 mm, 5  $\mu\text{m}$  particle size) and isocratic elution with 60/40, (v/v);  $\text{CH}_3\text{CN}/\text{H}_2\text{O}$  (140 mM  $\text{NH}_4^+\text{HCO}_2^-$ , pH 4.0). The amino column was stored in a solution of 5/95, (v/v); methanol/hexane when it was received from the manufacture. In order to convert the column to weak base ion-exchange mode, the column was washed with 1 L of reagent grade isopropanol (0.2 mL/min) followed by 1 L of HPLC grade acetonitrile (0.2 mL/min) prior to the first use. Shikimic acid molecular standard was obtained from Roche. *p*-Hydroxybenzoic acid and *m*-hydroxybenzoic acid were separated from one another with baseline resolution and quantified by HPLC using an Agilent ZORBAX SB-C18 (4.6 x 150 mm, 5  $\mu\text{m}$  particle size) column and isocratic elution with 15/85, (v/v);  $\text{CH}_3\text{CN}/\text{H}_2\text{O}$  (100 mM  $\text{NH}_4^+\text{HCO}_2^-$ ,

pH 2.5). The ZORBAX was stored in a solution of 85/15, (v/v); methanol/H<sub>2</sub>O when it was received from the manufacture. The column was washed with 1 L of HPLC grade acetonitrile prior to the first use. *p*-Hydroxybenzoic acid molecular standard was obtained from Spectrum while the *m*-hydroxybenzoic acid molecular standard was obtained from Sigma-Aldrich. The deionized, distilled water used to make the required buffer solutions was filtered with a DURAPORE® 0.45 µm HV filter (MILLIPORE). The acetonitrile was HPLC grade. Syringe filtration (0.45 µm Whatman filter) was followed by HPLC analysis for all the sample.

### 7.3. Culture Medium

All solutions were prepared in distilled, deionized water. M9 salts (1 L) contained Na<sub>2</sub>HPO<sub>4</sub> (6 g), KH<sub>2</sub>PO<sub>4</sub> (3 g), NH<sub>4</sub>Cl (1 g), and NaCl (0.5 g). M9 minimal medium (1 L) contained D-glucose (10 g), MgSO<sub>4</sub> (0.24 g), thiamine pyrophosphate (0.010 g), L-phenylalanine (0.040 g), L-tyrosine (0.040 g), L-tryptophan (0.040 g), *p*-hydroxybenzoic acid (0.010 g), *p*-aminobenzoic acid (0.010 g), and 2,3-dihydroxybenzoic acid (0.010 g) in 1 L of M9 salts. Solutions of M9 salts, MgSO<sub>4</sub>, and glucose were autoclaved individually and then mixed. Solutions of amino acids, aromatic vitamins and thiamine pyrophosphate were sterilized through 0.22 µm membranes. Solid medium was prepared by addition of Bacto™ agar to a final concentration of 1.5% (w/v) to the liquid medium.

The fermentation medium was prepared with water (16 L), K<sub>2</sub>HPO<sub>4</sub> (150 g), ammonium iron (III) citrate (6 g), citric acid monohydrate (42 g), concentrated H<sub>2</sub>SO<sub>4</sub> (24 mL), concentrated NH<sub>4</sub>OH (82 mL), L-phenylalanine (14 g), L-tyrosine (14 g), and L-tryptophan (7 g). This solution was sterilized in the fermentor using a built-in sterilization function. The solution (2 L) containing following supplements were added immediately prior to initiation of the fermentation: glucose (600 g), MgSO<sub>4</sub> (2.4 g), thiamine hydrogenchloride (0.010 g), *p*-hydroxybenzoic acid

(0.100 g), *p*-aminobenzoic acid (0.100 g), 2,3-dihydroxybenzoic acid (0.100 g) and trace minerals, including  $(\text{NH}_4)_6(\text{Mo}_7\text{O}_{24})\cdot 4\text{H}_2\text{O}$  (0.037 g),  $\text{ZnSO}_4\cdot 7\text{H}_2\text{O}$  (0.029 g),  $\text{B}(\text{OH})_3$  (0.247 g),  $\text{CuSO}_4\cdot 5\text{H}_2\text{O}$  (0.025 g), and  $\text{MnCl}_2\cdot 4\text{H}_2\text{O}$  (0.158 g). Glucose and  $\text{MgSO}_4$  (1 M) were autoclaved separately, while solutions of aromatic vitamins, thiamine pyrophosphate and trace minerals were sterilized through 0.22  $\mu\text{m}$  membranes.

#### **7.4. Bacteria Strain and Plasmid**

*E. coli* SP 1.1 was previously engineered in the group.<sup>6b,c</sup> Plasmid pKD15.071B, which was constructed previously in the group<sup>6a</sup> was transformed into *E. coli* SP1.1.

#### **7.5. Fed-Batch Fermentation (General)**

A B. Braun BIOSTAT® C-DCU fermentor (30 L) connected to a DCU-3 system was used for fed-batch fermentations at 20 L scale. Data acquisition utilized MFCS/win 3.0 software (Sartorius Stedim Systems), which was installed in a personal computer (Digilink) operated by Windows® 7 Professional. Matson Marlow 101U/R peristaltic pump was used for administration of feed glucose solution. Temperature and pH were controlled with PID loop maintaining at 33 °C and pH 7.0±0.1 with 2N  $\text{H}_2\text{SO}_4$  and  $\text{NH}_4\text{OH}$ . Impeller speed was varied between 100 and 600 rpm to maintain dissolved oxygen (D.O.) levels at 10% air saturation. Airflow was increased from 0.5 L/min to 20 L/min to maintain dissolved oxygen (D.O.) levels at 10% air saturation. The air was supplemented with pure oxygen when the 20 L/min air flow could not provide enough oxygen. DO was measured using a Hamilton OxyFerm FDA 120 (catalogue number 237450) fitted with an Optiflow FDA membrane (catalogue number 237140). pH was measured with Mettler Toledo 405-DPAS-SC-K85/120 (catalogue number 104054479). The concentration of glucose in the medium was maintained at glucose-rich culture conditions

defined as a glucose concentration in the range of 19-43 g/L. Glucose levels were maintained throughout the run by addition of feed glucose solution (60% w/v). Glucose concentration was measured with GlucCell™ and glucose test strip (CESCO Bioengineering Co., Ltd.). Antifoam 204 (Sigma-Aldrich) was added as needed to mitigate foam accumulation.

Inoculant was started by introduction of a single colony picked from an agar plate into 5 mL of M9 medium. The culture was grown at 37 °C with agitation at 250 rpm until turbid (24h) and subsequently transferred to 100 mL of M9 medium. This 100 mL culture was grown at 37 °C and 250 rpm until the OD<sub>600</sub> reached 2.0-3.0 (12 h). Two flasks containing 1 L of M9 media were inoculated with a portion of this 100 mL culture such that the initial OD<sub>600</sub> = 0.05. These two 1 L cultures were grown at 37 °C and 250 rpm until the OD<sub>600</sub> reached 1.0-2.0 (9-11 h). The fermentation vessel was inoculated with these two 1 L of cultures thus initiating the fermentation run ( $t = 0$  h).

## **7.6. Fed-Batch Fermentation of Shikimic Acid**

The supplement solution (2 L) was added to the fermentation medium (16 L) followed by inoculation with the two 1 L inoculants. The initial volume of fermentation broth was 20 L with 30 g/L glucose concentration. The concentration of glucose in the medium was maintained in the range of 19-43 g/L throughout the run by addition of feed glucose solution (60% w/v). Oxygen supplementation was required at  $t = 16-22$  h in order to maintain dissolved oxygen (D.O.) levels at 10% air saturation. The cell growth reached stationary phase at  $t = 30$  h. A total of 6.6 kg of glucose was consumed after 61 h based on <sup>1</sup>H NMR. The broth volume increased gradually due to cell growth, product, addition of glucose solution and NH<sub>4</sub>OH (1600 mL), which was used to adjust pH. Final broth volume was approximately 30 L. For <sup>1</sup>H NMR

quantification of shikimic acid, the broth was concentrated to dryness under reduced pressure, concentrated to dryness one additional time from D<sub>2</sub>O, and then dissolved in D<sub>2</sub>O containing a known concentration of the sodium salt of 3-(trimethylsilyl) propionic-2,2,3,3-d<sub>4</sub> acid. The concentration of shikimic acid was determined by comparison of integral corresponding to shikimic acid (2.75 ppm, ddt,  $J = 18.1, 5.3, 1.6$  Hz, 1H) with integral corresponding to TSP ( $\delta = 0.00$  ppm, s, 9H).

The instrument setting was split into two phase. During first phase, DO was maintained at 10 % by impeller speed primarily until the impeller speed reached to the maximum (600 rpm). And then airflow was increased until it reached to the maximum (20.0 L/min). The pO<sub>2</sub> control loop setting for first phase was following (Table 3.5.) :

Table 3.5. Instrument Setting of First Phase

DEADB 0.5% sat							
CASCADE							
1	STIR						
2	AIRF						
Cascade	Minimum	Maximum	XP	TI	TD	Hysteresis	Mode
STIR	5.0%	30.0%	150.0%	100.0 s	0.0 s	01:00 m:s	auto
AIRF	1.2%	40.0%	90.0%	50.0 s	0.0 s	01:00 m:s	auto
SUBS	0.0%	100.0%	90.0%	50.0 s	0.0 s	05:00 m:s	off
O2EN	0.0%	100.0%	90.0%	50.0 s	0.0 s	05:00 m:s	auto
STIR: 5.0% = 100 rpm, 30.0% = 600 rpm AIRF: 0.2% = 1.00 L/min, 40.0% = 20.00 L/min SUBS setting did not matter since it was off.							

The cascade setting was altered to second phase when both impeller speed and airflow reached to their maximum. During second phase, DO was maintained at 10 % by impeller speed while the airflow was held at 20.0 L/min. The airflow was supplemented with O<sub>2</sub> automatically when the impeller speed was not sufficient to maintain DO at 10%. The pO<sub>2</sub> control loop setting for second phase was following (Table 3.6.) :

Table 3.6. Instrument Setting of Second Phase

DEADB 0.5% sat							
CASCADE							
1	AIRF						
2	STIR						
Cascade	Minimum	Maximum	XP	TI	TD	Hysteresis	Mode
STIR	5.0%	30.0%	150.0%	100.0 s	0.0 s	01:00 m:s	auto
AIRF	40.0%	40.0%	90.0%	50.0 s	0.0 s	01:00 m:s	auto
SUBS	0.0%	100.0%	90.0%	50.0 s	0.0 s	05:00 m:s	off
O2EN	0.0%	100.0%	90.0%	50.0 s	0.0 s	05:00 m:s	auto
STIR: 5.0% = 100 rpm, 30.0% = 600 rpm AIRF: 40.0% = 20.00 L/min SUBS setting did not matter since it was off.							

The antifoam was added automatically and manually as needed. The position of foam sensor was gradually raised while total broth volume was increasing. The auto-antifoam setting was following (Table 3.7.) :

Table 3.7. Auto-antifoam Setting

SENSI	Med-High
CYCLE	15:00
PULSE	00:01

## 7.7 Cell Removal

Raw fermentation broth was filtered with a hollow fiber cartridge (GE Healthcare xFP-x-x-55), equipped with a portable utility/sprinkler pump (Simer 2825ss) to remove cells. The hollow fiber cartridge passes cell free broth through 0.1 µm cutoff membrane and recirculates the retentate through 1 mm diameter hollow fibers. When the retentate became approximately 2 L, it was not enough volume to sustain the broth flow. The retentate was diluted with 2 L of water to increase the volume and reduce the viscosity. The diluted retentate was filtered until the flow ceased. This filtration afforded 30.1 L of cell free broth containing 2,160 g of shikimic acid.

### **7.8. Protein Removal**

The protein in the cell free broth was removed with four Sartocan® ECO Hydrostart® membrane cut off 10 kD cassettes equipped with SartoJet® Pump 4-Piston Diaphragm Pump. This tangential flow filtration of cell free broth was performed with the pressure toward the membrane of 25±5 psi and a back pressure of 6±1 psi. When the retentate became approximately 1 L, it was not enough volume to sustain the broth flow. The retentate was diluted with 2 L of water to increase the volume and reduce the viscosity. The diluted retentate was filtered until the flow ceased.

### **7.9. Shikimic Acid Extraction Solvent Screening in Vials**

Cell-free, protein-free shikimic acid fermentation broth was concentrated by boiling off water to approximately 1/5 of the original broth volume and then acidified with H<sub>2</sub>SO<sub>4</sub> to pH 2.5. The final volume was adjusted with water to 1/4 of original broth volume. The extraction was performed in a vial (8 × 25 mm). Each vial contained 0.5 mL concentrated broth and 0.5 mL solvent. The solvent and the broth were mixed by continuously rotating vertically (7 rotations/min) for 12 h using a hybridization incubator. The shikimic acid concentration of extracts and raffinates were determined by HPLC.

### **7.10. KARR® Column General**

The bench-top KARR® column (220 mL) was manufactured by Koch Modular Process Systems, KMPS). A Teflon and a stainless-steel plate stack assembly built on stainless steel shafts were supplied with the KARR® column. All the KARR® column extraction experiment utilized the Teflon plates stack shaft. The solvent, broth feed and raffinate flow rates were regulated with QD High Speed-High Flows Metering Pump (Fluid Metering Inc.).

### 7.11. Comparison of Shikimic Acid Extraction Solvents in KARR® Column

Cell-free, protein-free shikimic acid fermentation broth was concentrated by boiling off water to approximately 1/5 of the original broth volume, and then acidified with H<sub>2</sub>SO<sub>4</sub> to pH 2.5. The final volume was adjusted with water to 1/4 of original broth volume. This concentrated broth (100 mL) containing shikimic acid (30 g) was subjected to countercurrent extraction using *n*-butanol, 2-butanol and *t*-butanol. *t*-Butanol was melted before use. A broth feed flow rate of 5 mL/min and a solvent flow rate of 40 mL/min were used. The amount of extracted shikimic acid from the fermentation broth to *n*-butanol, 2-butanol and *t*-butanol were 17 g (57%), 18 g (60%) and 22 g (73%) respectively based on HPLC. The concentrated broth (100 mL) containing shikimic acid (30 g) was additionally submitted to countercurrent extraction using *n*-propanol, acetone and isopropanol. A broth feed flow rate of 5 mL/min and a solvent flow rate of 10 mL/min were used. The amount of extracted shikimic acid from the fermentation broth to *n*-propanol, acetone and isopropanol were 23 g (77%), 24 g (80) and 24 g (80%) respectively based on HPLC. Finally, the concentrated broth (1000 mL) containing shikimic acid (272 g) was submitted to countercurrent extraction using isopropanol/water, 9:1, v/v. A broth feed flow rate of 10 mL/min and a solvent flow rate of 20 mL/min were used. The amount of extracted shikimic acid from the fermentation broth to isopropanol/water, 9:1, v/v solution was 259 g (95%) based on HPLC.

### 7.12. Comparison of Shikimic Acid Crystallization Solvents

Extracts contained shikimic acid as a function of solvent were as follows: *n*-butanol 17.0 g, 2-butanol 17.5 g, *n*-propanol 23.3 g, isopropanol 24.4 g, *t*-butanol 22.1 g and acetone 23.6 g. The extract was vacuum filtered through Whatman® #1 filter paper to remove particulate. The

extracts were concentrated using a rotary evaporator until formation of the first solid was observed, and crystallization subsequently allowed to proceed at rt overnight. The crystallized solid was collected by filtration and washed with the extraction solvent followed by acetone. After drying under vacuum, the amount of shikimic acid obtained, % recovery, and purity as a function of solvent were: *n*-butanol 13.6 g (75% recovery, 94.3% purity), 2-butanol 9.5 g (51% recovery, 93.1% purity), *n*-propanol 8.8 g (34% recovery, 89.4 % purity), isopropanol 12.2 g (47% recovery, 94.1 % purity). No precipitate of shikimic acid was observed after standing at rt overnight for *t*-butanol and acetone extracts.

### **7.13. Decolorizing Isopropanol/Water (9:1 v/v) Extract and Evaporative Crystallization from *n*-Butanol of Shikimic Acid**

Isopropanol/water. 9:1, v/v extract (2910 mL) containing shikimic acid (257 g) was separated into three 2 L Erlenmyer flasks. Activated charcoal (DARCO™ G-60, decolorizing, ACROS Organics™, 8.6 g) was added to each flask. The flasks were shaken on an orbital shaker at 150 rpm at rt for 1 h. The activated charcoal was removed by vacuum filtration through 64 g of Celite 545 in an OD 17 cm Buchner funnel fitted with Whatman #1 filter paper. This filtrate was concentrated using a rotary evaporator. The residue was dissolved in boiling water (250 mL), and then *n*-butanol (1500 mL) was added. The water was removed azeotropically with a rotary evaporator until crystallization began. The solution was poured into a crystallization dish to afford a first crop of shikimic acid. A dark, brown-colored solid remained in the stripping flask, which was dissolved in boiling water (100 mL). *n*-Butanol (550 mL) was added to the solution. The water was again removed azeotropically with a rotary evaporator until crystallization began. The solution was poured into a crystallization dish to afford a second crop

of shikimic acid. After overnight crystallization, the crystallized solid was collected by filtration and washed with cold *n*-butanol followed by acetone. The solid was dried under vacuum to afford shikimic acid, which was analyzed with HPLC. For the first crop, 160 g of off-white colored shikimic acid was obtained (61% recovery) with a purity of 98.4%. For the second crop, 35.6 g of off-white shikimic acid was obtained (14% recovery) with a purity of 97.9%. This overall process afforded 196 g of off-white shikimic acid (75% recovery, 98.1% purity). <sup>1</sup>H NMR (D<sub>2</sub>O, TSP δ = 0.00) δ = 6.80 (dt, *J* = 3.8, 1.8 Hz, 1H), 4.45 (td, *J* = 4.0, 1.9 Hz, 1H), 4.04 (ddd, *J* = 8.3, 6.5, 5.2 Hz, 1H), 3.78 (dd, *J* = 8.2, 4.3 Hz, 1H), 2.75 (ddt, *J* = 18.1, 5.3, 1.6 Hz, 1H), 2.23 (ddt, *J* = 18.2, 6.6, 1.5 Hz, 1H). <sup>13</sup>C NMR (D<sub>2</sub>O, TSP δ = 0.00) δ = 175.0, 137.9, 134.9, 74.3, 69.6, 68.9, 34.1. mp: 1<sup>st</sup> crop 182-184 °C, 2<sup>nd</sup> crop 184-185 °C (lit.<sup>17</sup> 184-185 °C).

#### 7.14. Scale-up Dehydration of Shikimic Acid in 1-Butyl-3-methylimidazolium Bromide

Ionic liquid 1-butyl-3-methylimidazolium bromide was synthesized *in situ*. 1-Bromobutane (491 mL, 4.57 mol) was added to 228 mL (2.86 mol) of 1-methylimidazole in a 2 L three-neck round bottom flask heated in a 70 °C oil bath fitted with two reflux condensers open to the atmosphere. A vigorous exothermic reaction was observed after heating at 70 °C for approximately 15 min. The flask was removed from the oil bath until the vigorous exothermic reaction ceased and then placed back in the 70 °C oil bath for 20 h. Unreacted 1-bromobutane and water were removed by distillation under reduced pressure at 55 °C. This afforded 1-butyl-3-methylimidazolium bromide (619 g, 99%) as a yellow oil. <sup>1</sup>H NMR (CDCl<sub>3</sub>) δ = 10.6 (s, 1H), 7.32 (dd, *J* = 3.5, 2 Hz, 1H), 7.25 (dd, *J* = 3.5, 2 Hz, 1H), 4.31 (dd, *J*<sub>1</sub> = *J*<sub>2</sub> = 7.5 Hz, 2H), 4.11 (s, 3H), 1.86-1.92 (m, 2H), 1.37 (m, 2H), 0.950 (dd, *J* = 7.5, 7.0 Hz, 3H). <sup>13</sup>C NMR (CDCl<sub>3</sub>) δ = 138.2, 123.6, 122.0, 50.3, 37.1, 32.5, 19.8, 13.8.

*In situ* synthesized 1-Butyl-3-methylimidazolium bromide ([BMIm]Br) was first dried at 55 °C under vacuum in the 2 L three-neck round bottom flask in which this ionic liquid was generated. The flask containing dry [BMIm]Br (618 g, 3.23 mol) was opened under N<sub>2</sub> and shikimic acid (purity 94%, 262 g, 1.42 mol) was added. The flask was fitted with an overhead stirrer and two gas adaptors. The reaction vessel was swept with an active N<sub>2</sub> flow. The reaction solution temperature was maintained at 90 °C. After the shikimic acid dissolved, H<sub>2</sub>SO<sub>4</sub> (15.1 mL, 283 mmol) was added. The reaction solution was heated at 90 °C for 24 h under an active flow of N<sub>2</sub> to afford 145 g (74%) of *p*-hydroxybenzoic acid and 37.2 g (19%) of *m*-hydroxybenzoic acid based on HPLC analysis. The reaction solution was diluted with H<sub>2</sub>O (1000 mL) and separated into two portions. Each portion was extracted with EtOAc (1400 mL) for 18 h in a continuous liquid-liquid extractor. The brown EtOAc extracts were then combined and it contained 140 g of *p*-hydroxybenzoic acid (71%), and 36.7 g of *m*-hydroxybenzoic acid (19%) based on HPLC analysis. The brown organic extract was concentrated to approximately 1.5 L. This solution was decolorized using continuous flow conditions. A decolorizing column (D = 8.0 cm) was constructed with a piece of Kimwipe to plug the column outlet below a layer of 75 g Celite® 545 topped with a layer consisting of 75 g activated charcoal (DARCO® G-60, 100 mesh) dispersed in 375 g flash chromatography grade silica gel (60 Å pore size, 40-63µm mesh). After loading, the decolorizing column was washed with an EtOAc/AcOH, 98.6:1.4, v/v solution. Concentrating this solution gave a gray solid. This gray solid was dissolved in 1000 mL boiling H<sub>2</sub>O, crystallized at rt, filtered, and dried to afford *p*-hydroxybenzoic acid 126 g (64%) as a white solid with purity 98.9% based on HPLC analysis. <sup>1</sup>H NMR (CD<sub>3</sub>OD): δ = 7.89-7.92 (m, 2H), 6.83-6.86 (m, 2H). <sup>13</sup>C NMR (CD<sub>3</sub>OD) δ = 170.9, 164.2, 133.9, 123.6, 116.9. mp: 208-212 °C (Lit.<sup>18</sup> 210-211 °C).

## REFERENCES

## REFERENCES

1. Draths, K. M.; Knop, D. R.; Frost, J. W. Shikimic acid and quinic acid: replacing isolation from plant sources with recombinant microbial biocatalysis. *J. Am. Chem. Soc.* **1999**, *121*, 1603-1604. (b) Knop, D. R.; Draths, K. M.; Chandran, S. S.; Barker, J. L.; von Daeniken, R.; Weber, W.; Frost, J. W. Hydroaromatic equilibration during biosynthesis of shikimic acid. *J. Am. Chem. Soc.* **2001**, *123*, 10173-10182. (c) Chandran, S. S.; Yi, J.; Draths, K. M.; von Daeniken, R.; Weber, W.; Frost, J. W. Phosphoenolpyruvate availability and the biosynthesis of shikimic acid. *Biotechnol. Prog.* **2003**, *19*, 808-814.
2. (a) Herrmann, K. M. The Common Aromatic Biosynthetic Pathway. In *Amino Acids: Biosynthesis and Genetic Regulation*. Herrmann, K. M., Ed.; Somerville, R. L., Ed.; Addison-Wesley: Massachusetts, 1983; p301-322. (b) Roberts, F.; Roberts, C. W.; Johnson, J. J.; Kyle, D. E.; Krell, T.; Coggins, J. R.; Coombs, G. H.; Milhous, W. K.; Tzipori, S.; Ferguson, D. J. P.; Chakrabarti, D.; McLeod, R. Evidence for the shikimate pathway in apicomplexan parasites. *Nature* 1998, *393*, 801-805. (c) Bentley, R. The shikimate pathway-A metabolic tree with many branches. *Crit. Rev. Biochem. Molbiol.* **1990**, *25*, 307-384.
3. (a) Garner, C.; Herrmann, K. M. Biosynthesis of Phenylalanine. In *Amino Acids: Biosynthesis and Genetic Regulation*. Herrmann, K. M., Ed.; Somerville, R. L., Ed.; Addison-Wesley: Massachusetts, 1983; p323-338. (b) Camakaris, H.; Pittard, J. Tyrosine Biosynthesis. In *Amino Acids: Biosynthesis and Genetic Regulation*. Herrmann, K. M., Ed.; Somerville, R. L., Ed.; Addison-Wesley: Massachusetts, 1983; p339-350. (c) Somerville, R. L. Tryptophan: Biosynthesis, Regulation, and Large-Scale Production. In *Amino Acids: Biosynthesis and Genetic Regulation*. Herrmann, K. M., Ed.; Somerville, R. L., Ed.; Addison-Wesley: Massachusetts, 1983; p351-378.
4. (a) Dell, K. A.; Frost, J. W. Identification and removal of impediments to biocatalytic synthesis of aromatics from D-glucose: Rate-limiting enzymes in the common pathway of aromatic amino acid biosynthesis. *J. Am. Chem. Soc.* **1993**, *115*, 11581-11589. (b) Li, K.; Mikola, M. R.; Draths, K. M.; Worden, R. M.; Frost, J. W. Fed-batch fermentor synthesis of 3-dehydroshikimic acid using recombinant *Escherichia coli*. *Biotechnol. Bioeng.* **1999**, *64*, 61-73. (c) Frost, J. W.; Bender, J. L. Kadonaga, J. T.; Knowles, J. R. Dehydroquinase synthase from *Escherichia coli*: purification, cloning, and construction of overproducers of the enzyme. *Biochemistry* **1984**, *23*, 4470-4475. (d) Takeda, Y.; Nishimura, A.; Nishimura, Y.; Yamada, M.; Yasuda, S.; Suzuki, H.; Hirota, Y. Synthetic ColE1 plasmids carrying genes for oenicillin-binding proteins in *Escherichia coli*. *Plasmid* **1981**, *6*, 86-98.
5. Lobner-Olesen, A.; Marinus, M. G. Identification of the gene (*aroK*) encoding shikimic acid kinase I of *Escherichia coli*. *J. Biotechnol.* **1992**, *174*, 525-529.
6. (a) Anton, I. A.; Coggins, J. R. Sequencing and overexpression of the *Escherichia coli aroE* gene encoding shikimate dehydrogenase. *Biochem. J.* **1988**, *249*, 319-326. (b) Anton, J. A.; Coggins, J. R. Subcloning of the *Escherichia coli* shikimate dehydrogenase gene (*aroE*) from the transducing bacteriophage *spc1*. *Biochem. Soc. T.* **1984**, *12*, 275-276. (c) Jaskunas, S.

- R.; Lindahl, L.; Nomura, M. Specialized transducing phages for ribosomal protein genes of *Escherichia coli*. *Proc. Natl. Acad. Sci. U.S.A.* **1975**, *72*, 6-10.
7. (a) Draths, K. M.; Pompiano, D. L. Conley, D. L.; Frost, J. W.; Berry, A.; Disbrow, G. L.; Staversky, R. J.; Lievens, J. C. Biocatalytic synthesis of aromatics from D-glucose: The role of transketolase. *J. Am. Chem. Soc.* **1992**, *114*, 3956-3962. (b) Blackmore, P. F.; Williams, J. F.; MacLeod, J. K. Dimerization of erythrose 4-phosphate. *Febs Lett.* **1976**, *64*, 222-226.
  8. (a) Li, K. Kai Li Laboratory Notebook KL I p018-113 1995. (b) Schaub, J.; Mauch, K.; Reuss, M. Metabolic flux analysis in *Escherichia coli* by integrating isotopic dynamic and isotopic stationary <sup>13</sup>C labeling data. *Biotechnol. Bioeng.* **2008**, *99*, 1170-1185.
  9. Hecquet, L.; Fessner, W.-D.; Helanine, V.; Charmantray, F. *New Applications of Transketolase: Cascade Reactions for Assay Development*. In *Cascade Biocatalysis*; Riva, S.; Fessner, W.-D., Ed.; Wiley-VCH Verlag GmbH & Co. KGaA, Weinheim: Germany, 2014; pp315-337.
  10. (a) Koch Modular Process System, LLC. Liquid Extraction Overview. <https://modularprocess.com/liquid-liquid-extraction/> (accessed Jan 04, 2017). (b) Chemical Engineering, College of Engineering, University of Michigan. Extractor. <http://encyclopedia.che.engin.umich.edu/Pages/SeparationsChemical/Extractors/Extractors.html#GJ5VCUA23E0CST2FYB5C> (accessed Apr 06, 2017).
  11. Suggestion from my own experience.
  12. Spectrum Labs. Competitive Edge. <http://spectrumlabs.com/filtration/Edge.html> (accessed Mar 25, 2017)
  13. (a) Reichardt, C. *Solvents and Solvent Effects in Organic Chemistry*, 3rd ed.; Wiley-Vch: Weinheim, 2003; p 418-424. (b) SciFinder, Predicted properties. Calculated using Advanced Chemistry Development (ACD/Labs) Software V11.02 (©1994-2017 ACD/Labs)
  14. Smallwood, I. M. *Solvent Recovery Handbook*, 2nd ed.; CRC Press: Boca Raton, 2002.
  15. Van der Does, T.; Booij, J.; Kers, E. E.; Leenderts, E. J. A. M.; Sibeijn, M.; Agayn, V. Process for the recovery of shikimic acid. WO 0206203, January 24, 2002.
  16. (a) Hanabatake, M. Production method of aromatic polyesters. JP S5657821, May 20, 1981. (b) Layton, R.; Cleay, J. W. Wholly aromatic polyesters with reduced char content. EP 0347228, December 20, 1989. (c) Huspeni, P. J.; Stern, B. A.; Frayer, P. D. Blends of liquid crystalline polymers of hydroquinone poly(iso-terephthalates) p-hydroxybenzoic acid polymers and another LCP containing oxybisbenzene and naphthalene derivatives. WO 9004002, April 04, 1990. (d) Waggoner, M. Liquid crystalline polymer composition. WO 9606888, July 03, 1996. (e) Shepherd, J. P.; Linstid, C. H. III. Stretchable liquid crystal polymer composition. WO 02064661, August 22, 2002.
  17. Payne, R.; Edmonds, M. Isolation of shikimic acid from star aniseed. *J. Chem. Educ.* **2005**,

82, 599-600.

18. Kikuchi, M.; Sato, K.; Shiraishi, Y.; Nakayama, R.; Watanabe, R.; Sugiyama, M.  
Constituents of *Berchemia racemosa* Sieb. et Zucc. *Yakugaku Zasshi* **1990**, *110*, 354-357.

## CHAPTER FOUR

### Synthesis of Biobased Terephthalic Acid

#### 1. Introduction

1,4-Benzenedicarboxylic acid (terephthalic acid) and 1,3-benzenedicarboxylic acid (isophthalic acid) are used in polymers, particularly polyethylene terephthalate (PET). In 2012, the world PET consumption was over 19.8 million tons.<sup>1</sup> The global consumption of terephthalic acid was 47 million tons with a market value of \$60 billion in 2012.<sup>2</sup> Other significant uses of terephthalic acid are in synthetic fibers<sup>3</sup> and liquid crystalline polymers (LCPs)<sup>4</sup>. In PET, 5-7% of isophthalic acid is introduced into the polymer in order to disrupt the crystallization of the molten resin as it cools. This affords a transparent polymer and lowers the melt process temperature.<sup>5</sup> Isophthalic acid is also used for alkyd resins, high-temperature-resistant nylon, plasticizers<sup>5</sup> and LCPs<sup>4</sup>. Terephthalic acid and isophthalic acid are currently produced in industry via catalytic oxidation of *p*-xylene and *m*-xylene, respectively.<sup>6a,b</sup>

## 2. Terephthalic Acid and Isophthalic Acid Production

Terephthalic acid and isophthalic acid are produced from *para*- and *meta*-xylene by the Amoco Mid-Century process, which is an aerobic catalytic oxidation in acetic acid. The reaction is catalyzed by cobalt, manganese and bromide compounds.<sup>6a,7</sup> It is a radical process, which is depicted in Scheme 1.<sup>6a,8</sup> In the first step, a bromine radical abstracts a hydrogen from the methyl group of *p*-xylene **1** producing 4-methylbenzyl radical **2** and HBr. The 4-methylbenzyl radical **2** reacts with oxygen to form the peroxide **3**, which becomes 4-methylbenzaldehyde **4** upon oxidizing Co<sup>II</sup> to Co<sup>III</sup>. A bromine radical abstracts another hydrogen from 4-methylbenzaldehyde **4** producing radical intermediate **5**, which reacts with oxygen to form the peracid **7**. This peracid **7** reacts with 4-methylbenzaldehyde **4** producing two molecules of *p*-toluic acid **10** in a Baeyer-Villiger type reaction via intermediates **8** and **9**.<sup>8</sup> Repetition of this process upon the other methyl group produces terephthalic acid **11** (Scheme 4.1).<sup>6a,8</sup> The role of manganese is to reduce Co<sup>III</sup> back to Co<sup>II</sup> and oxidize bromide back to bromine radical (Scheme 4.2).<sup>6a</sup>



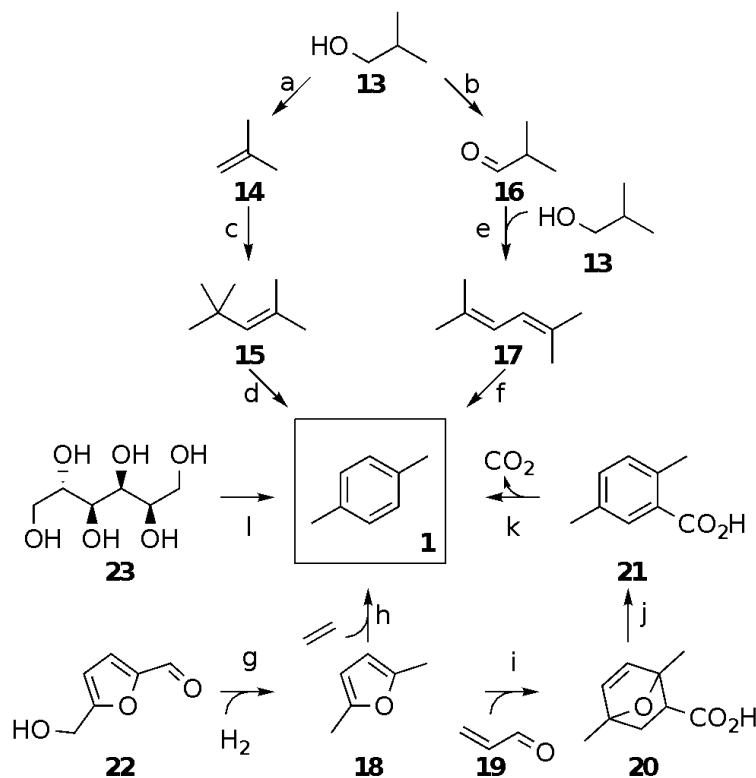
Overoxidation of *p*-xylene to CO<sub>2</sub> and acetic acid oxidation to both CO<sub>2</sub> and methane creates a large carbon footprint.<sup>6a</sup> Methane has a 25-fold greater impact on climate change relative to CO<sub>2</sub> on a wt/wt basis.<sup>6c</sup> During production of 1000 kg terephthalic acid from *p*-xylene, 165 kg CO<sub>2</sub> is generated. Of this CO<sub>2</sub>, 40% comes from overoxidation of *p*-xylene and 60% comes from oxidation of acetic acid.<sup>9</sup> Switching to biobased terephthalic acid production, which being with starting materials that have one or both carboxylic acids are already in the place, can reduce the overall emission of greenhouse gas. Several routes of biobased terephthalic acid production have been proposed.

### 3. Biobased Terephthalic Acid

There are two broad routes in the syntheses of biobased terephthalic acid. One involves *p*-xylene intermediacy (Scheme 4.3) while the other does not (Scheme 4.4). An example of a route using *p*-xylene as an intermediate proceeds through biobased isobutanol **13**, which is microbially synthesized from glucose.<sup>10</sup> It can then be dehydrated to isobutene<sup>11,12</sup> **14** or oxidized to isobutanal<sup>13</sup> **16** (Scheme 4.3). Dimerization of isobutene **14** produces 2,4,4-trimethylpentene **15**,<sup>11</sup> which undergoes catalytic dehydrocyclization to *p*-xylene.<sup>12</sup> Isobutanol **13** can also be reacted with isobutanal<sup>13</sup> **16** producing 2,5-dimethylhexadiene **17**, which is dehydrocyclized to *p*-xylene.<sup>13</sup> *p*-Xylene also can be synthesized from cycloaddition of 2,5-dimethylfuran **18** with ethylene followed by dehydration of the cycloaddition product.<sup>14</sup> Cycloaddition of 2,5-dimethylfuran **18** with acrolein **19** followed by an oxidation, dehydration, and decarboxylation also leads to *p*-xylene.<sup>15</sup> Biobased 2,5-dimethylfuran **18** can be synthesized by hydrogenation<sup>16</sup> of 5-hydroxymethylfurfural **22**, which is chemically derived from glucose or fructose.<sup>17</sup> Catalytic reforming of glucose-derived sorbitol<sup>18</sup> **23** followed by hydrogenation and dehydration

affords a mixture of aromatics.<sup>19</sup>

Scheme 4.3. Biobased *p*-Xylene



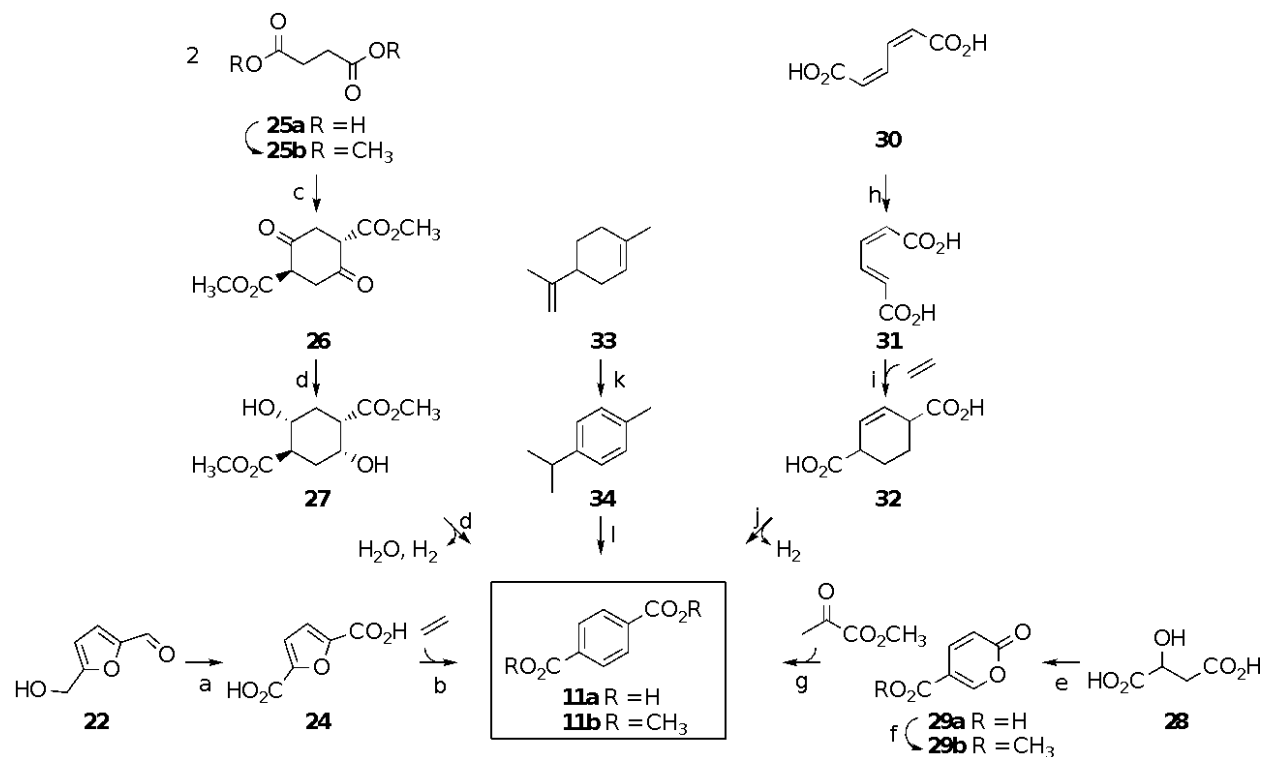
- (a)  $\gamma$ -Al<sub>2</sub>O<sub>3</sub>, 325 °C, 95%. (b) CuO, 325 °C, 95%. (c) ZSM-5, 160 °C, 69%.  
 (d) CrO<sub>x</sub>/Al<sub>2</sub>O<sub>3</sub>, 550 °C, 42%. (e) Nb<sub>x</sub>O<sub>y</sub>•H<sub>2</sub>O, 225 °C, 35%. (f) CrO<sub>x</sub>/Al<sub>2</sub>O<sub>3</sub>, 450 °C, 68%. (g) CuRu/C, *n*-BuOH, 220 °C, 6.8 bar H<sub>2</sub>, 71%. (h) C, 200-335 °C, 35-41 bar, 30%. (i) i) Sc(OTf)<sub>3</sub>, MS (4Å), CDCl<sub>3</sub>, -55 °C ii) NaClO<sub>2</sub>, H<sub>2</sub>O<sub>2</sub>, NaH<sub>2</sub>PO<sub>4</sub>, H<sub>2</sub>O, CH<sub>3</sub>CN, 0 °C, 77%. (j) H<sub>2</sub>SO<sub>4</sub>, 0 °C, 48%. (k) Cu<sub>2</sub>O, bathophenanthroline, NMP/quinoline, 210 °C, 91%. (l) i) Pt-Re/C, H<sub>2</sub>, 230 °C, 27 bar; ii) Ru/C, H<sub>2</sub>, 160 °C, 55 bar; iii) H-ZSM-5, 400 °C.

One method of synthesizing biobased terephthalic without *p*-xylene intermediacy

(Scheme 4.4) starts with 5-hydroxymethylfurfural **22**. Oxidation of 5-hydroxymethylfurfural **22** to 2,5-furandicarboxylic acid **24**<sup>20</sup> followed by cycloaddition with ethylene leads to trace levels of biobased terephthalic acid **11a**.<sup>21</sup> Another route involves dimerization of dimethyl succinate **25b**,<sup>22</sup> which is derived from esterification of microbially synthesized<sup>23</sup> succinic acid **25a**, affords succinylsuccinate **26**. Hydrogenation of succinylsuccinate **26** to **27** followed by dehydration and dehydrogenation gives dimethyl terephthalate **11b**.<sup>24</sup> This can then be hydrolyzed to terephthalic

acid. A third route to terephthalic acid that avoids *p*-xylene utilizes dimerization of microbially synthesized<sup>26</sup> malic acid **28** followed by esterification affording methyl coumalate **29b**.<sup>25</sup> Cycloaddition of **29b** with methyl pyruvate leads to dimethyl terephthalate **11b**.<sup>27</sup> Microbially synthesized<sup>28</sup> *cis,cis*-muconic acid **30** can also be used to make terephthalic acid.<sup>29</sup> *cis,cis*-Muconic acid **30** is isomerized to *cis,trans*-muconic acid **31**.<sup>29</sup> *In situ* isomerization of *cis,trans*-muconic acid **31** to *trans,trans*-muconic acid followed by cycloaddition with ethylene affords cycloadduct **32**.<sup>30</sup> Dehydrogenation of cycloadduct **32** leads to terephthalic acid **11a**.<sup>30</sup> Finally, conversion of biobased limonene **33** to *p*-cymene **34** is followed by oxidation of the side chains to give terephthalic acid **11a**.<sup>31</sup>

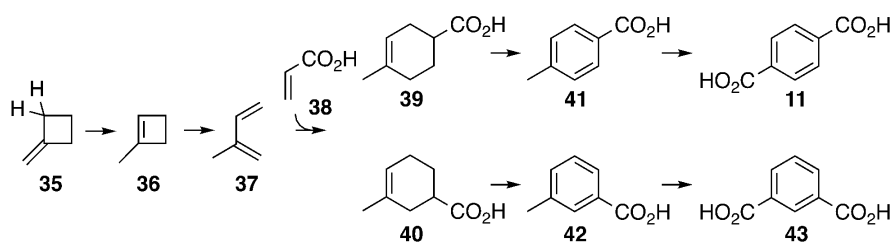
Scheme 4.4. Xylene-Free Synthesis of Biobased Terephthalic Acid



- (a) Pt/C, air, 95%, rt. (b) H<sub>2</sub>O, 200 °C, 13.8 bar, 0.1%. (c) NaOCH<sub>3</sub>, MeOH, 100 °C, 86%.  
 (d) i) Ru/C, H<sub>2</sub>, MeOH, 120 °C, 68.9 bar; ii) Ru/C, NaOH, MeOH, 195 °C, 68.9 bar, 24%.  
 (e) SO<sub>3</sub>/H<sub>2</sub>SO<sub>4</sub>, 75 °C, 65%. (f) DIPEA, NMP, (CH<sub>3</sub>O)<sub>2</sub>SO<sub>2</sub>, rt, 64%. (g) 200 °C, 59%.  
 (h) pH 4, 60 °C in fermentation broth, 100%. (i) I<sub>2</sub>, THF, 160 °C, 17.4 bar, 75%. (j) Pt/C, 150 °C, H<sub>2</sub>O, 55%.  
 (k) H<sub>2</sub>N(CH<sub>2</sub>)<sub>2</sub>NH<sub>2</sub>, FeCl<sub>3</sub>, Na, 50 °C to 100 °C, 99%. (l) H<sub>2</sub>N(CH<sub>2</sub>)<sub>2</sub>NH<sub>2</sub>, FeCl<sub>3</sub>, Na, 50 °C to 100 °C  
 (l) i) HNO<sub>3</sub>, H<sub>2</sub>O, reflux; ii) KMnO<sub>4</sub>, H<sub>2</sub>O, NaOH, reflux, 85%.

In 1952, Kurt Alder synthesized terephthalic acid **11** from acrylic acid **38** and isoprene **37**.<sup>32</sup> His intention was to prove that isoprene formed upon ring opening of methylenecyclobutane **35** (Scheme 4.5) by trapping the isoprene formed upon ring opening with acrylic acid, thereby affording 4-methyl-3-cyclohexenecarboxylic acid **39** and 3-methyl-3-cyclohexenecarboxylic acid **40**. The cycloadduct 4-methyl-3-cyclohexenecarboxylic acid **39** was then aromatized by  $\text{H}_2\text{SO}_4$  producing *p*-toluic acid **41**, which was then oxidized with  $\text{KMnO}_4$  to terephthalic acid **11**.<sup>32</sup>

Scheme 4.5. Alder's Reaction Sequence



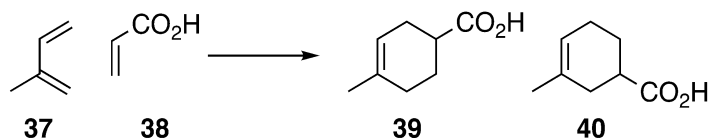
This reaction sequence developed by Alder can produce biobased terephthalic acid if microbially synthesized isoprene<sup>33</sup> **37** and biobased acrylic acid **38** are used.<sup>34,35</sup> The realization of commercial biobased terephthalic acid production with the Alder reaction sequence requires improvement of each step. Clery performed the cycloaddition of isoprene and acrylic acid in a high pressure reactor at 95 °C for 2 h and reported a “quantitative yield” of 4-methyl-3-cyclohexenecarboxylic acid **39** and 3-methyl-3-cyclohexenecarboxylic acid **40** as a 3:1 mixture.<sup>36a</sup> PET contains a 20:1 mixture of terephthalic acid **11** and isophthalic acid **43**.<sup>36b</sup> The selectivity of Clery's reaction was inadequate for commercial terephthalic acid production. Tong and Wang modified the Alder reaction sequence to synthesize biobased terephthalic acid by improving cycloaddition selectivity with the use of  $\text{BH}_3$  catalysis.<sup>37</sup> However, they used Alder's conditions for the next two steps: a stoichiometric  $\text{H}_2\text{SO}_4$  oxidation of 4-methyl-3-cyclohexenecarboxylic acid **39** to toluic acid **41** and stoichiometric  $\text{KMnO}_4$  oxidation of toluic

acid **41** to terephthalic acid **11**.<sup>32,37</sup> In this chapter, methods for aromatization of 4-methyl-3-cyclohexenecarboxylic acid **39** and 3-methyl-3-cyclohexenecarboxylic acid **40** to *p*-toluic acid **41** and *m*-toluic acid **42**, respectively, are improved. *p*-Toluic acid **41** synthesized by aromatization of 4-methyl-3-cyclohexenecarboxylic acid **39** with H<sub>2</sub>SO<sub>4</sub> requires a vapor phase filtration in order to utilize the Amoco Mid-Century oxidation process to yield terephthalic acid **11**. The purification method is established in this chapter. A vapor phase plug reactor was developed for dehydrogenation reaction to aromatize both 4-methyl-3-cyclohexenecarboxylic acid **39** and 3-methyl-3-cyclohexenecarboxylic acid **40** to *p*-toluic acids **41** and *m*-toluic acid **42**. Also heterogeneous catalysts for cycloaddition of isoprene and acrylic acid was explored.

## 4. Results

### 4.1. Cycloaddition of Acrylic Acid and Isoprene

Scheme 4.6. Cycloaddition of Acrylic Acid and Isoprene



Cycloaddition of acrylic acid **38** and isoprene **37** (Scheme 4.6) were performed using at various reaction conditions (Table 4.1). Uncatalyzed neat cycloaddition of acrylic acid **38** and isoprene **37** in a sealed tube at rt yielded 7% of 4-methyl-3-cyclohexenecarboxylic acid (*para* cycloadduct) **39** and 2% of 3-methyl-3-cyclohexenecarboxylic acid (*meta* cycloadduct) **40** (Table 4.1, entry 1). The uncatalyzed neat reaction performed in a high pressure reactor (6.9 bar) at 95 °C afforded 60% of *para* cycloadduct and 19% of *meta* cycloadduct (Table 4.1, entry 2). Since PET contains a 20:1 mixture of terephthalic acid **11** and isophthalic acid **43**,<sup>36b</sup> the selectivity of this reaction would be inadequate for commercial terephthalic acid production. Heterogeneous catalysts for cycloaddition of acrylic acid **38** and isoprene **37** were explored. Smit reported the use of silica gel as a heterogeneous catalyst in various cycloadditions.<sup>38</sup> This reaction uniquely featured a “dry state adsorption condition.” In this dry state adsorption condition, both the diene and dienophile were adsorbed and reacted on the silica gel in the absence of solvent.<sup>38</sup> Smit did not report any cycloaddition of dienophile with carboxylic acid moieties. However, he reported that the Diels-Alder reaction of isoprene **37** and methyl vinyl ketone or acrolein yielded 70% and 56 % cycloadducts, respectively, with 95-97% selectivity toward *para*.<sup>38</sup> This dry state adsorption condition was tested on the cycloaddition of acrylic acid **38** and isoprene **37**. A mixture of acrylic acid **38** and isoprene **37** were adsorbed onto pre-dried

chromatographic grade SiO<sub>2</sub> (230-400 mesh, pore size 60 Å) while the weight of the solution and SiO<sub>2</sub> was kept at a ratio of 1:15.

Table 4.1. Cycloaddition of Acrylic Acid and Isoprene

entry	equivalent		catalyst	solvent	temp, time	pressure	Yield	
	<b>38</b>	<b>37</b>					<b>39</b>	<b>40</b>
							(mol ratio)	
1	1.0	1.1	-	neat	rt, 24 h	< 1.6 bar <sup>b</sup>	7% <sup>e</sup> (3.5 : 1.0)	2% <sup>e</sup>
2	1.0	1.1	-	neat	95 °C, 2 h	8.3 bar <sup>c</sup>	60% <sup>e</sup> (3.1 : 1.0)	19% <sup>e</sup>
3	1.0	1.1	SiO <sub>2</sub>	neat	25 °C, 2 h	< 1.6 bar <sup>c</sup>	6% <sup>f</sup> (3.0 : 1.0)	2% <sup>f</sup>
4	1.0	1.1	SiO <sub>2</sub>	neat	50 °C, 2h	< 1.6 bar <sup>c</sup>	8% <sup>f</sup> (2.7 : 1.0)	3% <sup>f</sup>
5	1.0	1.5	SiO <sub>2</sub>	neat	95 °C, 2 h	< 1.6 bar <sup>c</sup>	10% <sup>f</sup> (5.0 : 1.0)	2% <sup>f</sup>
6	1.0	5.0	zeolite β 8 wt% <sup>a</sup>	hexanes	rt, 24 h	1 bar <sup>d</sup>	27% <sup>f</sup> (14 : 1.0)	2% <sup>f</sup>
7	1.0	5.0	zeolite β 36 wt% <sup>a</sup>	hexanes	rt, 24 h	1 bar <sup>d</sup>	35% <sup>f</sup> (9.0 : 1.0)	4% <sup>f</sup>
8	1.0	1.1	zeolite β 8 wt% <sup>a</sup>	hexanes	rt, 24 h	1 bar <sup>d</sup>	23% <sup>f</sup> (12 : 1.0)	2% <sup>f</sup>
9	1.0	1.1	zeolite β 16 wt% <sup>a</sup>	hexanes	rt, 24 h	1 bar <sup>d</sup>	27% <sup>f</sup> (14 : 1.0)	2% <sup>f</sup>

a: Zeolite β wt% of hexanes' weight. b: apparatus = sealed tube

c: apparatus = high pressure reactor. d: apparatus = flask

e: Both yields were quantified with GC. f: Yield based on <sup>1</sup>HNMR integration.

After acrylic acid **38** and isoprene **37** were adsorbed onto the SiO<sub>2</sub>, it was allowed to react at 25, 50, 95 °C in a high-pressure reactor (Table 4.1, entry 3, 4 and 5). A high pressure reactor was employed in order to prevent evaporation of isoprene **37**. The cycloadducts were collected by rinsing the SiO<sub>2</sub> with EtOAc. The total yield of cycloadducts from the reactions at 25, 50, 95 °C were 8%, 11% and 12% respectively (Table 4.1, entry 3, 4 and 5). Although, a slight improvement in the selectivity toward *para* cycloadduct was observed in the reaction at 95 °C (5.0:1.0), it was still far below the ideal selectivity (20:1). Carlson employed zeolites in Diels-Alder reactions of isoprene and various dienophiles.<sup>39</sup> Carlson did not report any cycloaddition

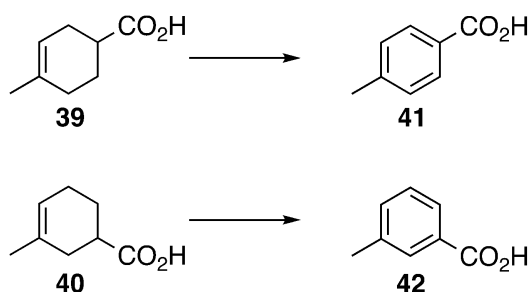
of a dienophile with a carboxylic acid. In his report, zeolite  $\beta$  showed 94-99% selectivity toward *para* cycloadduct with a reasonable yield when zeolite  $\beta$  was used as suspension in the reaction solution.<sup>39</sup> Carlson's reaction conditions were used for the cycloaddition of acrylic acid **38** and isoprene **37**. Flame activated zeolite  $\beta$  was suspended in the hexanes solution of acrylic acid **38** and isoprene **37** for 24 h at rt. Two reaction variables were compared in this reaction: the ratio of acrylic acid **38** to isoprene **37** and wt% of zeolite  $\beta$  (Table 4.1, entry 6,7,8 and 9). The crude products were collected by filtration and concentrated. An improvement in the selectivity toward to *para* cycloadduct was observed in all four reactions with better yields than the uncatalyzed reaction at rt (Table 4.1, entry 1 vs 6, 7, 8 and 9). However, the crude products after filtration to remove the zeolite  $\beta$  and concentration solidified to an intractable solid mass upon standing at room temperature overnight.

Investigation into improvement of the yield and *para* selectivity of the cycloaddition of acrylic acid **38** and isoprene **37** was continued by a co-worker, Kelly K. Miller.<sup>40</sup> He discovered that this cycloaddition catalyzed by 2 mol% of  $\text{TiCl}_4$  could afford a 94% yield of cycloadducts with 97% selectivity (23:1) favoring the *para* cycloadduct.<sup>40</sup> The pure *para* cycloadduct **39** was provided by Kelly to me to examine aromatization of *para* cycloadduct **39**.<sup>40</sup> Isolation of *meta* cycloadduct **40** was unsuccessful by column chromatography or distillation. The mixture of *para* and *meta* cycloadducts (ratio 1.00:1.26) was obtained from the uncatalyzed neat reaction performed in a high-pressure reactor. A crystallization of *para* cycloadduct **39** in hexanes gave *meta* cycloadduct **40** enhanced mother liquor. The crystallization of *para* cycloadduct **39** from the mother liquor gave more *meta* cycloadduct **40** enhanced mother liquor.

## 4.2. Aromatization of 4-Methyl-3-cyclohexenecarboxylic Acid and 3-Methyl-3-cyclohexenecarboxylic Acid

4-Methyl-3-cyclohexenecarboxylic acid **39** and 3-methyl-3-cyclohexenecarboxylic acid **40** were aromatized to *p*-toluic acid **41** and *m*-toluic acid **42** (Scheme 4.7) by three approaches: (1) oxidation using H<sub>2</sub>SO<sub>4</sub>; (2) solution phase dehydrogenation using Pd(0) or Pd(II); (3) vapor phase dehydrogenation using Pd(0).

Scheme 4.7. Aromatization of 4-Methyl-3-cyclohexenecarboxylic acid **39** and 3-methyl-3-cyclohexenecarboxylic acid **40**

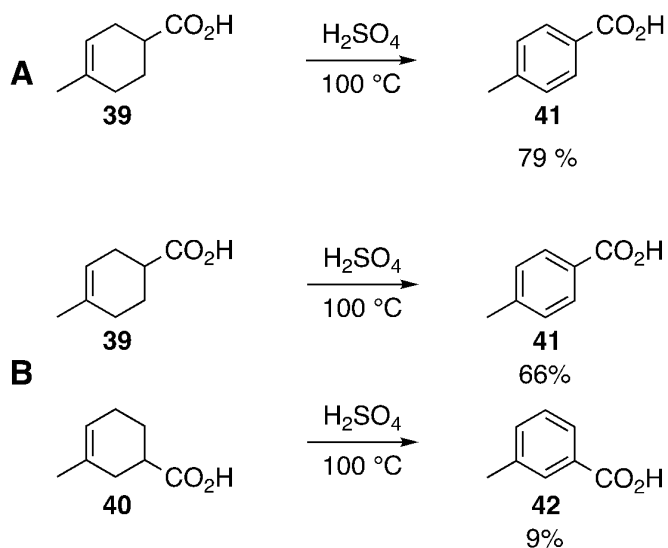


Alder reported<sup>32</sup> the aromatization of *para* cycloadduct **39** by oxidation using H<sub>2</sub>SO<sub>4</sub>, which was utilized by Tong<sup>37</sup> recently. The problem of this reaction was that 21% of the consumed *para*-cycloadduct **39** could not be accounted.

### 4.2.1. H<sub>2</sub>SO<sub>4</sub> Oxidation

As reported by Alder<sup>32</sup> and Tong,<sup>37</sup> *para* cycloadduct **39** was heated in concentrated H<sub>2</sub>SO<sub>4</sub> at 100 °C until vigorous SO<sub>2</sub> gas evolution ceased. Quenching the reaction solution with ice followed by filtration afforded 79% of *p*-toluic acid **41** (Scheme 4.8A). The proposed mechanism is depicted in Scheme 4.9.

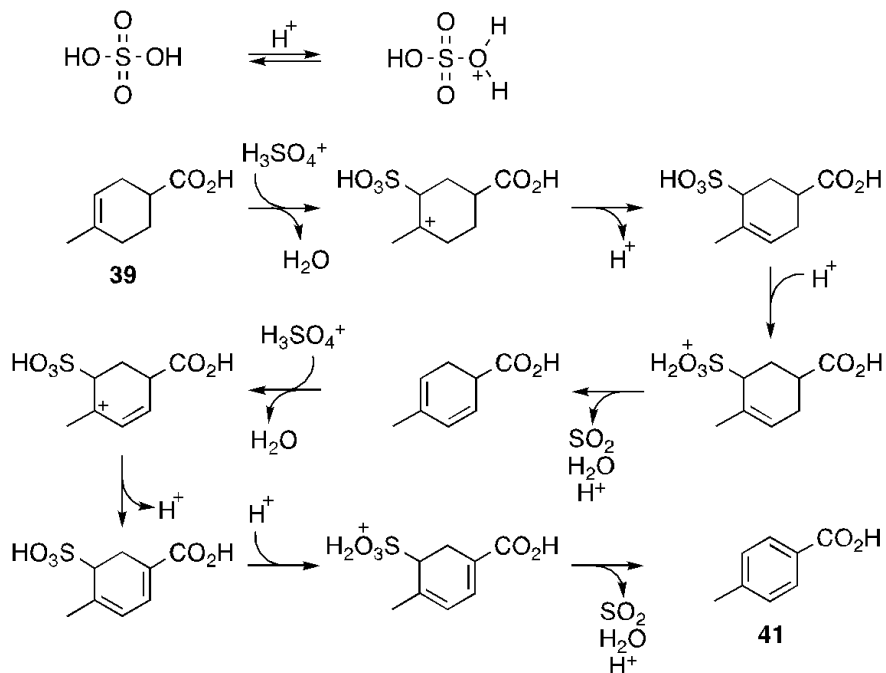
Scheme 4.8. H<sub>2</sub>SO<sub>4</sub> Oxidation



A: reaction with **39** only

B: reaction with mixture of **39** and **40** (**41** yield from **39**; **42** yield from **40**)

Scheme 4.9. Proposed Reaction mechanism of H<sub>2</sub>SO<sub>4</sub> Oxidation



The *p*-toluic acid **41** from this reaction contained impurities, which inhibit the subsequent

Amoco Mid-Century oxidation of *p*-toluic acid **41**. This problem was solved by purification of

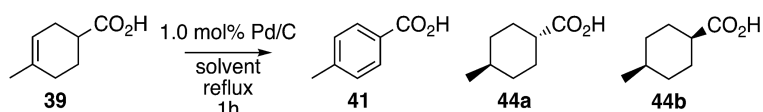
the *p*-toluic acid by distillation through a plug of chromatographic grade silica gel. A

disadvantage of this reaction was a loss of 21% of the *p*-toluic acid originally in the crude oxidation product. The use of H<sub>2</sub>SO<sub>4</sub> became more problematic when the 1.0:1.3 mixture of *para* **39** : *meta* **40** cycloadducts were aromatized to *p*-toluic acid **41** and *m*-toluic acid **42**, respectively. This reaction afforded 60% of *p*-toluic acid **41** from the *para* cycloadduct **39** and 9% of *m*-toluic acid **42** from the *meta* cycloadduct **40**, respectively (Scheme 4.8B).

#### 4.2.2. Dehydrogenation Catalyzed by Pd/C in Solvents

Due to the problem in H<sub>2</sub>SO<sub>4</sub> oxidation reaction, aromatization of *para*- and *meta*-cycloadducts was redirected towards dehydrogenation. The *para* cycloadduct **39** was aromatized by dehydrogenation with 1.0 mol% Pd/C in various solvents at their boiling points (Table 4.2).

Table 4.2. Dehydrogenation of 4-Methyl-3-cyclohexenecarboxylic Acid in Various Solvents



entry	solvent	temp (°C)	yield <sup>a</sup>	
			<b>41</b>	<b>44</b>
1	water	100	34%	63%
2	acetic acid	117	36%	60%
3	<i>p</i> -xylene	138	55%	45%
4	mesitylene	165	39%	59%
5	<i>n</i> -decane	175	39%	63%

a: yields were quantified by GC

Unlike H<sub>2</sub>SO<sub>4</sub> oxidation, almost all of the consumed *para*-cycloadduct **39** could be accounted for in product *para*-toluic acid **41** and side products *cis*-4-methyl-3-cyclohexanecarboxylic acid **44a** and *trans*-4-methyl-3-cyclohexanecarboxylic acid **44b** (Table 4.2). Separate dehydrogenative aromatizations of *para*-cycloadduct **39** with 1.0 mol% Pd/C in water, acetic acid, *n*-decane and mesitylene resulted in higher yields of cyclohexane side products **44a** and **44b** than desired product *p*-toluic acid (Table 4.2, entry 1, 2, 4 and 5). The reaction in *p*-xylene showed slightly

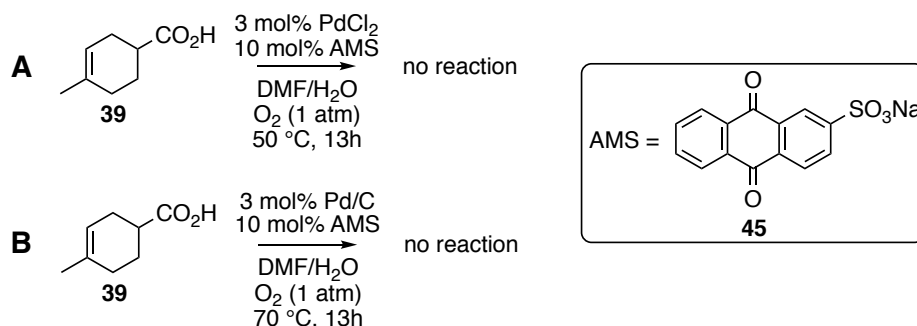
better selectivity: 55% of *p*-toluic acid and 45% of cyclohexanes (Table 4.2, entry 3).

Nitrobenzene is a hydrogen acceptor reported by Johnson Matthey<sup>41</sup> to improve the selectivity of dehydrogenations. Theoretically, transfer of hydrogen from a substrate to nitrobenzene results in formation of aniline and water. Nitrobenzene (17 mol%) was examined as the hydrogen acceptor in dehydrogenation of *para* cycloadduct **39** with 1 mol% Pd/C in mesitylene. It appeared that the reaction was inhibited by the nitrobenzene as evidenced by 69% of unreacted starting material after 6 days with 31% yield of *p*-toluic acid. This phenomenon was also reported by Trost and Metzner<sup>42</sup> during aromatization of cyclohexene.

#### 4.2.3. Catalytic Oxidative Dehydrogenation

Sheldon and Sobczak utilized anthraquinone-2-sulfonate sodium salt (AMS) **45** as a cocatalyst with either PdCl<sub>2</sub> or Pd/C for aromatization of cyclohexene to benzene.<sup>43</sup> They reported quantitative yields of benzene on a Pd/AMS catalytic system with molecular oxygen. We examined their reaction conditions on the aromatization of *para* cycloadduct **39** (Scheme 4.10). There was no reaction in either PdCl<sub>2</sub> with AMS or Pd/C with AMS.

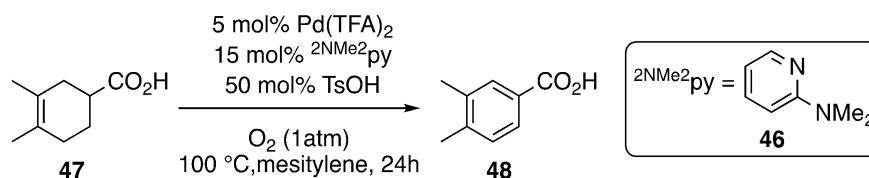
Scheme 4.10. Dehydrogenation of 4-Methyl-3-cyclohexenecarboxylic Acid on Pd/AMS



#### 4.2.4. Aerobic Dehydrogenation

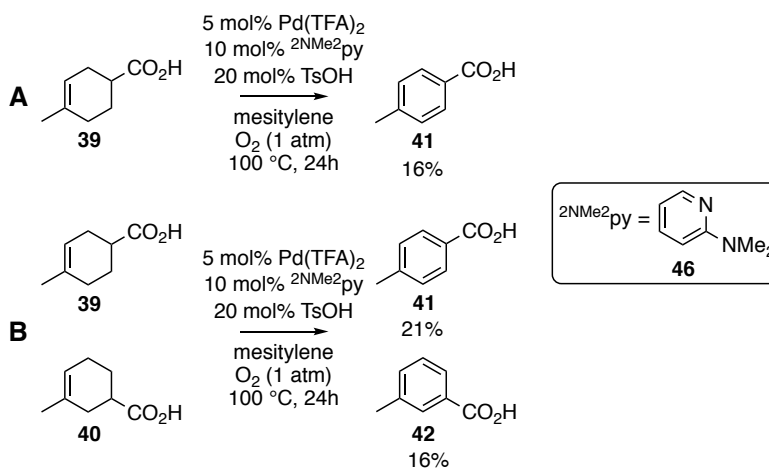
Stahl reported<sup>44</sup> a quantitative yield of aromatization of 3,4-dimethyl-3-cyclohexenecarboxylic acid **47** with Pd-catalyzed aerobic dehydrogenation (Scheme 4.11).

Scheme 4.11. Stahl's Reported Reaction



Despite the only difference between his substrate and the cycloadducts **39**, **40** is possession of one extra methyl at either C-3 or C-4, aromatization of both *para* **39** and *meta* **40** cycloadducts showed poor yields (Scheme 4.12). There was no unreacted substrate remaining and the <sup>1</sup>H NMR spectrum showed multiple unidentified products.

Scheme 4.12. Aerobic Dehydrogenation of 4-Methyl-3-cyclohexenecarboxylic Acid and 3-Methyl-3-cyclohexenecarboxylic Acid

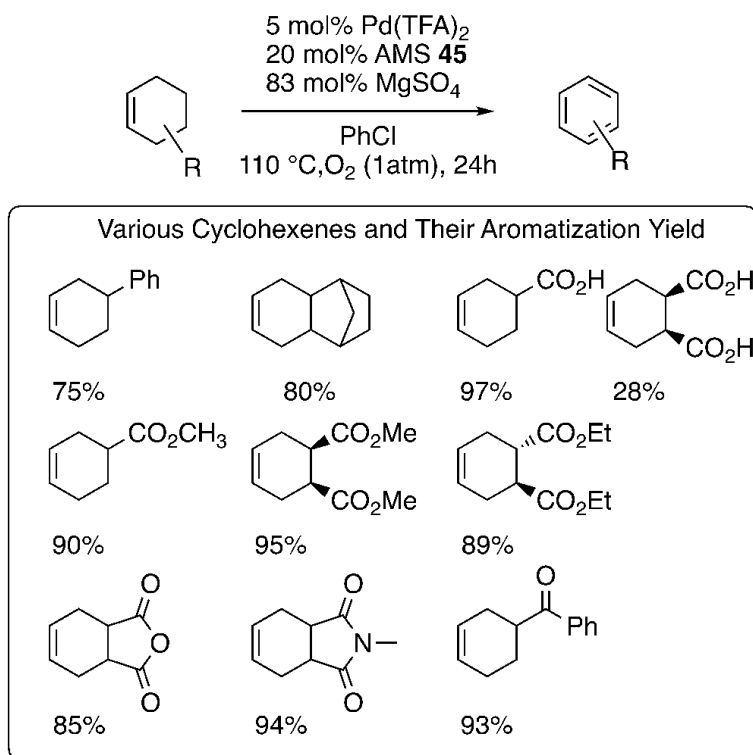


#### 4.2.5. Aerobic Oxidative Dehydrogenation

Recently, Stahl reported a modified catalyst system which could aromatize cyclohexenes. It consisted of Pd(TFA)<sub>2</sub>, AMS **45** and MgSO<sub>4</sub> as a drying agent.<sup>45</sup> The quantitative or near quantitative yields were reported with various substituted cyclohexenes (Scheme 4.13).

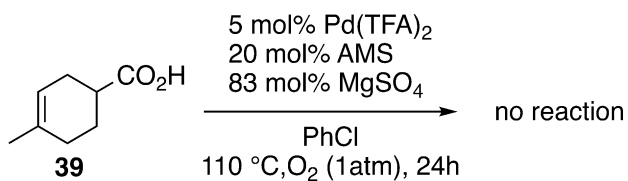
However, all of his reported successes were limited to substituents in the 4- and/or 5-position of the cyclohexenes without any substituent at other positions.

Scheme 4.13. Aerobic Oxidative Dehydrogenation of Cyclohexenes to Arene Derivatives<sup>45</sup>



His aerobic oxidative dehydrogenation reaction conditions were tested on aromatization of *para* cycloadduct **39** (Scheme 4.14). The methyl substituent evidently has a significant impact on the function of the catalyst. No reaction was observed using *para* **39** as a substrate.

Scheme 4.14. Aerobic Oxidative Dehydrogenation of 4-Methyl-3-cyclohexenecarboxylic Acid



#### 4.2.6. Vapor Phase Dehydrogenation

H<sub>2</sub>SO<sub>4</sub> oxidation reaction gave the highest yield (79%) of *p*-toluic acid **41** in the liquid phase aromatization of *para* cycloadduct **39**. However, the biggest disadvantage of this reaction is the inability to structurally account for 21% of the consumed *para*-cycloadduct. Also, we would like to avoid the use of hot, concentrated H<sub>2</sub>SO<sub>4</sub> as a stoichiometric oxidant and solvent. Fortunately, the cycloadducts **39** and **40** possess reasonable vapor pressures and therefore vapor phase dehydrogenative aromatization was realizable.

A vapor phase dehydrogenation reactor was developed with common laboratory glassware and instruments (Figure 4.1). The reaction substrate placed in a round bottom flask was distilled through Pd/C dispersed in macroporous silica gel (200-425 mesh, pore size 150 Å). The flask containing substrate and a glass tube containing the catalyst were inserted in an oven. The reaction product was collected in collection bulbs at ambient temperature and a U-shaped tube cooled to -78 °C. The entire glassware was rocked by an oscillating pneumatic motor (Sigma) to ensure even heating of the substrate and the catalyst. This apparatus was connected to a water recirculating aspirator pump. In order to avoid deactivation of the catalyst from moisture, a trap filled with a drying agent was placed between the reactor and the aspirator pump (Figure 4.1).

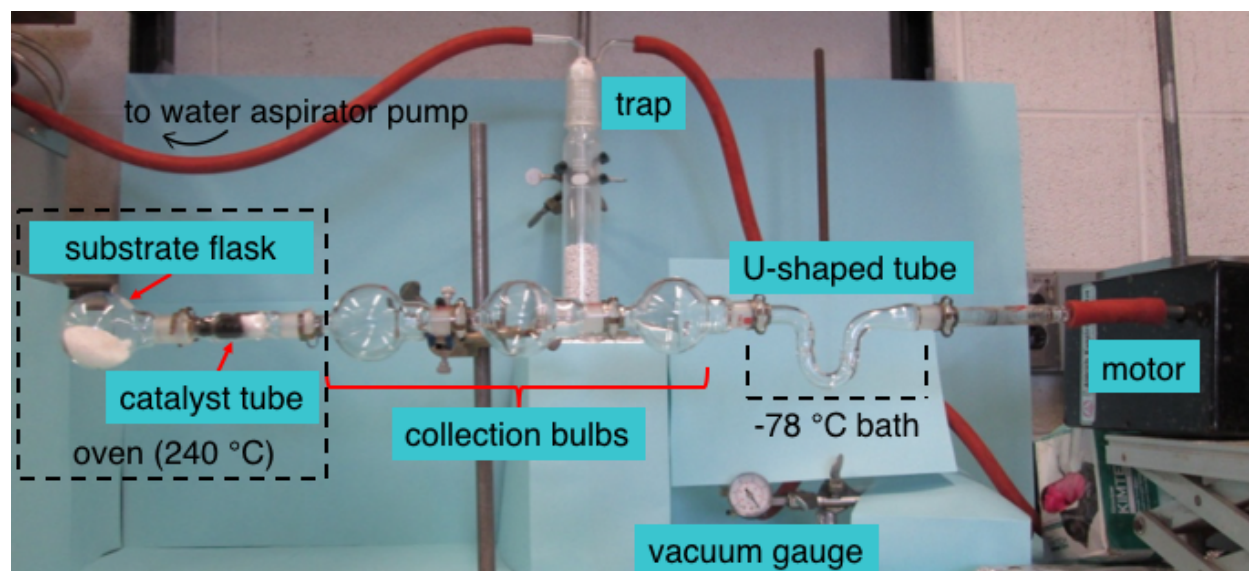
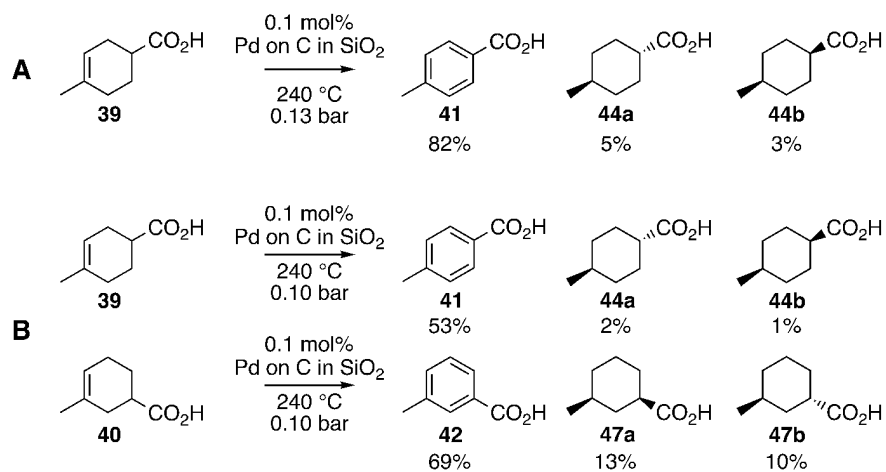


Figure 4.1. Vapor Phase Plug Reactor

*Para* cycloadduct **39** was distilled at 0.13 bar and 240 °C through Pd/C dispersed in macroporous silica gel. *p*-Toluic acid was obtained in 82% yield along with *trans*-4-methylcyclohexanecarboxylic acid **44a** and *cis*-4-methylcyclohexanecarboxylic acid **44b** in 5% and 3% yields, respectively (Scheme 4.15A). Not only this yield was comparable with the H<sub>2</sub>SO<sub>4</sub> oxidation reaction but also 90% of the mass of consumed *para*-cycloadduct could be structurally accounted for in *p*-toluic acid product 82% and side products *cis*- and *trans*- 8%. The aromatization of *meta* cycloadduct **40** with H<sub>2</sub>SO<sub>4</sub> gave a poor yield (9%) of *m*-toluic acid **42** (Scheme 4.8B). The vapor phase dehydrogenation of the 3.1:1.0 mixture of *para* **39**:*meta* **40** resulting from uncatalyzed cycloaddition led to a 69% yield of *m*-toluic acid **42** from *meta* cycloadduct **40** along with *trans*-3-methylcyclohexanecarboxylic acid **49b**, *cis*-3-methylcyclohexanecarboxylic acid **49a** and unreacted *meta* cycloadduct **40** in 10%, 13% and 17% yields, respectively (Scheme 4.15B).

Scheme 4.15. Vapor Phase Aromatization of 4-Methyl-3-cyclohexenecarboxylic Acid and 3-Methyl-3-cyclohexenecarboxylic Acid



A: reaction with **39** only.

B: reaction with mixture of **39** and **40** (**41** and **44** yields from **39**; **42** and **47** yields from **40**)  
 unreacted para cycloadduct **39** 28%, unreacted meta cycloadduct **40** 17%.

## 5. Discussion

Alder's and Tong's reaction conditions involve a stoichiometric  $\text{H}_2\text{SO}_4$  oxidation of 4-methyl-3-cyclohexenecarboxylic acid **39** to toluic acid **41** and stoichiometric  $\text{KMnO}_4$  oxidation of toluic acid **41** to terephthalic acid **11**.<sup>32,37</sup> *p*-Toluic acids **41** synthesized by aromatization of 4-methyl-3-cyclohexenecarboxylic acid **39** with  $\text{H}_2\text{SO}_4$  oxidation required a vapor phase filtration in order to use an Amoco Mid-Century oxidation to produce terephthalic acid **11**. Distillation of *p*-toluic acid **41** synthesized by  $\text{H}_2\text{SO}_4$  oxidation through a plug of chromatographic grade silica gel enabled use of an Amoco Mid-Century oxidation of *p*-toluic acid to obtain. Even though this purification method avoided the use of stoichiometric  $\text{KMnO}_4$  oxidation of toluic acid **41** to terephthalic acid **11**, there were still problems with the  $\text{H}_2\text{SO}_4$  oxidation reaction. Those problems included 21% of missing mass and the use of hot, concentrated  $\text{H}_2\text{SO}_4$  as a stoichiometric oxidant and solvent. The development of the vapor phase plug reactor for dehydrogenative aromatization solved both of these issues.

## 6. Experimental

### 6.1. General

<sup>1</sup>H NMR spectra were recorded on a 500 MHz spectrometer. Chemical shifts for <sup>1</sup>H NMR spectra are reported (in parts per million) relative to CDCl<sub>3</sub> ( $\delta = 7.26$  ppm). <sup>13</sup>C NMR spectra were recorded at 125 MHz and the shifts for these spectra are reported (in parts per million) relative to CDCl<sub>3</sub> ( $\delta = 77.0$  ppm). GC spectra were recorded on an Agilent 6890N chromatograph equipped with an autosampler. Zeolite  $\beta$  ammonium and 5 wt% Pd on C (A503023-5) were purchased from Alfa Aesar. All other reagents were purchased from Sigma-Aldrich. Chemicals were used as received without further purification.

### 6.2. Cycloaddition Products **39** and **40** Analysis

The total concentration of *para* cycloadduct **39** and *meta* cycloadduct **40** was quantified using an Agilent DB-FFAP nitroterephthalic acid modified polyethylene glycol coated capillary column (30 m  $\times$  0.320 mm i.d., 0.25  $\mu$ m film thickness). Isolated cycloadduct **39** was used as the standard, which was kindly provided by Kelly Miller.<sup>40</sup> The series of standard solutions contained 0.464–23.86 mg/mL of cycloadduct **39**, 50.3 mg/mL of 3-methylcyclohexanone as an internal standard and toluene as the solvent. The samples from cycloaddition were prepared in the same way as the standard solution. Syringe filtration (0.45  $\mu$ m Whatman filter) was followed by chromatographic analysis to determine the total concentration of *para* **39** and *meta* **40** cycloadducts.

The ratio of *para* cycloadduct **39** and *meta* cycloadduct **40** was determined using an Agilent HP-5 (5%-Phenyl)-methylpolysiloxane coated capillary column (30 m  $\times$  0.320 mm i.d., 0.25  $\mu$ m film thickness). A weighed quantity of the cycloaddition reaction products (12.6 mg,

0.0899 mmol) was added to toluene (2 mL) and *N,O*-bis(trimethylsilyl)trifluoroacetamide (BSTFA) (376  $\mu$ L, 1.42 mmol) were then added. Derivatization was complete upon mixing. Syringe filtration (0.45  $\mu$ m Whatman filter) was followed by chromatographic analysis to determine the ratio of *para* **39** and *meta* **40** cycloadducts.

### **6.3. Analysis of Aromatization Products: *p*-Toluic Acid **41** and 4-Methyl-3-cyclohexanecarboxylic Acid **44****

The concentrations of *p*-toluic acid **41** and 4-methylcyclohexanecarboxylic acid **44** were quantified using an Agilent DB-FFAP nitroterephthalic acid modified polyethylene glycol coated capillary column (30 m  $\times$  0.320 mm i.d., 0.25 $\mu$ L film thickness). *p*-Toluic acid **41** and 4-methylcyclohexanecarboxylic acid **44** obtained from Sigma-Aldrich were used as the standards. The series of standard solutions contained 0.51-5.04 mg/mL of *p*-toluic acid **41** and 1.14-5.02 mg/mL of 4-methylcyclohexanecarboxylic acid **44** with 3.20 mg/mL of 3-methylcyclohexanone as an internal standard and EtOH as the solvent. The samples from aromatization reaction were prepared in the same way as the standard solution. Syringe filtration (0.45  $\mu$ m Whatman filter) was followed by chromatographic analysis to determine the concentration of *p*-toluic acid **41** and 4-methylcyclohexanecarboxylic acid **44**.

**6.4. Analysis of Aromatization Products: *p*-Toluic Acid 41, *m*-Toluic Acid 42, 4-Methylcyclohexanecarboxylic Acid 44, 3-Methylcyclohexanecarboxylic Acid 47, Unreacted 4-Methyl-3-cyclohexenecarboxylic Acid 39 and Unreacted 3-Methyl-3-cyclohexenecarboxylic Acid 40**

*p*-Toluic **41** acid and *m*-toluic acid **42** were separated from one another with baseline resolution and quantified by HPLC using an Agilent ZORBAX SB-C18 (4.6 × 150 mm, 5 μm particle size) column and isocratic elution with 20/80, (v/v); CH<sub>3</sub>CN/H<sub>2</sub>O (100 mM NH<sub>4</sub><sup>+</sup>HCO<sub>2</sub><sup>-</sup>, pH 2.5). A series of standard solutions in EtOH of *p*-Toluic **41** acid (0.508-5.01 mg/mL) and *m*-toluic acid **42** (1.02-5.32 mg/mL) were prepared with *p*-toluic **41** and *m*-toluic acid **42** obtained from Sigma-Aldrich. The samples from aromatization reaction were prepared in the same way as the standard solution. Syringe filtration (0.45 μm Whatman filter) was followed by chromatographic analysis to determine the concentration of *p*-toluic acid **41** and *m*-toluic acid **42**.

The concentration of [4-methylcyclohexanecarboxylic acid **44** + 3-methylcyclohexanecarboxylic acid **47**] and [unreacted 4-methyl-3-cyclohexenecarboxylic acid **39** and 3-methyl-3-cyclohexenecarboxylic acid **40**] were quantified using an Agilent DB-FFAP nitroterephthalic acid modified polyethylene glycol coated capillary column (30 m × 0.320 mm i.d., 0.25 μm film thickness). 4-methylcyclohexanecarboxylic acid **44** obtained from Sigma-Aldrich were used as the standards. Isolated cycloadduct **39** was used as the standard, which was provided by Kelly Miller.<sup>40</sup> The series of standard solutions contained 0.49-5.10 mg/mL of 4-methylcyclohexanecarboxylic acid **44** and 0.97-4.94 mg/mL of cycloadduct **39** with 3.20 mg/mL of 3-methylcyclohexanone as an internal standard and EtOH as the solvent. The samples from aromatization reaction were prepared in the same way as the standard solution. Syringe filtration (0.45 μm Whatman filter) was followed by chromatographic analysis.

The ratio of *trans*-4-methylcyclohexanecarboxylic acid **44a**: *cis*-4-methylcyclohexanecarboxylic acid **44b**: *trans*-3-methylcyclohexanecarboxylic acid **47a**: *cis*-3-methylcyclohexanecarboxylic acid **47b** and unreacted 4-methyl-3-cyclohexenecarboxylic acid **39** to 3-methyl-3-cyclohexenecarboxylic acid **40** were determined using an Agilent HP-5 (5%-Phenyl)-methylpolysiloxane coated capillary column (30 m × 0.320 mm i.d., 0.25 μm film thickness). *N,O*-bis(trimethylsilyl)trifluoroacetamide (BSTFA) (600 μL, 1.42 mmol) and acetonitrile (400 μL, 2.26 mmol) were added to a reaction crude solid (20.6 mg). Derivatization was complete upon mixing. Syringe filtration (0.45 μm Whatman filter) was followed by analysis to determine the ratio of *trans*-4-methylcyclohexanecarboxylic acid **44a**: *cis*-4-methylcyclohexanecarboxylic acid **44b**: *trans*-3-methylcyclohexanecarboxylic acid **47a**: *cis*-3-methylcyclohexanecarboxylic acid **47b** and unreacted 4-methyl-3-cyclohexenecarboxylic acid **39** to 3-methyl-3-cyclohexenecarboxylic acid **40**.

### 6.5. Uncatalyzed Cycloaddition of Acrylic Acid **38** and Isoprene **37** at rt

A 100 mL glass pressure vessel (10.3 bar max) equipped with a magnetic stir bar was charged with acrylic acid **38** (8.36g, 116 mmol) and isoprene **37** (8.32g, 122 mmol). This solution was stirred for 24 h at rt. Concentrating this reaction solution afforded 7% of *para* cycloadduct **39** and 2% of *meta* cycloadduct **40** based on GC.

## 6.6. Uncatalyzed Cycloaddition of Acrylic Acid and Isoprene in a High Pressure Reactor

Isoprene (77.5 g, 1.14 mol) **37** was added to acrylic acid (71.4 g, 0.991 mol) **38** in a Parr Series 4575 high pressure reactor interfaced with a Series 4842 temperature controller. The reactor was flushed with N<sub>2</sub> and then pressurized to 8.3 bar with N<sub>2</sub>. Heating the reactor at 95 °C with stirring (100 rpm) for 2 h led to an initial increase in pressure to 13.8 bar followed by a decline in pressure to 9.7 bar. After allowing the reactor to cool, a yellow heterogeneous reaction crude was obtained containing a 79% yield of a 3.1:1.0 ratio of *para* cycloadduct **39**: *meta* cycloadduct **40** (83.3 g of *para* cycloadduct **39** and 26.4 g of *meta* cycloadduct **40**).

## 6.7. Silica Gel Catalyzed Cycloaddition of Acrylic Acid **38** and Isoprene **37** at 25 °C

Chromatographic grade silica gel was dried in a vacuum oven at 55 °C overnight. A solution containing isoprene **37** (2.70 g, 39.6 mmol) and acrylic acid **38** (2.70 g, 37.5 mmol) was added to the dry silica gel (79.1 g) in a 1 L stripping flask. This flask was rotated for 3 min in an iced-bath. This reaction solution adsorbed on the silica gel was transferred into a Parr Series 4575 high pressure reactor interfaced with a Series 4842 temperature controller in order to prevent evaporation of isoprene **37**. The reactor was maintained at 25 °C for 2 h. The reaction product was extracted into EtOAc from the silica gel. Concentrating this extract afforded 8% yield of a 3.0:1.0 ratio of *para* cycloadduct **39**: *meta* cycloadduct **40** (0.42g of *para* cycloadduct **39** and 0.11 g of *meta* cycloadduct **40**) based product mass and <sup>1</sup>H NMR integration.

### 6.8. Silica Gel Catalyzed Cycloaddition of Acrylic Acid **38** and Isoprene **37** at 50 °C

Chromatographic grade silica gel was dried in a vacuum oven at 55 °C overnight. A solution containing isoprene **37** (2.70 g, 39.6 mmol) and acrylic acid **38** (2.70 g, 37.5 mmol) was added to the dry silica gel (70.8 g) in a 1 L stripping flask. This flask was rotated for 3 min in an ice-bath. This reaction solution adsorbed on the silica gel was transferred into a Parr Series 4575 high pressure reactor interfaced with a Series 4842 temperature controller in order to prevent evaporation of isoprene **37**. The reactor was maintained at 50 °C for 2 h. The reaction product was extracted into EtOAc from the silica gel. Concentrating this extract afforded 11% yield of a 2.7:1.0 ratio of *para* cycloadduct **39**: *meta* cycloadduct **40** (0.42g of *para* cycloadduct **39** and 0.16 g of *meta* cycloadduct **40**) based on product mass and <sup>1</sup>H NMR integration.

### 6.9. Silica Gel Catalyzed Cycloaddition of Acrylic Acid **38** and Isoprene **37** at 95 °C

Chromatographic grade silica gel was dried in a vacuum oven at 55 °C overnight. A solution containing isoprene **37** (3.83 g, 56.2 mmol) and acrylic acid **38** (2.70 g, 37.5 mmol) was added to the dry silica gel (83.2 g) in a 1 L stripping flask. This flask was rotated 3 min in an ice-bath. This reaction solution adsorbed on silica gel was transferred into a Parr Series 4575 high pressure reactor interfaced with a Series 4842 temperature controller in order to prevent evaporation of isoprene **37**. The reactor was maintained at 95 °C for 2 h. The reaction product was extracted into EtOAc from the silica gel. Concentrating this extract afforded 12% yield of a 5.0:1.0 ratio of *para* cycloadduct **39**: *meta* cycloadduct **40** (0.56 g of *para* cycloadduct **39** and 0.11 g of *meta* cycloadduct **40**) based on product mass and <sup>1</sup>H NMR integration.

**6.10. Zeolite  $\beta$  Catalyzed Cycloaddition of Acrylic Acid **38** and Isoprene **37** (Table 4.1, entry 6)**

Zeolite  $\beta$  (5.29 g) was flame activated under vacuum. Hexanes (67.2 g) and acrylic acid **38** (3.75 g, 52.0 mmol) were added to the flame activated zeolite  $\beta$  under  $N_2$ . The mixture was stirred for 30 min at rt prior to addition of isoprene **37** (17.7 g, 260 mmol). This reaction mixture was stirred for 24 h at rt under  $N_2$ . Filtration of the reaction mixture followed by concentrating the filtrate afforded 29% yield of a 14:1.0 ratio of *para* cycloadduct **39**: *meta* cycloadduct **40** (2.00 g of *para* cycloadduct **39** and 0.14 g of *meta* cycloadduct **40**) based on product mass and  $^1H$  NMR integration. This crude product was a yellow oil initially however, it became an undissolvable solid after standing at rt overnight.

**6.11. Zeolite  $\beta$  Catalyzed Cycloaddition of Acrylic Acid **38** and Isoprene **37** (Table 4.1, entry 7)**

Zeolite  $\beta$  (5.28 g) was flame activated under vacuum. Hexanes (14.5 g) and acrylic acid **38** (3.75 g, 52.0 mmol) were added to the flame activated zeolite  $\beta$  under  $N_2$ . The mixture was stirred for 30 min at rt prior to addition of isoprene **37** (17.7 g, 260 mmol). This reaction mixture was stirred for 24 h at rt under  $N_2$ . Filtration of the reaction mixture followed by concentrating the filtrate afforded 39% yield of a 9.0:1.0 ratio of *para* cycloadduct **39**: *meta* cycloadduct **40** (2.57 g of *para* cycloadduct **39** and 0.29 g of *meta* cycloadduct **40**) based on the mass of product and  $^1H$  NMR integration. This crude product was a yellow oil initially however, it became an undissolvable solid after standing at rt overnight.

**6.12. Zeolite  $\beta$  Catalyzed Cycloaddition of Acrylic Acid **38** and Isoprene **37** (Table 4.1, entry 8)**

Zeolite  $\beta$  (5.24 g) was flame activated under vacuum. Hexanes (67.2 g) and acrylic acid **38** (3.75 g, 52.0 mmol) were added to the flame activated zeolite  $\beta$  under  $N_2$ . The mixture was stirred for 30 min at rt prior to addition of isoprene **37** (3.90 g, 57.3 mmol). This reaction mixture was stirred for 24 h at rt under  $N_2$ . Filtration of the reaction mixture followed by concentrating the filtrate afforded 25% yield of a 12:1.0 ratio of *para* cycloadduct **39**: *meta* cycloadduct **40** (1.65 g of *para* cycloadduct **39** and 0.14 g of *meta* cycloadduct **40**) based on the mass of product and  $^1H$  NMR integration. This crude product was a yellow oil initially however, it became an undissolvable solid after standing at rt overnight.

**6.13. Zeolite  $\beta$  Catalyzed Cycloaddition of Acrylic Acid **38** and Isoprene **37** (Table 4.1, entry 9)**

Zeolite  $\beta$  (5.25 g) was flame activated under vacuum. Hexanes (33.6 g) and acrylic acid **38** (3.75 g, 52.0 mmol) were added to the flame activated zeolite  $\beta$  under  $N_2$ . The mixture was stirred for 1 h at rt prior to addition of isoprene **37** (3.90 g, 57.3 mmol). This reaction mixture was stirred for 24 h at rt under  $N_2$ . Filtration of the reaction mixture followed by concentrating the filtrate afforded 29% yield of a 14:1.0 ratio of *para* cycloadduct **39**: *meta* cycloadduct **40** (1.97 g of *para* cycloadduct **39** and 0.14 g of *meta* cycloadduct **40**) based on the mass of product and  $^1H$  NMR integration. This crude product was a yellow oil initially however, it became an undissolvable solid after standing at rt overnight.

#### 6.14. H<sub>2</sub>SO<sub>4</sub> Oxidation of 4-Methyl-3-cyclohexenecarboxylic Acid **39** to *p*-Toluic Acid **41**

Concentrated H<sub>2</sub>SO<sub>4</sub> (80.0 mL, 1.50 mol) previously chilled in an ice bath was added dropwise to (20.1 g, 143 mmol) of *para* cycloadduct **39** (from a TiCl<sub>4</sub>-catalyzed cycloaddition<sup>40</sup>) in a 250 mL round bottom flask chilled in an ice bath and fitted with a reflux condenser open to the atmosphere. The solution was heated to 100 °C. Vigorous gas formation was first observed when the reaction mixture temperature reached 60 °C. Heating of the reaction mixture at 100 °C was continued until gas formation ceased. This gas was captured into a vacuumed Erlenmeyer flask and submitted to a GC/MS analysis confirming SO<sub>2</sub>. Sulfur dioxide: MS (EI) m/z = calculated [M]<sup>+</sup> 64.0, measured 63.9. The reaction mixture was heated for a total of 50 min from the time gas evolution was first observed at 60 °C. The reaction mixture was poured into ice (400 g) immediately after gas formation ceased, and 17.7 g of a tan-colored solid precipitated from solution. This solid was collected by filtration to afford 15.4 g (79%) of *p*-toluic acid **41** based HPLC. Kugelrohr distillation (50 mL bulbs, 14/20 joint size) of this solid through a plug (9 cm x 1.7 cm) of chromatographic grade silica gel (60 Å pore size, 40-63 μm mesh) under vacuum afforded 15.2 g (78%) of *p*-toluic acid **5** as a white solid. *p*-Toluic acid **41**: <sup>1</sup>H NMR (CDCl<sub>3</sub>) δ = 8.00-8.02 (m, 2H), 7.27-7.29 (m, 2H), 2.44 (s, 3H). <sup>13</sup>C NMR (CDCl<sub>3</sub>) δ = 127.5, 145.0, 130.6, 129.6, 126.9, 22.1. mp: 178-180 °C (Lit.<sup>46</sup> 178-180 °C).

#### 6.15. H<sub>2</sub>SO<sub>4</sub> Oxidation of a Mixture of 4-Methyl-3-cyclohexenecarboxylic Acid **39** and 3-Methyl-3-cyclohexenecarboxylic Acid **40** to *p*-Toluic Acid **41** and *m*-Toluic Acid **42**

The mixture of 4-methyl-3-cyclohexenecarboxylic acid **39** and 3-methyl-3-cyclohexenecarboxylic acid **40** were prepared from the uncatalyzed cycloaddition of acrylic acid **38** and isoprene **37** in a high pressure reactor. The concentration of *meta* cycloadduct **40** was

increased by removal of *para* cycloadduct **39** with multiple crystallization in hexanes. Concentrated H<sub>2</sub>SO<sub>4</sub> (3.99 mL, 74.9 mmol) previously chilled in an ice bath was added dropwise to a cycloadducts mixture consisting of *para* cycloadduct **39** (0.446 g, 3.18 mmol) and *meta* cycloadduct **40** (0.562 g, 4.01 mmol) in a 15 mL round bottom flask chilled in an ice bath and fitted with a reflux condenser open to the atmosphere. The solution was heated to 100 °C. Vigorous gas formation was first observed when the reaction mixture temperature reached 60 °C. Heating of the reaction mixture at 100 °C was continued until gas formation ceased. The reaction mixture was heated for a total of 13 min from the time gas evolution was first observed at 60 °C. The reaction mixture was poured into ice (20 g) immediately after gas formation ceased, and 0.630 g of a tan-colored solid precipitated from solution. This solid was collected by filtration to afford 0.286 g (66%) of *p*-toluic acid **39** and 0.0477g (9%) of *m*-toluic acid **40** based on HPLC analysis.

#### **6.16. Dehydrogenation of 4-Methyl-3-cyclohexanecarboxylic Acid **39** in Water**

Pd (5 wt%) on C containing approximately 50 wt% water was dried for 3 h under reduced pressure at 70 °C. Water (6.6 mL) followed by *para* cycloadduct **39** (1.32g, 9.42 mmol) were added to the 50 mL round bottom flask with three neck (14/20) containing dry Pd/C (0.20g, 0.094 mmol). The flask was fitted with a thermometer and reflux condenser open to the atmosphere. The reaction mixture was refluxed at 100 °C for 1 h. This reaction mixture was diluted with EtOH to 200 mL. Based on GC analysis, the reaction yield was 34% (0.441 g) of *p*-toluic acid **41** and 63% (0.849 g) of 4-methylcyclohexanecarboxylic acid **44**. <sup>1</sup>H NMR integration indicated the ratio of *trans*-4-methylcyclohexanecarboxylic acid **44a**: *cis*-4-methylcyclohexanecarboxylic acid **44b** was 1.3:1.0.

### 6.17. Dehydrogenation of 4-Methyl-3-cyclohexenecarboxylic Acid **39** in Acetic Acid

Pd (5 wt%) on C containing approximately 50 wt% water was dried for 3 h under reduced pressure at 70 °C. Acetic acid (5.3 mL) followed by *para* cycloadduct **39** (1.12g, 7.99 mmol) were added to the 50 mL round bottom flask with three neck (14/20) containing dry Pd/C (0.17 g, 0.080 mmol). The flask was fitted with a thermometer and reflux condenser open to the atmosphere. The reaction mixture was refluxed at 117 °C for 1 h. This reaction mixture was diluted with EtOH to 200 mL. Based on GC analysis, the reaction yield was 36% (0.391 g) of *p*-toluic acid **41** and 60% (0.686 g) of 4-methylcyclohexanecarboxylic acid **44**. <sup>1</sup>H NMR integration indicated the ratio of *trans*-4-methylcyclohexanecarboxylic acid **44a**: *cis*-4-methylcyclohexanecarboxylic acid **44b** was 1.4:1.0.

### 6.18. Dehydrogenation of 4-Methyl-3-cyclohexenecarboxylic Acid **39** in *p*-Xylene

Pd (5 wt%) on C containing approximately 50 wt% water was dried for 3 h under reduced pressure at 70 °C. *p*-Xylene (7.7 mL) followed by *para* cycloadduct **39** (1.32g, 9.42 mmol) were added to the 50 mL round bottom flask with three neck (14/20) containing dry Pd/C (0.20 g, 0.094 mmol). The flask was fitted with a thermometer and reflux condenser open to the atmosphere. The reaction mixture was refluxed at 138 °C for 1 h. This reaction mixture was diluted with EtOH to 200 mL. Based on GC analysis, the reaction yield was 55% (0.703 g) of *p*-toluic acid **41** and 45% (0.606 g) of 4-methylcyclohexanecarboxylic acid **44**. <sup>1</sup>H NMR integration indicated the ratio of *trans*-4-methylcyclohexanecarboxylic acid **44a**: *cis*-4-methylcyclohexanecarboxylic acid **44b** was 1.5:1.0.

### 6.19. Dehydrogenation of 4-Methyl-3-cyclohexenecarboxylic Acid **39** in Mesitylene

Pd (5 wt%) on C containing approximately 50 wt% water was dried for 3 h under reduced pressure at 70 °C. Mesitylene (6.5 mL) followed by *para* cycloadduct **39** (1.12g, 7.99 mmol) were added to the 50 mL round bottom flask with three neck (14/20) containing dry Pd/C (0.17 g, 0.080 mmol). The flask was fitted with a thermometer and reflux condenser open to the atmosphere. The reaction mixture was refluxed at 165 °C for 1 h. This reaction mixture was diluted with EtOH to 200 mL. Based on GC analysis, the reaction yield was 39% (0.428 g) of *p*-toluic acid **41** and 59% (0.672 g) of 4-methylcyclohexanecarboxylic acid **44**. <sup>1</sup>H NMR integration indicated the ratio of *trans*-4-methylcyclohexanecarboxylic acid **44a**: *cis*-4-methylcyclohexanecarboxylic acid **44b** was 1.7:1.0.

### 6.20. Dehydrogenation of 4-Methyl-3-cyclohexenecarboxylic Acid **39** in *n*-Decane

5% Pd on C containing approximately 50 wt% water was dried for 3 h under reduced pressure at 70 °C. *n*-Decane (8.2 mL) followed by *para* cycloadduct **39** (1.19g, 8.49 mmol) were added to the 50 mL round bottom flask with three neck (14/20) containing dry 5 wt% Pd/C (0.18 g, 0.085 mmol). The flask was fitted with a thermometer and reflux condenser open to the atmosphere. The reaction mixture was refluxed at 175 °C for 1 h. This reaction mixture was diluted with EtOH to 200 mL. Based on GC analysis, the reaction yield was 39% (0.458 g) of *p*-toluic acid **41** and 63% (0.765 g) of 4-methylcyclohexanecarboxylic acid **44**. <sup>1</sup>H NMR integration indicated the ratio of *trans*-4-methylcyclohexanecarboxylic acid **44a**: *cis*-4-methylcyclohexanecarboxylic acid **44b** was 1.5:1.0.

### 6.21. Dehydrogenation of 4-Methyl-3-cyclohexenecarboxylic Acid **39** and 3-Methyl-3-cyclohexenecarboxylic Acid **40** with Pd/C and Nitrobenzene in Mesitylene

To a solid containing *para* cycloadduct **39** (0.478g, 3.41 mmol) and *meta* cycloadduct **40** (0.0305 g, 0.218 mmol) in a 50 mL round bottom flask with three neck (14/20), are added 5 wt% Pd on C containing approximately 50 wt% water (0.184 g, 0.040 mmol), mesitylene (2.9 mL), AcOH 145  $\mu$ L and nitrobenzene (77.5 mg, 0.630 mmol). The flask was fitted with a thermometer and reflux condenser open to the atmosphere. The mixture was refluxed at 166 °C for 6 days. The mixture was gravity hot filtered, and the filtrate was concentrated under vacuum. The residue was dissolved in EtOH (100 mL as the final volume) and analyzed with HPLC. This afforded 0.145 g (31 %) *p*-toluic acid **41** and 8.14 mg (28%) of *m*-toluic acid **42**.

### 6.22. PdCl<sub>2</sub>-AMS Catalyzed Dehydrogenation of 4-Methyl-3-cyclohexenecarboxylic Acid **39**<sup>43</sup>

PdCl<sub>2</sub> (0.07 g, 0.4 mmol) and 0.32 g (1.0 mmol) of antoraquinone-2-sulfonate sodium salt (AMS) was added to a 100 mL round bottom flask (14/20) fitted with a magnetic stir bar. DMF (3.0 mL) and water (1.0 mL) were added to the flask. The flask was purged with O<sub>2</sub> followed by addition of *para* cycloadduct **39**. The flask was connected to a O<sub>2</sub> balloon through an air condenser after purging with O<sub>2</sub>. The reaction mixture was heated at 50 °C for 13 h. Based on <sup>1</sup>H NMR observation, there was no reaction.

### 6.23. Pd/C-AMS Catalyzed Dehydrogenation of 4-Methyl-3-cyclohexenecarboxylic Acid **39**<sup>43</sup>

Pd (5 wt%) on C containing approximately 50 wt% water (1.28 g, 0.30 mmol) and AMS (0.31 g, 1.0 mmol) was added to a 100 mL round bottom flask (14/20) fitted with a magnetic stir

bar. DMF (3.0 mL) and water (1.0 mL) were added to the flask. The flask was purged with O<sub>2</sub> followed by addition of *para* cycloadduct **39**. The flask was connected to an O<sub>2</sub> balloon through an air condenser after purging with O<sub>2</sub>. The reaction mixture was heated at 70 °C for 13 h.

Based on <sup>1</sup>H NMR observation, there was no reaction.

#### **6.24. Aerobic Dehydrogenation of 4-Methyl-3-cyclohexenecarboxylic Acid **39****<sup>44</sup>

To a glass test tube (20 × 150 mm) fitted with a magnetic stir bar was added Pd(TFA)<sub>2</sub> (32.7 mg, 0.0984 mmol), *p*-toluenesulfonic acid (76.0 mg, 0.400 mmol), 2-(*N,N*-dimethylamino)pyridine (24.5 mg, 0.201 mmol), *para* cycloadduct **39** (274 mg, 1.96 mmol) and mesitylene (0.90 mL). The test tube was sealed with a rubber septum and O<sub>2</sub> was sparged into the mixture for 10 min. The test tube was fitted with O<sub>2</sub> balloon and heated at 100 °C for 24 h. Water 10 mL was added to the reaction mixture, and then extracted in EtOAc (10 mL × 3). The organic layer was dried over MgSO<sub>4</sub> and concentrated to afford 43.5 mg (16%) of *p*-toluic acid based on HPLC analysis.

#### **6.25. Aerobic Dehydrogenation of 4-Methyl-3-cyclohexenecarboxylic Acid **39** and 3-Methyl-3-cyclohexenecarboxylic Acid **40****<sup>44</sup>

To a glass test tube (20 × 150 mm) fitted with a magnetic stir bar was added Pd(TFA)<sub>2</sub> (37.8 mg, 0.114 mmol), *p*-toluenesulfonic acid (84.1 mg, 0.442 mmol), 2-(*N,N*-dimethylamino)pyridine (34.5 mg, 0.282 mmol), a mixture of *para* cycloadduct **39** (138 mg, 0.984 mmol) and *meta* cycloadduct **40** (174 mg, 1.24 mmol), and mesitylene (0.94 mL). The test tube was sealed with a rubber septum and O<sub>2</sub> was sparged into the mixture for 10 min. The test tube was fitted with O<sub>2</sub> balloon and heated at 100 °C for 24 h. Water 10 mL was added to the

reaction mixture, and then extracted in EtOAc (10 mL × 3). The organic layer was dried over MgSO<sub>4</sub> and concentrated to afford 27.1 mg (21%) of *p*-toluic acid and 27.1 mg (16%) of *m*-toluic acid based on HPLC analysis.

#### 6.26. Aerobic Oxidative Dehydrogenation of 4-Methyl-3-cyclohexenecarboxylic Acid **39**<sup>45</sup>

To a glass test tube (20 × 150 mm) fitted with a magnetic stir bar was added *para* cycloadduct **39** (139 mg, 0.994 mmol), Pd(TFA)<sub>2</sub> (16.8 mg, 0.0505 mmol), AMS (62.5 mg, 0.201 mmol), MgSO<sub>4</sub> (99.8 mg) and chlorobenzene (1.0 mL). The test tube was sealed with a rubber septum and O<sub>2</sub> was sparged into the mixture for 10 min while the mixture was stirred. The test tube was fitted with O<sub>2</sub> balloon and heated at 110 °C for 24 h. Water 10 mL was added to the reaction mixture, and then extracted in EtOAc (10 mL × 3). There was no reaction based on GC analysis and <sup>1</sup>H NMR observation.

#### 6.27. Vapor Phase Dehydrogenation of 4-Methyl-3-cyclohexenecarboxylic Acid **39**

Davisil Grade 643 silica gel (150Å pore size, 35-70 μm mesh) was dried in a vacuum oven (150 °C, 15 mbar) overnight. Pd (5wt%) on C containing approximately 50 wt% water was dried for 3 h under reduced pressure at 70°C. The dried silica gel (1.67 g) and dried Pd (5wt%) on C (0.18g, 0.085mmol) were thoroughly mixed and then packed into a 9 cm × 1.7cm glass tube using glass wool to immobilize the plug reactor material. 4-Methyl-3-cyclohexenecarboxylic acid **39** (10.1 g, 72.0 mmol) obtained from a TiCl<sub>4</sub>-catalyzed cycloaddition was placed in a 50 mL, 14/20 round bottom flask. Vaporization/dehydrogenation of *para* cycloadduct **39** employed a Kugelrohr apparatus assembled as follows: the 50 mL flask containing **39**, the 9 cm × 1.7 cm glass tube containing the plug reactor, three 50 mL collection bulbs in series, a U-shaped tube

and finally a straight gas adaptor connected to a water recirculating aspirator pump (Figure 1). The flask containing **39** and plug reactor were inserted into the Kugelrohr oven. The second 50 mL collection bulb and U-shaped tube were cooled to  $-78^{\circ}\text{C}$ . Vaporization/dehydrogenation proceeded at  $240^{\circ}\text{C}$  under vacuum (0.13 bar) with reciprocal oscillating agitation. The white solid that accumulated in the collection bulbs and the U-shaped tube was collected with EtOH washes. The plug reactor contents were suspended in EtOH followed by filtration to remove the Pd on C and silica gel. All of the EtOH washes were combined, concentrated and dried to afford 8.03 g (82 %) of *p*-toluic acid **41**, 0.495 g (5%) of *trans*-4-methylcyclohexanecarboxylic acid **44a**, and 0.405 g (3%) of *cis*-4-methylcyclohexanecarboxylic acid **44b**.

#### **6.28. Vapor Phase Dehydrogenation of a Mixture of 4-Methyl-3-cyclohexenecarboxylic Acid **39** and 3-Methyl-3-cyclohexenecarboxylic Acid **40****

Davisil Grade 643 silica gel (150Å pore size, 35-70µm mesh) was dried in a vacuum oven ( $150^{\circ}\text{C}$ , 15 mbar) overnight. Pd (5wt%) on C containing approximately 50 wt% water was dried for 3 h under reduced pressure at  $70^{\circ}\text{C}$ . The dried silica gel (1.73 g) and dried 5wt% Pd on C (0.20 g, 0.094mmol) were thoroughly mixed and then packed into a 9 cm × 1.7cm glass tube using glass wool to immobilize the plug reactor material. A mixture of *para* cycloadduct **39** (8.00 g, 57.1 mmol) and *meta* cycloadduct **40** (2.61 g, 18.6 mmol) resulting from an uncatalyzed cycloaddition was placed in a 50 mL, 14/20 round bottom flask. Vaporization/dehydrogenation of the mixture of *para* cycloadduct **39** and *meta* cycloadduct **40** employed a Kugelrohr apparatus assembled as follows: the 50 mL flask containing **39** and **40**, the 9 cm x 1.7 cm glass tube containing the plug reactor, three 50 mL collection bulbs in series, a U-shaped tube and finally a straight gas adaptor connected to a water recirculating aspirator pump (Figure 1). The flask

containing cycloadducts **39** and **40** and plug reactor were inserted into the Kugelrohr oven. The second 50 mL collection bulb and U-shaped tube were cooled to -78 °C.

Vaporization/dehydrogenation proceeded at 240 °C under vacuum (0.11 bar) with reciprocal oscillating agitation. The white solid that accumulated in the collection bulbs and the U-shaped tube was collected with EtOH washes. The plug reactor contents were suspended in EtOH followed by filtration to remove the Pd on C and silica gel. All of the EtOH washes were combined, concentrated and dried to afford 4.08 g (53 %) of *p*-toluic acid **41**, 0.17 g (2%) of *trans*-4-methylcyclohexanecarboxylic acid **44a**, 0.05 g (1%) of *cis*-4-methylcyclohexanecarboxylic acid **44b**, 2.23 g (28%) of unreacted 4-methyl-3-cyclohexenecarboxylic acid **39**, 1.74 g (69%) of *m*-toluic acid **42**, 0.34 g (13%) of *cis*-3-methylcyclohexanecarboxylic acid **47a**, 0.27 g (10%) of *trans*-3-methylcyclohexanecarboxylic acid **47b** and 0.44 g (17%) of unreacted 3-methyl-3-cyclohexenecarboxylic acid **40**.

## REFERENCES

## REFERENCES

1. Merchant Research & Consulting Ltd. Global PET Supply to Exceed 24.39Mln Tonnes in 2015. <https://mcgroup.co.uk/news/20140117/global-pet-supply-exceed-2439-mln-tonnes-2015.html> (accessed Jan 06, 2017).
2. Collias, D. I., Harris, A. M., Nagpal, V., Cottrell, I. W., Schultheis, M. W. Biobased terephthalic acid technologies: a literature review. *Ind. Biotechnol.* **2014**, *10*, 91-105. DOI: 10.1089/ind.2014.0002.
3. Sheehan, R. J. Terephthalic Acid, Dimethyl Terephthalate, and isophthalic Acid. In *Ullmann's Encyclopedia of Industrial Chemistry*; Wiley-VCH: Weinheim, 2012; pp 17-28. DOI: 10.1002/14356007.a26\_193.pud2.
4. (a) Hanabatake, M. Production method of aromatic polyesters. JP S5657821, May 20, 1981. (b) Layton, R.; Cleay, J. W. Wholly aromatic polyesters with reduced char content. EP 0347228, June 15, 1989. (c) Huspeni, P. J.; Stern, B. A.; Frayer, P. D. Blends of liquid crystalline polymers of hydroquinone poly(iso-terephthalates) p-hydroxybenzoic acid polymers and another LCP containing oxybisbenzene and naphthalene derivatives. WO 9004002, April 19, 1990. (d) Waggoner, M. Liquid crystalline polymer composition. WO 9606888, July 03, 1996.
5. Wittcoff, H. A., Reuben, B. G., Plotkin, J. S. Chemicals from Xylenes. In *Industrial Organic Chemicals* 3<sup>rd</sup> ed.; Wiley: New Jersey, 2013; p 383-405.
6. (a) Tomas, R. A. F.; Bordado, J. C. M.; Gomes, J. F. P. *p*-Xylene oxidation to terephthalic acid: a literature review oriented toward process optimization and development. *Chem. Rev.* **2013**, *113*, 7421-7469. DOI: 10.1021/cr300298j. (b) Franck, H.-G., Stadelhofer, J. W. Production and Uses of Xylene Derivatives. In *Industrial Aromatic Chemistry: Raw Materials•Process•Products*; Springer-Verlag: Berlin, 1988; p265-290. (c) U.S. Environmental Protection Agency. Overview of Greenhouse Gases. Methane Emissions, 2013. <http://www3.epa.gov/climatechange/ghgemissions/gases/ch4.html> (accessed August 16, 2017)
7. Saffer, A.; Bayside, N. Y.; Barker, R. S.; Plainfield, N. J. Preparation of Aromatic Polycarboxylic Acids. US 2833816, May 6, 1958.
8. Zhu, Y.; Wang, B.; Liu, X.; Wang, H.; Wu, H.; Licht, S. STEP organic synthesis: an efficient solar, electrochemical process for the synthesis of benzoic acid. *Green Chem.* **2014**, *16*, 4758-4766. DOI: 10.1039/c4gc01448k.
9. James Tibbitt, Research Director (retired), Chemical Intermediates – Amoco/BP, personal communication.

10. Feldman, R. M. R.; Gunawardena, U.; Urano, J.; Meinhold, P.; Aristidou, A.; Dundon, C. A.; Smith, C. Yeast organism producing isobutanol at a high yield. US 20110183392, July 28, 2011.
11. Taylor, J. D.; Jenni, M. M.; Peters, M. W. Dehydration of fermented isobutanol for the production of renewable chemicals and fuels. *Top Catal.* **2010**, *53*, 1224-1230. DOI: 10.1007/s11244-010-9567-8.
12. Peters, M. W.; Taylor, J. D.; Jenni, M.; Manzer, L. E.; Henton, D. E. Integrated process to selectively convert renewable isobutanol to *p*-xylene. WO 2011044243 A1, April 14, 2011.
13. Taylor, T. J.; Taylor, J. D.; Peters, M. W.; Henton, D. E. Variations on prins-like chemistry to produce 2,5-dimethylhexadiene from isobutanol. US 20120271082, October 25, 2012.
14. (a) Brandvold, T. A. Carboxyhydrate route to *para*-xylene and terephthalic acid. US 8314267, December 30, 2010. (b) Cheng, Y.; Huber, G. W. Production of targeted aromatics by using Diels-Alder classes of reactions with furans and olefins over ZSM-5. *Green Chem.* **2012**, *14*, 3114-3125. DOI: 10.1039/c2gc35767d. (c) Takanishi, K.; Sone, S. Method for producing *para*-xylene. WO 2009110402 A1, September 11, 2009. (d) Wang, D.; Osmundsen, C. M.; Taarning, E.; Dumesic, J. A. Selective production of aromatics from alkylfurans over solid acid catalysts. *ChemCatChem* **2013**, *5*, 2044-2050. DOI: 10.1002/cctc.201200757.
15. Shiramizu, M.; Toste, F. D. On the Diels-Alder approach to solely biomass-derived polyethylene terephthalate (PET): conversion of 2,5-dimethylfuran and acrolein into *p*-xylene. *Chem. Eur. J.* **2011**, *17*, 12452-12457. DOI: 10.1002/chem.201101580.
16. Roman-Leshkov, Y.; Barrett, C. J.; Liu, Z. Y.; Dumesic, J. A. Production of dimethylfuran for liquid fuels from biomass-derived carbohydrates. *Nature* **2007**, *447*, 982-986. DOI: 10.1038/nature05923.
17. Zhao, H.; Holladay, J. E.; Brown, H.; Zhang, Z. C. Metal chloride in ionic liquid solvents convert sugars to 5-hydroxymethylfurfural. *Science* **2007**, *316*, 1597-1600. DOI: 10.1126/science.1141199.
18. Davda, R. R.; Dumesic, J. A. Renewable hydrogen by aqueous-phase reforming of glucose. *Chem. Comm.* **2004**, 36-37.
19. Kunkes, E. L.; Simonetti, D. A.; West, R. M.; Serrano-Ruiz, J. C.; Gartner, C. A. Dumesic, J. A. Catalytic conversion of biomass to monofunctional hydrocarbons and targeted liquid-fuel classes. *Science* **2008**, *322*, 417-421. DOI: 10.1126/science.1159210.
20. (a) Van Putten, R.-J.; van der Waal, J. C.; de Jong, E.; Rasrendra, C. B.; Heeres, H. J. Hydroxymethylfurfural, a versatile platform chemical made from renewable resources. *Chem. Rev.* **2013**, *113*, 1499-1597. DOI: 10.1021/cr300182k. (b) Lew, B. W. Method of Producing Dehydromucic Acid. US 3326944, June 20, 1967.

21. Gong, W. H. Terephthalic Acid Composition and Process for the Production Thereof. US 7385081, June 10, 2008.
22. Campbell, C. D.; Cole, D. T.; Taylor, H. R. III Process for the Preparation of Dialkyl Succinylsuccinates. US 5783723, July 21, 1998.
23. Cheng, K.; Zhao, X.; Zeng, J.; Zhang, J. Biotechnological production of succinic acid: current state and perspectives. *Biofuels Bioprod. Bior.* **2012**, *6*, 302-318. DOI: 10.1002/bbb.1327.
24. Kruper, W. Jr.; Rand, C. L.; Molzahn, D. C. Processes for Producing Terephthalic Acid and Terephthalic Esters. US 20130345467, December 26, 2013.
25. Ashworth, I. W.; Bowden, M. C.; Dembofsky, B.; Levin, D.; Moss, W.; Robinson, E.; Szczur, N.; Virica, J. A new route for manufacture of 3-cyano-1-naphthalenecarboxylic acid. *Org. Process Res. Dev.* **2003**, *7*, 74-81. DOI: 10.1021/op025571l.
26. Brown, S. H.; Bashkirova, L.; Berka, R.; Chandler, T.; Doty, T.; McCall, K.; McCulloch, M.; McFarland, S.; Thompson, S.; Yaver, D.; Berry, A. Metabolic engineering of *Aspergillus oryzae* NRRL 3488 for increased production of L-malic acid. *Appl. Microbiol. Biot.* **2013**, *97*, 8903-8912. DOI: 10.1007/s00253-013-5132-2.
27. Lee, J. J.; Kraus, G. A. One-pot formal synthesis of biorenewable terephthalic acid from methyl coumalate and methyl pyruvate. *Green Chem.* **2014**, *16*, 2111-2116. DOI: 10.1039/c3gc42487a.
28. Bui, V.; Lau, M. K.; MacRae, D.; Schweitzer, D. Methods for Producing Isomers of Muconic Acid and Muconate Salts. US 20130030215, January 31, 2013.
29. Niu, W.; Draths, K. M.; Frost, J. W. Benzene-free synthesis of adipic acid. *Biotechnol. Prog.* **2002**, *18*, 201-211. DOI: 10.1021/bp010179x.
30. Frost, J. W.; Miermont, A.; Schweitzer, D.; Bui, V.; Wicks, D. A. Novel Terephthalic and Trimellitic Based Acids and Carboxylate Derivatives Thereof. US 20120288311, November 24, 2011.
31. (a) Du Pont. An Improved Process for the preparation of Terephthalic Acid. GB 655074, July 11, 1951. (b) Colonna, M.; Berti, C.; Fiorini, M.; Binassi, E.; Mazzacurati, M.; Vannini, M.; Karanam, S. Synthesis and radiocarbon evidence of terephthalate polyesters completely prepared from renewable resources. *Green Chem.* **2011**, *13*, 2543-2548. DOI: 10.1039/c1gc15400a.
32. Alder, K.; Dortmann, H. A. Über substituierende addition und dien-synthese beim methylene-cyclobutan. *Chem. Ber.* **1952**, *85*, 556-565.

33. Whited, G. M.; Feher, F. J.; Benko, D. A.; Cervin, M. A.; Chotani, G. K.; McAuliffe, J. C.; LaDuca, R. J.; Ben-Shoshan, E. A.; Sanford, K. J. Development of a gas-phase bioprocess for isoprene-monomer production using metabolic pathway engineering. *Ind. Biotechnol.* **2010**, *6*, 152-163.
34. (a) Kumar, R.; Ashok, S.; Park, S. Recent advances in biological production of 3-hydroxypropionic acid. *Biotechnol. Adv.* **2013**, *31*, 945-961. (b) Lilga, M. A.; White, J. F.; Holladay, J. E.; Zacher, A. H.; Muzatko, D. S.; Orth, R. J. Method for Conversion of beta-Hydroxy Carbonyl Compounds. US 20070219391, September 20, 2007.
35. Yan, B.; Tao, L.; Liang, Y.; Xu, B. Sustainable production of acrylic acid: catalytic performance of hydroxyapatites for gas-phase dehydration of lactic acid. *ACS Catal.* **2014**, *4*, 1931-1943. DOI: 10.1021/cs500388x.
36. (a) Cahiez, G.; Rivas-Enterrios, J.; Clery, P. Organomanganese(II) reagents: a short and efficient synthesis of diastereoisomeric ( $\pm$ )- $\beta$ -bisaboloids and ( $\pm$ )-chiloperphenoxamine. *Tetrahedron Letters*, **1988**, *29*, 3659-3662. (b) East, A. J. Polyesters, Thermoplastic. In *Encyclopedia of Polymer Science and Technology*; Wiley: Hoboken, 2004; p504-529. DOI: 10.1002/0471440264.pst263.
37. Wang, F.; Tong, Z. Dehydro-aromatization of cyclohexene-carboxylic acids by sulfuric acid: critical route for bio-based terephthalic acid synthesis. *RSC Adv.* **2014**, *4*, 6314-6317. DOI: 10.1039/c3ra46670a.
38. Veselovsky, V. V.; Gybin, A. S.; Lozanova, A. V.; Moiseenkov, A. M.; Smit, W. A. Dramatic Acceleration of the Diels-Alder Reaction by adsorption on chromatography adsorbents. *Tetrahedron, Lett.* **1988**, *209*, 175-178.
39. Eklund, L.; Axelsson, A.-K.; Nordahl, A.; Carlson, R. Zeolite and Lewis acid catalysis in Diels-Alder reactions of isoprene. *Acta Chem. Scand.* **1993**, *47*, 581-591.
40. Miller, K. K.; Zhang, P.; Nishizawa-Brennen, Y.; Frost, J. W. Synthesis of biobased terephthalic acid from cycloaddition of isoprene with acrylic acid. *ACS Sustainable Chem. Eng.* **2014**, *2*, 2053-2056. DOI: 10.1021/sc5003038.
41. Johnson Matthey Catalysts. The Catalyst Technical Handbook. 2008.
42. Trost, B. M.; Metzner, P. J. Reaction of olefins with palladium trifluoroacetate. *J. Am. Chem. Soc.* **1980**, *102*, 3572-3577.
43. Sheldon, R. A.; Sobczak, J. M. Catalytic oxidative dehydrogenation of cyclohexene. *J. Mol. Catal.* **1991**, *68*, 1-6
44. Izawa, Y.; Pun, D.; Stahl, S. S. Palladium-catalyzed aerobic dehydrogenation of substituted cyclohexanones to phenols. *Science* **2011**, *333*, 209-213. DOI: 10.1126/science.1204183.

45. Iosub, A. V.; Stahl, S. S. Palladium-catalyzed aerobic oxidative dehydrogenation of cyclohexenes to substituted arene derivatives. *J. Am. Chem. Soc.* **2015**, *137*, 3454-3457. DOI: 10.1021/ja512770u.
46. Yavari, I.; Karimi, E. N-Hydroxyphthalimide-catalyzed oxidative production of phthalic acids from xylenes using O<sub>2</sub>/HNO<sub>3</sub> in an ionic liquid. *Synthetic Commun.* **2009**, *39*, 3420-3427. DOI: 10.1080/00397910902770461.

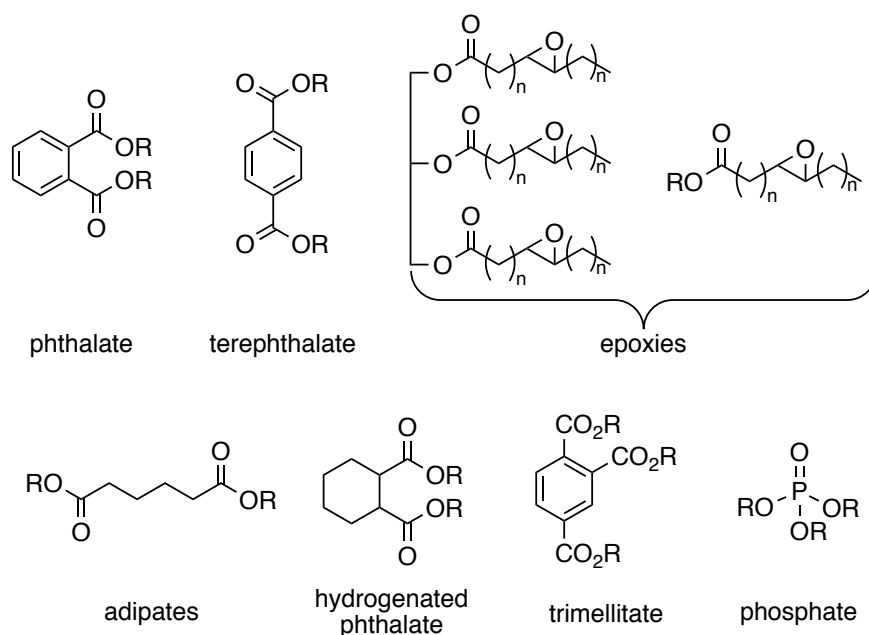
## CHAPTER FIVE

### Synthesis of Biobased Trimethyl Trimellitate

#### 1. Introduction

Plasticizers are used in resins to improve processability and to provide flexibility and strength. In 2010,  $6.0 \times 10^9$  kg of plasticizers were consumed globally.<sup>1a</sup> Flexible polyvinylchloride (PVC) constitutes 80-90% of global plasticizer production.<sup>1b</sup> Classes of plasticizers include phthalates, terephthalates, epoxies, aliphatics (adipates and hydrogenated phthalates), trimellitates, polymeric, and phosphates (Scheme 5.1).<sup>2</sup> In 2005, phthalates accounted for 88% of world plasticizer consumption. Phthalate usage declined to 70% of plasticizer consumption in 2014 and is projected to continue declining to 65% of plasticizer consumption in 2019.<sup>1b</sup> This decline is attributed to a demand for higher performance plasticizers and concerns regarding the impact of phthalates on human health and the environment.

Scheme 5.1. Plasticizers



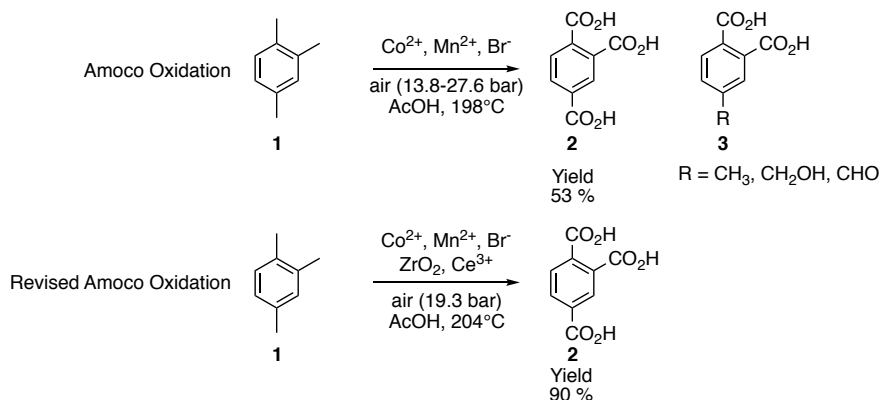
Testicular atrophy in adult male rats exposed to di-*n*-butyl phthalate was reported more than 40 years ago.<sup>3,4</sup> More recent studies have shown that exposing pregnant female rats to di-*n*-butyl or diethyl phthalate can lead to deformities in reproductive organs of male fetuses. These deformities caused structural and functional problems that persisted throughout the rats' lifetime.<sup>5-7</sup> Other reports have correlated elevated concentrations of phthalate diester or phthalate monoester, a metabolite of phthalate, in urine and semen of human males with various abnormalities. Takahashi examined the urine and blood of workers exposed to high levels of di-*n*-butyl and diethyl phthalates.<sup>8</sup> He reported a relationship between a high concentration of phthalate monoester in the urine with a significantly lower concentration of free-testosterone in the blood.<sup>8</sup> Calafat related a high concentration of monoethyl phthalate ester in urine with a high incidence of DNA damage in male test subjects sperm cells.<sup>9</sup> Saxena found that men who have a high concentration of diethyl / di-*n*-butyl / diethylhexyl phthalates in their semen tend to suffer from infertility, low sperm count, abnormal sperm cells or DNA fragmentation within sperm cells.<sup>10</sup> Since the toxicity of phthalate varies with the carbon chain of esters, each phthalate needs to be evaluated separately.<sup>11</sup>

Of the non-phthalate plasticizers, trimellitates and diisononyl cyclohexane-1,2-dicarboxylate (DINCH) have limited evidence of antiandrogenicity<sup>11</sup> and are resistant to high temperatures because they are very structurally stable and have extremely low volatility. These characteristics make trimellitates suitable for use in automobile interiors, high-specification electrical cable insulation and sheathing, construction materials, toys and medical devices. The demand for trimellitates is expected to grow in Asia Pacific, Europe and North America.<sup>12</sup>

## 2. Trimellitic Acid Production

Trimellitic acid **2** is commercially produced by oxidation of pseudocumene **1** (Scheme 5.2),<sup>13,14</sup> which is produced from catalytic reforming of crude oil fractions such as naphtha.<sup>15,16</sup> The oxidation of pseudocumene **1** employs a modified Amoco oxidation process.<sup>14</sup> Amoco oxidation ( $\text{Co}^{2+}$ ,  $\text{Mn}^{2+}$ ,  $\text{Br}^-$  in AcOH with air) produced a 53% yield of trimellitic acid<sup>17</sup> **2** along with undesired partial oxidation products **3** (Scheme 5.2).<sup>13,18</sup> Byproducts are attributed to incomplete aryl methyl group oxidations. Subsequent methyl group oxidations have higher energy barriers than initial oxidations. Thus, the last methyl substituent at C-4 is more difficult to oxidize than the first two. Even though increasing reaction temperature could theoretically help the oxidation of the last methyl substituent, it instead induced decarboxylation at C-4 producing a higher concentration of phthalic acid than trimellitic acid **2**.<sup>17</sup> Another significant problem during oxidation of pseudocumene is precipitation of the catalysts.<sup>18</sup> Higher yields of trimellitic acid were obtained with three metals ( $\text{Co}^{2+}$ ,  $\text{Mn}^{2+}$ ,  $\text{Ce}^{3+}$ ,  $\text{Br}^-$  in AcOH with air)<sup>13,14,19</sup> oxidation schemes. Amoco Corporation patented a revised Amoco process to produce trimellitic acid **2** from oxidation of pseudocumene **1** with a  $\text{Ce}^{3+}$ ,  $\text{ZrO}_2$ ,  $\text{Co}^{2+}$ ,  $\text{Mn}^{2+}$ ,  $\text{Br}^-$  in AcOH with air system (Scheme 5.2).<sup>14</sup> The main role of  $\text{ZrO}_2$  is to prevent the precipitation of the catalysts and increase the catalysts activity.<sup>18</sup>

Scheme 5.2. Oxidation of Pseudocumene

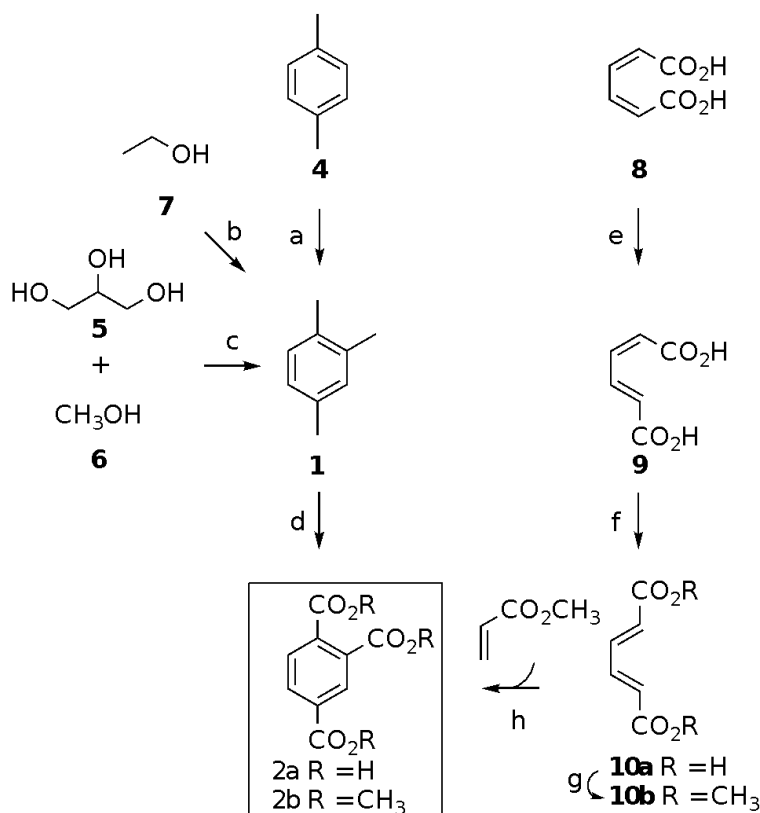


### 3. Biobased Trimellitic Acid / Trimethyl Trimellitate

Two general routes toward the synthesis of biobased trimellitate **2** have been published in the literature. One route involves a pseudocumene **1** intermediate while the other route does not (Scheme 5.3). Disproportionation of xylenes with shape-selective zeolite ZSM-5 produces pseudocumene **1** as a major product.<sup>15</sup> Synthesis of biobased *p*-xylene **4** was discussed in Chapter 4. Ethanol **7** can be reformed to pseudocumene **1**, along with fifteen other hydrocarbon products, using Cu-ZSM-5.<sup>20</sup> Catalytic reforming of glycerol **5** with methanol **6** over H-ZSM-5 affords pseudocumene **1** in addition to xylenes, toluene and benzene.<sup>21</sup> Glycerol and methanol are byproducts of biodiesel and wood pulp production, respectively.<sup>22,23</sup>

One route to trimethyl trimellitate that does not involve a pseudocumene intermediate utilizes microbially synthesized<sup>24</sup> *cis,cis*-muconic acid **8**, isomerized stepwise to *trans,trans*-muconic acid **10a**<sup>25,26</sup> prior to esterification to dimethyl *trans,trans*-muconate **10b** (Scheme 5.3). Cycloaddition of dimethyl *trans,trans*-muconate **10b** with methyl acrylate, followed by dehydrogenation affords trimethyl trimellitate **2b**.<sup>26</sup> Biobased methyl acrylate can be synthesized by esterification of biobased acrylic acid.<sup>27-29</sup>

Scheme 5.3. Biobased Trimellitate

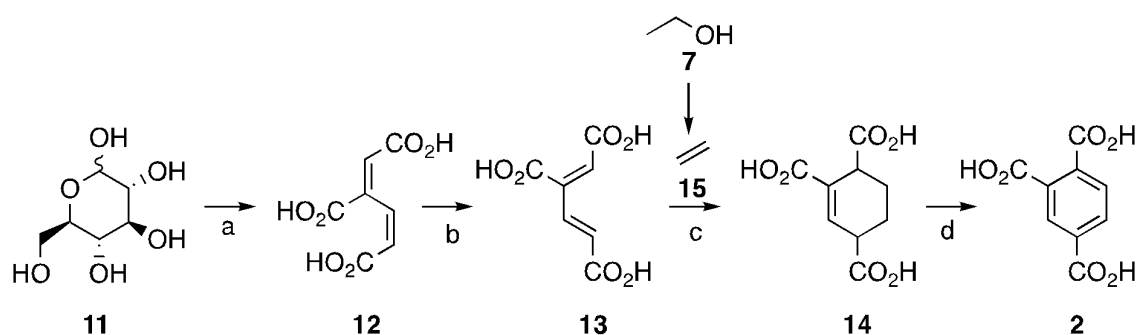


(a) ZSM-5, 427-538 °C (b) Cu-ZSM-5, 400 °C (c) HZSM-5, 400 °C, 16 % (d)  $\text{Co}^{2+}$ ,  $\text{Mn}^{2+}$ ,  $\text{Ce}^{3+}$ ,  $\text{ZrO}_2$ ,  $\text{Br}^-$ , AcOH, air, 19.3 bar, 204 °C, 90% (e) pH 4, 60 °C in fermentation broth, 100% (f)  $\text{I}_2$ , THF, rt, 84% (g)  $\text{H}_2\text{SO}_4$ , MeOH, reflux, 95% (h) i) neutral  $\text{Al}_2\text{O}_3$ , 4-*t*-butylcatechol, diglyme, 150 °C ii) Pd/C, diglyme, reflux, 46%

#### 4. New Synthetic Route to Biobased Trimellitic Acid

3-Carboxy-2*E*,4*Z*-muconic acid **12**, which is microbially synthesized from glucose can lead to another route for synthesis of biobased trimellitic acid **2** (Scheme 5.4). Isomerization of 3-carboxy-2*E*,4*Z*-muconic acid **12** to 3-carboxy-2*Z*,4*E*-muconic acid **13** followed by Diels-Alder reaction with bioethanol **7**-derived ethylene<sup>30</sup> **15** and subsequent aromatization would lead to trimellitic acid (Scheme 5.4). Additionally, hydrogenation of the cycloadduct **14** would lead to a new aliphatic plasticizer core. This proposed microbial synthesis of 3-carboxy-2*E*,4*Z*-muconic acid **12** uses the previous microbial synthesis of 2*Z*,4*Z*-muconic acid as its biosynthetic foundation.

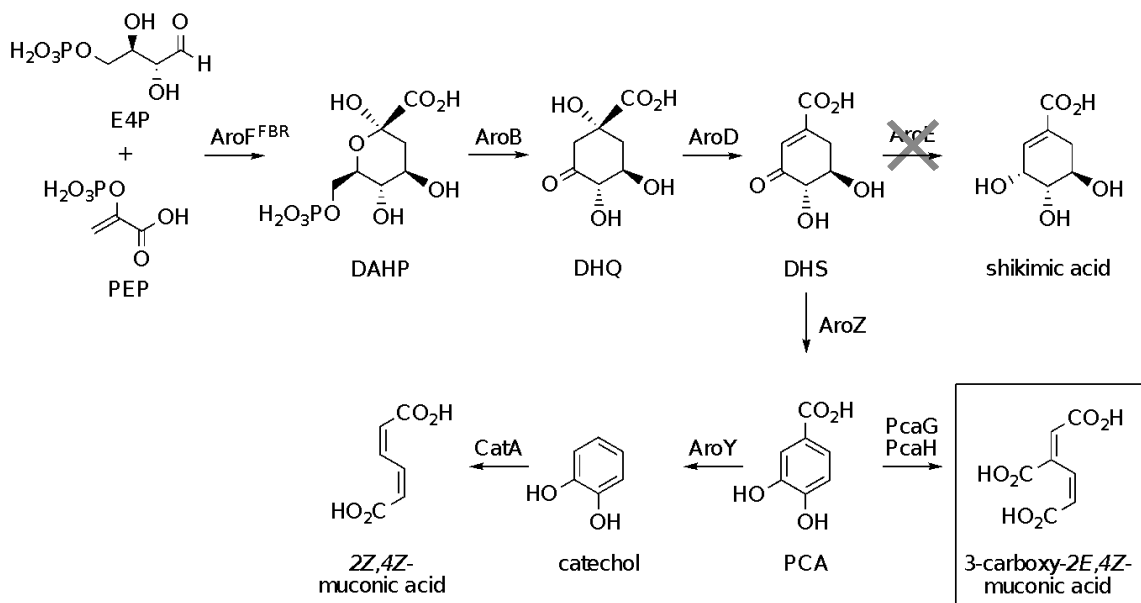
Scheme 5.4. New Synthetic Route to Biobased Trimellitic Acid



2Z,4Z-Muconic acid is microbially synthesized with *E. coli* WN1/pWN2.248, which was previously engineered in Frost group (Scheme 5.5).<sup>24</sup> Modification of the host genome for microbial synthesis of 2Z,4Z-muconic acid included the insertion of an *aroBaroZ* cassette into the *serA* locus<sup>31</sup>, insertion of a *tktAaroZ* cassette into the *lacZ* locus<sup>24</sup> and mutation of the *aroE* gene<sup>32,33</sup> in the genome of *E. coli* WN1. The extra genomic copy of *aroB* eliminates accumulation of 3-deoxy-D-arabino-heptulosonic acid 7-phosphate (DAHP), while mutation of *aroE* prevents carbon flow in the common pathway from proceeding beyond 3-dehydroshikimic acid (DHS).<sup>24</sup> In order to increase the availability of erythrose 4-phosphate (E4P), the genomic *tktA* insert results in overexpression of transketolase.<sup>24</sup> Two genomic copies of the *Klebsiella pneumoniae aroZ* gene, which encodes DHS dehydratase, enables the conversion of DHS to protocatechuic acid (PCA).<sup>24</sup> Disruption of L-serine biosynthesis is due to loss of genomic *serA*-encoded phosphoglycerate dehydrogenase. This ensures that WN1 retains plasmid pWN2.248, which encodes *serA*, *aroY*, *catA*, and *aroF<sup>FBR</sup>*. The *K. pneumoniae aroY* gene encoding PCA decarboxylase enables the conversion of PCA to catechol, and the *Acinetobacter calcoaceticus catA* gene encoding catechol 1,2-dioxygenase leads to production of 2Z,4Z-muconic acid.<sup>24</sup> Plasmid-localized *aroF<sup>FBR</sup>* encodes a mutant isozyme of 3-deoxy-D-arabino-heptulosonic acid 7-phosphate synthase, AroF<sup>FBR</sup>, which is insensitive to feedback inhibition by tyrosine increases

carbon flow into the common pathway of aromatic amino acid biosynthesis.<sup>24</sup>

Scheme 5.5. Biosynthetic Pathway of 2*E*,4*Z*-3-carboxymuconic Acid



E4P: erythrose 4-phosphate; PEP: phosphoenolpyruvate; DAHP: 3-deoxy-D-*arabino*-heptulosonic acid 7-phosphate; DHQ: 3-dehydroquinic acid; DHS: 3-dehydroshikimic acid; PCA: protocatechuic acid  
AroF<sup>FBR</sup>: DAHP synthase (tyrosine insensitive); AroB: DHQ synthase; AroD: DHQ dehydratase;  
AroE: shikimate dehydrogenase; AroZ: DHS dehydratase from *Klebsiella pneumoniae*;  
AroY: PCA decarboxylase from *K. pneumoniae*; CatA: catechol 1,2-dioxygenase from *Acinetobacter calcoaceticus*;  
PcaG PcaH: protocatechuate 3,4-dicarboxylase

3-Carboxy-2*E*,4*Z*-muconic acid synthesizing *E. coli* can be constructed with the same host strain WN1,<sup>24</sup> which already has the pathway to produce PCA from E4P and PEP (Scheme 5.5). The only new catalytic activity needed is *pcaGpcaH*-encoded protocatechuate 3,4-dioxygenase.

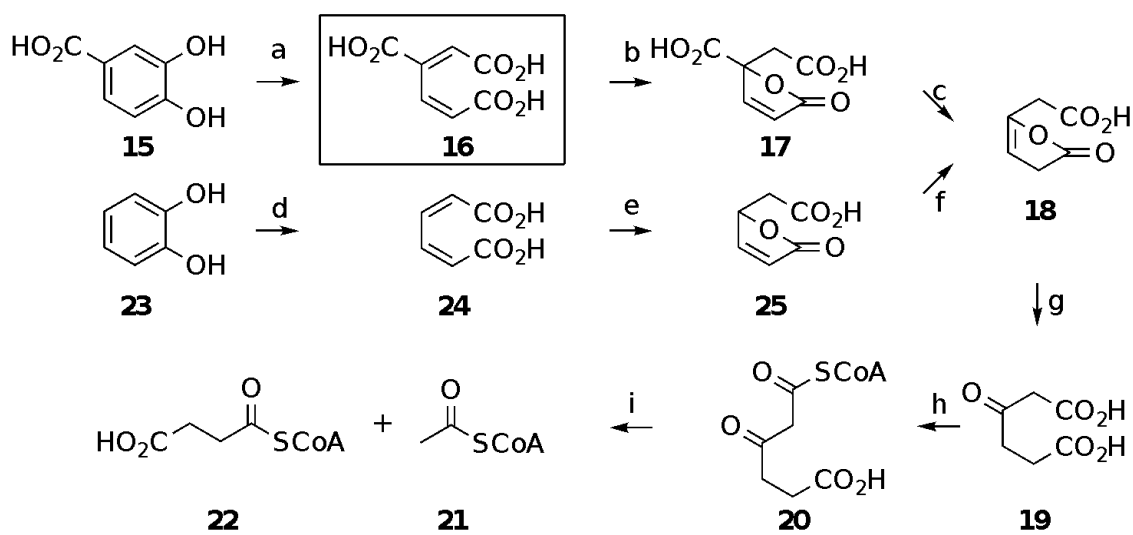
## 5. Protocatechuate 3,4-Dioxygenase

Protocatechuate 3,4-dioxygenase is endogenous to many bacteria.<sup>34-39</sup> A crystal structure of protocatechuate 3,4-dioxygenase has been determined.<sup>34</sup> Protocatechuate 3,4-dioxygenase contains sets of a nonheme ferric ion, an  $\alpha$ -subunit and a  $\beta$ subunit ( $[\alpha\beta\text{Fe}^{3+}]_x$ ).<sup>35-39</sup> The number of  $[\alpha\beta\text{Fe}^{3+}]$  depends on the species. Protocatechuate 3,4-dioxygenase of *Pseudomonas cepacia*

is  $[\alpha\beta\text{Fe}^{3+}]_4$ ; *Geobacillus sp.* is  $[\alpha\beta\text{Fe}^{3+}]_5$ , *Pseudomonas putida* is  $[\alpha\beta\text{Fe}^{3+}]_{12}$ .<sup>35-39</sup> The  $\alpha$ -subunit is encoded by *pcaG* and the  $\beta$ -subunit is encoded by *pcaH*.<sup>35,40</sup> The *pcaGpcaH* genes encoding protocatechuate 3,4-dioxygenase have been cloned and sequenced<sup>35,40</sup> from a variety of different bacterial sources and heterologously expressed in catalytically active form in *Escherichia coli*.<sup>39,41,42</sup>

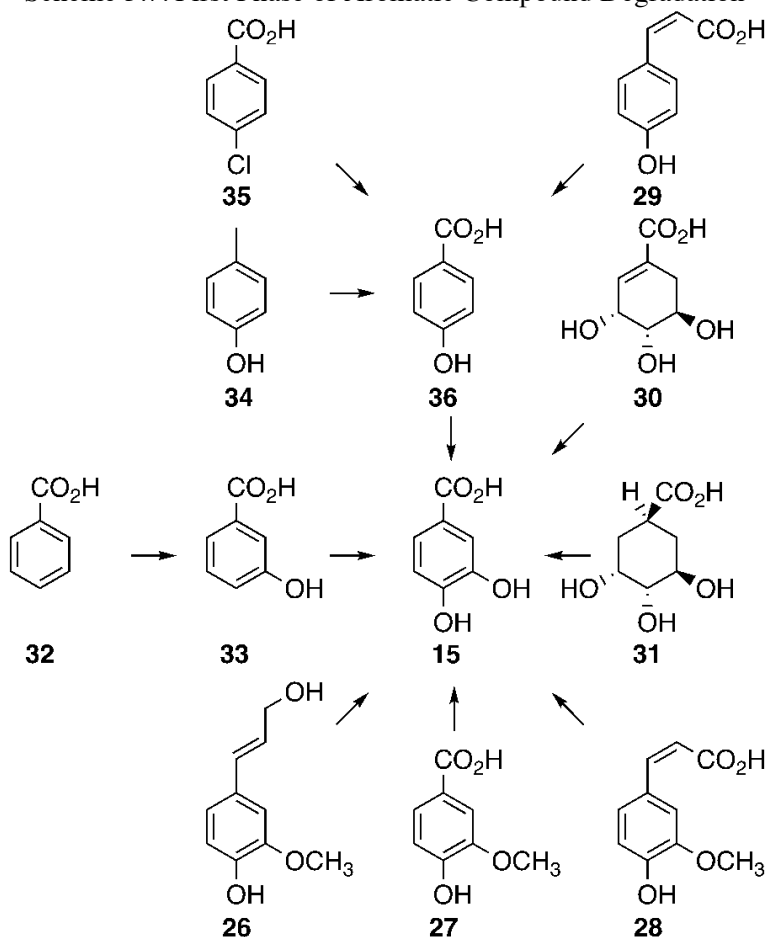
Protocatechuate 3,4-dioxygenase is found in the  $\beta$ -ketoacid pathway. This aromatic degradation pathway has two branches. One branch degrades protocatechuic acid **15**. The other branch degrades catechol **23** (Scheme 5.6).<sup>43</sup> Various aromatic compounds are first degraded to protocatechuic acid **15** (Scheme 5.7).<sup>43</sup> Protocatechuic acid **15** is then converted by enzymes of the  $\beta$ -ketoacid pathway to succinyl-CoA **21** and acetyl-CoA **22** via intermediacy of  $\beta$ -ketoacid **19** (Scheme 5.6).<sup>43</sup> The compounds converted to protocatechuic acid depend on the microbial species, which are frequently isolated from soil.<sup>43</sup> Coniferyl alcohol **26**, vanillic acid **27**, ferulic acid **28** and 4-coumaric acid **29** (Scheme 5.7) are lignin-related monomers from decaying plant materials.<sup>44</sup> Shikimic acid **30** and quinic acid **31** (Scheme 5.7) are also from decaying plant materials.<sup>43</sup> Benzoic acid **32**, p-cresol **34** and 4-chlorobenzoic acid **35** (Scheme 5.7) are pollutants found in soil, which result from human activity.<sup>45-47</sup>

Scheme 5.6.  $\beta$ -Ketoadipate Pathway



- (a) protocatechuate 3,4-dioxygenase (b)  $\beta$ -carboxy-*cis,cis*-muconate lactonizing enzyme E.C.5.5.1.2  
 (c)  $\gamma$ -carboxymuconolactone decarboxylase E.C.4.1.44 (d) catechol 1,2-dioxygenase  
 (e) *cis,cis*-muconate lactonizing enzyme (f) muconolactone isomerase (g) enollactone hydrolase  
 (h)  $\beta$ -ketoadipate:succinyl-CoA transferase (i)  $\beta$ -ketoadipyl-CoA thiolase

Scheme 5.7. First Phase of Aromatic Compound Degradation

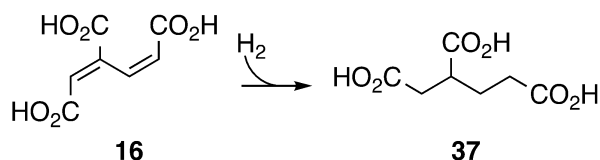


## 6. 1,2,4-Butanetricarboxylic Acid

### 6.1. Introduction

Another valuable biobased molecule that can be derived from 3-carboxy-2*E*,4*Z*-muconic acid **16** is 1,2,4-butanetricarboxylic acid **37** (Scheme 5.8).

Scheme 5.8. Synthesis of 1,2,4-Butanetricarboxylic Acid from 2*E*,4*Z*-3-Carboxymuconic Acid



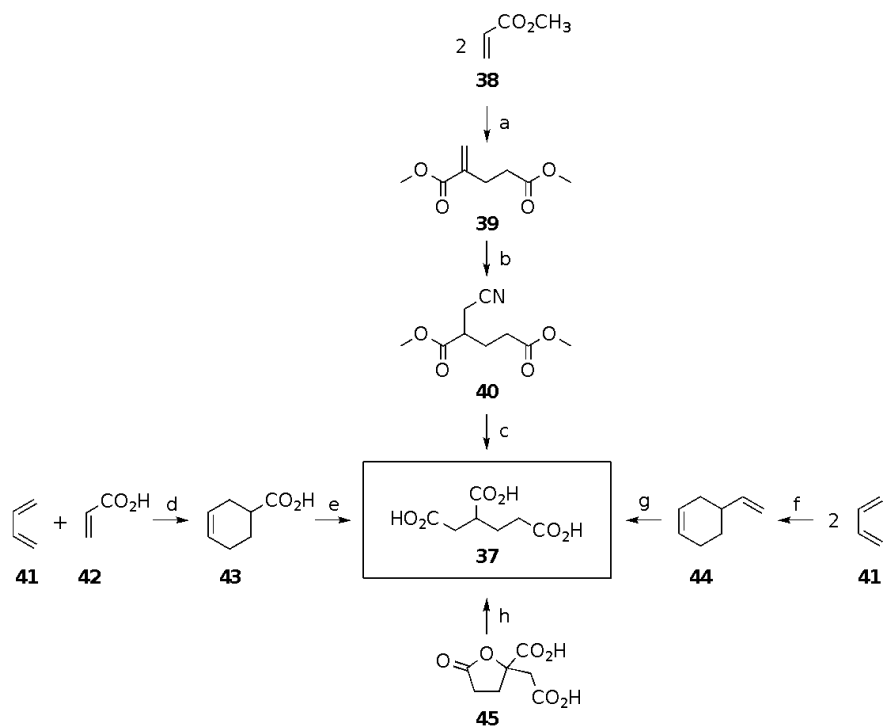
1,2,4-Butanetricarboxylic acid is used as a cross-linker in polyurethane coating formulations. These speciality coatings can tolerate 50 °C water, acidic water and prolonged exposure to sunlight.<sup>48</sup> 1,2,4-Butanetricarboxylic acid is also used in inkjet cartridges to prevent pigment bleeding.<sup>49</sup> Other applications include its utilization as a raw material for gellant in cosmetics,<sup>50</sup> a binder in electrochemical cells,<sup>51</sup> and used as a synthetic elastomer for cardiac tissue.<sup>52</sup> This synthetic elastomer will act as scaffolding for engineered tissue implants.<sup>52</sup>

### 6.2. Synthesis of Biobased 1,2,4-Butanetricarboxylic Acid

There are some reports in the literature suggesting 1,2,4-butanetricarboxylic acid can be made renewable by employing biobased starting materials (Scheme 5.9). Dimerization of methyl acrylate **38**, synthesized by esterification of biobased acrylic acid,<sup>27</sup> yields molecule **39**.<sup>53</sup> Hydrocyanation of **39** followed by hydrolysis affords 1,2,4-butanetricarboxylic acid **37**.<sup>53</sup> Two routes employ microbially synthesized<sup>54</sup> butadiene **41** as the starting material. Cycloaddition of butadiene **41** with biobased acrylic acid<sup>28,29</sup> **42** forms 3-cyclohexenecarboxylic acid **43**,<sup>55</sup> which is oxidized to 1,2,4-butanetricarboxylic acid **37**.<sup>56</sup> Dimerization of butadiene<sup>57</sup> **41** followed by oxidation of the dimer<sup>58</sup> **44** also affords 1,2,4-butanetricarboxylic acid. Hydrogenolysis of

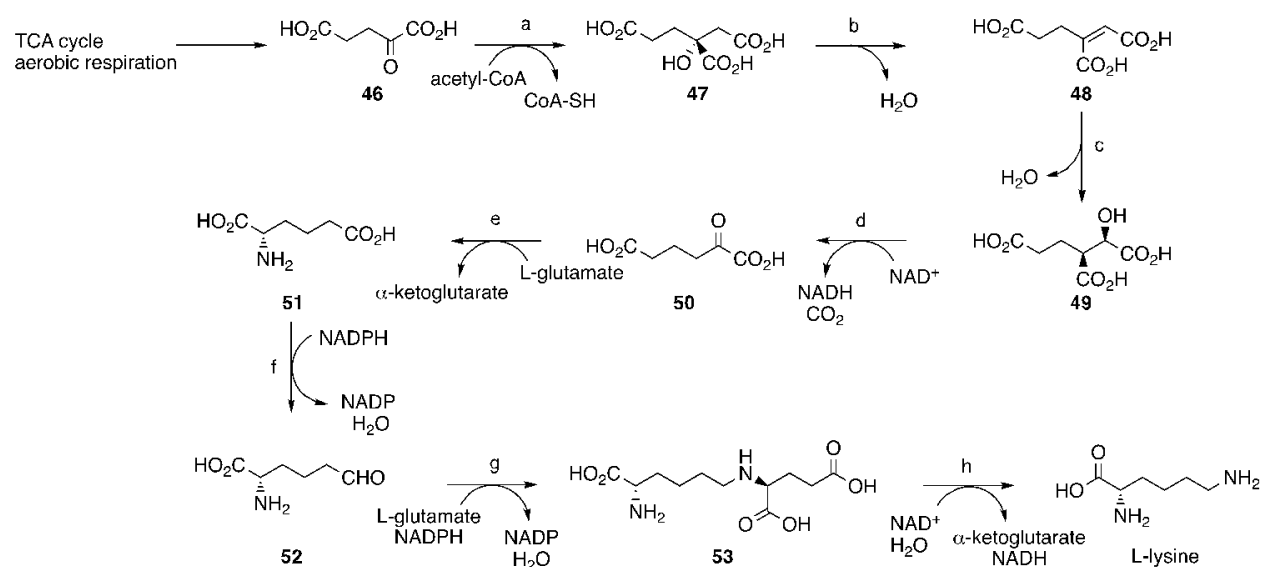
homocitric acid lactone **45** produced by genetically engineered *Issatchenkia orientalis* can also afford 1,2,4-butanetricarboxylic acid **37**.<sup>59</sup> Homocitric acid **47** is an intermediate of lysine biosynthesis pathway in *Issatchenkia orientalis* (Scheme 5.9).<sup>59</sup> The homocitric acid **47** lactonizes to homocitric acid lactone **45** in the acidic fermentation broth.<sup>59</sup>

Scheme 5.9. Biobased 1,2,4-Butanetricarboxylic Acid Synthesis Route



(a) tricyclohexylphosphine, chlorobenzene, 60 °C, 40% (b) HCN, CH<sub>3</sub>CN, 75 °C, 100% (c) 12N HCl, 110 °C, 80% (d) tetraacetyl diborate, -78 °C→rt, 99% (e) HNO<sub>3</sub>, NH<sub>4</sub>VO<sub>3</sub>, Cu<sup>0</sup>, 50-60 °C, 85%. (f) (C<sub>4</sub>H<sub>9</sub>)<sub>4</sub>N<sup>+</sup>[Fe(CO)<sub>3</sub>NO]<sup>-</sup>, FeCl<sub>2</sub>, 1.5 bar, 100 °C, 96% (g) HNO<sub>3</sub>, NH<sub>4</sub>VO<sub>3</sub>, 1-methylpicolinium chloride, 170 °C, 100%. (h) Pt/Pd on C, H<sub>2</sub>O, 150 °C, quantitative yield.

Scheme 5.10. Lysine Biosynthesis Pathway



(a) homocitrate synthase (b) homocitrate dehydratase (c) homoaconitase (d) homoisocitrate dehydrogenase  
 (e) 2-aminoadipate aminotransferase (f) alpha-aminoadipate reductase (g) saccharophine dehydrogenase 1.5.1.10  
 (h) saccharophine dehydrogenase 1.5.1.7

## 7. Results

### 7.1 Microbial Synthesis of 2*E*,4*Z*-3-Carboxymuconic Acid

#### 7.1.1. *E. coli* WN1/pYNB6.009A

##### 7.1.1.1. Cloning Overview

2*Z*,4*Z*-Muconic acid is microbially synthesized with *E. coli* WN1/pWN2.248, which was previously engineered in Frost group (Scheme 5.5).<sup>24</sup> Modification of the host genome for microbial synthesis of 2*Z*,4*Z*-muconic acid included the insertion of an *aroBaroZ* cassette into the *serA* locus<sup>31</sup>, insertion of a *tktAaroZ* cassette into the *lacZ* locus<sup>24</sup> and mutation of the *aroE* gene<sup>32,33</sup> in the genome of *E. coli* WN1. The extra genomic copy of *aroB* eliminates accumulation of 3-deoxy-D-*arabino*-heptulosonic acid 7-phosphate (DAHP), while mutation of *aroE* prevents carbon flow in the common pathway from proceeding beyond 3-dehydroshikimic acid (DHS).<sup>24</sup> In order to increase the availability of erythrose 4-phosphate (E4P), the genomic

*tktA* insert results in overexpression of transketolase.<sup>24</sup> Two genomic copies of the *Klebsiella pneumoniae aroZ* gene, which encodes DHS dehydratase, enables the conversion of DHS to protocatechuic acid (PCA).<sup>24</sup> Disruption of L-serine biosynthesis is due to loss of genomic *serA*-encoded phosphoglycerate dehydrogenase. This ensures that WN1 retains the plasmid pYNB6.009A, which contains *pcaHG*, *serA*, *aroF<sup>FBR</sup>* genes and *P<sub>aroF</sub>* DNA sequence. The *pcaHG* genes encode protocatechuate 3,4-dioxygenase, which converts protocatechuic acid into 2*E*,4*Z*-3-carboxymuconic acid.<sup>35,40</sup> The *aroF<sup>FBR</sup>* encodes a mutant isozyme of DAHP synthase whose expression is insensitive to feedback inhibition by tyrosine.<sup>24</sup> This allows elevated DAHP synthase activity when cells were cultured in medium containing aromatic amino acids. Transcription of *aroF* is repressed by the TyrR repressor-tyrosine complex.<sup>60a</sup> There are three sites (TYR R boxes) in the promoter of *aroF* where the TyrR repressor-tyrosine complex can bind.<sup>60a,b</sup> Even though, the TYR R boxes of *aroF<sup>FBR</sup>* possess weaker affinity to TyrR repressor-tyrosine complex than wild type, addition of tyrosine to the culture medium still causes some repression of *aroF* gene.<sup>60a</sup> The sequence of unmodified native promoter of *aroF* (*P<sub>aroF</sub>*) can titrate away the TyrR repressor-tyrosine complex.<sup>60c</sup>

#### **7.1.1.2. Construction of pKD16.179A and pYNB6.009A**

A 1.5 kb DNA fragment encoding *pcaHG* with its native promoter was amplified from *Klebsiella pneumoniae* subsp. *pneumoniae* (ATCC25597) and subsequently digested by EcoRI. Ligation of this fragment into the EcoRI digested pJF118EH resulted in pKD16.179A (Figure 5.1). The resulting *pcaHG* genes were transcribed in the same direction as the *tac* promoter located on pJF118EH.

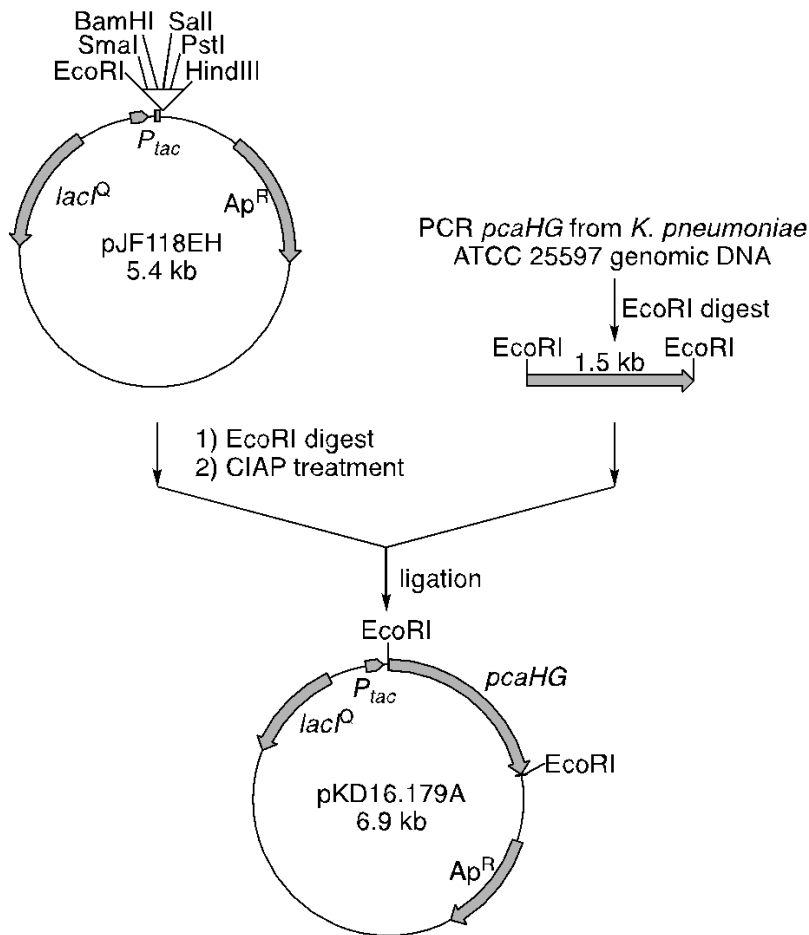


Figure 5.1. Preparation of Plasmid pKD16.179A

A 3.3 kb DNA fragment containing *serA* gene, *aroF<sup>FBR</sup>* gene and  $P_{aroF}$  DNA sequence was amplified from pWN1.162A<sup>24</sup> and subsequently digested by SmaI. Ligation of this fragment into the SmaI digested pKD16.179A resulted in pYNB6.009B (Figure 5.2). The resulting *serA* and *aroF<sup>FBR</sup>* genes were transcribed in the opposite direction to the *tac* promoter located on pKD16.179A.

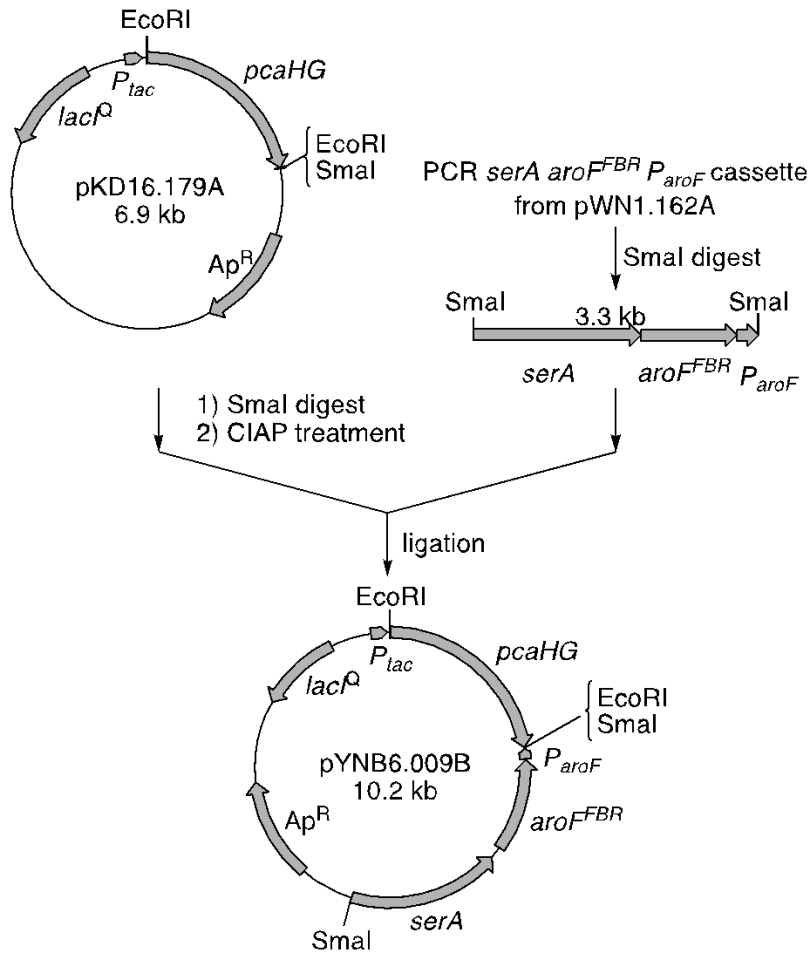


Figure 5.2. Preparation of Plasmid pYNB6.009B

The 3.3 kb DNA fragment containing *serA* gene, *aroF<sup>FBR</sup>* gene and  $P_{aroF}$  DNA sequence was digested from pYNB6.009B by *SmaI*. Ligation of this fragment into the *SmaI* digested pKD16.179A resulted in pYNB6.009A (Figure 5.2). The resulting *serA* and *aroF<sup>FBR</sup>* genes were transcribed in the same direction as the *tac* promoter located on pKD16.179A.

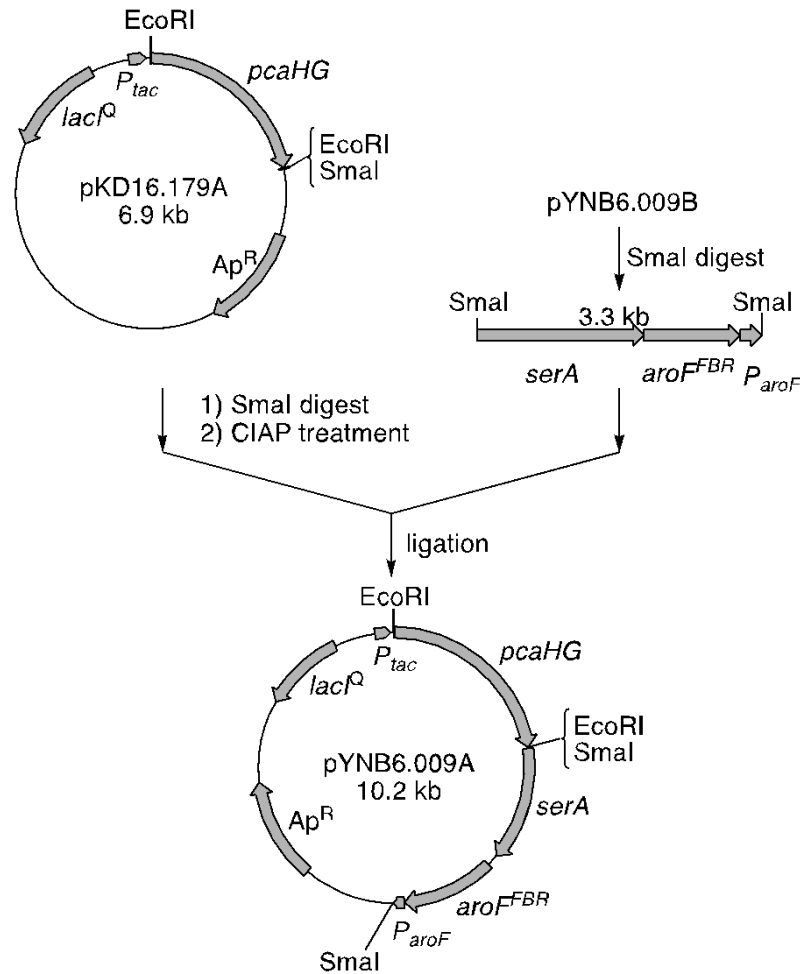


Figure 5.3. Preparation of Plasmid pYNB6.009A

### 7.1.1.3. Host Strain *E. coli* WN1 Phenotype Confirmation

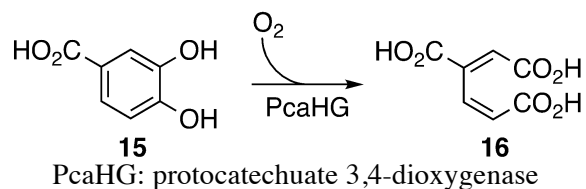
The host strain *E. coli* WN1 was previously engineered by Wei Niu in the Frost group.<sup>24</sup> The modifications of the host genome included the insertion of an *aroBaroZ* cassette into the *serA* locus<sup>31</sup>, insertion of *tktAaroZ* cassette into the *lacZ* locus<sup>24</sup> and mutation of the *aroE* gene<sup>32,33</sup> in the genome of *E. coli* WN1. Therefore, this strain requires supplementation of aromatic amino acids and serine. An insertion of *tktAaroZ* cassette into the *lacZ* locus results in a loss of lactose metabolism. A glycerol freeze *E. coli* WN1 was streaked on a LB Plate. Six isolated colonies were tested on multiple plates to confirm their phenotype. The growth

characteristics of the six colonies were: growth as a white colony on MacConkey agar containing lactose; no growth on M9 containing aromatic amino acids and aromatic vitamins; no growth on M9 containing serine, growth on M9 containing aromatic amino acids, aromatic vitamin and serine; growth on LB; and no growth on LB containing ampicillin (Ap).

### 7.1.2. Protocatechuate 3,4-Dioxygenase Activity

In order to measure the protocatechuate 3,4-dioxygenase activity, pKD16.179A was transformed into *E. coli* DH5 $\alpha$ . *E. coli* DH5 $\alpha$ /pKD16.179A was harvested from LB/Ap/1 mM IPTG culture. The specific activity of protocatechuate 3,4-dioxygenase was assayed with crude cell-free lysate. The consumption of protocatechuic acid (PCA) was measured by the slope of absorption at 290 nm over 30 seconds (Scheme 5.11). The specific activity of protocatechuate 3,4-dioxygenase of the cell-free lysate was 1.0  $\mu\text{mol min}^{-1} \text{mg}^{-1}$ .

Scheme 5.11. Protocatechuate 3,4-Dioxygenase



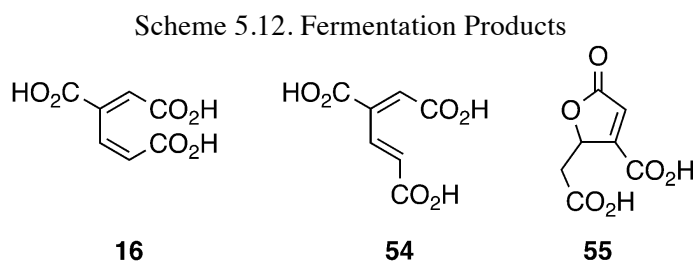
### 7.1.3. Fed-Batch Fermentor Synthesis of 2E,4Z-3-Carboxymuconic Acid

#### 7.1.3.1. Glucose-rich Condition Fermentation

The 2E,4Z-3-carboxymuconic acid **16** synthesizing strain, *E. coli* WN1/pYNB6.009A was cultured at 1 L scale in a 2 L working volume fermentor at pH 7.0 and 33 °C. The impeller speed and airflow were allowed to vary in order to maintain dissolved oxygen (DO) level at 10% of air saturation. Antifoam was added manually as needed. Glucose-rich culture conditions

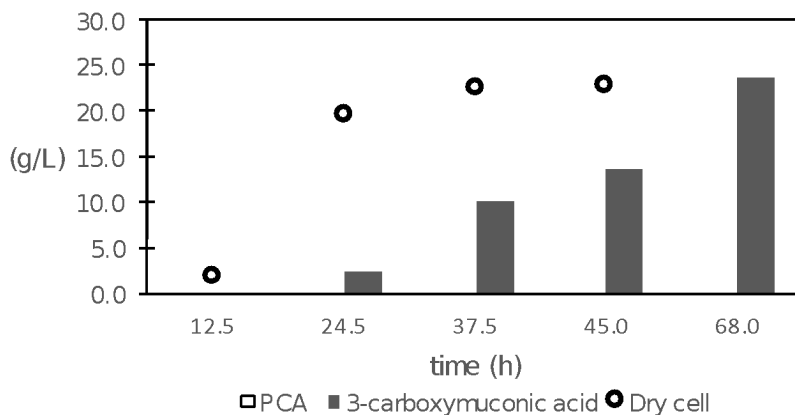
were employed such that the concentration of glucose in the medium was maintained in the range of 19-45 g/L (average 28 g/L) throughout the run.

Inoculant was initially grown in 5 mL M9 medium in an incubator shaker (37 °C, 250 rpm) for 20 h. This culture was then transferred to 100 mL of M9 medium, cultured in an incubator shaker (37 °C, 250 rpm) for an additional 9 h. The fermentation was initiated when this culture was transferred to the fermentor (t = 0). The initial glucose concentration in the fermentation medium was 30 g/L. For glucose-rich/IPTG(+) experiments, sterile 100 mM IPTG stock solution (12 mg IPTG / each addition) was added at 19 h, 27 h, 38 h, 45 h and 51h. Some of the microbially-synthesized *2E,4Z*-3-carboxymuconic acid **16** isomerized to *2E,4E*-3-carboxymuconic acid **54** and 2-(carboxymethyl)-5-oxo-2,5-dihydrofuran-3-carboxylic acid (lactone) **55** (Scheme 5.12).



The total products **16** and **54** concentration, PCA concentration, lactone **55**, calculated dry cell mass and protocatechuate 3,4-dioxygenase activity were observed during fermentation.

In glucose-rich/IPTG(+) fermentation, steady accumulation of products **16/54** continued during the entire fermentation (Figure 4). After 68 h of cultivation, 23.7 g/L of 3-carboxymuconic acid was synthesized in a 12% (mol/mol) yield from glucose.



t =	PCA 3,4-dioxygenase activity
24 h	29 U/mg
45 h	29 U/mg

Figure 5.4. Glucose-rich/IPTG(+) Fermentation

### 7.1.3.2. Glucose-limited Condition Fermentation

The *2E,4Z*-3-carboxymuconic acid **16** synthesizing strain, *E. coli* WN1/pYNB6.009A was cultured at 1 L scale in a 2 L working volume fermentor at pH 7.0 and 33 °C. The instrument setting was split into two phases. During first phase, the impeller speed (50-750 rpm) and airflow (0.06-1.00 L/min) were allowed to vary in order to maintain DO level at 10% of air saturation. When the airflow reached to 1.00 L/min with impeller speed 750 rpm, both airflow and impeller speed were kept constant. DO level started increasing when all the initial glucose was consumed. Here, the instrument settings were switched to the second phase. During the second phase, airflow and impeller speed remained constant at 1.00 lpm and 750 rpm respectively. Automatic oxygen-sensor-controlled glucose feeding was used to maintain a glucose-limited condition. The impeller speed was lowered as needed. Antifoam was added manually as needed.

Inoculant was initially grown in 5 mL M9 medium in an incubator shaker (37 °C, 250

rpm) for 20 h. This culture was then transferred to 100 mL of M9 medium and cultured in an incubator shaker (37 °C, 250 rpm) for an additional 7 h. The fermentation was initiated when this culture was transferred to the fermentor (t = 0). The initial glucose concentration in the fermentation medium was 20 g/L. The sterile 100 mM IPTG stock solution (12 mg IPTG / each addition) was added at 19 h, 25 h, 31 h, 37 h, 43 h and 49 h. The total products **16** and **54** concentration, PCA concentration, calculated dry cell mass and protocatechuate 3,4-dioxygenase activity were determined over the course of the fermentation.

The glucose-limited/IPTG(+) fermentation condition showed a poor accumulation of products **16/54** during the entire fermentation (Figure 5.5). After 63 h of cultivation, only 1.2 g/L of 3-carboxymuconic acid was synthesized in a 2% (mol/mol) yield from glucose. The synthesis of *2E,4Z*-3-carboxymuconic acid **16** with *E. coli* WN1/pYNB6.009A preferred glucose-rich conditions.

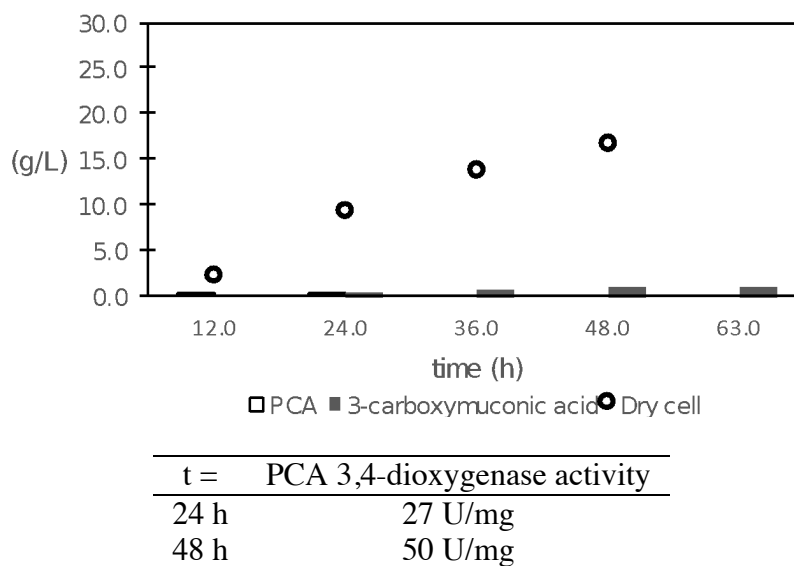


Figure 5.5. Glucose-limited/IPTG(+) Fermentation

## 7.2. Isolation of *2E,4E*-3-Carboxymuconic Acid from Fermentation Broth

Prior to isolating *2E,4E*-3-carboxymuconic acid from the glucose-rich fermentation broth, cells were removed by centrifugation. Protein was then removed using a tangential flow apparatus fitted with four 10 kD ultrafiltration cassettes (Sartorius). A portion of the cell-free/protein-free fermentation broth containing 5.4 g of *2E,4Z*-3-carboxymuconic acid **16**, 2.9 g of *2E,4E*-3-carboxymuconic acid **54** and 2.9 g of lactone **55** was treated with activated charcoal twice. This charcoal-treated broth was concentrated to 1/5 of the original volume with a rotary evaporator. The concentrated broth was chilled in an ice-bath followed by acidification in an ice-bath with H<sub>2</sub>SO<sub>4</sub> to pH 2. A white solid precipitated as the acidified broth was stirred at rt for 2 h. Filtration afforded 4.9 g of a white solid containing 4.3 g of *2E,4E*-3-carboxymuconic acid **54** (52% recovery of the **54** in the clarified fermentation broth).

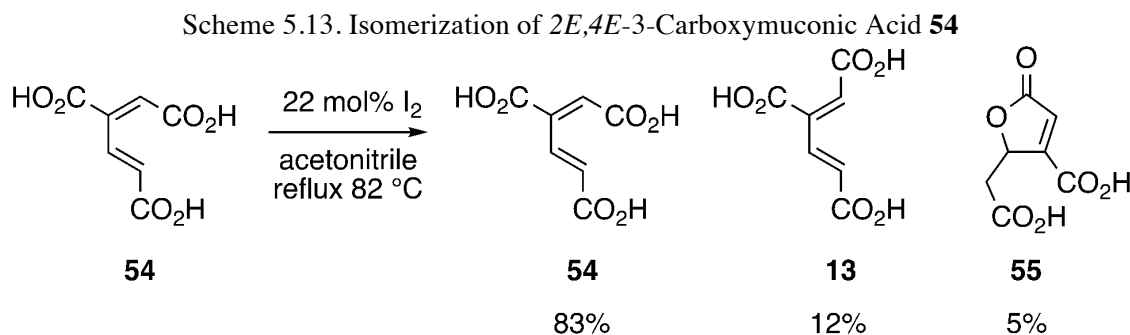
In order to investigate the fate of the half of the product not recovered during the isolation process, the same isolation procedure was performed with a another cell-free/protein-free fermentation broth containing 2.1 g of *2E,4Z*-3-carboxymuconic acid **16**, 2.7 g of *2E,4E*-3-carboxymuconic acid **54** and 1.4 g of lactone **55**. The isolated white solid contained 2.4 g of *2E,4E*-3-carboxymuconic acid **54** (50% recovery of the **54** in the clarified fermentation broth). The mother liquor contained 1.3 g of *2E,4E*-3-carboxymuconic acid **54** (27% of the **54** in the clarified fermentation broth) and 1.0 g of lactone **55** (21% of the **54** in the clarified fermentation broth). Extraction of the product from this mother liquor afforded a residue containing both *2E,4E*-3-carboxymuconic acid **54** and lactone **55**. Separation of the two molecules was unsuccessful.

### 7.3. Synthesis of Biobased Trimethyl Trimellitate

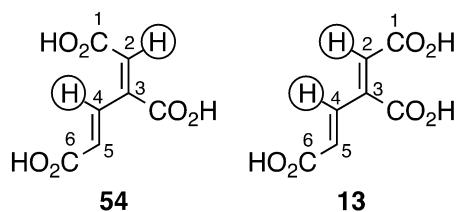
#### 7.3.1. Isomerization of *2E,4E*-3-Carboxymuconic Acid **54** to *2Z,4E*-3-Carboxymuconic Acid **13**

**13**

*2E,4E*-3-Carboxymuconic acid **54** was isomerized to *2Z,4E*-3-carboxymuconic acid **13** with 22 mol% of iodine in acetonitrile (Scheme 5.13). *2E,4E*-3-carboxymuconic acid **54** isomerized to 12% of *2Z,4E*-3-carboxymuconic acid **13** and 5% of lactone **55** but 83% of *2E,4E*-3-carboxymuconic acid **54** remained unreacted. *2Z,4E*-3-Carboxymuconic acid **13** was distinguished from *2E,4E*-3-carboxymuconic acid **54** by <sup>1</sup>H NMR and nuclear Overhauser effect spectroscopy (NOE). The magnetic interactions between the protons on C-2 and C-4 was observed using NOE experiments (Scheme 5.14). The peak of the proton on C-2 was observed after the proton on C-4 was magnetically excited.



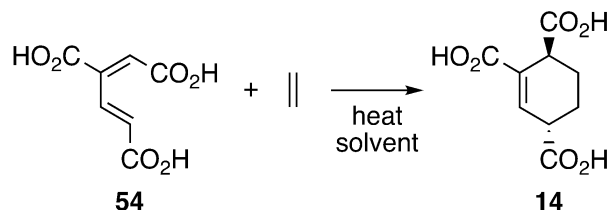
Scheme 5.14. Nuclear Overhauser Effect



### 7.3.2. Cycloaddition of 2*E*,4*E*-3-Carboxymuconic Acid **54** and Ethylene

Cycloaddition of 2*E*,4*E*-3-carboxymuconic acid **54** and ethylene was attempted in a high pressure reactor (Scheme 5.15).

Scheme 5.15. Cycloaddition of 2*E*,4*E*-3-Carboxymuconic Acid **54** and Ethylene



Even though the reaction of 2*E*,4*E*-3-carboxymuconic acid **54** and ethylene in 1,4-dioxane at 164 °C consumed all the starting material **54**, this reaction did not yield the cycloadduct **14** (Table 5.1, entry 1). <sup>1</sup>H NMR of this reaction crude and extract showed many unidentifiable resonances. The reaction in *m*-xylene at 150 °C also consumed all of the starting material **54** but did not yield any cycloadduct **14** (Table 5.1, entry 2). The reaction in 1,4-dioxane at 100 °C yielded no product (Table 5.1, entry 3). <sup>1</sup>H NMR observation showed mostly unreacted 2*E*,4*E*-3-carboxymuconic acid **54** with some unidentifiable resonances. The reaction in *m*-xylene at 100 °C yielded no product (Table 5.1, entry 4). <sup>1</sup>H NMR observation showed mostly unreacted 2*E*,4*E*-3-carboxymuconic acid **54** with some unidentifiable resonances.

entry	solvent	temperature	ethylene	rxn time	yield <b>14</b>
1	1,4-dioxane	164 °C	34.5 bar	24 h	0%
2	<i>m</i> -xylene	150 °C	34.5 bar	12 h	0%
3	1,4-dioxane	100 °C	34.5 bar	12 h	0%
4	<i>m</i> -xylene	100 °C	34.5 bar	12 h	0%

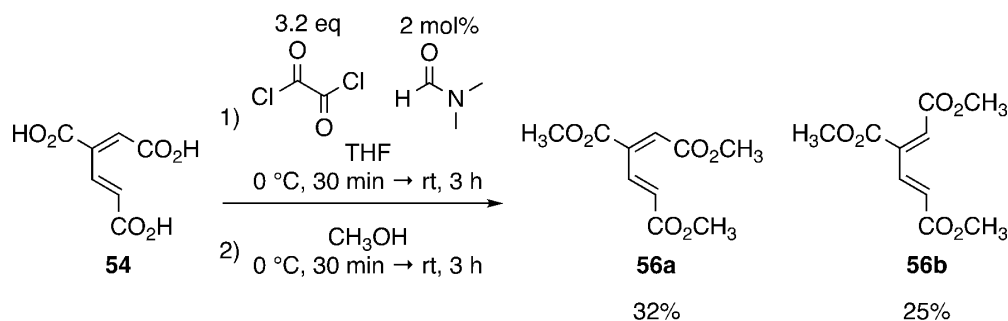
### 7.3.3 Esterification of 2*E*,4*E*-3-Carboxymuconic Acid **54**

Esterification of 2*E*,4*E*-3-carboxymuconic acid **54** was attempted with dry methanol and H<sub>2</sub>SO<sub>4</sub> as a catalyst. The Fischer esterification reaction at either rt or reflux (65 °C) yielded

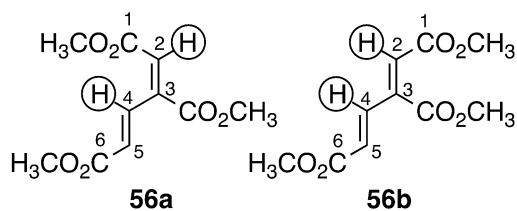
partially esterified products but no triester.

*2E,4E*-3-Carboxymuonic acid **54** was successfully fully esterified using oxalyl chloride with catalytic DMF (Scheme 5.16). Purification by flush chromatography afforded a 32% yield of isolated trimethyl *2E,4E*-3-carboxymuonate **56a** and a 25% yield of trimethyl *2Z,4E*-3-carboxymuonate **56b**. Trimethyl *2E,4E*-3-carboxymuonate **56a** was distinguished from *2Z,4E*-3-carboxymuonic acid **56b** by <sup>1</sup>H NMR and nuclear Overhauser effect spectroscopy (NOE). The magnetic interactions between the protons on C-2 and C-4 was observed in NOE experiments (Scheme 5.17). The peak of the proton on C-2 was observed after the proton on C-4 was magnetically excited.

Scheme 5.16. Esterification of *2E,4E*-3-Carboxymuonic Acid **54**



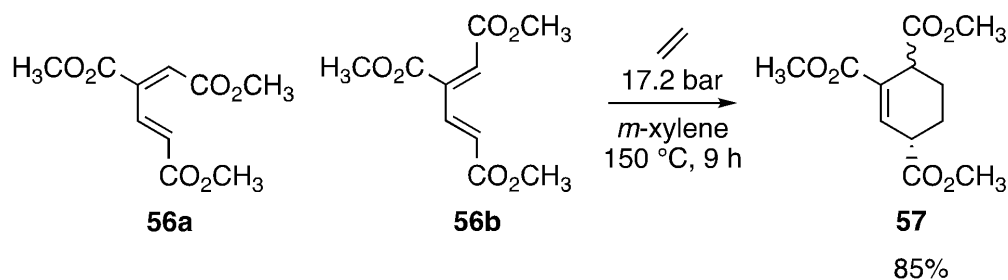
Scheme 5.17. Nuclear Overhauser Effect



### 7.3.4. Cycloaddition of Trimethyl 3-Carboxymuonate **56** and Ethylene

Cycloaddition of trimethyl 3-carboxymuonate **56** was conducted with ethylene (17.2 bar) in *m*-xylene at 150 °C for 9 h (Scheme 5.18).

Scheme 5.18. Cycloaddition of Trimethyl 3-Carboxymuconates **56a,b** and ethylene



This reaction yielded total 85% of *trans*-cycloadduct **57a** and *cis*-cycloadduct **57b**. The concentrated reaction crude product was subsequently aromatized without purification. A unique feature of this cycloaddition was that trimethyl *2E,4E*-3-carboxymuconate **56a** could react with ethylene while dimethyl *cis,trans*-muconate required an isomerization to dimethyl *trans,trans*-muconate<sup>61</sup> in order to react with ethylene.

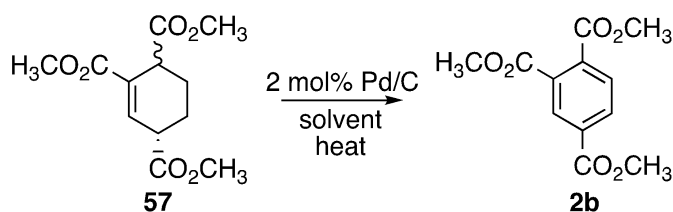
### 7.3.5. Aromatization of Cycloadduct **57**

Cycloadduct **57** was aromatized to trimethyl trimellitate **2b** by three strategies: dehydrogenation catalyzed by Pd/C in solvents, aerobic oxidative dehydrogenation,<sup>62</sup> and vapor phase dehydrogenation catalyzed by Pd/SiO<sub>2</sub>.

#### 7.3.5.1 Dehydrogenation Catalyzed by Pd/C in Solvents

Cycloadduct **57** was aromatized to trimethyl trimellitate **2b** with dehydrogenation catalyzed by Pd/C in solvents (Scheme 5.19).

Scheme 5.19. Dehydrogenation of Cycloadduct **57** Catalyzed by Pd/C in Solvents



A commercially available Pd (5 wt%) on C contained approximately 50 wt% water. It was dried for 3 h under reduced pressure at 70 °C. The Dry 2 mol% Pd on C and decane were added to cycloadduct **57** and refluxed at 174 °C for 3 days. Decane and Pd/C were removed with a silica gel column. A dark brown material remained at the leading edge of the column. The collected fraction was concentrated affording 17% yield of trimethyl trimellitate **2b** with no unreacted cycloadduct **57** (Table 5.2, entry 1). Dry 2 mol% Pd/C and dichlorobenzene were added to cycloadduct **57** and heated at 172 °C for 2 days. Pd/C was removed by filtration. The filtrate was concentrated affording 19% of trimethyl trimellitate **2b** with no unreacted cycloadduct **57** (Table 5.2, entry 2).

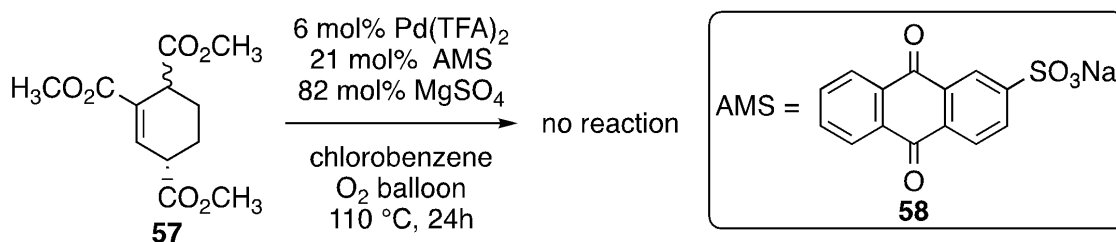
Table 5.2. Dehydrogenation of Cycloadduct **57** Catalyzed by Pd/C in Solvents

entry	solvent	temp	rxn time	Yield <b>2b</b>
1	decane	174 °C	3 d	17%
2	dichlorobenzene	172 °C	2 d	19%

### 7.3.5.2. Aerobic Oxidative Dehydrogenation of Cycloadduct **57**

Aromatization of cycloadduct **57** was attempted by Stahl's aerobic oxidative dehydrogenation reaction conditions.<sup>62</sup> These consisted of 6 mol% of Pd(TFA)<sub>2</sub>, 21 mol% anthraquinone-2-sulfonate sodium salt (AMS) **58**, 82 mol% MgSO<sub>4</sub> and oxygen (1 atm) in chlorobenzene (Scheme 5.20).

Scheme 5.20. Aerobic Oxidative Dehydrogenation of Cycloadduct **57**



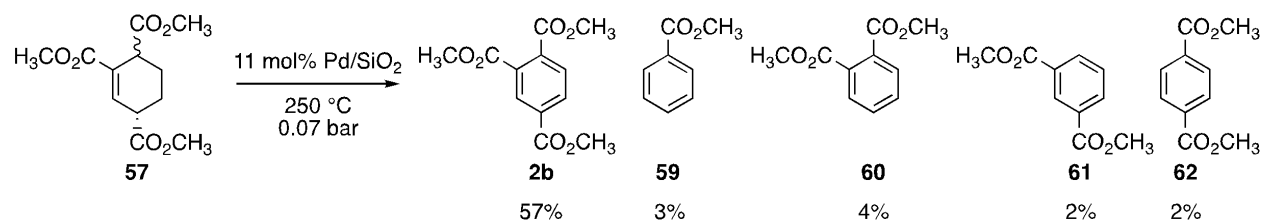
All of Stahl's reported successful aromatization of cyclohexenes were limited to substituents in

the 4- and/or 5-position of the cyclohexene. Other substitution patterns for mono- and disubstituted cyclohexenes were not examined for aerobic oxidative dehydrogenation. Also, no 1,3,6-trisubstituted cyclohexenes were examined as substrates for oxidative dehydrogenation. The aerobic oxidative dehydrogenation gave no reaction to cyclohexene **57** (Scheme 5.20).

### 7.3.5.3. Vapor Phase Dehydrogenation of Cycloadduct **57** Catalyzed by Pd/SiO<sub>2</sub>

A vapor phase dehydrogenation reactor was employed for aromatization of cycloadduct **57** (Chapter 4, Figure 4.1). The cycloadduct **57** was distilled at 0.07 bar and 250 °C through 11 mol% Pd/SiO<sub>2</sub> dispersed in macroporous silica gel. Trimethyl trimellitate **2b** was obtained in 57% yield. In addition, methyl benzoate **59**, dimethyl phthalate **60**, dimethyl isophthalate **61** and dimethyl terephthalate **62** were obtained as side products in 3%, 4%, 2% and 2% yields, respectively (Scheme 5.21).

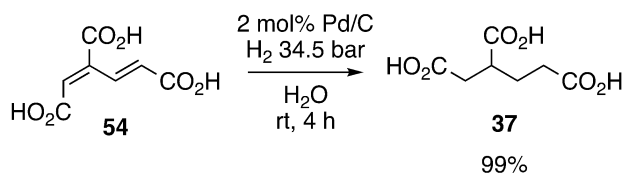
Scheme 5.21. Vapor Phase Dehydrogenation of Cycloadduct **57** Catalyzed by Pd/SiO<sub>2</sub>



#### 7.4. Synthesis of Biobased 1,2,4-Butanetricarboxylic Acid

The synthesis of 1,2,4-butanetricarboxylic acid **37** employed a high pressure reactor (34.5 bar). *2E,4E*-3-carboxymuconic acid **54** was hydrogenated with 2 mol% Pd/C at rt in water (Scheme 5.22).

Scheme 5.22. Synthesis of 1,2,4-Butanetricarboxylic acid **37**



This reaction afforded 99% yield of 1,2,4-butanetricarboxylic acid **37**. The reaction mixture was filtered and then concentrated to 1/10 of the filtrate volume. The filtrate was acidified with H<sub>2</sub>SO<sub>4</sub> to pH 2 followed by extraction with EtOAc. The extract was dried with MgSO<sub>4</sub> subsequently concentrated affording a white residue. This residue was crystallized in acetonitrile at 4 °C. This afforded a 79 % isolated yield of 1,2,4-butanetricarboxylic acid **37**. The <sup>1</sup>H NMR, <sup>13</sup>C NMR, and mp of biobased 1,2,4-butanetricarboxylic acid **37** synthesized from glucose was identical with 1,2,4-butanetricarboxylic acid purchased from Sigma.

## 8. Discussion

A recombinant strain of *Escherichia coli* capable of synthesizing 2*E*,4*Z*-3-carboxymuconic acid **16** from glucose was engineered and called WN1/pYNB6.009A. This strain synthesized 23.7 g/L of 3-carboxymuconic acids **16** and **54** in a 12% (mol/mol) yield from glucose under fermentor-controlled conditions. The isolated product, 2*E*,4*E*-3-carboxymuconic acid **54** was used to synthesize biobased trimethyl trimellitate **2b** and 1,2,4-butanetricarboxylic acid **37**. A quantitative yield of biobased 1,2,4-butanetricarboxylic acid **37** was synthesized from 2*E*,4*E*-3-carboxymuconic acid **54** with only one step process.

The cycloaddition of trimethyl 2*E*,4*E*-3-carboxymuconate **56a** with ethylene was achieved without an isomerization to trimethyl 2*Z*,4*E*-3-carboxymuconate **56b**. Cycloadduct **57** was aromatized to trimethyl trimellitate **2b** with three methods: dehydrogenation catalyzed by Pd/C in solvents, Stahl's aerobic oxidative dehydrogenation reaction,<sup>62</sup> and vapor phase dehydrogenation catalyzed by Pd/SiO<sub>2</sub>. Neither of the solution phase aromatization of cycloadduct **57** was successful. The vapor phase dehydrogenation catalyzed by Pd/SiO<sub>2</sub> gave the highest yield of trimethyl trimellitate among the three methods tested.

## 9. Experimental

### 9.1. Spectroscopic Measurements

$^1\text{H}$  NMR spectra were recorded on a 500 MHz spectrometer. Chemical shifts for  $^1\text{H}$  NMR spectra are reported (in parts per million) relative to  $\text{CDCl}_3$  ( $\delta = 7.26$  ppm) or sodium 3-(trimethylsilyl)propionate-2,2,3,3- $\text{d}_4$  (TSP,  $\delta = 0.00$  ppm) with  $\text{D}_2\text{O}$  as the solvent.  $^{13}\text{C}$  NMR spectra were recorded at 125 MHz and the shifts for these spectra are reported (in parts per million) relative to  $\text{CDCl}_3$  ( $\delta = 77.0$  ppm).

UV and visible measurements were recorded on an Agilent 8453 UV-visible Spectroscopy System with UV-visible ChemStation as the operating software in Dell Dimension 8100.

### 9.2. Gas Chromatography

GC spectra were recorded on an Agilent 6890N chromatograph equipped with an autosampler. The trimethyl trimellitate **2b** concentration was determined using an Agilent HP-5 (5%-Phenyl)-methylpolysiloxane coated capillary column (30 m  $\times$  0.320 mm i.d., 0.25  $\mu\text{m}$  film thickness). The reaction crude product was diluted with acetonitrile in a volumetric flask. Syringe filtration (0.45  $\mu\text{m}$  Whatman filter) was followed by analysis to determine the concentration of trimethyl trimellitate **2b**.

### 9.3. Bacterial Strains and Plasmids

*E. coli* DH5 $\alpha$  [F  $\phi$ 80*lacZ* $\Delta$ M15  $\Delta$ (*lacZYA-argF*)U169 *recA1 endA1 hsdR17*( $r_k, m_k+$ ) *PhoA supE44*  $\lambda$  *thi1 gyrA96 relA1*] was obtained previously from Invitrogen. *E. coli* WN1 [*tsx-352 supE42*  $\lambda$  *aroE353 malA352*( $\lambda^R$ ) *serA::aroBaroZ lacZ::tkTAaroZ*] was constructed by Wei

Niu in the Frost group.<sup>24</sup> Plasmid pJF118EH was previously obtained from professor M. Bagdasarian (Michigan State University). Plasmid pWN1.162A was constructed by Wei Niu in the Frost group.<sup>24</sup>

#### **9.4. Storage of Bacterial Strains and Plasmids**

All *E. coli* was stored at -78 °C in glycerol. Plasmids were transformed into *E. coli* DH5 $\alpha$  for a long-term storage. Preparation of a bacterial glycerol freeze started from an inoculation of 5 mL medium with a single colony of the desired strain. *E. coli* strains were cultured in 5 mL LB medium (with antibiotic when it was appropriate) at 37 °C with agitation for 14 h. Glycerol freeze samples were prepared by addition of bacterial culture 0.75 mL to sterile 80% (v/v) aqueous glycerol solution 0.25 mL). The solutions were gently mixed, allowed to stand at room temp. for 6 h, and then stored at -78 °C.

#### **9.5. Culture Medium**

Bacto™ tryptone, Difco™ yeast extract and Bacto™ agar were obtained from BD. Ampicillin, thiamine hydrogen chloride, 2,3-dihydroxybenzoic acid, 4-aminobenzoic acid, 4-hydroxybenzoic acid was obtained from Spectrum. Isopropyl- $\beta$ -D-thiogalactoside was obtained from Gold Biotechnology. Ammonium heptamolybdate tetrahydrate was obtained from Mallinckrodt. All solutions were prepared in deionized distilled water.

LB medium (1 L) contained Bacto™ tryptone (10 g), Difco™ yeast extract (5 g) and NaCl (10 g).<sup>63</sup> 2 $\times$ Yeast-tryptone (1 L) contained Difco™ yeast extract (10 g), Bacto™ tryptone (16 g) and NaCl (5 g).<sup>63</sup> SOB medium (1 L) contained Bacto™ tryptone (20 g), Difco™ yeast extract (5 g) and NaCl (5 g).<sup>64</sup> SOC medium was prepared with SOB medium (1 L), 250 mM

KCl (10 mL), 2M MgCl<sub>2</sub>(5 mL), 1M glucose (20 mL).<sup>64</sup> Modified M9 salts (1 L) contained Na<sub>2</sub>HPO<sub>4</sub> (6 g), KH<sub>2</sub>PO<sub>4</sub> (3 g), NH<sub>4</sub>Cl (1 g) and NaCl (0.5 g).<sup>63</sup> M9 minimal medium contained D-glucose (10 g), MgSO<sub>4</sub> (0.24 g), and thiamine hydrogen chloride (0.001 g) in 1 L of M9 salts.<sup>63</sup> M9 medium (1 L) was supplemented where appropriate with L-phenylalanine (0.040 g), L-tyrosine (0.040 g), L-tryptophan (0.040 g), *p*-hydroxybenzoic acid (0.010 g), *p*-aminobenzoic acid (0.010 g), 2,3-dihydroxybenzoic acid (0.010 g). L-Serine was added to a final concentration of 33 mg/L where indicated. Ampicillin was added where appropriate to a final concentration of 50 µg/mL where indicated. Solutions of LB medium, M9 salts, MgSO<sub>4</sub>, D-glucose, SOB medium, KCl, MgCl<sub>2</sub> were autoclaved. Solutions of aromatic vitamins (containing *p*-hydroxybenzoic acid, *p*-aminobenzoic acid, and 2,3-dihydroxybenzoic acid), aromatic amino acids (containing L-phenylalanine, L-tyrosine, L-tryptophan), L-serine, ampicillin and isopropyl-β-D-thiogalactoside (IPTG) were sterilized through 0.22 µm membrane.

## 9.6. Preparation and Transformation of Electrocompetent Cells

Electrocompetent cells were prepared using procedures modified from Sambrook and Russell.<sup>65</sup> Preparation of electrocompetent cells started with inoculation of LB (5 mL) from a single colony followed by incubation in an incubator shaker (37 °C, 250 rpm) for 14 h. The seed culture (2 mL) was transferred to a 2 L Erlenmeyer flask containing 500 mL 2×YT. The cells were cultured in an incubator shaker (37 °C, 250 rpm) until they reached the mid-log phase of growth (OD<sub>600</sub> = 0.5-0.7). The flask containing the culture was chilled in an ice-bath for 10 min. The culture was transferred to a sterile centrifuge bottle. The cells were harvested by centrifugation (2000 g, 5 min, 4 °C) and the supernatant was discarded. The cells were kept cold in an ice-bath as much as possible until the end of the procedure. The cells were resuspended in

400 mL of ice-cold sterile water, and harvested by centrifugation (2000 g, 10 min, 4 °C). The cells were resuspended in 200 mL of ice-cold sterile water, and harvested by centrifugation (2000 g, 10 min, 4 °C). Once again, the cells were resuspended in 200 mL of ice-cold sterile water, and harvested by centrifugation (2000 g, 10 min, 4 °C). The cells were suspended in 100 mL of sterile ice-cold 10 %(v/v) glycerol aqueous solution. The cells were harvested by centrifugation (2000 g, 10 min, 4 °C). The cells were suspended in 1.5 mL of sterile ice-cold 10%(v/v) glycerol aqueous solution. Aliquots (50 µL) were dispensed into ice-cold 1.5 mL sterile microfuge tubes and immediately frozen in liquid nitrogen. The competent cells were stored at -78 °C.

Electroporation was performed by Bio-Rad Gene Pulser® II with Gene Pulser® Cuvette (catalogue # 165-2086, 0.2 cm electrode gap). The cuvettes were chilled on ice for 5 min prior to use. Plasmid DNA (dissolved in sterile water 1-5 µL) or purified DNA ligation reaction solution was mixed with 50 µL of electrocompetent cells. The mixture of cells and DNA was transferred into a cuvette. The instrument was set at 2.5 kV, 25 µF and 200 Ω. A single pulse was applied to a sample which typically resulted in a time constant of 5.2 ms. SOC medium (1 mL) was added into the cuvette and the mixture was transferred into a sterile test tube (20 × 150 mm). It was incubated in an incubator shaker (37 °C, 250 rpm) for 1 h, and plated on the appropriate medium.

### **9.7. Small Scale Purification of Plasmid DNA**

A single colony of a strain possibly containing the desired plasmid was inoculated into LB/Ap (5 mL). A master plate was created for each colony. After incubation in an incubator shaker (37 °C, 250 rpm) for 14 h, cells were harvested from 3 mL of the culture in a 1.5 mL

microfuge tube by centrifugation (5000 g, 1 min). Qiagen® QIAprep® Spin Miniprep Kit (catalogue number 27104) was used for purification of the plasmid DNA by following the manufacturer's instructions. The plasmid DNA was eluted from the spin column with 50 µL of sterile water.

### **9.8. Large Scale Purification of Plasmid DNA**

A colony from the master plate created during small scale purification of plasmid DNA was used to inoculate 500 mL LB/Ap in a 2 L Erlenmeyer flask. After incubation in an incubator shaker (37 °C, 250 rpm) for 14 h, cells were harvested from approximately 400 mL of the culture in a centrifuge tube by centrifugation (3200 g, 5 min). Qiagen® Plasmid Maxi Kit (catalogue number 12163) was used for purification of the plasmid DNA by following manufacturer's instructions. The purified plasmid DNA pellet was dissolved with 500 µL of sterile water. In order to determine the concentration and purity of DNA, the absorbance at 260 nm and 280 nm were measured relative to water. The DNA concentration was calculated based on the absorbance at 260 nm of  $50 \text{ ng } \mu\text{L}^{-1} \text{ cm}^{-1}$  is 1.0.<sup>65</sup> The purity of DNA was assessed with the ratio of absorbance 260 nm / 280 nm.<sup>66</sup> A pure DNA solution should have the ratio of 1.8 or above. The ratio becomes low when it is contaminated with protein.<sup>66</sup> A sample with the ratio above 1.2 was stored as stock plasmid DNA solution.

### **9.9. Isolation of *Klebsiella pneumoniae* subsp. *pneumoniae* (ATCC 25597) Genomic DNA**

*Klebsiella pneumoniae* subsp. *pneumoniae* (ATCC 25597) was streaked on a LB plate with a glycerol freeze from the group strain collection. LB 5 mL was inoculated with single colony. After incubation in an incubator shaker (37 °C, 250 rpm) for 14 h, cells were harvested

from 1 mL of the culture in a 1.5 mL microfuge tube by centrifugation (10,000 g, 2 min). Promega Wizard® Genomic DNA Purification Kit (catalogue number A1120) was used to isolate the genomic DNA by following the manufacturer’s instructions. The DNA concentration was 617 ng/μL based on the absorbance at 260 nm. The ratio of absorbance 260 nm / 280 nm was 1.6.

### 9.10. Plasmid pKD16.179A

The 1.5 kb open reading frame of *pcaHG* was amplified from *Klebsiella pneumoniae* subsp. *pneumoniae* (ATCC 25597) genomic DNA using the following primers containing EcoRI restriction sequences: 5’-AGGAATTCAGTGCGCAAACATAACCCA and 5’-AGGAATTCGTCACCGCGACGGCTAAATA. The primers were synthesized by Integrated DNA Technologies. Bio-Rad DNA Engine® Peltier Thermal Cycler was used for polymerase chain reaction (PCR). Each reaction (50 μL) contained 0.2 mM dNTPs (Promega), 0.5 μM of each primer, template DNA 250 ng, 1×Phusion buffer and 1 unit of Phusion DNA polymerase (New England BioLabs).

PCR cycles were set as follows (Table 5.3.) :

Table 5.3. PCR Cycle for *pcaHG*

number of cycle	step	temperature	time length
1	initial denaturation	98 C	2 min
	denaturation	98 C	30 sec
30	annealing	60-68 C	30 sec
	extension	72 C	1 min
1	final extension	72 C	5 min
1	storing	4 C	hold

The PCR product (1.5 kb) was purified with Zymo Research DNA Clean & Concentrator™-25 (catalogue number D4006) by following the manufacturer’s protocol.

The PCR product (insert) and pJF118EH (vector) were digested with EcoRI-HF (New England BioLabs) at 37 °C for 1 h. The linearized vector was dephosphorylated at 5' and 3' end of DNA with New England BioLabs Calf Intestinal Alkaline Phosphate (catalogue number M0290) by following the manufacturer's protocol. The digested insert and dephosphorylated vector were purified from 0.7 % agarose gel with Zymo Research Zymoclean™ Gel DNA Recovery Kit (catalogue number D4001) by following the manufacturer's protocol. The insert and vector were ligated with New England BioLabs T4 DNA Ligase (catalogue number M0202S) by following the manufacturer's protocol. The ligation product was purified with Zymo Research DNA Clean & Concentrator™-25.

The ligation product was transformed into electrocompetent *E. coli* DH5α and plated on LB/Ap. Small scale purification of plasmid DNA was performed for six colonies from the LB/Ap plate followed by enzyme digestion with EcoRI-HF at 37 °C for 1 h. Further enzyme digestions were performed on two possible candidate plasmids with BamHI-HF, PvuI-HF, Sall-HF and Sall/NdeI, confirming both plasmids were pKD16.179A. Large scale purification of plasmid DNA was performed on those two plasmids and stored as pKD16.179A stock solution after confirmation of the products by enzyme digestion with EcoRI-HF, BamHI-HF, PvuI-HF, Sall-HF and Sall/NdeI.

### **9.11. Plasmid pYNB6.009B**

pWN1.162A<sup>24</sup> was linearized by enzyme digestion with HindIII-HF at 37 °C for 1 h followed by purification with Zymo Research DNA Clean & Concentrator™-25. The 3.3 kb DNA fragment containing *serA* gene, *aroF*<sup>FBR</sup> gene and *P<sub>aroF</sub>* DNA sequence was amplified from the linearized pWN1.162A using the following primers containing SmaI restriction sequences:

5'-TCCCCCGGGTAAATAGTGCAAGG and 5'-TCCCCCGGGATGACGTAACGATAA. The primers were synthesized by Integrated DNA Technologies. Each reaction (50  $\mu$ L) contained 0.2 mM dNTPs (Promega), 0.2  $\mu$ M of each primer, template DNA 20 ng, 1.0 mM MgCl<sub>2</sub>, 1 $\times$  thermopol buffer and 2.5 units of Taq DNA polymerase (New England BioLabs).

PCR cycles were set as follows (Table 5.4.) :

Table 5.4. PCR Cycle for *serA* - *aroF*<sup>FBR</sup> - *P*<sub>aroF</sub> Cassette

number of cycle	step	temperature	time length
1	initial denaturation	94 C	3 min
	denaturation	94 C	1 min
30	annealing	56 C	1 min
	extension	72 C	3 min 18 sec
1	final extension	72 C	4 min
1	storing	4 C	hold

The PCR product (1.5 kb) was isolated from 0.7 % agarose gel with Zymo Research Zymoclean™ Gel DNA Recovery Kit.

The resulting DNA (insert) and pKD16.179A (vector) were digested with SmaI (New England BioLabs) at 37 °C for 2 h. The linearized vector was dephosphorylated at 5' and 3' end of DNA with New England BioLabs Calf Intestinal Alkaline Phosphate. The digested insert was purified from 0.7 % agarose gel with Zymo Research Zymoclean™ Gel DNA Recovery Kit. The dephosphorylated vector was purified with Zymo Research DNA Clean & Concentrator™-25. The insert and vector were ligated with New England BioLabs T4 DNA. The ligation product was purified with Zymo Research DNA Clean & Concentrator™-25.

The ligation product was transformed into electrocompetent *E. coli* DH5 $\alpha$  and plated on LB/Ap. Small scale purification of plasmid DNA was performed for 30 colonies from the LB/Ap plate followed by enzyme digestion with SmaI at 37 °C for 1 h. One plasmid contained the insert fragment. Further enzyme digestion was performed on the plasmids with NdeI,

confirming the plasmid as pYNB6.009B. Large scale purification of plasmid DNA was performed on this plasmid and stored as pYNB6.009B stock solution after confirmation of the product by enzyme digestion with SmaI and NdeI.

### **9.12. Plasmid pYNB6.009A**

pKD16.179A (vector) was digested with SmaI at 37 °C for 2 h. The linearized vector was dephosphorylated at 5' and 3' end of DNA with New England BioLabs Calf Intestinal Alkaline Phosphate. The dephosphorylated vector was purified with Zymo Research DNA Clean & Concentrator™-25. pYNB6.009B was digested with SmaI at 37 °C for 2 h. The 3.3 kb DNA fragment containing *serA* gene, *aroF<sup>FBR</sup>* gene and *P<sub>aroF</sub>* DNA sequence was isolated from 0.7 % agarose gel with Zymo Research Zymoclean™ Gel DNA Recovery Kit. The insert and vector were ligated with New England BioLabs T4 DNA. The ligation product was purified with Zymo Research DNA Clean & Concentrator™-25.

The ligation product was transformed into electrocompetent *E. coli* DH5α and plated on LB/Ap. Small scale purification of plasmid DNA was performed for 10 colonies from the LB/Ap plate followed by enzyme digestion with SmaI at 37 °C for 1 h. Nine plasmids contained the insert fragment. Further enzyme digestion was performed on those plasmids with NdeI, confirming six plasmids were pYNB6.009A. Large scale purification of plasmid DNA was performed on one of the plasmids and stored as pYNB6.009A stock solution after confirmation of the product by enzyme digestion with SmaI and NdeI.

### **9.13. *E. coli* WN1**

The host strain *E. coli* WN1 was previously engineered by Wei Niu in the Frost group.<sup>24</sup>

A glycerol freeze *E. coli* WN1 was streaked on a LB Plate and incubated at 37 °C for 14 h. Six isolated colonies were inoculated on multiple plates and incubated at 30 °C for 17 h. The growth characteristics of the six colonies were: growth as a white colony on MacConkey agar containing lactose; no growth on M9 containing aromatic amino acids and aromatic vitamins; no growth on M9 containing serine, growth on M9 containing aromatic amino acids, aromatic vitamins and serine; growth on LB; and no growth on LB containing ampicillin (Ap).

#### **9.14. Protocatechuate 3,4-Dioxygenase Activity**

pKD16.179A was transformed into *E. coli* DH5 $\alpha$ , and plated on LB/Ap. A single colony was inoculated into 100 mL LB/Ap in 500 mL Erlenmeyer flask followed by incubation in an incubator shaker (37 °C, 250 rpm) for 15 h. This culture was used to inoculate 500 mL LB/Ap in 2 L Erlenmeyer flask, and incubated in an incubator shaker (37 °C, 250 rpm) until OD<sub>600</sub> became 0.6. This culture was incubated further for 4 h after addition of 1mM IPTG. The cells were harvested by centrifugation (3200 g, 5 min, 4 °C) and the supernatant was discarded. The mass of wet cells was 2.6 g. The cells were kept cold in an iced-bath as much as possible until the end of the procedure. The cells were resuspended in 250 mL of ice-cold 20 mM tris-acetate pH 7.5, and harvested by centrifugation (3200 g, 5 min, 4 °C). The cells were resuspended in 6 mL of ice-cold 50 mM tris-acetate pH 7.5. The cells were lysed with French Pressure Cell Press (SLM instrument). The instrument setting was following: piston diameter 1 inch, medium ratio, 1100 psig = cell pressure 18000 psig. The cell debris was removed by centrifugation (29000 g, 30 min, 4 °C). The crude cell-free lysate was kept cold in an ice-bath as much as possible until the end of the procedure.

Bio-Rad Quick Start<sup>TM</sup> Bradford 1 $\times$  dye Reagent (catalogue number 500-0205) and Quick

Start™ Bovine Serum Albumin Standard (catalogue number 500-0206) were used to quantify the concentration of protein by following manufacture procedure.

The specific activity of protocatechuate 3,4-dioxygenase was assayed with crude cell-free lysate. The consumption of protocatechuic acid was measured by the slope of absorption at 290 nm ( $\epsilon = 3890 \text{ L mol}^{-1} \text{ cm}^{-1}$ ).<sup>67a</sup> Each reaction solution 1 mL contained 320  $\mu\text{M}$  protocatechuic acid, 50 mM tris-acetate pH 7.5 and 110  $\mu\text{L}$  of diluted cell lysate.<sup>67b</sup> The specific activity of protocatechuate 3,4-dioxygenase of the cell-free lysate was  $1.0 \mu\text{mol min}^{-1} \text{ mg}^{-1}$ .

### 9.15. Fed-Batch Fermentation General

The fermentation medium was prepared with water (800 mL),  $\text{K}_2\text{HPO}_4$  (7.5 g), ammonium iron (III) citrate (0.3 g), citric acid monohydrate (2.1 g), concentrated  $\text{H}_2\text{SO}_4$  (1.2 mL), concentrated  $\text{NH}_4\text{OH}$  (4.1 mL), L-phenylalanine (0.7 g), L-tyrosine (0.7 g), and L-tryptophan (0.35 g) in a 2 L fermentation vessel. This vessel containing the medium with antifoam (5 drops) was autoclaved. The solution (100 mL) containing following supplements were added immediately prior to initiation of the fermentation: glucose (30 g),  $\text{MgSO}_4$  (0.12 g), thiamine hydrogen chloride (0.001 g), *p*-hydroxybenzoic acid (0.010 g), *p*-aminobenzoic acid (0.010 g), 2,3-dihydroxybenzoic acid (0.010 g) and trace minerals, including  $(\text{NH}_4)_6(\text{Mo}_7\text{O}_{24}) \cdot 4\text{H}_2\text{O}$  (3.7 mg),  $\text{ZnSO}_4 \cdot 7\text{H}_2\text{O}$  (2.9 mg),  $\text{B}(\text{OH})_3$  (24.7 mg),  $\text{CuSO}_4 \cdot 5\text{H}_2\text{O}$  (2.5 mg), and  $\text{MnCl}_2 \cdot 4\text{H}_2\text{O}$  (15.8 mg). The initial glucose solution, feed glucose solution and  $\text{MgSO}_4$  solutions were autoclaved. Solutions of aromatic vitamins (containing *p*-hydroxybenzoic acid, *p*-aminobenzoic acid, and 2,3-dihydroxybenzoic acid), trace minerals solution and IPTG solution were sterilized through 0.22  $\mu\text{m}$  membrane. Antifoam (Sigma 204) was added to the fermentation broth as needed.

Fermentations employed BIOSTAT® B-DCU system controlled by DCU Tower with a 2 L working volume fermentor vessel. Data acquisition utilized MFCS/win 3.0 software (Sartorius Stedim Systems), which was installed in a personal computer (Digilink) operated by Windows® 7 Professional. Matson Marlow 101U/R peristaltic pump was used for administration of feed glucose solution. Temperature and pH were controlled with PID loop maintaining at 33 °C and pH 7.0±0.1 with 2N H<sub>2</sub>SO<sub>4</sub> and NH<sub>4</sub>OH. Impeller speed was varied between 50 and 1800 rpm to maintain dissolved oxygen (DO) levels at 10% air saturation. Airflow was increased from 0.06 L/min to 1.0 L/min to maintain DO levels at 10% air saturation. DO was measured using a Hamilton OxyFerm FDA 225 (catalogue number 237452) fitted with an Optiflow FDA membrane (catalogue number 237140). pH was measured with Hamilton EasyFerm Plus K8 200 (catalogue number 238627). Glucose concentration was measured with GlucCell™ and glucose test strip (CESCO Bioengineering Co., Ltd.). Antifoam 204 (Sigma-Aldrich) was added as needed to mitigate foam accumulation.

For <sup>1</sup>H NMR quantification of product concentration, the broth was concentrated to dryness under reduced pressure, concentrated to dryness one additional time from D<sub>2</sub>O, and then dissolved in D<sub>2</sub>O containing a known concentration of the sodium salt of 3-(trimethylsilyl) propionic-2,2,3,3-d<sub>4</sub> acid. The concentration was determined by the integral corresponding to 2*E*,4*Z*-3-carboxymuconic acid **16** (5.99 ppm, d, *J* = 12 Hz, 1H); 2*E*,4*E*-3-carboxymuconic acid **54** (6.14 ppm, d, *J* = 16 Hz, 1H); protocatechuic acid **15** (6.94 ppm, d, *J* = 8.5 Hz, 1 H); lactone **55** (5.60 ppm, ddd, *J* = 2.5, 3.5, 8.5 Hz, 1H) with integral corresponding to TSP (δ = 0.00 ppm, s, 9H). Cell densities were determined by dilution of fermentation broth with M9 salts followed by measurement of absorption at 600 nm (OD<sub>600</sub>). Dry cell weight of *E. coli* cells (g/L) was calculated using a conversion coefficient of 0.39 g L<sup>-1</sup> OD<sub>600</sub><sup>-1</sup>.<sup>68</sup>

### 9.16. Glucose-rich Condition Fermentation

Glucose-rich culture condition was employed such that the concentration of glucose in the medium was maintained in the range of 19-45 g/L (average 28 g/L) throughout the run. Inoculant was initially grown in 5 mL M9 medium in an incubator shaker (37 °C, 250 rpm) for 20 h and subsequently transferred to 100 mL of M9 medium. This 100 mL culture was grown at 37 °C and 250 rpm until the OD<sub>600</sub> reached 1.0-2.0 (9 h). Baffles were installed in the 2 L fermentor vessel for glucose-rich experiments. The fermentation was initiated when this culture was transferred to the fermentor (t = 0). The initial glucose concentration in the fermentation medium was 30 g/L. For glucose-rich/IPTG(+) experiment, sterile 100 mM IPTG stock solution (12 mg IPTG / each addition) was added at 19 h, 27 h, 38 h, 45 h and 51h. The instrument settings were split into two phases. During the first phase, DO was maintained at 10 % by increasing impeller speed until the speed reached the set maximum (750 rpm). Airflow was then increased until it reached the set maximum (1.00 L/min). The pO<sub>2</sub> control loop setting for first phase was as follows (Table 5.5) :

Table 5.5. First Phase of Glucose-rich Fermentation

DEADB 0.5% sat							
CASCADE							
1	STIR						
2	AIRF						
Cascade	Minimum	Maximum	XP	TI	TD	Hysteresis	Mode
STIR	2.5%	37.5%	150.0%	100.0 s	0.0 s	01:00 m:s	auto
AIRF	2.0%	33.3%	90.0%	50.0 s	0.0 s	01:00 m:s	auto
O2EN	0.0%	100.0%	90.0%	50.0 s	0.0 s	05:00 m:s	off
STIR: 2.5% = 50 rpm, 37.5% = 750 rpm AIRF: 2.0% = 0.06 L/min, 33.3% = 1.00 L/min O2EN setting did not matter since it was off.							

The cascade settings were switched to the second phase when both impeller speed and airflow reached their set maximum values. During the second phase, DO was maintained at 10 % by

changing the impeller speed while the airflow was held at 1.00 L/min. The pO<sub>2</sub> control loop setting for second phase was as follows (Table 5.6.) :

Table 5.6. Second Phase of Glucose-rich Fermentation

DEADB 0.5% sat							
CASCADE							
1	AIRF						
2	STIR						
Cascade	Minimum	Maximum	XP	TI	TD	Hysteresis	Mode
STIR	37.5%	90.0%	150.0%	100.0 s	0.0 s	01:00 m:s	auto
AIRF	33.3%	33.3%	90.0%	50.0 s	0.0 s	01:00 m:s	auto
O <sub>2</sub> EN	0.0%	100.0%	90.0%	50.0 s	0.0 s	05:00 m:s	off
STIR: 37.5% = 750 rpm, 90.0% = 1800 rpm AIRF: 33.3% = 1.00 L/min O <sub>2</sub> EN setting did not matter since it was off.							

The impeller speed (STIR) minimum was changed to 400 rpm (20%) at t = 24 h.

### 9.17. Glucose-limited Condition Fermentation

Glucose limited conditions consisted of two phases. The preparation of inoculant and the first phase of fermentation were essentially the same as described for glucose rich conditions. Inoculant was initially grown in 5 mL M9 medium in an incubator shaker (37 °C, 250 rpm) for 20 h and subsequently transferred to 100 mL of M9 medium. This 100 mL culture was grown at 37 °C and 250 rpm until the OD<sub>600</sub> reached 1.0-2.0 (7 h). The baffles for the 2 L fermentor vessel were removed for these experiments. The fermentation was initiated when the 100 mL culture was transferred to the fermentor (t = 0). The initial glucose concentration in the fermentation medium was 20 g/L. The sterile 100 mM IPTG stock solution (12 mg IPTG / each addition) was added at 19 h, 25 h, 31 h, 37 h, 43 h and 49 h. The instrument settings were split into two phases. During the first phase, DO was maintained at 10 % by increasing the impeller speed until the impeller speed reached the set maximum (750 rpm). Airflow was then increased

increased until it reached the set maximum (1.00 L/min).

The pO<sub>2</sub> control loop settings for the first phase was as follows (Table 5.7.) :

Table 5.7. First Phase of Glucose-limited Fermentation

DEADB 0.5% sat							
CASCADE							
1	STIR						
2	AIRF						
Cascade	Minimum	Maximum	XP	TI	TD	Hysteresis	Mode
STIR	2.5%	37.5%	150.0%	100.0 s	0.0 s	01:00 m:s	auto
AIRF	2.0%	33.3%	90.0%	50.0 s	0.0 s	01:00 m:s	auto
O2EN	0.0%	100.0%	90.0%	50.0 s	0.0 s	05:00 m:s	off
STIR: 2.5% = 50 rpm, 37.5% = 750 rpm AIRF: 2.0% = 0.06 L/min, 33.3% = 1.00 L/min O2EN setting did not matter since it was off.							

The pO<sub>2</sub> control loop was turned off when both impeller speed and airflow reached their maximum values. The airflow was held at 1.00 L/min and the impeller speed was held at 750 rpm. DO level started increasing when all the initial glucose was consumed. The instrument setting was switched to pO<sub>2</sub> Nutrient control loop while the airflow was held at 1.00 L/min and the impeller speed was held at 750 rpm. The pO<sub>2</sub> Nutrient control loop setting for second phase was as follows (Table 5.8.) :

Table 5.8. Second Phase of Glucose-limited Fermentation

MIN	0.0%	MAX	100.0%
DEADB	0.5% sat	XP	950.0%
TI	999.9 s	TD	0.0 s
impeller speed = 750 rpm airflow = 1.0 L/min			

These settings created the glucose-limited conditions by restricting the addition of feed glucose to only when DO rose above 10%. The impeller speed was lowered to 600 rpm at 31 h and then 400 rpm at 52 h. Antifoam was added manually as needed.

### 9.18. Removal of Cells and Protein

The cells were removed by centrifugation (4600 g, 30 min, 4 °C). The protein in the cell free broth was removed with four Sartocan® ECO Hydrostart® membrane cut off 10 kD cassettes equipped with a SartoJet® Pump 4-Piston Diaphragm Pump. This tangential flow filtration of cell free broth was performed with the pressure toward the membrane of 25±5 psi and a back pressure of 6±1 psi. When the retentate became approximately 200 mL, it was not enough volume to sustain the broth flow. The retentate was diluted with 200 mL of water to increase the volume. The diluted retentate was filtered until the flow ceased.

### 9.19. Isolation of 2*E*,4*E*-3-carboxymuconic acid **54**

The cell-free/protein-free broth 627 mL contained 5.4 g of 2*E*,4*Z*-3-carboxymuconic acid **16**, 2.9 g of 2*E*,4*E*-3-carboxymuconic acid **54** and 2.9 g of lactone **55**. An activated charcoal (Sigma 242276, Darco G-60, mesh 100-325) 10 g was added to a 2 L Erlenmeyer flask containing 627 mL of the broth. It was swirled for 1h in an incubator shaker (250 rpm, rt). The activated charcoal was removed by filtration with a filter paper. The filtrate was treated with 10 g of the activated charcoal one more time followed by filtration. The filtrate was concentrated to 125 mL with a rotary evaporator. The concentrated broth was chilled in an ice-bath and acidified with H<sub>2</sub>SO<sub>4</sub> to pH 2 while it was kept in an ice-bath. This acidified broth was stirred at rt for 2 h to allow precipitation of the product. The white solid was collected by filtration with a filter paper and dried under reduced pressure overnight. Filtration afforded 4.9 g of white solid containing 4.3 g of 2*E*,4*E*-3-carboxymuconic acid **54** (52% recovery) based on <sup>1</sup>H NMR analysis. <sup>1</sup>H NMR (D<sub>2</sub>O, TSP δ = 0.00) δ = 7.94 (d, *J* = 16 Hz, 1H), 6.48 (s, 1H), 6.33 (d, *J* = 16 Hz, 1H). <sup>13</sup>C NMR (D<sub>2</sub>O, TSP δ = 0.00) δ = 175.8, 174.1, 173.6, 145.0, 140.2, 132.0, 128.5.

mp: decomposed at 169 °C (lit.<sup>69</sup> 155-159 °C).

### 9.20. *2E,4E*-3-Carboxymuconic Acid **54** Isolation Process Investigation

The cell-free/protein-free broth 500 mL containing 2.1 g of *2E,4Z*-3-carboxymuconic acid **16**, 2.7 g of *2E,4E*-3-carboxymuconic acid **54** and 1.4 g of lactone **55** was processed as aforementioned. The isolated white solid and the mother liquor were analyzed with <sup>1</sup>H NMR. The isolated white solid (2.7 g) contained 2.4 g of *2E,4E*-3-carboxymuconic acid **54** (50% recovery). The mother liquor contained 1.3 g of *2E,4E*-3-carboxymuconic acid **54** (27%) and 2.4 g of lactone **55**. Since the original cell-free/protein-free broth contained 1.4 g of lactone **55**, 1.0 g of the lactone **55** (21%) was produced during this isolation process.

### 9.21. Isomerization of *2E,4E*-3-Carboxymuconic Acid **54** to *2Z,4E*-3-Carboxymuconic Acid **13**

Iodine (0.03 g, 0.12 mmol) and acetonitrile (10 mL) were added to a 25 mL stripping flask (14/20 neck size) containing a magnetic stir bar and *2E,4E*-3-carboxylic acid **54**. This flask was connected to a reflux condenser, which was opened to air. This mixture was refluxed at 82 °C for 24 h. The reaction mixture was concentrated and dried under reduced pressure. The brown residue was analyzed by <sup>1</sup>H NMR and NOE. For <sup>1</sup>H NMR quantification of products, the residue was dissolved in D<sub>2</sub>O. <sup>1</sup>H NMR (D<sub>2</sub>O, TSP δ = 0.00) *2E,4E*-3-carboxymuconic acid **54** δ = 7.94 (d, *J* = 16 Hz, 1H), 6.48 (s, 1H), 6.33 (d, *J* = 16 Hz, 1H); *2Z,4E*-3-carboxymuconic acid **13** δ = 7.27 (d, *J* = 16 Hz, 1H), 6.15 (d, *J* = 16 Hz, 1H), 6.01 (s, 1H); lactone **55** δ = 6.43 (d, *J* = 2Hz, 1H), 5.62 (ddd, *J* = 2.5, 3.5, 8.5 Hz, 1H), 3.21 (dd, *J* = 3.5, 16.5 Hz, 1H), 2.73 (dd, *J* = 8.5, 16.5 Hz, 1H). The ratio of three products was determined by the integral corresponding to *2E,4E*-3-carboxymuconic acid **54** at 7.94 ppm, *2Z,4E*-3-carboxymuconic acid **13** at 7.27 ppm

and lactone **55** at 5.60 ppm. This reaction afforded 12% of *2Z,4E*-3-carboxymuconic acid **13**, 5% of lactone **55** and 83% of *2E,4E*-3-carboxymuconic acid **54**. The magnetic interactions between the protons on C-2 and C-4 was observed using NOE technique (Scheme 13). There was no interaction between protons on C-2 (6.48 ppm) and C-4 (7.94 ppm) of *2E,4E*-3-carboxymuconic acid **54**. There was an interaction between the protons on C-2 (6.01 ppm) and C-4 (7.27 ppm) of *2Z,4E*-3-carboxymuconic acid **13**.

## **9.22. Cycloaddition of *2E,4E*-3-Carboxymuconic Acid **54** and Ethylene**

*2E,4E*-3-Carboxymuconic acid **54** and a solvent were added in a Parr Series 4590 Micro Bench Top Reactor (25 mL) interfaced with 4848 Reactor Controller. The reactor was flushed with N<sub>2</sub> five times, and then flushed with ethylene five times. The reactor was charged with ethylene (34.5 bar).

### **9.22.1. Reaction in 1,4-Dioxane at 164 °C**

Heating the reactor at 164 °C with stirring (100 rpm) for 24 h led to a maximum pressure to 72.4 bar. After allowing the reactor to cool, a dark brown reaction crude was obtained. The entire reaction crude was concentrated and an aliquot of the residue was dissolved in DMSO-d<sub>6</sub>. This reaction did not yield cycloadduct **14** based on <sup>1</sup>H NMR.

### **9.22.2. Reaction in *m*-Xylene at 150 °C**

Heating the reactor at 150 °C with stirring (200 rpm) for 12 h led to a maximum pressure to 79.3 bar. After allowing the reactor to cool, a dark brown reaction crude was obtained. The entire reaction crude was concentrated and an aliquot of the residue was dissolved in DMSO-d<sub>6</sub>. This reaction did not yield cycloadduct **14** based on <sup>1</sup>H NMR.

### 9.22.3. Reaction in 1,4-Dioxane at 100 °C

Heating the reactor at 100 °C with stirring (300 rpm) for 12 h led to a maximum pressure to 56.9 bar. After allowing the reactor to cool, a white reaction crude was obtained. The reactor was rinsed with water. The water solution was acidified with H<sub>2</sub>SO<sub>4</sub> to pH 1 followed by extraction with Et<sub>2</sub>O 10 mL × 6. The extracted was dried over MgSO<sub>4</sub> and concentrated. The residue was dissolved in DMSO-d<sub>6</sub>. This reaction did not yield cycloadduct **14** with mostly unreacted 2*E*,4*E*-3-carboxymuconic acid **54** and some unidentifiable peaks in <sup>1</sup>H NMR.

### 9.22.4. Reaction in *m*-Xylene at 100 °C

Heating the reactor at 100 °C with stirring (300 rpm) for 12 h led to a maximum pressure to 58.6 bar. After allowing the reactor to cool, a white reaction crude was obtained. The reactor was rinsed with water. The water solution was acidified with H<sub>2</sub>SO<sub>4</sub> to pH 1 followed by extraction with EtOAc 10 mL × 6. The extracted was dried over MgSO<sub>4</sub> and concentrated. The residue was dissolved in DMSO-d<sub>6</sub>. This reaction did not yield cycloadduct **14** with mostly unreacted 2*E*,4*E*-3-carboxymuconic acid **54** and some unidentifiable peaks in <sup>1</sup>H NMR.

### 9.23. Esterification of 2*E*,4*E*-3-Carboxymuconic Acid **54**

Tetrahydrofuran (20 mL) was added to a 100 mL RBF (2 × 24/40 necks) containing 2*E*,3*E*-3-carboxymuconic acid (1.02 g, 5.50 mmol) and a magnetic stir bar. The flask was purged with N<sub>2</sub>, and connected to a N<sub>2</sub> bubbler line while the side neck was closed with a rubber septum. The flask was chilled in an iced-bath followed by addition of oxalyl chloride (1.50 mL, 17.7 mmol). The reaction mixture was stirred in an iced-bath for 30 min after addition of dimethylformamide (10 μL, 0.1 mmol). The reaction mixture was continued to stir for 3 h at rt. The reaction solution became dark brown gradually during this 3 h. The flask was chilled in an

ice-bath prior to addition of dry cold methanol (20 mL, 494 mmol). The reaction solution was stirred in an ice-bath for 30 min and then continued stirring at rt for 19 h. The reaction solution was concentrated under reduced pressure. The residue was loaded on a silica column. Chromatographic purification (EtOAc/hexanes, 1:11 to 1:5, v/v) gave 746 mg of light white oil containing Trimethyl *2E,4E*-3-carboxymuconate **56a** and Trimethyl *2Z,4E*-3-carboxymuconate **56b**. The magnetic interactions between the protons on C-2 and C-4 was observed using NOE technique (Scheme 16). There was no interaction between protons on C-2 (6.70 ppm) and C-4 (8.22 ppm) of trimethyl *2E,4E*-3-carboxymuconate **56a**. There was an interaction between the protons on C-2 (6.14 ppm) and C-4 (7.23 ppm) of trimethyl *2Z,4E*-3-carboxymuconate **56b**. The products were quantified by the integral corresponding to trimethyl *2E,4E*-3-carboxymuconate **56a** (6.61 ppm, d,  $J = 16$  Hz, 1H); trimethyl *2Z,4E*-3-carboxymuconate **56b** (6.07 ppm, d,  $J = 16$  Hz, 1H) with integral corresponding to maleic anhydride ( $\delta = 7.03$  ppm, s, 2H). Trimethyl *2E,4E*-3-carboxymuconate **56a** (32%) and trimethyl *2Z,4E*-3-carboxymuconate **56b** (25%) were isolated as a mixture.  $^1\text{H}$  NMR for trimethyl *2E,4E*-3-carboxymuconate **56a**:  $\delta = 8.22$  (dd,  $J = 1, 16$  Hz, 1H), 6.70 (d,  $J = 1$  Hz, 1H), 6.61 (d,  $J = 16$  Hz, 1H), 3.83 (s, 3H), 3.78 (s, 3H), 3.76 (s, 3H).  $^1\text{H}$  NMR for trimethyl *2Z,4E*-3-carboxymuconate **56b**:  $\delta = 7.23$  (d,  $J = 16$  Hz, 1H), 6.14 (s, 1H), 6.07 (d,  $J = 16$  Hz, 1H), 3.87 (s, 3H), 3.75 (s, 3H), 3.74 (s, 3H).

#### 9.24. Cycloaddition of Trimethyl 3-Carboxymuconates **56** and Ethylene

A solution of trimethyl 3-carboxymuconic acid **56** (0.520 g, 2.28 mmol) in *m*-xylene was added in a Parr Series 4590 Micro Bench Top Reactor (25 mL) interfaced with 4848 Reactor Controller. The reactor was flushed with  $\text{N}_2$  five times and then flushed with ethylene five times. The reactor was charged with ethylene (17.2 bar). Heating the reactor at 150 °C with stirring

(300 rpm) for 9 h led to a maximum pressure to 34.5 bar. After allowing the reactor to cool, a colorless reaction crude was obtained. A sticky solid remained in the reactor that did not dissolve in common solvents. The crude solution was concentrated under reduced pressure affording a total 85% yield of *trans*-cycloadduct **57a** and *cis*-cycloadduct **57b**. The products were quantified by the integral corresponding to cycloadduct-1 (3.74 ppm, s, 3H); cycloadduct-2 (3.72 ppm, s, 3H) with integral corresponding to *tert*-butyl methyl ether ( $\delta = 3.21$  ppm, s, 3H). The ratio of cycloadduct-1 : cycloadduct-2 were 1.0:1.1.  $^1\text{H}$  NMR ( $\text{CDCl}_3$ ) for mixture of *trans*-cycloadduct **57a** and *cis*-cycloadduct **57b**:  $\delta = 7.21$  (d,  $J = 3$  Hz, 1H), 7.18 (dd,  $J = 1.5, 4$  Hz, 1 H), 3.750 (s, 3H), 3.746 (s, 3H), 3.736 (s, 3H), 3.722 (s, 3H), 3.693 (s, 3H), 3.684 (s, 3H), 3.49-3.51 (m, overlap 2H), 3.31-3.34 (m, 1H), 3.24-3.28 (m, 1H), 2.13-2.18 (m, 1H), 2.01-2.08 (m, 1H), 1.89-1.97 (m, overlap 4H), 1.81-1.88 (m, overlap 2 H).

### 9.25. Dehydrogenation of Cycloadducts **57** Catalyzed by Pd/C in Decane

5 wt% Pd/C (Alfa Aesar A102023-5) containing approximately 50 wt% water was dried for 3 h under reduced pressure at 70 °C. Dry Pd/C (17.3 mg, 0.008 mmol) and decane (3.0 mL) were added to a 25 mL stripping flask (14/20) containing cycloadduct **57** (77.0 mg, 0.300 mmol). The flask was connected to a reflux condenser opening to air. The mixture was refluxed at 174 °C while reaction progress was observed by TLC (EtOAc : hexanes = 1:2, UV). After 3 days, the reaction mixture was loaded on a silica gel column in order to remove decane. Dark brown material remained at beginning of the column. The collected fraction was concentrated affording 41.7 mg of yellow oil containing 12.9 mg of trimethyl trimellitate **2b** (17%) based on GC analysis.

### 9.26. Dehydrogenation of Cycloadducts **57** Catalyzed by Pd/C in Dichlorobenzene

5 wt% Pd/C (Alfa Aesar A102023-5) containing approximately 50 wt% water was dried for 3 h under reduced pressure at 70 °C. Dry Pd/C (38.3 mg, 0.018 mmol) and dichlorobenzene (3.0 mL) were added to a 25 mL stripping flask (neck size 14/20) containing cycloadduct **57** (230 mg, 0.897 mmol). The flask was connected to a reflux condenser open to air. The mixture was heated at 172 °C while reaction progress was monitored by TLC (EtOAc : hexanes = 1:2, UV). After 2 days, the reaction mixture was filtered in order to remove Pd/C. The filtrate was concentrated affording 273 mg of light brown oil containing 43.0 mg of trimethyl trimellitate **2b** (19%) based on GC analysis.

### 9.27. Aerobic Oxidative Dehydrogenation of Cycloadduct **57**<sup>61</sup>

To a glass test tube (20 × 150 mm) fitted with a magnetic stir bar was added Pd(TFA)<sub>2</sub> (18.8 mg, 0.0565 mmol), AMS (64.9 mg, 0.209 mmol), MgSO<sub>4</sub> (100 mg, 0.831 mmol) and cycloadduct **57** (259 mg, 1.01 mmol) dissolved in chlorobenzene (1.0 mL). The test tube was sealed with a rubber septum and O<sub>2</sub> was sparged into the mixture for 10 min while the mixture was stirred. The test tube was fitted with O<sub>2</sub> balloon and heated at 110 °C for 24 h. <sup>1</sup>H NMR spectrum showed nothing but starting material, cycloadduct **57**.

### 9.28. Vapor Phase Dehydrogenation of Cycloadduct **57**

Pd/SiO<sub>2</sub> (2.4 wt%) was prepared by Kelly Miller and Sebastien Thueillon. Davisil Grade 643 silica gel (150 Å pore size, 35-70 µm mesh) and Pd/SiO<sub>2</sub> (2.4 wt%) were dried under reduced pressure (0.3 mbar) at 100 °C for 3h. The dried silica gel (1.00 g) and dried Pd/SiO<sub>2</sub> (0.50 g, 0.113 mmol) were thoroughly mixed and then packed into a 9 cm × 1.7cm glass tube

using glass wool to immobilize the plug reactor material. Vaporization/dehydrogenation of cycloadduct **57** employed a Kugelrohr apparatus assembled as follows: the 50 mL flask containing **57**, the 9 cm × 1.7 cm glass tube containing the plug reactor, three 5 mL collection bulbs in series, a U-shaped tube and finally a straight gas adaptor connected to two water recirculating aspirator pumps through an oscillating motor and a trap (Chapter 4, Figure 1). The flask containing **57** and plug reactor were inserted into an oven. The U-shaped tube was cooled to -78 °C. Prior to the reaction, the glassware was assembled without the flask containing the substrate. The glass tube containing the catalyst was closed with a glass cap. The catalyst was preheated at 250 °C for 10 min at 0.07 bar and the vacuum was gently released from the system. The 50 mL flask containing cycloadduct **57** was connected to the catalyst tube. Vaporization/dehydrogenation proceeded at 250 °C under vacuum (0.07 bar) with reciprocal oscillating agitation. The colorless clear liquid that accumulated in the collection bulbs and the U-shaped tube was collected with acetonitrile washes into a 10 mL volumetric flask. The plug reactor contents were suspended in acetonitrile followed by filtration to remove the Pd/SiO<sub>2</sub>. The filtrate was collected in a 5 mL volumetric flask. The acetonitrile solutions contained 148 mg of trimethyl trimellitate **2b** (57%), 4.04 mg of methyl benzoate **59** (3%), 8.24 mg of dimethyl phthalate **60** (4%), 4.52 mg of dimethyl isophthalate **61** (2%) and 3.10 mg of dimethyl terephthalate **62** (2%).

### 9.29. Synthesis of Biobased 1,2,4-Butanetricarboxylic Acid **37**

2*E*,4*E*-3-Carboxymuconic acid (875 mg, 4.70 mmol) **54** and 5 wt% Pd/C (Alfa Aesar A102023-5) containing approximately 50 wt% (0.46 g, 0.11 mmol) were added to water (130 mL) in a Parr Series 4575 high pressure reactor (500 mL) interfaced with a Series 4842

temperature controller. The reactor was flushed with H<sub>2</sub> and then pressurized to 34.5 bar with H<sub>2</sub>. It was kept stirring (200 rpm) at rt for 4 h. Pd/C was removed by filtration affording clear colorless filtrate containing 892 mg of 1,2,4-butanetricarboxylic acid **37** (99%). The product **37** was quantified by the calibration curve generated from integral corresponding to 1,2,4-butanetricarboxylic acid **37** (1.87 ppm, dtd, 2H) with integral corresponding to TSP ( $\delta = 0.00$  ppm, s, 9H). This filtrate was concentrated with a rotary evaporator down to 20 mL and then acidified with H<sub>2</sub>SO<sub>4</sub> to pH 1.8. The product was extracted by hand with EtOAc 20 mL 6. The extract was dried over MgSO<sub>4</sub> and concentrated to afford a white residue. This white residue was dissolved in acetonitrile (8 mL) by heating followed by crystallization at 4 °C overnight. Filtration of the white crystal afforded 702 mg of 1,2,4-butanetricarboxylic acid **37** (79%). <sup>1</sup>H NMR (D<sub>2</sub>O, TSP  $\delta = 0.00$ ):  $\delta = 2.76$ - $2.82$  (m, 1H), 2.66 (dd,  $J = 10, 15$  Hz, 1H), 2.55 (dd,  $J = 5, 15$  Hz, 1H), 2.38- $2.48$  (m, 2H), 1.81- $1.93$  (m, 2H). <sup>13</sup>C NMR (D<sub>2</sub>O, TSP  $\delta = 0.00$ ):  $\delta = 184.0, 182.3, 181.1, 45.6, 40.4, 35.7, 30.2$ . mp: 124-125 °C.

## REFERENCES

## REFERENCES

1. (a) Emanuel, C. B. Plasticizer Market Update <http://www.cpsc.gov/PageFiles/126090/spi.pdf> (accessed Feb 6, 2017). (b) Bizzari, S. N.; Blagoev, M.; Kishi, A. Chemical Economics Handbook-SRI Consulting. CEH Marketing Research Report: Plasticizers, 2007.
2. Gooch, J. W. Encyclopedic Dictionary of Polymers, 2nd ed.; Springer Nature: Berlin, 2011.
3. Cater, B. R.; Cook, M. W.; Gangolli, S. D. Zinc metabolism and dibutyl phthalate-induced testicular atrophy in the rat. *Biochem. Soc. Trans.* **1976**, *4*, 652–653. DOI: 10.1042/bst0040652.
4. Cater, B. R.; Cook, M. W.; Gangolli, S. D.; Grasso, P. Studies on dibutyl phthalate-induced testicular atrophy in the rat: Effect on zinc metabolism. *Toxicol. Appl. Pharmacol.* **1977**, *41*, 609-618. DOI: 10.1016/S0041-008X(77)80014-8.
5. Mylchreest, E.; Wallace, D. G.; Cattley, R. C.; Foster, P. M. Dose-dependent alterations in androgen-regulated male reproductive development in rats exposed to Di(*n*-butyl) phthalate during late gestation. *Toxicol. Sci.* **2000**, *55*, 143-151. DOI: 10.1093/toxsci/55.1.143.
6. Parks, L. G.; Ostby, J. S.; Lambright, C. R.; Abbott, B. D.; Klinefelter, G. R.; Barlow, N. J.; Gray, L. E., Jr. The plasticizer diethylhexyl phthalate induces malformations by decreasing fetal testosterone synthesis during sexual differentiation in the male rat. *Toxicol. Sci.* **2000**, *58*, 339-349. DOI: 10.1093/toxsci/58.2.339.
7. Fisher, J. S.; Macpherson, S.; Marchetti, N.; Sharpe, R. M. Human ‘testicular dysgenesis syndrome’: a possible model using in-utero exposure of the rat to dibutyl phthalate. *Hum. Reprod.* **2003**, *18*, 1383-1394. DOI: 10.1093/humrep/deg273.
8. Guowei Pan; Hanaoka, T.; Mariko Yoshimura; Shujuan Zhang; Wang, P.; Hiromasa Tsukino; Inoue, K.; Nakazawa, H.; Tsugane, S.; Ken Takahashi. Decreased serum free testosterone in workers exposed to high levels of di-*n*-butyl Phthalate (DBP) and di-2-ethylhexyl Phthalate (DEHP): A cross-sectional study in China. *Environ. Health Perspect.* **2006**, *114*, 1643-1648.
9. Hauser, R.; Meeker, J. D.; Singh, N. P.; Silva, M. J.; Ryan, L.; Duty, S.; Calafat, A. M. DNA damage in human sperm is related to urinary levels of phthalate monoester and oxidative metabolites. *Hum. Reprod.* **2007**, *22*, 688-695. DOI: 10.1093/humrep/del428.
10. Pant, N.; Shukla, M.; Kumar Patel, D.; Shukla, Y.; Mathur, N.; Kumar Gupta, Y.; Saxena, D. K. Correlation of phthalate exposures with semen quality. *Toxicol. Appl. Pharmacol.* **2008**, *231*, 112-116. DOI: 10.1016/j.taap.2008.04.001.
11. Erickson, B. E. *Chem. Eng. News* **2015**, *93*, 11-15.

12. Research, P. M. Trimellitates Market <http://www.persistencemarketresearch.com/market-research/trimellitates-market.asp> (accessed Feb 6, 2017).
13. Ember, G.; Park, P.; Hannemann, D. E.; Darin, J. K.; Zimmerschied, W. J. Production of aromatic tricarboxylic acids having only two vicinal carboxylic acid group. US 3491144, January 20, 1970.
14. Schammel, W. P. Process for the production of trimellitic acid. US 4992579, February 12, 1991.
15. Yan, T. Y. Pseudocumene and mesitylene production and coproduction thereof with xylene. US 5004854, April 2, 1991.
16. Favilli, S. Process and equipment for separating 1,2,4-trimethylbenzene (pseudocumene) from a mixture containing aromatic hydrocarbons. US 20130267751, October 10, 2013.
17. Saffer, A.; Barker, R. S. Preparation of aromatic polycarboxylic acids. US 2833816, May 6, 1958.
18. (a) Partenheimer, W. The effect of zirconium in metal/bromide catalysts during the autoxidation of *p*-xylene Part I. Activation and changes in benzaldehyde intermediate formation. *J. Mol. Catal. A-Chem.* **2003**, *206*, 105-119. DOI: 10.1016/S1381-1169(03)00407-2.  
(b) Partenheimer, W. The effect of zirconium in metal/bromide catalysts during the autoxidation of *p*-xylene Part II. Alternative metals to zirconium and the effect of zirconium on manganese (IV) dioxide formation and precipitation with pyromellitic acid. *J. Mol. Catal. A-Chem.* **2003**, *206*, 131-144. DOI: 10.1016/S1381-1169(03)00421-7.
19. (a) Darin, J. K.; Kanitkar, D. R. Staged catalyst addition for catalytic liquid phase oxidation of pseudocumene to trimellitic acid. US 3683016, August 8, 1972 (b) Northbridge, C. S. U. Standard Reduction Potentials <https://www.csun.edu/~hcchm003/321/Ered.pdf> (accessed Feb 9, 2017).
20. Narula, C. K.; Davison, B. H.; Keller, M. Zeolitic catalytic conversion of alcohols to hydrocarbons. US 2012174205, December 20, 2012.
21. Suh, Y.; Jang, H.; Bae, K. Method for producing bio-aromatics from glycerol. US 2015336856, November 26, 2015.
22. Uprety, B. K.; Chaiwong, W.; Ewelike, C.; Rakshit, S. K. Biodiesel production using heterogeneous catalysts including wood ash and the importance of enhancing byproduct glycerol purity. *Energy Convers. Manage.* **2016**, *115*, 191-199. DOI: 10.1016/j.enconman.2016.02.032.
23. Der, B.; Jense, A. S. Methanol purification method and apparatus. US 2011306807, December 15, 2011.

24. Niu, W.; Draths, K. M.; Frost, J. W. Benzene-free synthesis of adipic acid. *Biotechnol. Prog.* **2002**, *18*, 201-211. DOI: 10.1021/bp010179x.
25. Bui, V.; Lau, M. K.; MacRae, D.; Schweitzer, D. Methods for producing isomers of muconic acid and muconate salts. US 2013030215, January 31, 2013.
26. Frost, J. W.; Miermont, A.; Schweitzer, D.; Bui, V.; Wicks, D. A. Novel terephthalic acid trimellitic based acids and carboxylate derivatives thereof. US 2011288311, November 24, 2011.
27. Fauconet, M.; Roundy, R. L.; Denis, S.; Daniel, S. M. Method for continuous production of light acrylates by esterification of a raw ester-grade acrylic acid. US 2016159725, June 9, 2016.
28. (a) Kumar, R.; Ashok, S.; Park, S. Recent advances in biological production of 3-hydroxypropionic acid. *Biotechnol. Adv.* **2013**, *31*, 945-961. DOI: 10.1016/j.biotechadv.2013.02.008. (b) Lilga, M. A.; White, J. F.; Holladay, J. E.; Zacher, A. H.; Muzatko, D. S.; Orth, R. J. Method for Conversion of beta-Hydroxy Carbonyl Compounds. US 20070219391, September 20, 2007.
29. Yan, B.; Tao, L.; Liang, Y.; Xu, B. *ACS Catal.* **2014**, *4*, 1931-1943.
30. Taheri, H.; Sarin, Y.; Ozero, B. Reactor and process for dehydration of ethanol to ethylene. US 2013178674, July 11, 2013.
31. Li, K.; Frost, J. W. Synthesis of vanillin from glucose. *J. Am. Chem. Soc.* **1998**, *120*, 10545-10546. DOI: 10.1021/ja9817747.
32. Pittard, J.; Wallace, B. J. Distribution and function of genes concerned with aromatic biosynthesis in *Escherichia coli*. *J. Bacteriol.* **1966**, *91*, 1494-1508.
33. *E. coli* Genetic Resources at Yale CGSC, T. C. G. S. C. Strain AB2834 <http://cgsc2.biology.yale.edu/Strain.php?ID=8219> (accessed Feb 28, 2017).
34. Ohlendorf, D. H.; Lipscomb, J. D.; Weber, P. C. Structure and assembly of protocatechuate 3,4-dioxygenase. *Nature* **1988**, *336*, 403-405. DOI: 10.1038/336403a0.
35. Hartnett, C.; Neidle, E. L.; Ngai, t. K.-L.; Nicholas Ornston, L. DNA Sequences of genes encoding *Acinetobacter calcoaceticus* protocatechuate 3,4-Dioxygenase: evidence indicating shuffling of genes and of DNA sequences within genes during their evolutionary divergence. *J. Bacteriol.* **1990**, *172*, 956-966.
36. Zylstra, G. J.; Olsen, R. H.; Ballou, D. P. Genetic organization and sequence of the *Pseudomonas cepacia* genes for the alpha and beta subunits of protocatechuate 3,4-dioxygenase. *J. Bacteriol.* **1989**, *171*, 5915-5921.

37. Giedraityte, G.; Kalėdienė, L. Biotransformation of eugenol via protocatechuic acid by thermophilic *Geobacillus* sp. AY 946034 strain. *J. Microbiol. Biotechnol.* **2014**, *24*, 475-482. DOI: 10.4014/jmb.1309.09069.
38. Eulberg, D.; Lakner, S.; Golovleva, L. A.; Schlömann, M. Characterization of a protocatechuate catabolic gene cluster from *Rhodococcus opacus* ICP: evidence for a merged enzyme with 4-carboxymuconolactone-decarboxylating and 3-oxoadipate enol-lactone-hydrolyzing activity. *J. Bacteriol.* **1998**, *180*, 1072-1081.
39. Frazee, R. W.; Livingston, D. M.; LaPorte, D. C.; Lipscomb, J. D. Cloning, sequencing, and expression of the *Pseudomonas putida* protocatechuate 3,4-dioxygenase genes. *J. Bacteriol.* **1993**, *175*, 6194-6202.
40. National Center for Biotechnology Information (NCBI). *Klebsiella pneumoniae* subsp. *rhinoscleromatis* Strain SB3432, Complete Genome <https://www.ncbi.nlm.nih.gov/nuccore/499527875?report=graph> (accessed Mar 2, 2017).
41. Contzen, M.; Stolz, A. Characterization of the genes for two protocatechuate 3, 4-dioxygenases from the 4-sulfocatechol-degrading bacterium *Agrobacterium radiobacter* strain S2. *J. Bacteriol.* **2000**, *182*, 6123-6129.
42. Doten, R. C.; Ngai, K.-L.; Mitchell, D. J.; Nicholas Ornston, L. Cloning and genetic organization of the *pca* gene cluster from *Acinetobacter calcoaceticus*. *J. Bacteriol.* **1987**, *169*, 3168-3174.
43. Harwood and, C. S.; Parales, R. E. The  $\beta$ -keto adipate Pathway and the biology of self-identity. *Annu. Rev. Microbiol.* **1996**, *50*, 553-590 DOI:10.1146/annurev.micro.50.1.553.
44. Rinaldi, R.; Jastrzebski, R.; Clough, M. T.; Ralph, J.; Kennema, M.; Bruijninx, P. C. A.; Weckhuysen, B. M. Paving the way for lignin valorisation: recent advances in bioengineering, biorefining and catalysis. *Angew. Chem. Int. Ed Engl.* **2016**, *55*, 8164-8215. DOI: 10.1002/anie.201510351.
45. Hybholt, T. K.; Aamand, J.; Johnsen, A. R. Quantification of centimeter-scale spatial variation in PAH, glucose and benzoic acid mineralization and soil organic matter in roadside soil. *Environ. Pollut.* **2011**, *159*, 1085-1091. DOI:10.1016/j.envpol.2011.02.028.
46. Mazzeo, D. E. C.; Casado, M.; Piña, B.; Marin-Morales, M. A. Detoxification of sewage sludge by natural attenuation and implications for its use as a fertilizer on agricultural soils. *Sci. Total Environ.* **2016**, *572*, 978-985. DOI: 10.1016/j.scitotenv.2016.07.228.
47. Lesage, O.; Falk, L.; Tatoulian, M.; Mantovani, D.; Ognier, S. Treatment of 4-chlorobenzoic acid by plasma-based advanced oxidation processes. *Chemical Engineering and Processing: Process Intensification* **2013**, *72*, 82-9. DOI:10.1016/j.cep.2013.06.008.

48. Yamashita, M.; Shimoda, A. Triisocyanate and polyurethane coating. JP 2003277341, October 2, 2003.
49. Shirota, K.; Yamashita, Y. Inkjet recording reaction liquid, inkjet recording method and inkjet recording ink set. JP 2008265122, November 6, 2008.
50. Miyajima, T.; Ihara, T.; Mizushima, H. Amide compound. WO 2005082839, September 9, 2005.
51. Kunisawa, M.; Ohmori, M.; Yokouchi, H. Method for using electrochemical element. Wo 2014007330, January 9, 2014.
52. Davenport Huyer, L.; Zhang, B.; Korolj, A.; Montgomery, M.; Drecun, S.; Conant, G.; Zhao, Y.; Reis, L.; Radisic, M. Highly elastic and moldable polyester biomaterial for cardiac tissue engineering applications. *ACS Biomaterials Science & Engineering* **2016**, *2*, 780-788 DOI: 10.1021/acsbomaterials.5b00525.
53. Ichikawa, S.; Kiyoku, K. Production of 1,2,4-butanetricarboxylic acid. JP 2000044521, February 15, 2000.
54. Burk, M. J.; Burgard, A. P.; Sun, J.; Osterhout, R. E.; Pharkya, P. Microorganisms and methods for the biosynthesis of butadiene. US 2012225466, September 6, 2012.
55. Zhang, P.; Kriegel, R. M.; Frost, J. W. B–O–B Catalyzed Cycloadditions of Acrylic Acids. *ACS Sustainable Chemistry & Engineering* **2016**, *4*, 6991–6995. DOI: 10.1021/acssuschemeng.6b01908.
56. Lynn, J. W.; Roberts, R. L. Some Syntheses of 1,2,4-Butanetricarboxylic Acid. *J. Org. Chem.* **1961**, *26*, 4303-4305. DOI: 10.1021/jo01069a029.
57. Suzuki, N.; Shirosaki, Y.; Okago, Y. Cyclo-dimerization of conjugated diolefin. JP H101446, January 6, 1998.
58. Samura, H.; Suenaga, K.; Nukina, S. Preparation of high-purity 1,2,4-butanetricarboxylic acid. JP S56164136, December 17, 1981.
59. Baker, R. T.; White, J. F.; Manzer, L. E.; Ntais, S.; Baranova, O.; Thapa, I.; Lau, K. L.; Hass, C. S. Organic Acids from Homocitrate and Homocitrate Derivatives. WO 2015191763, December 17, 2015.
60. (a) Garner, C. C.; Herrmann, K. M. *J. Biol. Chem.* **1985**, *260*, 3820-3825. (b) Cobbett, C. S.; Delbridge, M. L. *J. Bacteriol.* **1987**, *169*, 2500-2506. (c) Li, K.; Mikola, M. R.; Draths, K. M.; Worden, R. M.; Frost, J. W. *Biotechnol. Bioeng.* **1999**, *64*, 61-73.
61. (a) Bui, V.; Lau, M. K.; MacRae, D.; Schweitzer, D. Methods for Producing Isomers of Muconic Acid and Muconate Salts. US 20130030215, January 31, 2013. (b) Frost, J. W.;

- Miermont, A.; Schweitzer, D.; Bui, V.; Wicks, D. A. Novel Terephthalic and Trimellitic Based Acids and Carboxylate Derivatives Thereof. US 20120288311, November 24, 2011.
62. Iosub, A. V.; Stahl, S. S. *J. Am. Chem. Soc.* **2015**, *137*, 3454-3457. DOI: 10.1021/ja512770u.
63. Miller, J. H. Experiments in Molecular Genetics; Cold Spring Harbor Laboratory: Plainview, NY, 1972, p431-435.
64. Hanahan, D. Studies on transformation of *Escherichia coli* with plasmids. *J. Mol. Biol.* **1983**, *166*, 557-580. DOI:10.1016/S0022-2836(83)80284-8.
65. Sambrook, J.; Russell, D. W. Molecular Cloning: A Laboratory Manual, 3<sup>rd</sup> ed.; Cold Spring Harbor Laboratory: Cold Spring Harbor, NY, 2001.
66. (a) Barbas, C. F. III; Burton, D. R.; Scott, J. K.; Silverman, G. J. Quantification of DNA and RNA in *Phage Display: A Laboratory Manual*. Cold Spring Harbor Laboratory: Cold Spring Harbor, NY, 2001; pA3.9. (b) Manchester, K. L. Value of A260/A280 ratios for measurement of purity of nucleic acids. *Biotechniques* **1995**, *19*, 208-210.
67. (a) Stroman, P.; Reinert, W. R.; Giles, N. H. Purification and characterization of 3-dehydroshikimate dehydratase, an enzyme in the inducible quinic acid catabolic pathway of *Neurospora crassa*. *J. Biol. Chem.* **1978**, *253*, 4593-4598. (b) Fujisawa, H. Protocatechuate 3,4-dioxygenase (*Pseudomonas*). *Methods Enzymol.* **1970**, *17A*, 526-529.
68. Glazyrina, J.; Materne, E.; Dreher, T.; Strom, D.; Junne, S.; Adams, T.; Greller, G.; Neubauer, P. High cell density cultivation and recombinant protein production with *Escherichia coli* in a rocking-motion-type bioreactor. *Microb. Cell Fact.* **2010**, *9*:42.
69. Ainsworth, A. T.; Kirby, G. W. Stereochemistry of  $\beta$ -carboxy- and  $\beta$ -hydroxymethylmuconic derivatives. *J. Chem. Soc. C* **1968**, *88*, 1483-1487.